DEVELOPMENT OF A SYNTHETIC METHODOLOGY FOR THIENOPYRIDINONE AND THIENODIAZEPINONE DERIVATIVES AND BENZIMIDAZO-OXAZEPINES

A THESIS SUBMITTED TO
THE GRADUATE SCHOOL OF NATURAL AND APPLIED SCIENCES
OF
MIDDLE EAST TECHNICAL UNIVERSITY

BY

NALAN KORKMAZ ÇOKOL

IN PARTIAL FULFILLMENT OF THE REQUIREMENTS
FOR
THE DEGREE OF DOCTOR OF PHILOSOPHY
IN
CHEMISTRY

SEPTEMBER 2018

Approval of the thesis:

DEVELOPMENT OF A SYNTHETIC METHODOLOGY FOR THIENOPYRIDINONE AND THIENODIAZEPINONE DERIVATIVES AND BENZIMIDAZO-OXAZEPINES

submitted by **NALAN KORKMAZ ÇOKOL** in partial fulfillment of the requirements for the degree of **Doctor of Philosophy in Department of Chemistry, Middle East Technical University** by,

Prof. Dr. Halil Kalıpçılar _____
Dean, Graduate School of **Natural and Applied Sciences**

Prof. Dr. Cihangir Tanyeli _____
Head of Department, **Chemistry**

Prof. Dr. Metin Balcı _____
Supervisor, **Chemistry Dept**., **METU**

Examining Committee Members:

Prof. Dr. Aliye Alaylı Altundaş _____
Chemistry Dept., Gazi University

Prof. Dr. Metin Balcı _____
Chemistry Dept., METU

Prof. Dr. Adnan Bulut _____
Chemistry Dept., Kırıkkale University

Prof. Dr. Özdemir Doğan _____
Chemistry Dept., METU

Assist. Prof. Dr. Çağatay Dengiz _____
Chemistry Dept., METU

Date: 25.09.2018

I hereby declare that all information in this document has been obtained and presented in accordance with academic rules and ethical conduct. I also declare that, as required by these rules and conduct, I have fully cited and referenced all material and results that are not original to this work.

Name, Last name: Nalan Korkmaz Çokol

Signature:

ABSTRACT

DEVELOPMENT OF A SYNTHETIC METHODOLOGY FOR THIENOPYRIDINONE AND THIENODIAZEPINONE DERIVATIVES AND BENZIMIDAZO-OXAZEPINES

Korkmaz Çokol, Nalan
Ph.D., Department of Chemistry
Supervisor: Prof. Dr. Metin Balcı

September 2018, 207 pages

Thienopyridinone and thienodiazepinone derivatives are known for their diverse pharmacological activities. Pyridinones and diazepinones play an important role in inhibition of some enzymes such as glycogen synthase kinase-3β and regulation of various cell functions. They also demonstrate an interesting property in the repair of damaged DNA. In the first part of this thesis, we synthesized thienopyridinone and thienodiazepinone derivatives. Aminothiophene derivatives were successfully synthesized *via* Gewald type reaction which was followed by the conversion to iodo- and bromo-thiophene derivatives *via* modified Sandmayer reaction. Sonogashira cross-coupling reaction was used to generate carbon-carbon single bond between the thiophene ring and alkyne derivatives. Cyclization of those compounds with hydrazine hydrate gave target molecules.

Imidazole derivatives exhibit a wide range of bioactivities, therefore they are of intensive synthetic interest. They are also used as precursors for the synthesis of heterocycles having pharmaceutical properties. In the second part of this thesis, a concise and efficient approach to the synthesis of benzimidazo-oxazepine derivatives was developed. The synthetic strategy relies on the *O*-propargylation of salicyl aldehyde derivatives followed by Sonogashira cross-coupling reaction for further derivatization. Resulting alkyne derivatives were converted into the corresponding

imidazole rings under acidic condition. NaH-mediated cyclization gave desired compounds, benzimidazo-oxazepines.

Keywords: thienopyridinone, thienodiazepinone, imidazole, benzimidazole, oxazepine, benzimidazo-oxazepine.

ÖZ

TİYENOPİRİDİNON, TİYENODİAZEPİNON VE BENZİMİDAZO-OKZAZEPİN TÜREVLERİNİN SENTEZİ İÇİN YÖNTEM GELİŞTİRME

Korkmaz Çokol, Nalan
Doktora, Kimya Bölümü
Tez Yöneticisi: Prof. Dr. Metin Balcı

Eylül 2018, 207 sayfa

Tiyenopiridinon ve tiyenodiazepinon türevleri ilaç kimyasında kullanılan önemli bileşiklerdir. Piridinon ve diazepinon türevlerinin bazı hücre fonksiyonlarının düzenlenmesinde ve glikozidaz enzimlerinin inhibisyonunda kullanıldığı literatürde belirtilmiştir. Bu çalışmada, tiyenopiridinon ve tiyenodiazepinon türevlerinin sentezi için yeni metotların geliştirilmesi planlandı. Başlangıç maddesi olarak aminotiyofen türevleri Gewald reaksiyonu ile başarıyla sentezlendikten sonra, Sandmayer reaksiyonu kullanılarak ilgili iyodotiyofen ve bromotiyofen molekülleri oluşturuldu. Sonogashira kenetlenme reaksiyonu aracılığı ile tiyofen halkasına farklı üçlü bağlar takıldı ve halkalaşma için ilgili fonksiyonel gruplar elde edildi. Daha sonra hidrazin hidrat aracılığı ile molekül içi kapanma gerçekleştirilerek, ilgili piridinon ve diazepinon türevleri başarıyla sentezlendi.

İmidazol türevleri, biyolojik aktivite gösteren özellikleri ile bilim dünyasında dikkat çekmeyi başaran moleküller sınıfına girmişlerdir. Aynı zamanda ilaç kimyasında kullanılan bazı heterosiklik bileşiklerin sentezi için kullanılan önemli çıkış bileşikleridir. Çalışmanın ikinci kısmında, benzimidazo-okzazepin türevi sentezi için yeni bir metotun geliştirimesi planlandı. İlk olarak, salisilaldehit ve türevlerinin hidroksil grubuna bazik ortamda farklı propargil grupları takıldı. Alkin grubundan türevlendirme çalışmaları için Sonogashira kenetlenmesi başarıyla uygulandı. Daha

sonra bu bileşiklerin *O*-diaminobenzen ile kondenzasyonu sağlanarak halkalaşma için gerekli fonksiyonel gruplar moleküle takıldı. İlgili imidazol türevleri sentezlendikten sonra bu bileşiklerin NaH ile reaksiyonu sonucunda hedeflenen kapanma ürünleri yüksek verimle elde edildi.

Anahtar Kelimeler: tiyenopiridinon, tiyenodiazepinon, imidazol, benzimidazol, okzazepin, benzimidazo-okzazepin.

To my husband Onur and daughter Nur…

ACKNOWLEDGEMENT

I would like to express my deep thanks to my supervisor Prof. Dr. Metin Balcı for his continuous guidance, endless support, valuable advices, patience, and encouragements. It was a great chance for me to be a student of Prof. Dr. Metin Balcı.

I would like to thank Dr. Serdal Kaya and Dr. Selbi Keskin for their sincere assistance, sharing experience and advices through this research.

I would like to thank NMR specialist Betül Eymur for the NMR experiments.

I am particularly grateful for working with all SYNTHOR Research Group members for their warm friendship, great support, and assistance.

I would like to thank all of the members of the Department of Chemistry of METU for their support, guidance, and help.

I would like to thank TÜBİTAK (Scientific and Technological Research Council of Turkey, Project no: TBAG 112T360)

Finally, my special appreciation and great gratitude are devoted to my family; my husband Onur Çokol, my daughter Nur Çokol, and my mother Zahide Korkmaz for their endless love and great support.

TABLE OF CONTENTS

LIST OF FIGURES

FIGURES

LIST OF SCHEMES

SCHEMES

LIST OF ABBREVIATIONS

ABBREVIATIONS

Chk1: Check point kinase 1

DHP: Dihydropyran

DIPA: Diisopropylamine

Fmoc: Fluorenylmethyloxycarbonyl

HMBC: Heteronuclear Multiple Bond Correlation

HOBt: Hydroxybenzotriazole

HSQC: Heteronuclear single quantum correlation

MCH: Melanin-concentrating hormone

MCHR: Melanin-concentrating hormone receptor

TBAI: Tetrabutylammonium iodide

TBTU: 2-(1*H*-Benzotriazole-1-yl)-1,1,3,3-tetramethylaminium tetrafluoroborate

TEA: Triethanolamine

TFA: Trifluoroacetic acid

Tf_2O: Trifluoromethanesulfonic anhydride

THP: Tetrahydropyranyl acetal

TLC: Thin layer chromotography

***p*-TsOH:** *p*-Toluenesulfonic acid

CHAPTER 1

DEVELOPMENT OF A SYNTHETIC METHODOLOGY FOR THIENOPYRIDINONE AND THIENODIAZEPINONE DERIVATIVES

1.1 INTRODUCTION

Cancer has become one of the most vital and incurable diseases in the world since there are many people died in recent years. According to a research in 2000, more than 10 million people developed a tumor inside their body and more than half of those people died.[1] Thiophene-based structures have attracted a great deal of attention due to their binding properties to tumor in a cell. Many modelings such as pharmacophore and atom based 3D-QSAR were applied to the structures with thiophene moiety, it was proven that it had binding affinity for antitumor activity.[2] The number of obese people have gradually increased in recent years.[3] Melanin-concentrating hormone (MCH) is involved in the feed control in human body and this hormone leads to increase in feeding and weight when it chronically treats with the rat.[4,5] The melanin-concentrating hormone receptor **1** (MCH1R) has recently attracted considerable interest as target molecule (Figure 1). There are already some ligands which have high affinity to MCH1R.[6] Scientists have drawn attention to design novel ligands having high affinity to MCH with thiophene moiety which has anorectic effect on those people.[7]

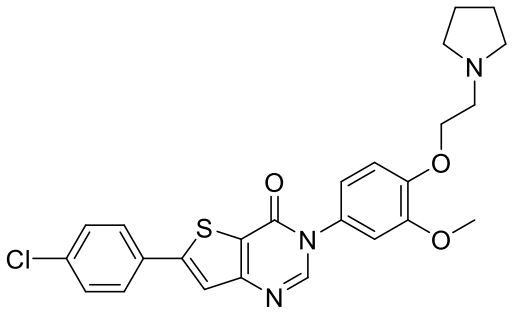

1

Figure 1. Structure of MCHR1 ligand

1.1.1 Pyridinone

Alzheimer's disease has become one of the most important diseases in the world because there have been 24 million people being effected worldwide.[8] Pyridinone derivatives are well-known drugs for Alzheimer's disease therapy. While H_3 receptor causes degradation in release of some neurotransmitters such as acetylcholine, serotonin, noradrenaline, and dopamine, H_3 receptor antagonists regulate the level of those neurotransmitters in the brain which provide mental health for patients with Alzheimer's disease. Pyridinone derivative **2** (Figure 2) has been employed as H_3 receptor antagonist and it demonstrated positive result as therapeutic agents.[9]

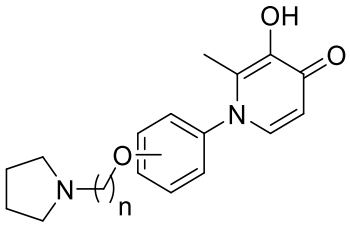

2

Figure 2. The H_3 receptor antagonist

1.1.2 Thienopyridinone

There have been various derivatives of thienopyridinone used in regulation of cell functions. To exemplify, compound **3** showed high cell activity as inhibition of

enzymes such as glycogen kinase synthase-β (Figure 3). Furthermore, this skeleton is well-known drug candidate structure.

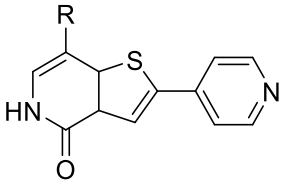

3

Figure 3. Biologically active thienopyridinone derivative

It has also effect on repair of DNA damage and is used as theurepatic agent for cancer cells. Its derivatives are known as to show great affinity to some receptors which are involved in regulation of some neurotransmitters. For instance, *N*-substituted thienopyridinone derivatives play an important role against Gram negative bacteria.[9]

1.1.3 Synthesis of thienopyridinone

Check point kinase 1 (Chk1), serine/threonine-specific protein kinase, plays an important role in cell regulation once DNA is damaged, that's why synthesis of its inhibitor has drawn attention by organic chemists. In literature, there are already published Chk1 inhibitors classified as first generation, however, there is no enough molecules having promosing affinity to Chk1. Thiophene-fused pyridine derivatives are well known compounds working as a Chk1 activator for DNA damage repair. Sahu *et al.*[9] (Scheme 1) investigated an efficient and economical way to synthesize *N*-aminothieno[3,2-*c*]pyridine-4-one from thieno[3,2-*c*]pyran-4-one (**7**) which was prepared from 4-(methylthio)-2-oxo-6-(*p*-tolyl)-*2H*-pyran-3-carbonitrile (**4**). Carbonitrile derivative **4** was reacted with methyl thioglycolate (**5**) to generate compound **6** *in situ* followed by addition of hydrazine hydrate to provide *N*-aminothieno[3,2-*c*] pyridine-4-one (**7**).

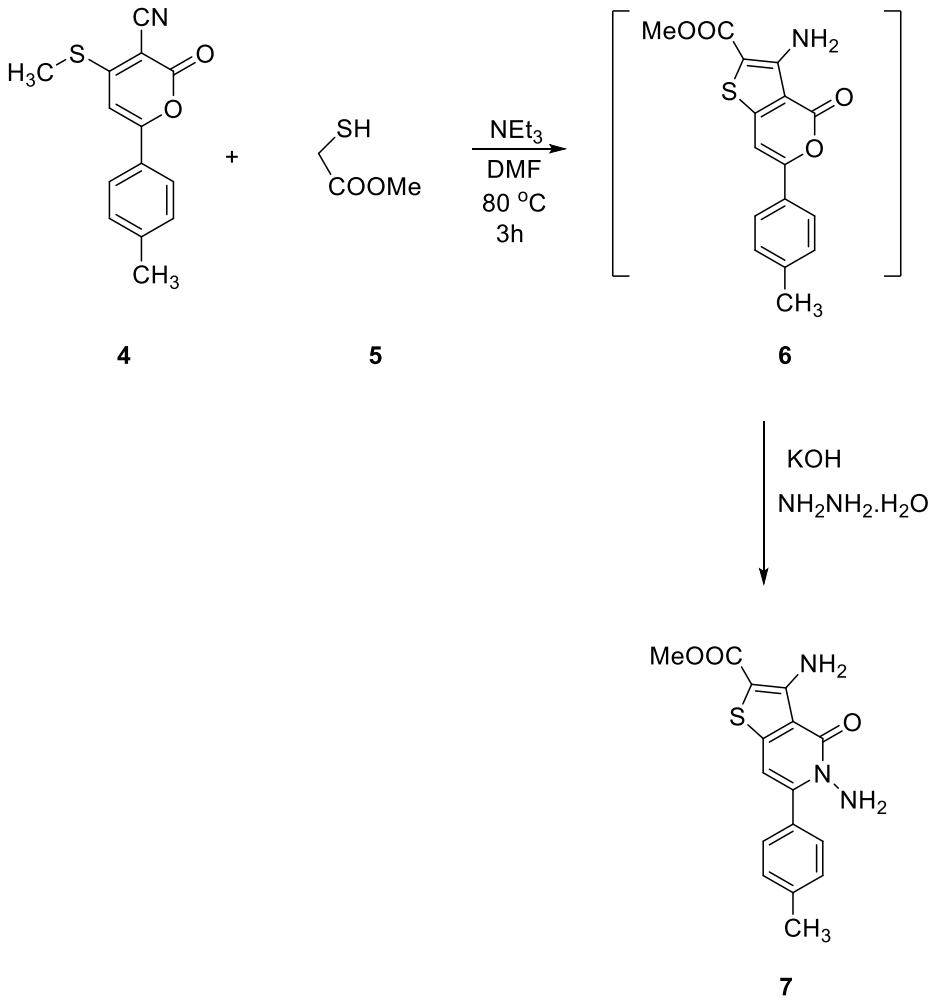

Scheme 1. Synthesis of *N*-aminothieno[3,2-*c*] pyridine-4-one (**7**)

In 2009, Brouillette *et al.*[10] developed a new methodology for synthesis of thienopyridinone derivatives **11** by using corresponding thienodiazepinones **8** as the starting materials (Scheme 2). After generation of Boc-protected thienodiazepinones **8**, they were treated with Grignard reagent to afford compound **9**. Abstraction of α-proton of ketone **9** in the presence of KO*t*Bu in THF was followed by attacking of the

resulting carbanion to the carbonyl group conjugated with the benzene ring to give **10**. Dehydration was carried out under acidic condition that afforded compound **11**.

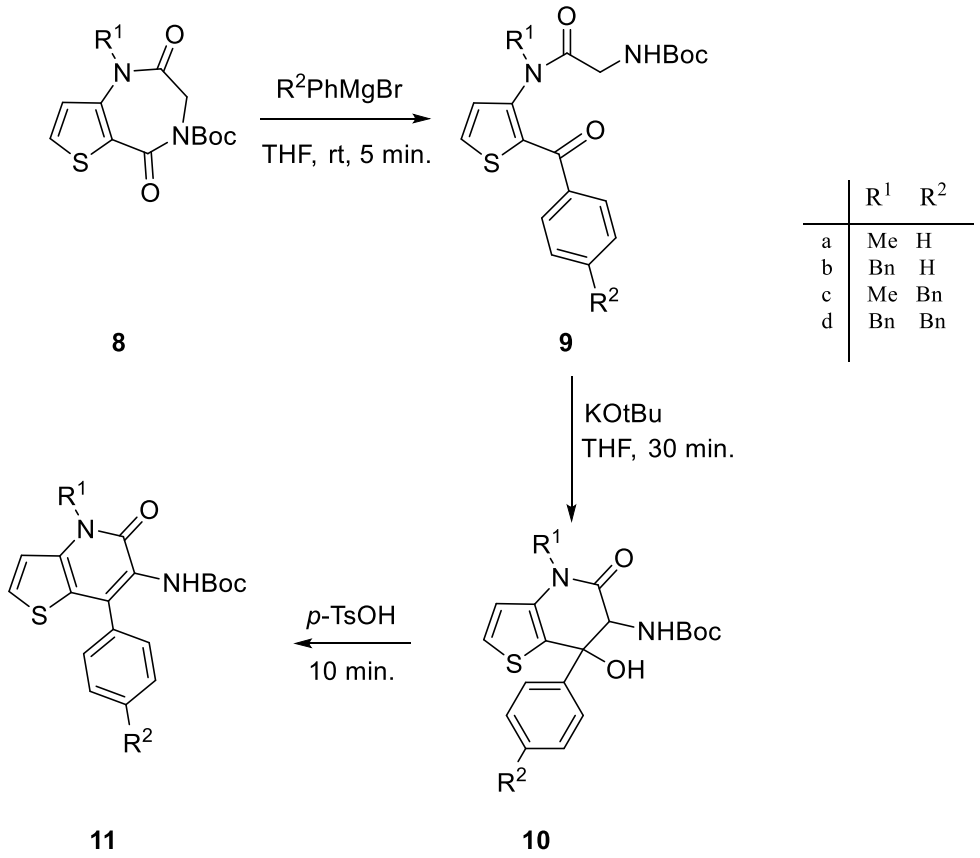

Scheme 2. Synthesis of thienopyridinone derivatives **11**

1.1.4 Thienopyrimidinone

Enzymes are proteins which are responsible for biochemical reactions in living cells. Some enzymes such as sirtuins (SIRTs) plays a significant role in many biological processes as deacylation of NAD^{+},[11] aging,[12] inflammation[13] and repair of DNA.[14] There are various isomers of sirtuins in human body all of which have different specifications. Since some of them have capability of linkage to disease cell to decrease its activity, scientists have drawn attention to synthesis of their derivatives. Selective SIRT2 suicide inhibitor has known to take a role in proteolytic degradation of c-Myc.[15] Previously, thienopyrimidinone SIRT2 inhibitor (**12**) (Figure 4) has been reported with high selectivity to SIRT2.[16]

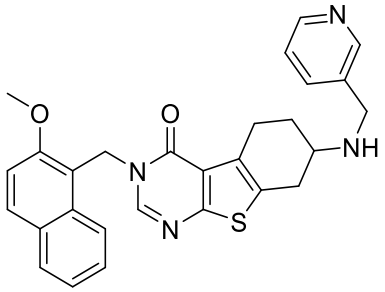

12

Figure 4. Thienopyrimidinone SIRT2 inhibitor

1.1.5 Pyridazinone

PDE4 has various types of cell functions such as controlling the level of cyclic nucleotide cAMP which is used for giving responses to biological agents through activation of adenylyl cyclase.[17] PDE4 is used as anti-inflammatory agent for asthma[18] as well as it is a member of nucleotide degrading enzyme family. Gr. cia *et al.*[20] prepared oral PDE4 program and tested a series of pyridazinone compounds used as inhaled inhibitors of PDE4. It gave a positive result as to show excellent activity like inhaled inhibition enzyme, PDE4[19] that's why at this point they aimed to synthesize pyridazinone analogues as **13** (Figure 5) used as inhaled inhibitor of PDE4.[20]

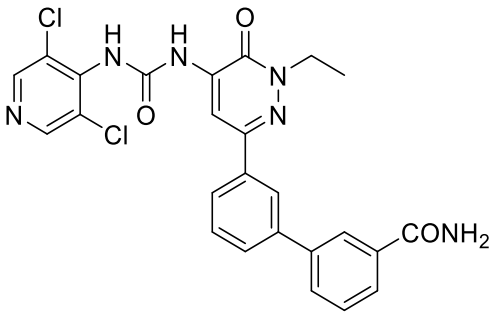

13

Figure 5. Biaryl-substituted pyridazinone **13**

1.1.6 Benzo- and thienopyridazinone

Some benzo- and thienopyridazinone derivatives have been used as mimics of melanin-concentrating hormone receptor. Thienopyridazinones have also been known

to show high affinity to this receptor and high brain penetration. It sends a signal to brain no food intake thus helps weight lose with dose-dependent. Synthesis of melanin-concentrating hormone receptor ligand antagonists has gained a great deal of importance by scientists because some evidence emerged that these structures have a significant role for such antagonists in the treatment of anxiety and depression as well.[21,22,23] Figure 6 shows thienopyridazinone **14** and benzopyridazinone **15** structures used as MCH1R antagonists.[7]

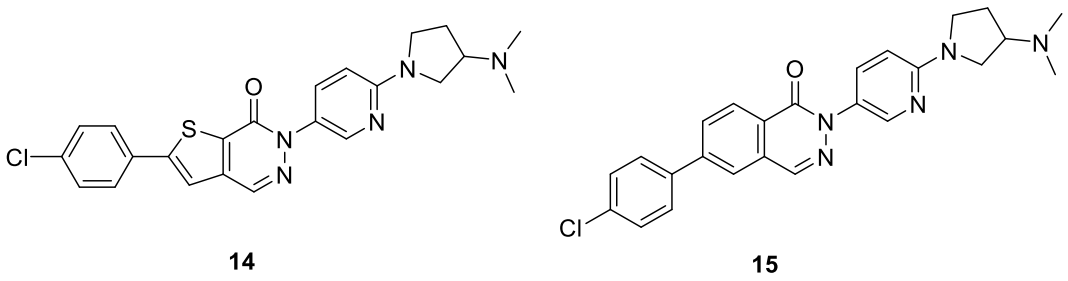

Figure 6. Melanin concentrating hormone receptor ligand antagonists

1.1.6.1 Synthesis of thienopyridazinone derivatives

Since thienopyridazinones and its derivatives have important role in regulation of nervous system, synthetic organic chemists draw attention to incorporation of new substituents to this skeleton. Dyck *et al.*[7] described a concise and efficient synthesis of derivatives of compound **14** utilized as MCH1R ligand (Scheme 3).

For this purpose, 4,5-dichloropyridazinone (**16**) was used as the starting material. NH-group was protected as tetrahydropyranyl acetal derivative and methanolysis was carried out selectively to give compound **17**. For introduction of arylacetone group compound **17** was first converted to the corresponding triflate followed by Sonogashira cross-coupling reaction to furnish compound **18**. Cyclization with Na_2S in DMF at 70 °C gave pyridazinone **19**.

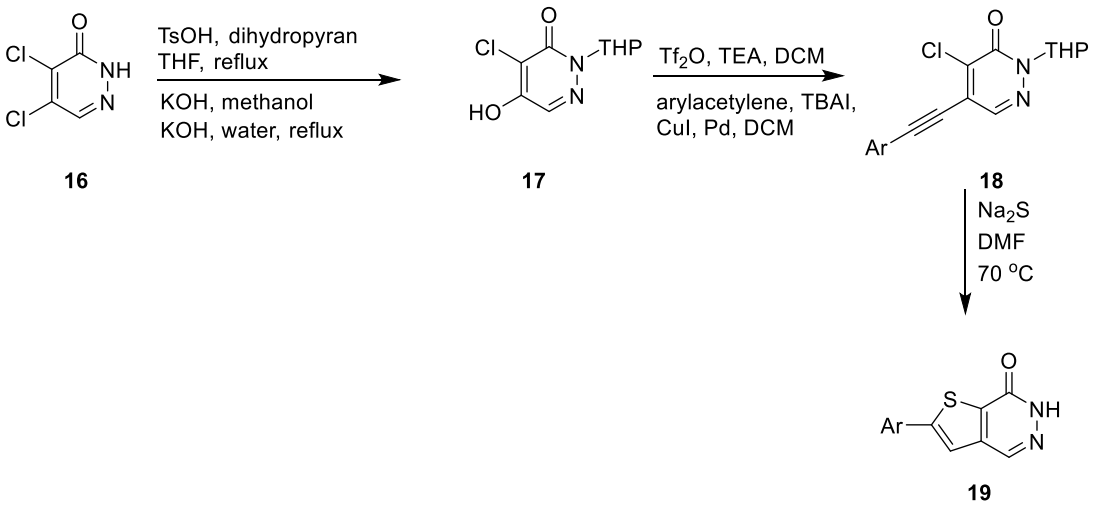

Scheme 3. Synthesis of fused pyridazinone **19**

For the construction of the compound **22** (Scheme 4), **20** was reacted with 3-(alkylamino)pyrrolidine in the presence of TsOH. Pyrrolidine functionality was successfully introduced to the system at 110 °C and **21** was formed exclusively. Compound **21** was reacted with **19** in the presence of CuI, 1,2-*trans*-aminocyclohexane, and Cs_2CO_3 in dioxane that resulted in the formation of **22**.

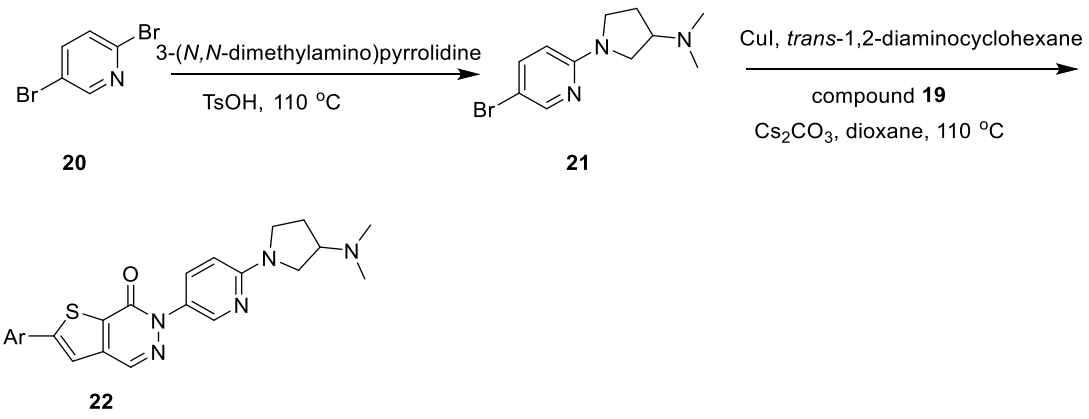

Scheme 4. Synthesis of MCH1R ligand **22**

1.1.7 Diazepinone

The synthesis of nitrogen containing heterocycles has attracted considerable interest due to their wide range of biological activities. In particular, seven-membered *N*-heterocycles are privileged structures such as **23** and **24** (Figure 7) are present in some

pharmaceuticals. The pyrrolobenzodiazepine **24** forms the natural anthramycin family of antitumor antibiotic skeleton. Synthetic pyrrolobenzodiazepines have recently been used as non-nucleoside reverse transcriptase inhibitors.[24]

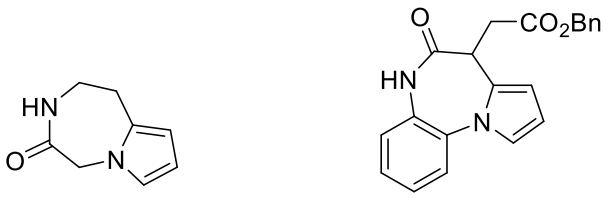

23 **24**

Figure 7. Pyrolodiazepinone **23** and pyrolobenzodiazepinone **24**

Benzo[1,4]diazepin-2-ones are privileged structures[25,26] due to the fact that they are present in various types of biologically active molecules. Synthesis of the heterocycles which are composed of these skeletons have attracted considerable attention since they are involved in the well-known drugs used in the treatment of coronary artery disease, peripheral vascular disease, and cerebrovascular disease.[27] Clotiazepam (**25**) (Figure 8) is thienodiazepine-based structure drug with anxiolytic, anticonvulsant, sedative, and muscle relaxant properties.[28,29] Furthermore, well-known compound **26** (Figure 8) is used in regulation of some cell functions as AMP-activated protein kinase regulators for the treatment of diabetes, metabolic syndrome, and obesity.[30,31]

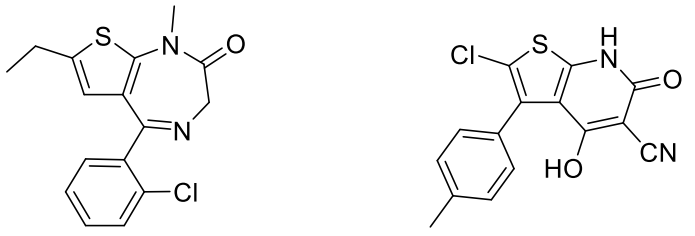

25
clotiazepam

26

Figure 8. Structures of biologically important thiophene-fused **25** and **26**

1.1.8 Synthesis of diazepinones

α-Aminoacyl-β-amino esters **28a-d** were synthesized by the reaction of β-amino esters **27a-d** with the *N*-Boc-amino acid using respectively 2-(1*H*-benzotriazole-1-yl)-

1,1,3,3-tetramethylaminium tetrafluoroborate (TBTU) and hydroxybenzotriazole (HOBt) in dichloromethane. Compound **28a-d** were isolated and treated with an excess of freshly prepared vinylmagnesium bromide (600 mol %) in the presence of copper cyanide (30-40 mol %) in THF at -78 °C to room temperature. Diazepinones **30a-d** were synthesized from homoallylic ketones **29a-d** by a route featuring deprotection of Boc group in the presence of TFA/DCM (1:1), treatment of the trifluoroacetate salt with triethylamine at 0 °C, and reduction of the imine intermediate with sodium triacetoxyborohydride in dilute dichloroethane (Scheme 5).[24]

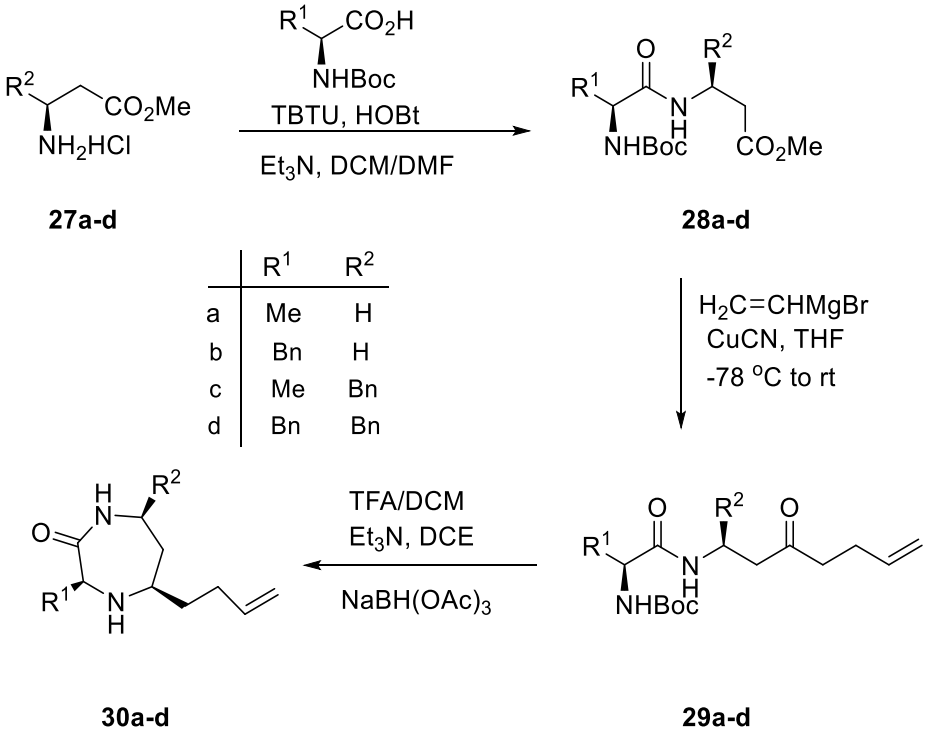

Scheme 5. Synthesis of diazepinones **30a-d**

1.1.8.1 Synthesis of fused diazepinones

Diazepinone-fused derivatives play an important role in medicinal chemistry because of their significant properties as therapeutics. This has encouraged the scientists for the synthesis of new classes of heterocyclic systems including diazepinone scaffold. Although heterocyclic systems having diazepinone system, imidazo[2,1-*b*][1,3,4]thiadiazole[32,33] and an imidazo[2,1-*b*][1,3]thiazole[34,35] indivually showed

incredible biological activities. Diazepinone system linked to those heterocycles have not been previously reported. Kolavi *et al.*[36] proposed a concise and efficient synthesis of diazepinone derivatives fused to those heterocycles (Scheme 6).

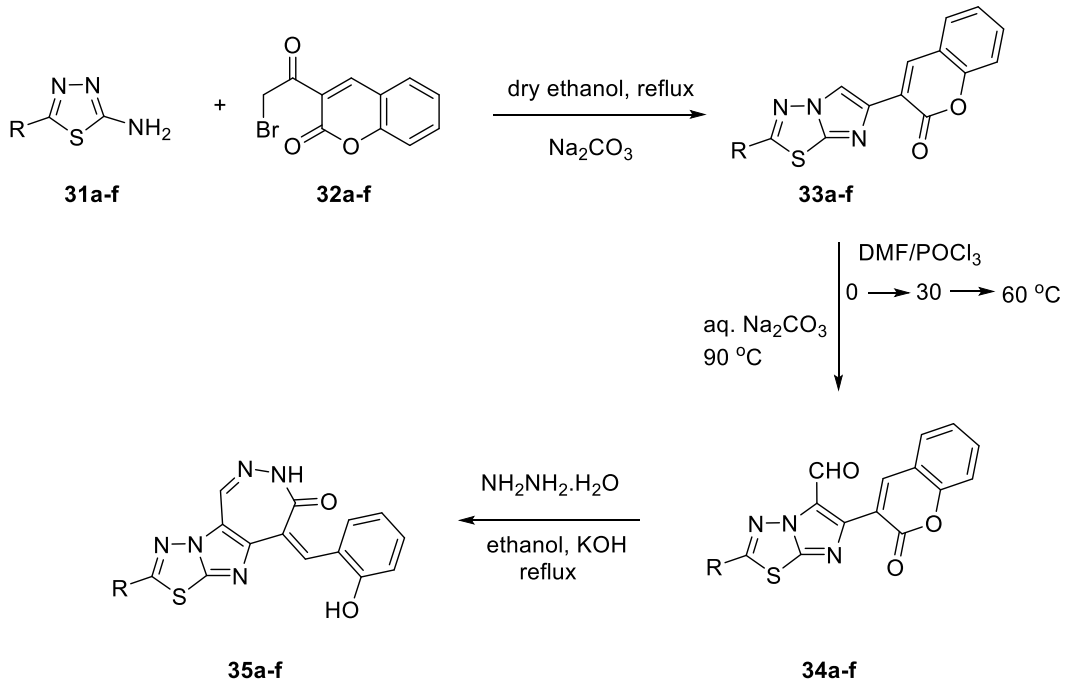

R= a) ethyl, b) *n*-propyl, c) cyclohexyl, d) benzyl, e) 2-furyl, f) 2-thienyl

Scheme 6. Synthesis of diazepinones **35a-f**

The benzopyran-2-ones **32a-f** were used for the synthesis of **35**. The required 3-(2-alky/arylimidazo[2,1-b]-[1,3,4]thiadiazol-6-yl)-2*H*-chromen-2-ones (**33**) were prepared by the reaction of 2-amino-5-alkyl/aryl-1,3,4- thiadiazoles (**31**) with 3-(bromoacetyl)coumarins (**32**). The 5-carbaldehydes **34a-f** were obtained by the Vilsmeier–Haack reaction on **33a-f**. Treatment of these compounds with hydrazine hydrate in ethanol/KOH under reflux conditions provided the ring-transformed derivatives *via* lactone ring opening by intramolecular nucleophilic attack of the $-NH_2$ group of the intermediate hydrazone which could not be isolated. Initial step in the mechanism of this reaction is intramolecular nucleophilic attack at the lactone carbonyl of the coumarin leading to the formation of diazepinones **35a-f**.

1.1.9 Aim of the study

The aim of this thesis was to develop a synthetic methodology for thienopyridinone and thienodiazepinone derivatives. For the formation of thiophene skeleton such as **37** and **40**, 1,4-dithiane-2,5-diol (**36)** and cyclohexanone (**39**) were planned to be used as starting materials (Scheme 7).

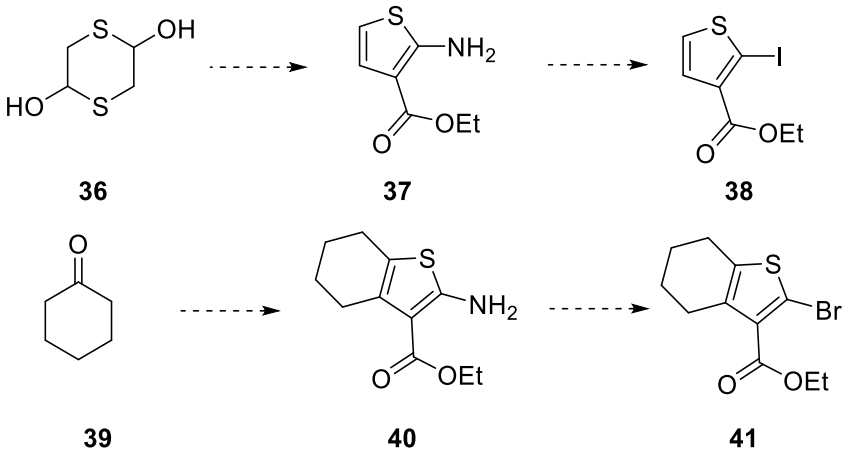

Scheme 7. Synthesis of aminothiophenes **37** and **40** and halothiophenes **38** and **41**

After the construction of aminothiophene skeletons as key compounds *via* Gewald type reaction, iodide and bromide will be attached to the alpha position of thiophene ring with replacement of amino moiety through modified Sandmayer reaction. Application of Sonogashira cross-coupling reaction to halothiophenes **38** and **41** will result in the formation of **42** and **45**.

The final step, cyclization of **42** and **45** with hydrazine monohydrate should provide the desired thienopyridinone **43** and **46** and thienodiazepinone derivatives **44** and **47** (Scheme 8).

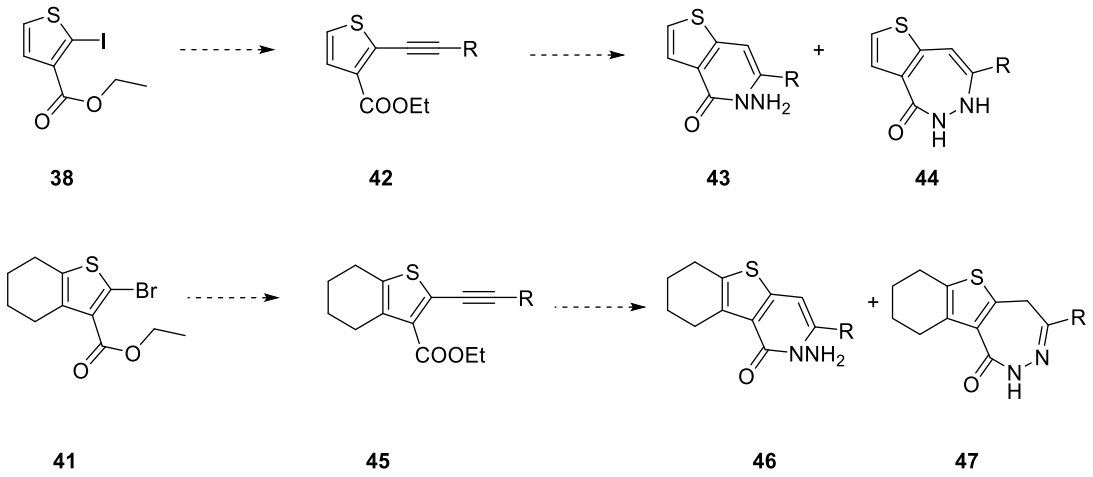

Scheme 8. Synthetic pathway for the formation of thienopyridinones and thienodiazepinones

1.2 RESULTS AND DISCUSSION

1.2.1 Synthesis of aminothiophene derivatives

1.2.1.1 Synthesis of ethyl 2-aminothiophene-3-carboxylate (37)

Dithiane **36** was used as starting material to form thiophene skeleton having amine functionality at its α–position using the Gewald type reaction (Scheme 9).[37]

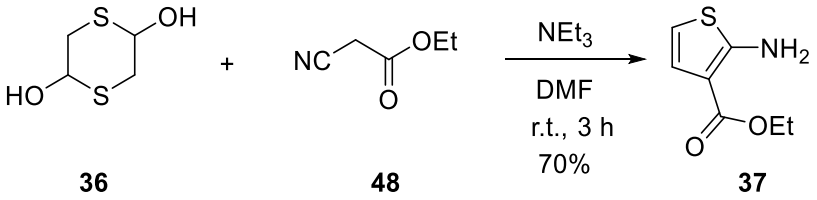

36 **48** **37**

Scheme 9. Synthesis of aminothiophene **37**

The methylene group in ethyl cyanoacetate (**48**) is activated by two electron-withdrawing groups for deprotonation. In this version of Gewald type reaction, the more stable dimeric form **36** of α-sulfonylaldehyde **49** was used to construct the thiophene skeleton. Compound **36** was dissolved in DMF at room temperature. After addition of ethyl cyanoacetate (**48**), followed by addition of NEt_3 compound **37** was formed.

We assume that the first step is the abstraction of a proton in **48**, in the presence of NEt_3. The resulting carbanion undergoes a nucleophilic attack to the aldehyde group in **49** to form the intermediate **50** accompanied by Knoevenagel-Cope condensation reaction. Intramolecular nucleophilic attack of the sulfur anion to the carbon atom of the cyano group affords **37** which in principle exists in equilibrium with the tautomeric forms cyclic imine **51** (Scheme 10). However, it was proven that amino-form **37** is the most stable structure and equilibrium is shifted to the side of amine.[38,39,40,41,42]

The ^{1}H- and ^{13}C-NMR spectral data were in agreement with the structure of **37.** Two thiophene protons resonate at 6.98 and 6.18 ppm with a coupling constant of J = 5.7 Hz. The NH_2 protons resonate as a broad singlet at 5.93 ppm.

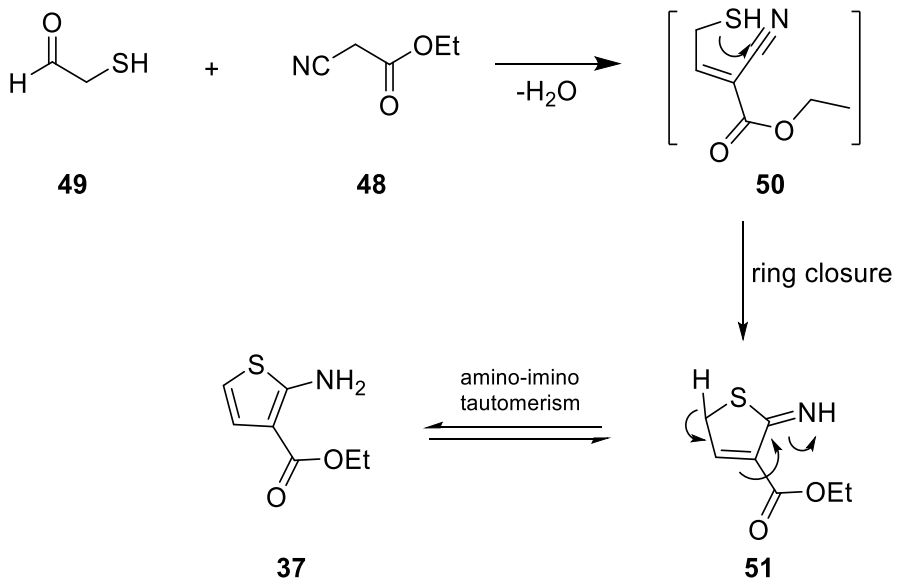

Scheme 10. Schematic pathway for the formation of compound **37**

1.2.1.1 Synthesis of ethyl 2-amino-4,5,6,7-tetrahydrobenzo[*b*]thiophene-3-carboxylate (40)

After successful synthesis of the aminothiophene derivative **37**, we focused on the synthesis of further substituted aminothiophenes. Base-promoted Gewald type reaction was used to generate **40**.[37] In the second version of the Gewald type reaction, any ketone having an α-proton can be used as starting material to form thiophene scaffold. Incorporation of cyclohexanone (**39**) into the system afforded corresponding amine **40** (Scheme 11).

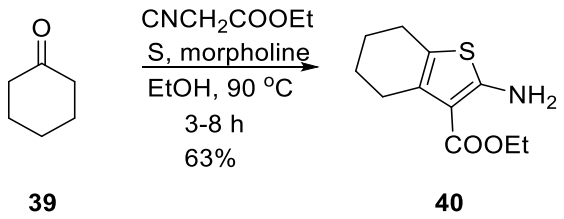

Scheme 11. Synthesis of ethyl 2-amino-4,5,6,7-tetrahydrobenzo[*b*] thiophene-3-carboxylate (**40**)

This particular version of Gewald type reaction involves a base-promoted sulfur addition. After deprotonation of **48**, the formed carbanion undergoes a nucleophilic addition to the carbonyl group in **39** to form intermediate **55**. Morpholine reacts with elemental sulfur **53** to form sulfur ylide **54**. Intermediate **55** reacts with **54** to generate sulfur adduct **56**. Intramolecular cyclization reaction of **56** involving sulfur attack to the carbon atom of cyano group affords **57** which is in equilibrium with its cyclic amine form **40** as shown in Scheme 12.

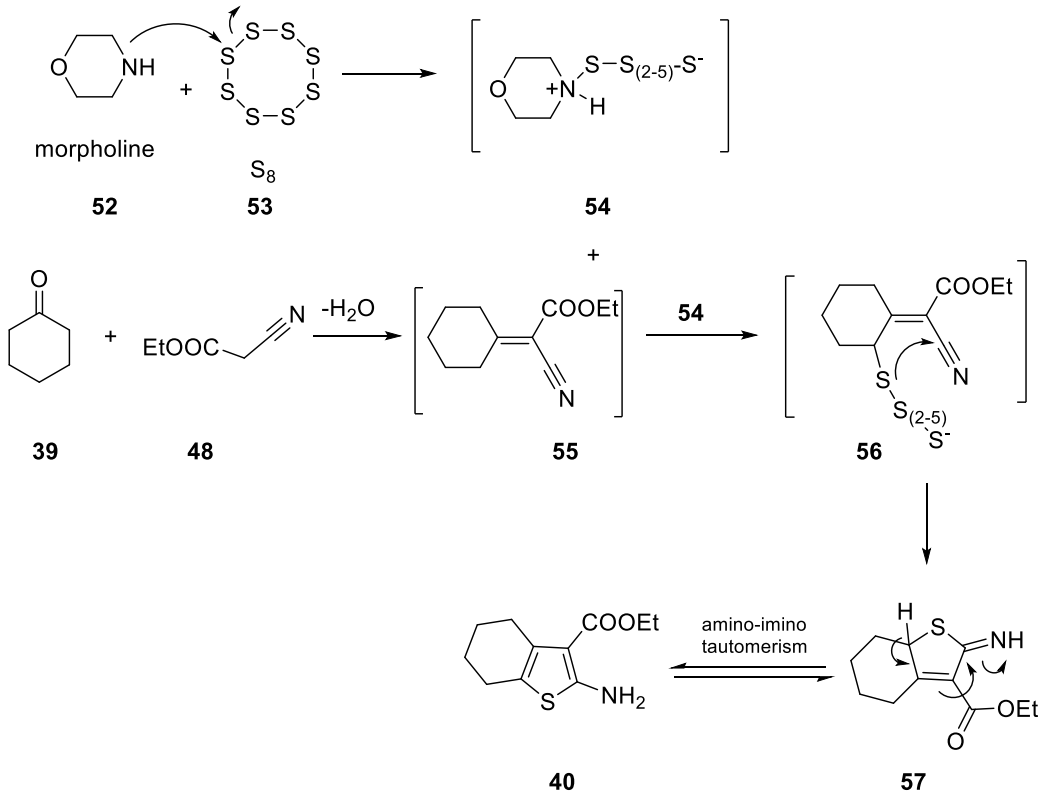

Scheme 12. Mechanism for the formation of **40**

The ^{1}H-NMR spectrum is in agreement with the structure **40**. The NH_2 protons resonate at 5.95 ppm as a broad singlet. The methylene protons attached to the thiophene ring resonate as multiplets at 2.70 and 2.49 whereas the remaining methylene protons appear at 1.75 ppm as multiplet as expected.

1.2.1.3 Synthesis of ethyl 2-amino-5,6-dihydro-4*H*-cyclopenta[*b*]thiophene-3-carboxylate (59)

Similar reaction was carried out with cyclopentanone. By application of the same methodology as described above, the expected product, cyclopentene-fused aminothiophene derivative **59** was obtained in a yield of 30% (Scheme 13).

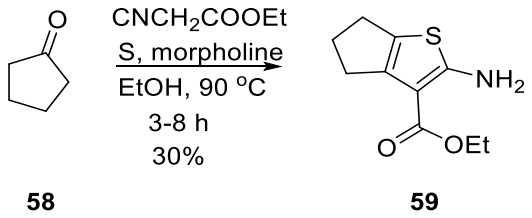

Scheme 13. Synthesis of ethyl 2-amino-5,6-dihydro-4H-cyclopenta[*b*] thiophene-3-carboxylate (**59**)

Completion of the reaction was followed by GC-MS which displayed a signal with the mass of 211.1 g/mol. The NMR spectral data were in agreement with the structure of **59**. In the ^{1}H-NMR spectrum, the NH_2 protons resonate at 5.84 ppm as a broad singlet. The CH_2 protons give rise to multiplets due to the coupling with neighboring methylene protons at 2.81, 2.72, and 2.31 ppm.

1.2.2 Synthesis of ethyl 2-iodothiophene-3-carboxylate (38)

Sandmayer reaction was applied to **37** for the formation of **38**. Conventional Sandmayer reaction involving initial diazotization of the arylamine followed by addition of the diazonium salt to the cuprous halide in an aqueous solution with the corresponding halogen acid is reported. Nevertheless, there are numerous competitive side reactions (Scheme 14) decreasing the yield of targeting Sandmayer products.[43]

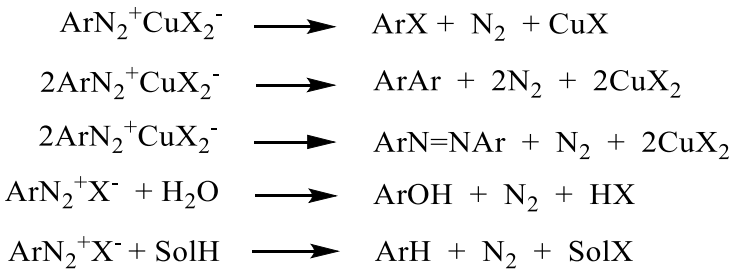

Scheme 14. Competitive side reactions

The overall reaction was reported in the literature as shown below.

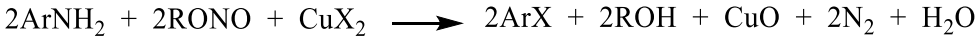

We applied the Sandmayer reaction to **37** in the presence of *t*-butyl nitrite and CuI in CH_3CN as shown in Scheme 15. Three side products **60**, **61**, and **62** were formed when the reaction was carried out in a non-dry solvent. The isolated yield of the desired product **38** was very low due to the fact that separation of **38** from **60** was very difficult. The yields of all compounds were determined by analysis of the ^{1}H-NMR spectrum of the mixture.

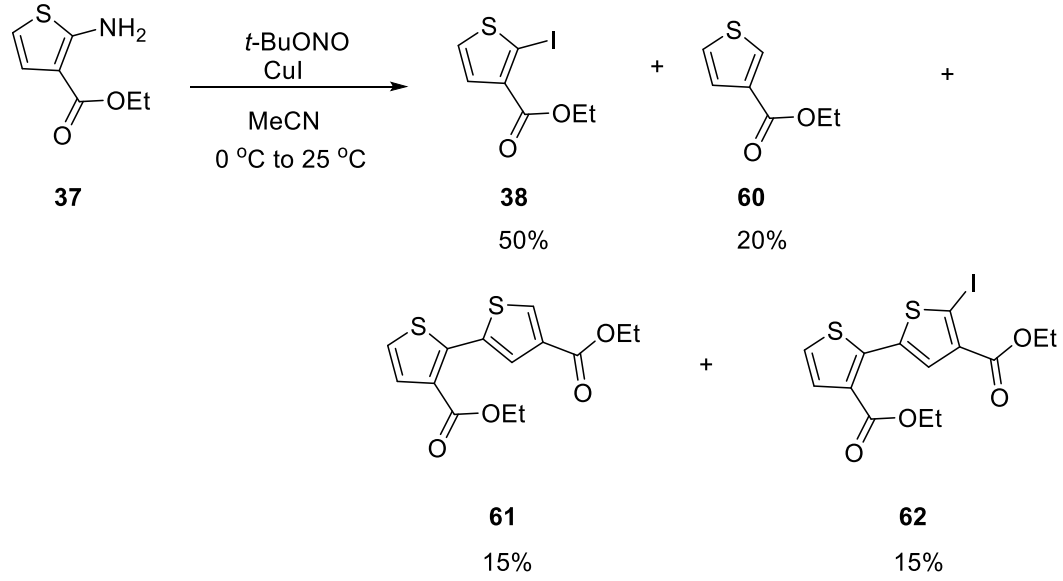

Scheme 15. Synthesis of iodothiophene **38** and side products **60-62**

The NMR spectral data were in agreement with the structure of **38** (Figure 9). Two thiophene protons resonates at 7.41 and 7.33 ppm with a coupling constants of $J = 5.6$ Hz which is in the expected range.

Since the chemical shift difference between adjacent protons is not much larger than the coupling constant, it gives an AB-system by which roof effect is obviously detected with the ratio $\Delta\delta/J = 5.72$.

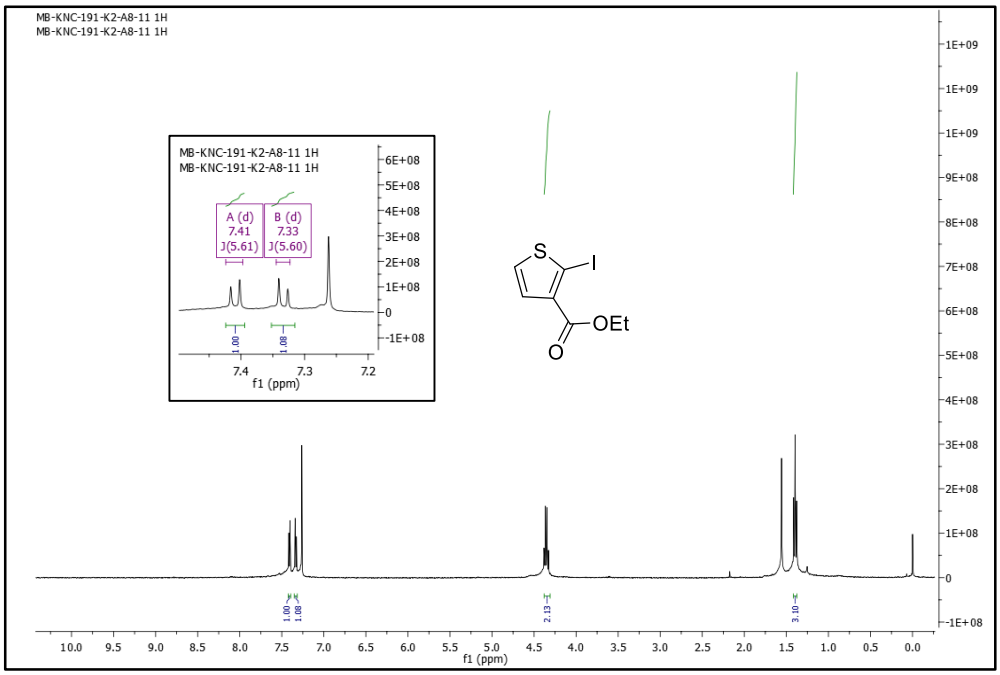

Figure 9. ^{1}H-NMR spectrum of compound **38**

The characterization of **61** and **62** was done by GC-MS and NMR analyses. It is known that the coupling constant ^{3}J between two adjacent protons of thiophene and that the ^{4}J coupling are in specific range, 5-6 Hz and 0-3 Hz, respectively. Careful inspection of the ^{1}H-NMR spectrum of **62**, shows the presence of two adjacent protons resonating at 7.49 and 7.24 ppm with a coupling constant of $J = 5.4$ Hz (Figure 10.). On the other hand, an additional thiophene proton attached to the other thiophene ring gives rise to a singlet at 7.58 ppm that means there is only one proton attached to thiophene ring. Compound **61** gives four different signals shown with black arrow (Figure 10) and two of which resonate at 7.50 and 7.23 ppm with a coupling constant of $J = 5.6$ Hz and the other thiophene protons appear as two distinct signals at 8.15 and 7.75 ppm with a coupling constant of $J = 1.4$ Hz clearly indicating 1,3 position of the protons.

When we evaluate the polarities of the products, one can easily notice that these compounds **61** and **62** have similar polarities which prevented the separation and isolation of individual products.

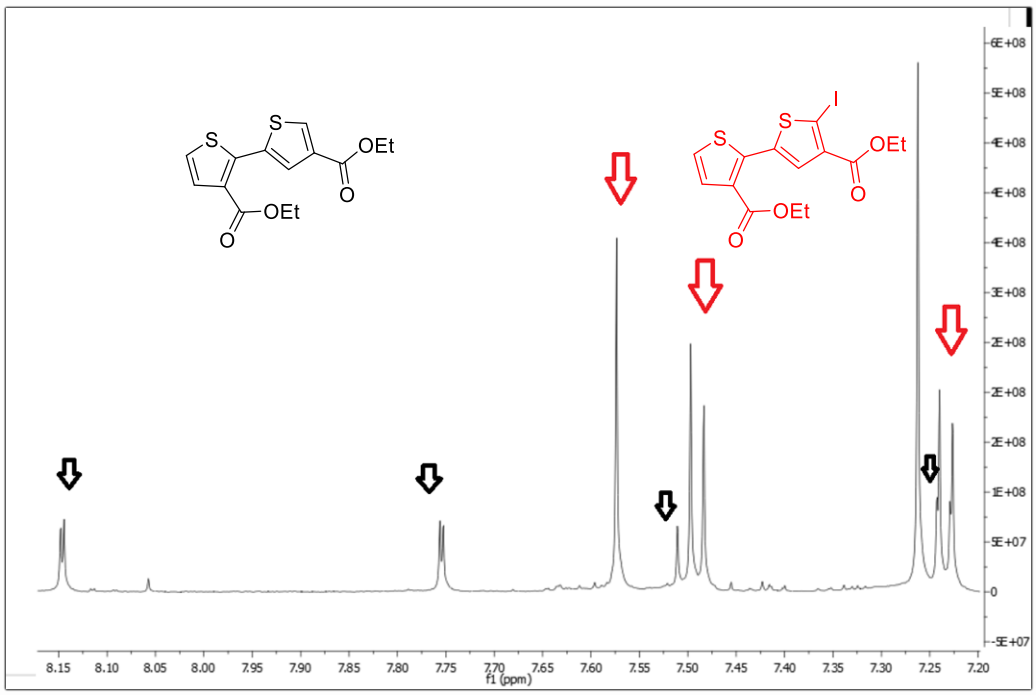

Figure 10. ^{1}H-NMR spectrum of a mixture **61** and **62**

1.2.3 Synthesis of ethyl 2,5-dibromothiophene-3-carboxylate (63)

During iodination of **37** several side products were formed. Therefore, we aimed to synthesize the corresponding bromo compounds according to literature procedure[44] with the expectation that the ratio of the side products would be reduced. For this reason **37** was treated with $CuBr_2$ in presence of *t*-butyl nitrite, surprisingly, 2,5-dibromo adduct **63** was formed as the sole product (Scheme 16). Unfortunately, mono-brominated compound was not formed even in traces.

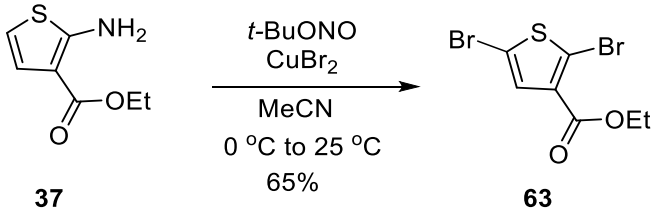

Scheme 16. Synthesis of dibromothiophene **63**

The fact that the only dibromo compound **63** was produced, can be explained on the basis of two steps reaction. We assume that the initially formed monobromide,

structure **64** formed after the Sandmayer reaction, undergoes subsequent bromination. It is likely that the compound **64** is much more reactive than the starting material so that the reaction cannot be controlled at the stage of monobromide **64**. At this stage, $CuBr_2$ has gained a great deal of importance while discussing reaction mechanism. Copper is an important catalyst involved in organometallic reactions with its complexes with oxidation states ranging from 0 to +4 although the +2 (cupric) and the +1 (cuprous) oxidation states are by far the most common. Hence, its reaction mechanism may change depending upon the condition and reactant structure. In recent years, researchers proposed Cu-mediated/catalyzed carbon–hydrogen activation reaction mechanisms for the formation of carbon–heteroatom bonds. In one of these mechanisms (Scheme 17), species of Cu(III) are suggested as key intermediates that can promote the transformation of carbon–hydrogen bonds. Cu(I) and Cu(II) are the most common oxidation states, while Cu(III) is scarce in inorganic and coordination chemistry. On the basis of the related literature we proposed a 2Cu(II) → Cu(III) + Cu(I) mechanism for the bromination reaction as shown in Scheme 17. The coordination of Cu(II) with the carbonyl group in **64** forms the Cu(II) intermediate **65**. Intermediate **65** is converted to the high valence Cu(III) intermediate **66** under the oxidation conditions of $CuBr_2$, and the $CuBr_2$ is converted into CuBr.[45,46,47,48]

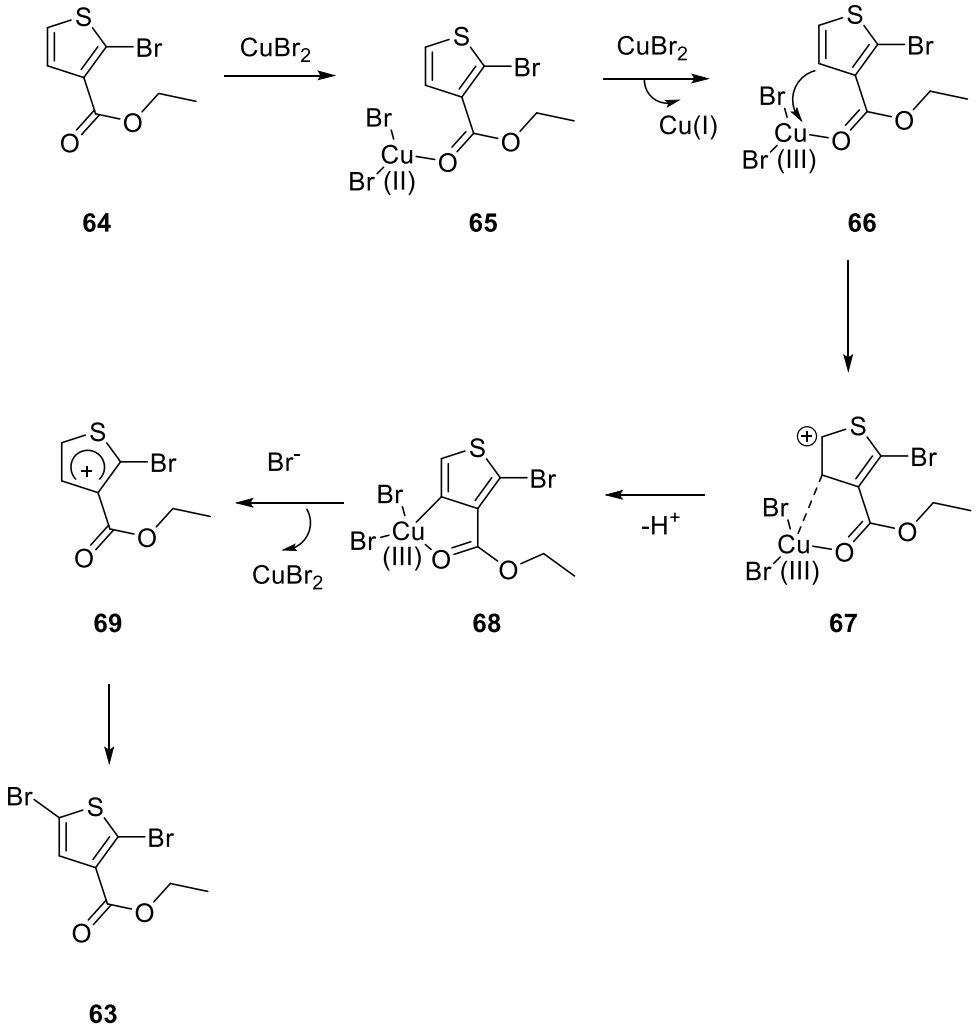

Scheme 17. Proposed mechanism for the Cu-mediated carbon–hydrogen bromination of thiophene derivative **63**.

Then, nucleophilic attack of the thiophene ring to the Cu(III) in the intermediate **67** generates Cu(III) intermediate **68** *via* intermediate **67** through a dearomatization and rearomatization processes.[49] Finally, the reductive elimination of intermediate **68** generates intermediate **69** and the nucleophilic attack of a bromine ion to the active intermediate **69** provides dibrominated product **63**.

1.2.4 Synthesis of ethyl 2-bromo-4,5,6,7-tetrahydrobenzo[*b*]thiophene-3-carboxylate (41)

As discussed in the previous section, there were numerous competitive side reactions during iodination of aminothiophene **37**. Therefore, our efforts were directed toward the use of substituted thiophenes such as **40** as the key compound to hinder possible coupling reactions between the thiophene rings. Modified Sandmayer reaction was applied to **40** in the presence of *t*-butyl nitrite with $CuBr_2$ in CH_3CN to obtain target compound **41**.[44] We obtained the desired compound **41** in a yield of 70%. However, the reduced product **70** was also formed in a yield of 15% (Scheme 18).

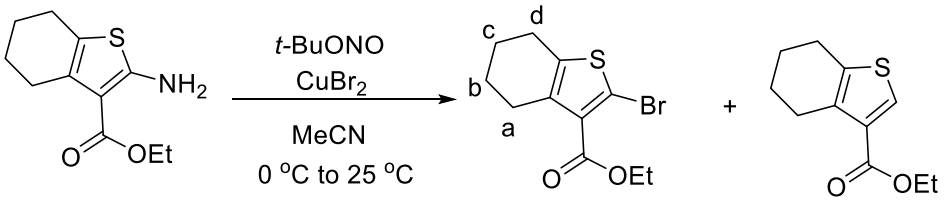

40 **41** **70**

	yield	
	41	**70**
a) (in non-dry solvent)	70%	15%
b) (in dry solvent)	90%	-

Scheme 18. Bromination of aminothiophene **40** with $CuBr_2$

When the reaction was carried out under the dry condition, product distribution was changed, the yield of the major product **41** was significantly increased and no trace of the side product **70** was detected.

Formation of compounds **41** and **70** was proven by ^{1}H-NMR. The ^{1}H-NMR spectrum of **41** shows two distinct signals at 2.75 and 2.63 ppm as quasi triplets arising from the protons **d** and **a**. Multiplet at 1.78 ppm belongs to the **b** and **c** protons. For the compound **70**, the thiophene proton resonates at 7.9 ppm as a singlet as expected from the structure. The other peaks present on cyclohexane ring resonate at 2.75 and 2.89 ppm as quasi triplets and multiplet at 1.81 ppm arising from other methylene protons on the cyclohexene ring.

1.2.5 Sonogashira cross-coupling reaction

The Sonogashira cross-coupling reaction is used for the coupling of aryl halides and terminal acetylenes for the formation of C(sp^2)−C(sp) bond.[50,51] Traditional palladium ligands in combination with CuI have been preferred although there are numerous metal catalysts claimed to be effective.[52] The most commonly used catalytic systems for this transformation include $PdCl_2(PPh_3)_2$, $PdCl_2/PPh_3$, and $Pd(PPh_3)_4$ together with CuI as the cocatalyst and amines are used as the solvents or cosolvents. This method is one of the most convenient methods for the straightforward construction of sp^2 –sp carbon–carbon bonds in synthetic chemistry.[53,54] Sonogashira reactions are carried out under inert atmosphere using dry solvents. General reaction representation of Sonogashira cross-coupling reaction is shown in Scheme 19.

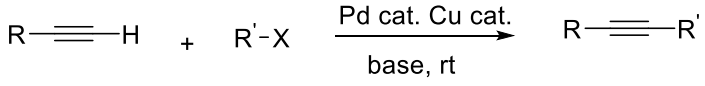

R' = aryl or vinyl
X= I, Br, Cl or OTf

Scheme 19. Sonogashira cross-coupling reaction

The Sonogashira cross-coupling reaction was first reported by Sonogashira *et al.* in 1975. Cassar, Dieck and Heck used relatively harsh reaction conditions, such as high temperature and obtained the same reaction products. While these researchers used only palladium catalyst for coupling, Sonogashira used both, palladium and copper as catalysts simultaneously. These results inspired the development of reaction conditions of Sonogashira cross-coupling reaction such as the ability to carry out the reactions at room temperature and to increase in the reactant reactivity. This development made the Sonogashira cross-coupling reaction very useful for alkynylation of aryl and alkenyl halides. [55,56] Although the reaction has attracted high attention of organic chemists who reported various coupling products with their proposed mechanism. Recent proposed mechanism represents the catalytic cycle of Sonogashira cross-coupling reaction as shown in Scheme 20.[56]

In this catalytic cycle, the first step is activation of palladium which involves conversion of palladium (II) into active palladium (0) through reduction. The active

palladium catalyst is the 14 electron compound $Pd(0)L_2$, complex **A**, which reacts with the organohalide compound in an oxidative addition to form a Pd(II) intermediate, complex **B**. This step is the rate-determining step of the reaction. In the copper catalytic cycle, copper coordinates to triple bond and plays a significant role in increasing the acidity of acetylene proton.

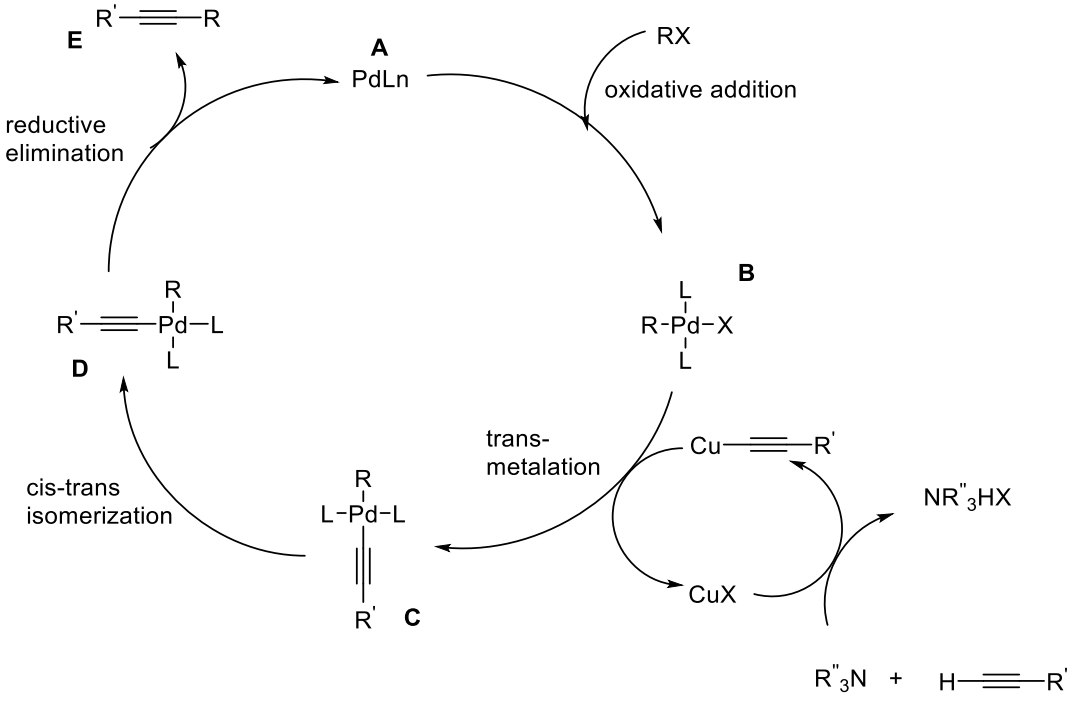

Scheme 20. Catalytic cycle of Sonogashira cross-coupling reaction

Amine base abstracts this proton and form its salt. Transmetallation involves the transfer of organic part of copper complex to palladium that provides complex **C**. Subsequent *cis-trans* isomerization gives complex **D** followed by reductive elimination which affords the coupling product **E** and palladium complex with palladium (0).

In the light of this information, we applied the Sonogashira cross-coupling reaction to our halothiophenes under the conditions which we developed. We used THF as a solvent and NEt_3/DIPA as a base. $PdCl_2$/CuI catalyst couple was used in presence of PPh_3 to afford our target alkyne substituted thiophenes.

1.2.5.1 Sonogashira cross-coupling reactions applied to iodothiophene 38

1.2.5.1.1 Synthesis of ethyl 2-(phenylethynyl)thiophene-3-carboxylate (42a)

The palladium-catalyzed Sonogashira coupling reaction of **38** with phenylacetylene using NEt_3 as a base was first examined. The reaction was carried out under nitrogen atmosphere at reflux temperature. At first, $PdCl_2$, PPh_3, and CuI in THF were added into reaction vessel and stirred under nitrogen atmosphere for 15 min. After subsequent addition of alkyne and NEt_3 the resulting mixture was stirred for 6 h at reflux temperature affording compound **42a** in 45% yield with the formation of homocoupling product **71** (Scheme 21).

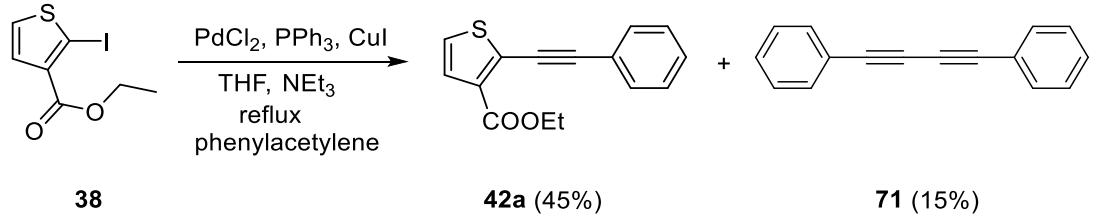

Scheme 21. Cross-coupling reaction to **38**

The formation of **42a** was confirmed by ^1H and ^{13}C-NMR spectra as shown in Figure 11 and Figure 12. As we described in the previous section, one could easily show the existence of thiophene skeleton by evaluating the coupling constant between the thiophene protons. There are two protons in aromatic region giving two distinct signals at 7.47 and 7.20 ppm with a coupling constant of J = 5.3 Hz. The resonance signals of the benzene ring appear as two separate multiplets at 7.57 and 7.36 ppm. Methyl and methylene protons of ester functionality resonate at 4.39 and 1.42 ppm, respectively.

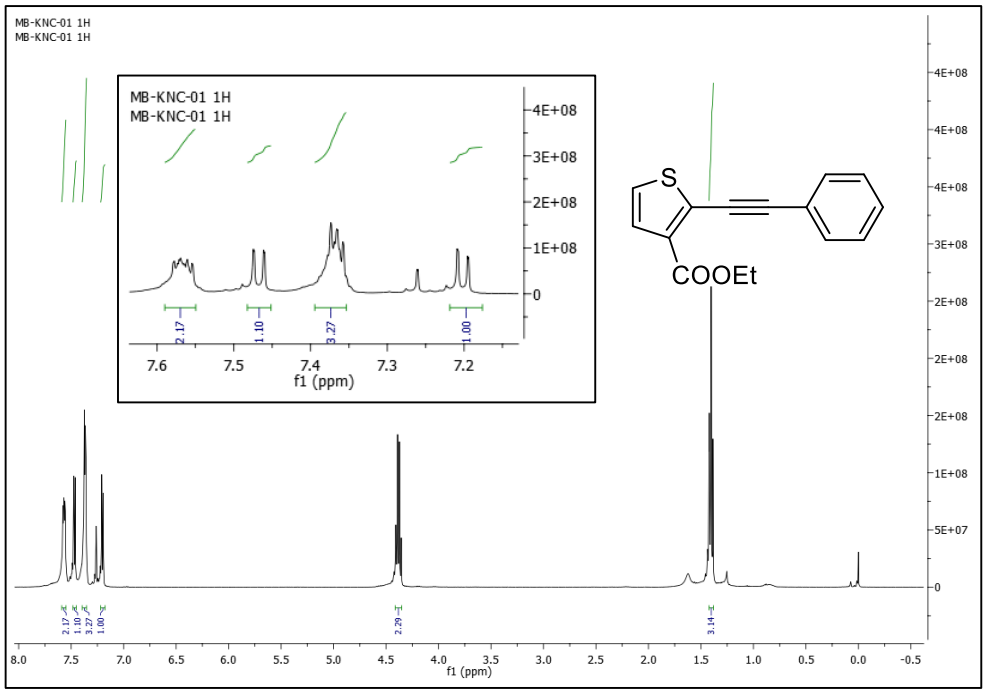

Figure 11. ^{1}H-NMR spectrum of compound **42a**

The ^{13}C-NMR spectrum also supported the formation of compound **42a**. If we analyze the ^{13}C-NMR spectrum, one can realiz the existence of two signals resonating at 98.9 and 81.8 ppm arising from the acetylene unit. In the sp^{2}-region, there are two intense peaks at 131.6 and 128.4 ppm arising from the *o*- and *m*-carbons of the phenyl group.

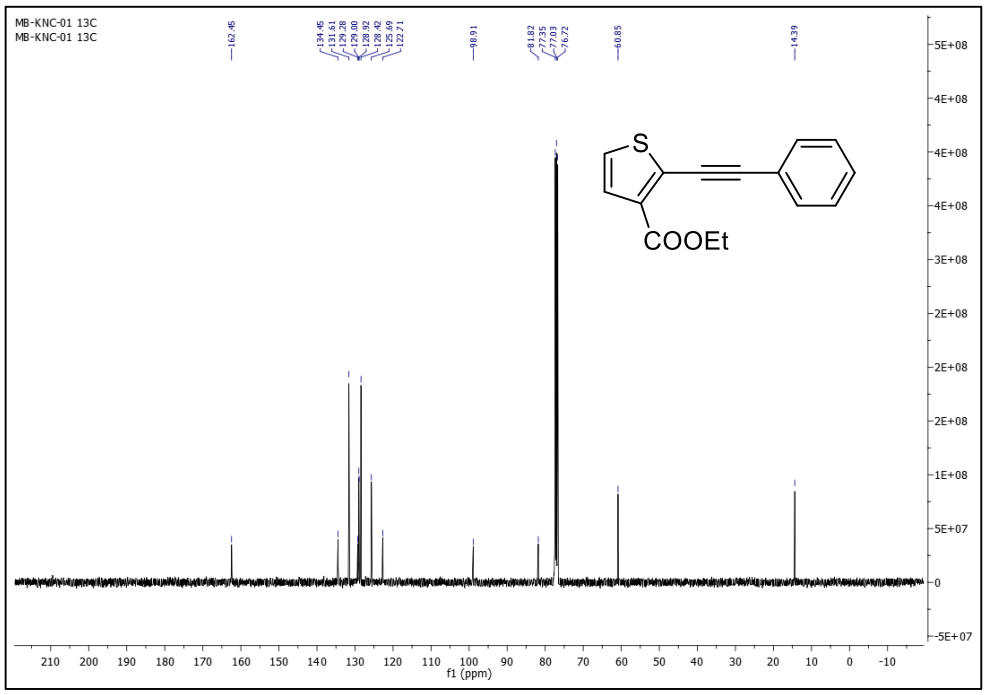

Figure 12. ^{13}C-NMR spectrum of compound **42a**

1.2.5.1.2 Synthesis of ethyl 2-(hept-1-yn-1-yl)thiophene-3-carboxylate (42b) and ethyl 2-(hex-1-yn-1-yl)thiophene-3-carboxylate (42c)

After successful synthesis of **42a**, we applied the coupling reaction to compound **38** with different alkynes such as hexyne and heptyne (Scheme 22).

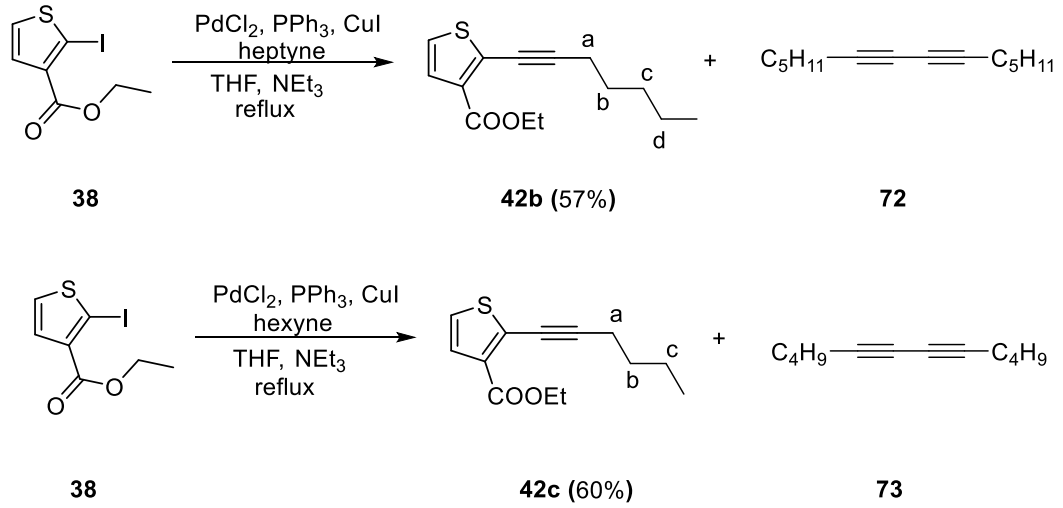

Scheme 22. Sythesis of heptyne- and hexyne-substituted thiophenes **42b** and **42c**

At first, we examined the reaction of compound **38** with heptyne. The reaction was monitored by TLC and we concluded that the reaction time was not affected significantly when compared to that of phenylacetylene coupling. However, in this case, only trace amount homocoupling product was formed as one can see from the crude NMR spectrum in Figure 13. The ^{1}H- and ^{13}C-NMR spectra are consistent with the proposed structure **42b**. In the ^{1}H-NMR spectrum of **42b**, there are two doublets in the aromatic region with a coupling constant of J = 5.4 Hz that belong to adjacent thiophene protons. The triplet signals at 2.5 ppm is arising from methylene protons **a** directly connected to acetylene unit.

Other aliphatic protons **b**, **c**, **d**, and methyls of alkyl chain and ethyl ester resonate in the range of 1.8-0.9 ppm.

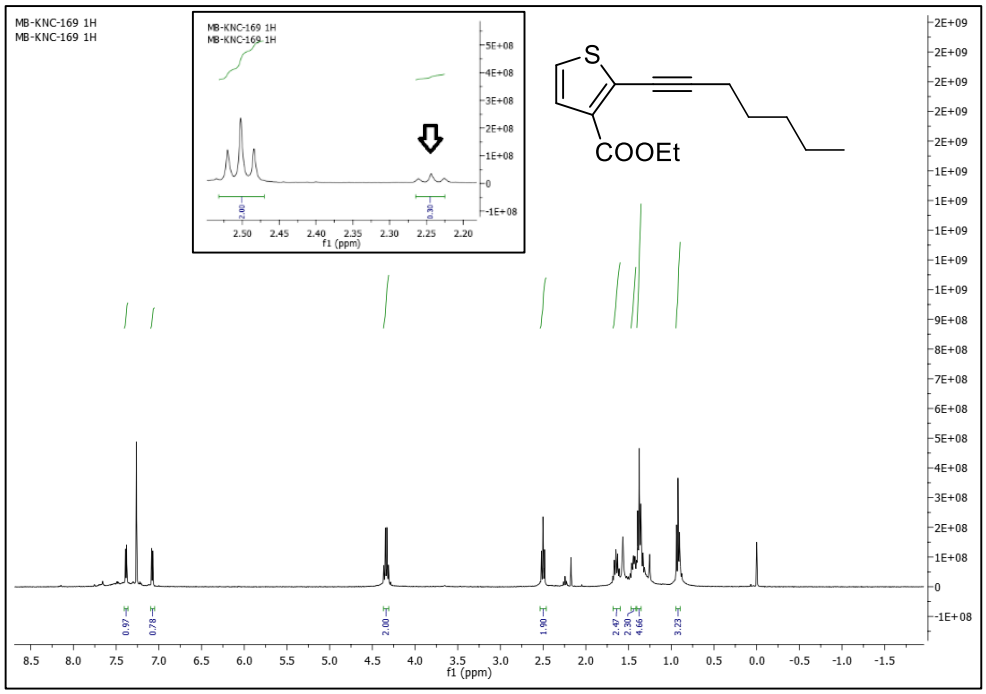

Figure 13. Crude ^{1}H-NMR spectrum of compound **42b**

We obtained similar results when hexyne was used as an alkyne source. The NMR spectrum of compound **42c** was straightforward. The fact that one methylene group was missing compared to the NMR spectrum of **42b** clearly indicated the formation of the desired coupling product.

1.2.5.2 Sonogashira cross-coupling reaction applied to bromothiophene 41

1.2.5.2.1 Synthesis of ethyl 2-(phenylethynyl)-4,5,6,7-tetrahydrobenzo [*b*]thiophene-3-carboxylate (45a)

As demonstrated in Scheme 23, coupling of **41** with phenylacetylene was also performed smoothly which gave the corresponding product **45a** in 60% yield. We used same coupling reagents which were used for the coupling reactions of **38** (Scheme 23). Additionaly diisopropylamine was used as a base as to increase the yield of the reaction.

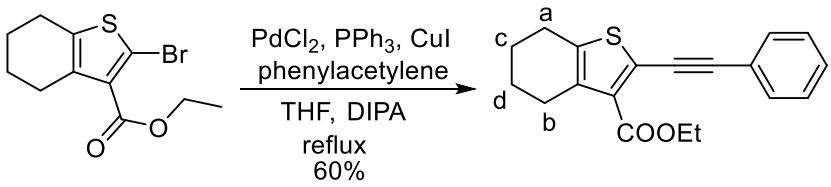

41 **45a**

Scheme 23. Phenylacetylene coupling to compound **41**

The ^{1}H- and ^{13}C-NMR spectra are compatible with the proposed structure **45a**. Phenyl protons resonate as two separate multiplets at 7.52 and 7.34 ppm. In aliphatic region, there are two quasi triplets at 2.83 and 2.73 arising from the **a** and **b** protons attached to thiophene skeleton. The reason for low field resonance of **a** protons is that it is close to the sulfur atom which inductively pulls its electrons (-I) through sigma bond.

The methylene proton resonances **c** and **d** are overlapped and appear as a multiplets at 1.8 ppm. The ^{13}C-NMR spectrum is also fully consistent with the proposed structure. The resonances at 97.6 and 82.9 ppm clearly demonstrate the incorporation of the alkyne unit into the molecule.

1.2.5.2.2 Synthesis of ethyl 2-(hept-1-yn-1-yl)-4,5,6,7-tetrahydrobenzo [*b*]thiophene-3-carboxylate (45b) and ethyl 2-(hex-1-yn-1-yl)-4,5,6,7-tetrahydrobenzo[*b*]thiophene-3-carboxylate (45c)

Treatment of compound **41** with Sonogashira coupling reagents in the presence of hexyne and heptyne at the reflux temperature provided thiophene substituted alkyne derivatives **45b** and **45c** (Scheme 24).

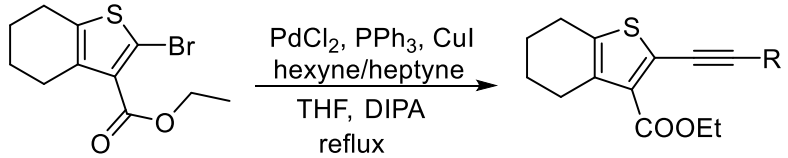

41

45b=R:C_5H_{11}(72%)
45c=R:C_4H_9 (45%)

Scheme 24. Synthesis of heptynyl and hexynyl substituted thiophenes **45b** and **45c**

The formation of compounds **45b** and **45c** was determined by ^{1}H- and ^{13}C-NMR spectra. Comparison of the ^{1}H-NMR spectrum of **45b** with those of **45a** shows the similarity of the resonances arising from the cyclohexene ring showing the presence of two quasi triplets and two multiplets overlapped at 1.8 ppm as in the ^{1}H-NMR spectrum of **45a**. The heptynyl resonances of **45b** has also similar chemical shifts and coupling constants as described in the ^{1}H-NMR spectrum of **42b**. Eleven carbon resonances observed in the sp^{3}-region also support the proposed structure. Again the presence of two distinct resonances at 99.8 and 73.7 ppm in ^{13}C-NMR shows the presence of alkyne unit in the structure. The other five carbon peaks in sp^{2}-region belong to thiophene quaternary carbons and carbonyl carbon.

We applied the coupling reaction to compound **41** in presence of hexyne. The formation of **45c** was also proven by ^{1}H- and ^{13}C-NMR spectra. The ^{1}H-NMR spectrum is similar to that of compound **45b**.

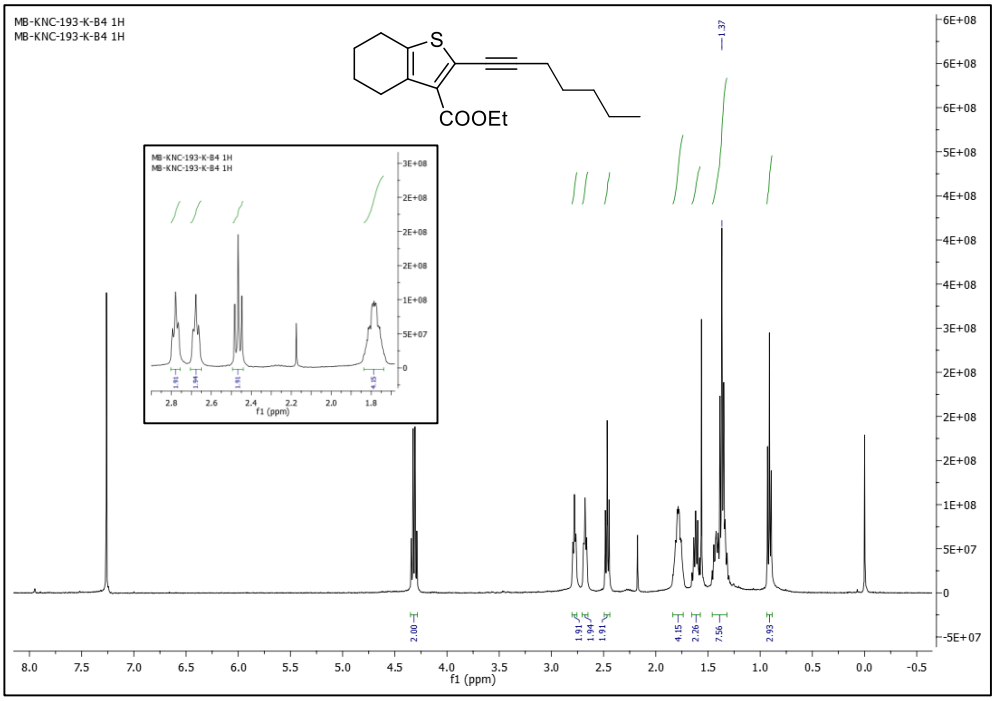

Figure 14. ^{1}H-NMR spectrum of compound **45b**

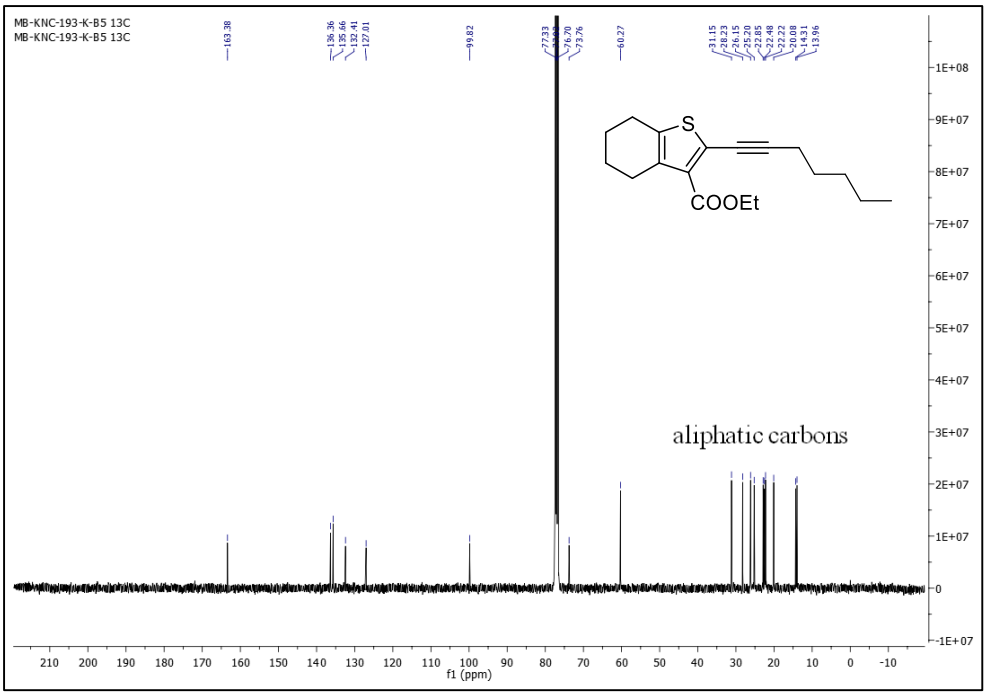

Figure 15. ^{13}C-NMR spectrum of compound **45b**

1.2.5.3 Synthesis of ethyl 2,5-bis(phenylethynyl)thiophene-3-carboxylate (74)

The versatility of Sonogashira coupling reaction was further demonstrated by the synthesis of coupling product **74** from dibromothiophene **63** in the presence of phenylacetylene (Scheme 25).

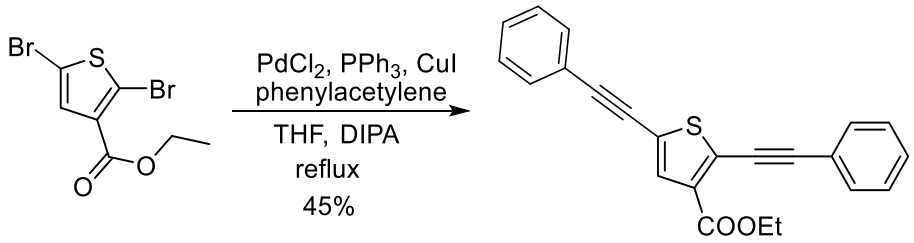

63 **74**

Scheme 25. Synthesis of ethyl 2,5-bis(phenylethynyl)thiophene-3-carboxylate (**74**)

Its formation was verified by ^{1}H- and ^{13}C-NMR spectra. In the ^{1}H-NMR spectrum, there are ten aromatic protons resonating as three distinct multiplets at 7.58, 7.52 and 7.38 ppm and the integral values of which are consistent with the number of phenyl protons. The other singlet resonating at 7.60 ppm belongs to the thiophene proton. The

^{13}C-NMR spectrum clearly shows us the incorporation of two alkynes into the system including four acetylene carbons. The resonances of those carbons are observed at 99.6, 94.5, 81.6, and 81.3 ppm.

1.2.6 Cyclization with hydrazine monohydrate

Hydrazine is a kind of a base and it can be used as nucleophile in organic reactions. Its basic character and nucleophilicity makes it very useful compound for organic synthesis. It has two lone pairs which provides attack to any electron deficient center. It is a kind of a base because when it is dissolved in water, its acidic form is readily formed. Moreover, it has two adjacent nitrogen atoms by which its addition reaction followed by cyclization reaction can afford biologically important heterocyclic compounds. In the light of this information, we used hydrazine monohydrate for cyclization to afford thienopyridinone and thienodiazepinone derivatives.

1.2.6.1 Cyclization of phenylethynylthiophene 42a with hydrazine mono hydrate

We treated **42a** with excess hydrazine monohydrate in methanol and the resulting reaction mixture was heated at reflux temperature and stirred well. The reaction was controlled by TLC.

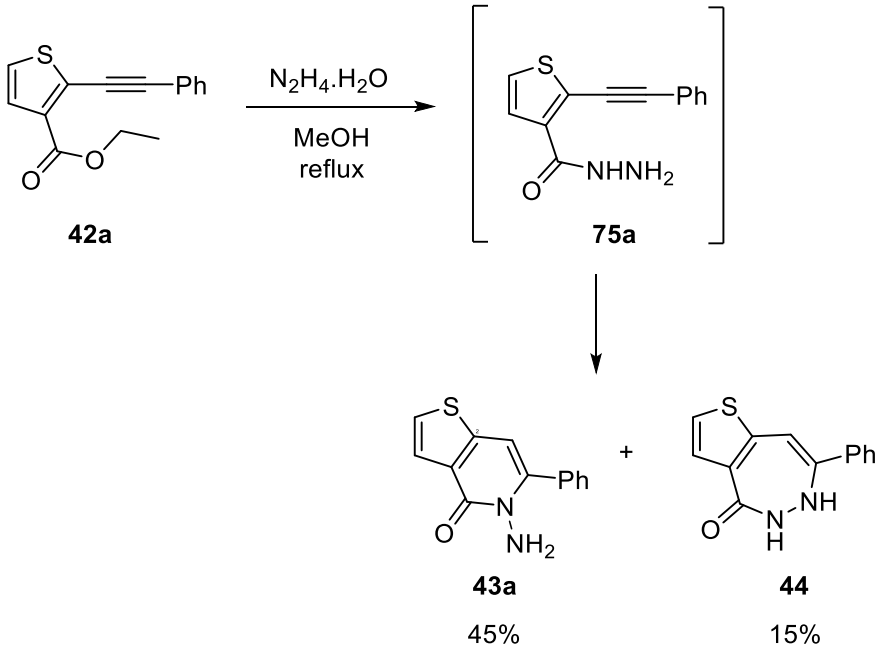

Scheme 26. Hydrazinolysis reaction of **42a**

We observed that hydrazinolysis of compound **42a** led to the cyclization products thienopyridinone **43a** and thienodiazepinone **44** with the formation of corresponding hydrazide **75a** as an intermediate as shown in Scheme 26.

The ^{1}H- and ^{13}C-NMR spectra are consistent with the proposed structure **43a**. The NH_2 protons resonate as a broad singlet at 5.03 ppm and the olefinic proton resonates at 6.64 ppm as singlet as shown in Figure 16. These two characteristic peaks and disappearance of ester group clearly show us the formation of compound **43a**.

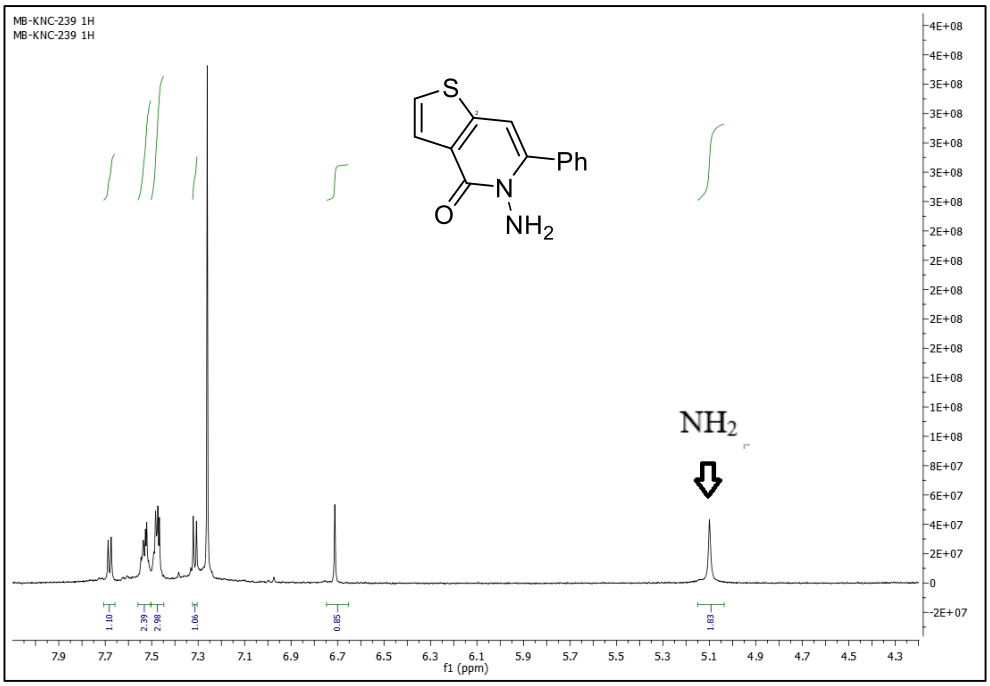

Figure 16. ^{1}H-NMR spectrum of compound **43a**

1.2.6.2 Cyclization of ethyl 2-(hept-1-yn-1-yl)thiophene-3-carboxylate (42b) and ethyl 2-(hex-1-yn-1-yl)thiophene-3-carboxylate (42c) with hydrazine monohydrate

To validate this methodology, we applied the cyclization reaction to compound **42b** and **42c**. The reaction proceeded under the same condition with that of compound **42a**. The reaction was monitored by TLC.

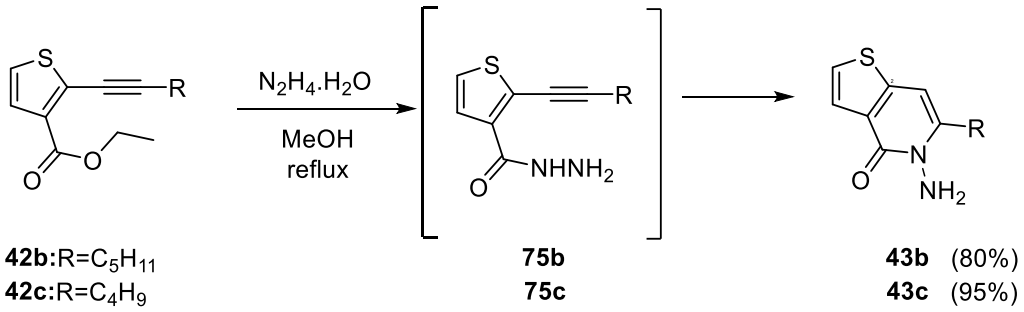

Scheme 27. Synthesis of thienopyridinone **43b** and **43c**

We treated compound **42b** and **42c** with hydrazine monohydrate to form hydrazides as intermediates. Subsequent intramolecular cyclization reaction involving nitrogen

attack to triple bond carbon afforded only compound **43b** and **43c** in high yields (Scheme 27). In this particular reaction, there was no diazepinone formation.

The formation of **43b** and **43c** was established by ^{1}H- and ^{13}C-NMR spectra. In the ^{1}H-NMR spectrum of the compound **43c** (Figure 17), there are two thiophene protons resonating at 7.59 and 7.20 ppm with a coupling constant of J = 5.4 Hz. The olefinic proton and NH_2 protons resonate as singlets at 6.56 and 4.96 ppm, respectively. The methylene protons attached directly to the double bond resonates as a broad triplet at 2.85 ppm.

The carbon chemical shifts of **43c** is shown in Figure 18. The ^{13}C-NMR spectrum clearly demonstrates the formation of cyclization products. Furthermore, disappearance of alkyne carbon signals and appearance of a singlet at 100.1 ppm supports the formation of a cyclization product. The remaining carbon atoms from the hydrocarbon tail resonate below 30.5 ppm which is an agreement with the proposed structure.

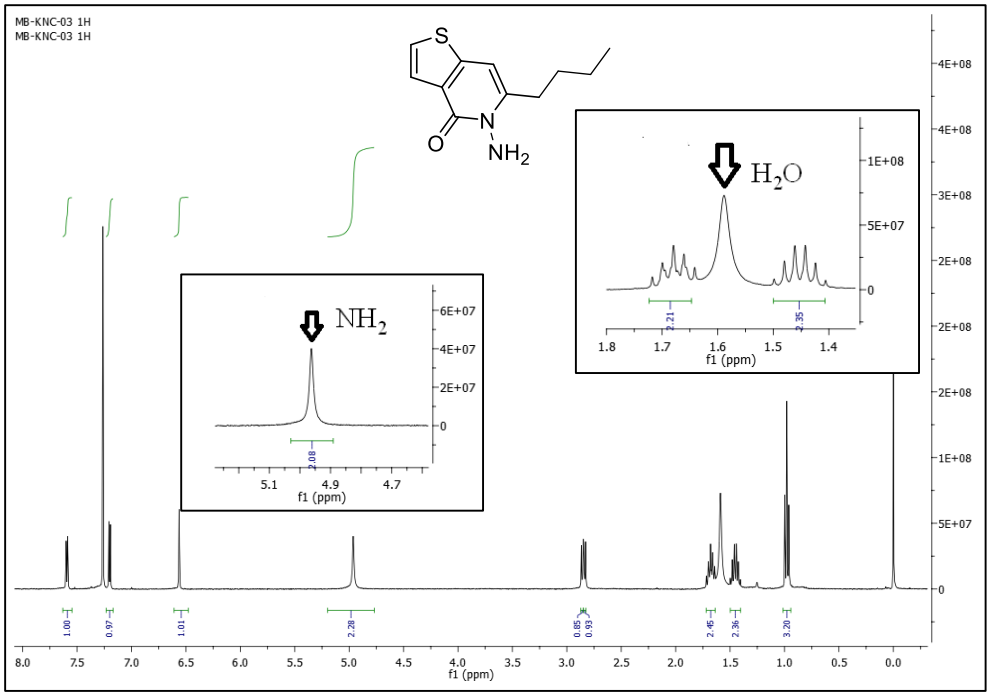

Figure 17. ^{1}H-NMR spectrum of compound **43c**

As we discussed in the previous section that the NMR spectra of the coupling products with hexyne and heptyne are not significantly affected by the presence of an additional

methylene group. The ^{1}H-NMR spectrum of **43c** differs from that of **43b** just by the presence of an additional methylene group.

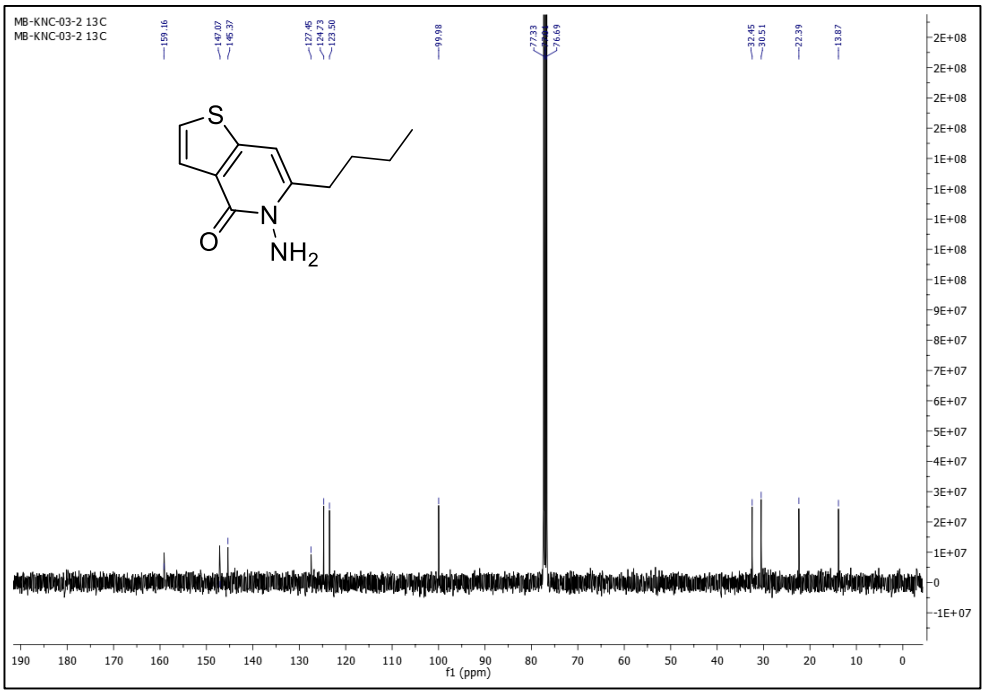

Figure 18. ^{13}C-NMR spectrum of compound **43c**

1.2.6.3 Cyclization of ethyl 2-(phenylethynyl)-4,5,6,7-tetrahydrobenzo [*b*]thiophene-3-carboxylate (45a) with hydrazine monohydrate

Access to these valuable scaffolds (thienopyridinone and thienodiazepinone) encouraged us to apply cyclization reaction to different alkyne substituted thiophenes. Treatment of compound **45a** with hydrazine monohydrate in methanol under reflux condition afforded thienopyridinone **46a** and thienodiazepinone **47** *via* 6-*endo-dig* and 7-*endo-dig* cyclization reactions (Scheme 28).

The ^{1}H- and ^{13}C-NMR spectra are consistent with the structures **46a** and **47**. Moreover, we determined the exact structures of those compounds by using 2D-NMR spectra.

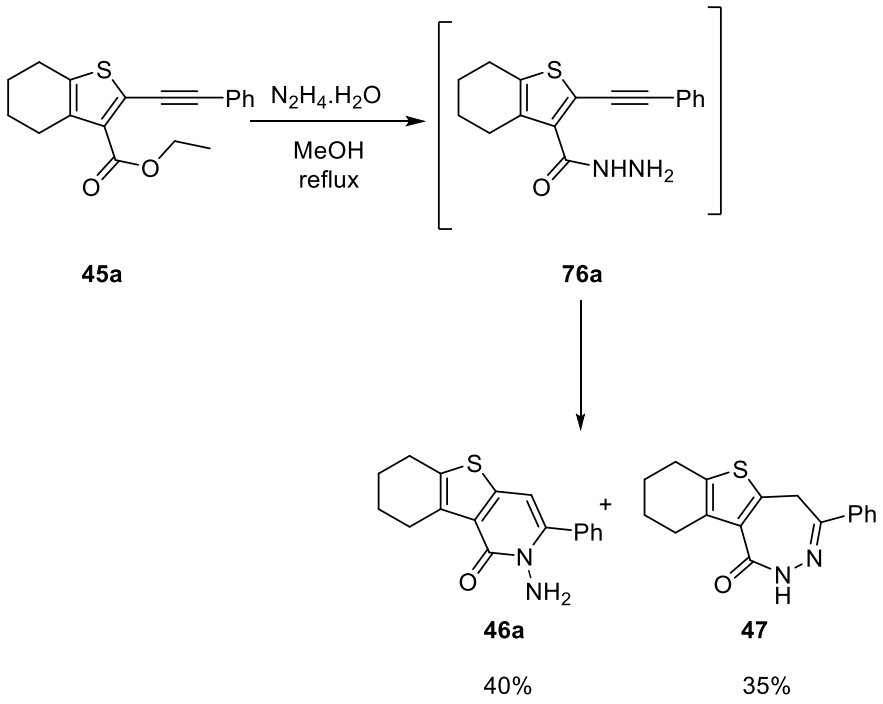

Scheme 28. Synthesis of thienopyridinone **46a** and thienodiazepinone **47**

In the ^{1}H-NMR spectrum of the seven-membered ring **47**, there are two significant resonances appearing at 4.10 and 8.6 ppm which were assigned to methylene protons and NH proton, respectively. These signals are the finger print of the formation of compound **47**. Eight protons in the aliphatic region and five protons in the aromatic region are arising from cyclohexene ring and phenyl group, respectively.

However, from the 1D NMR spectra we could not distinguish between the structures **47** and **77** (Figure 19). The 1D NMR spectra can also be in agreement with the structure **77** (Figure 20). In order to make a clear-cut differentiation between these two structures, we recorded 2D NMR spectra of the compound.

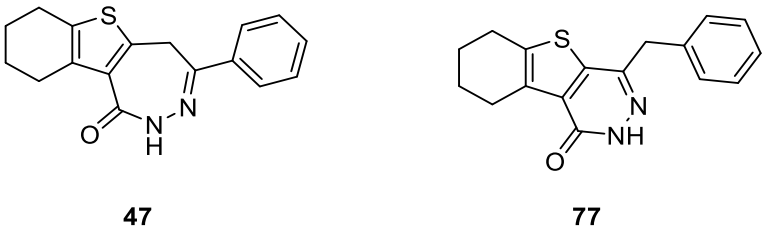

Figure 19. Plausible seven- and six-membered ring products **47** and **77**

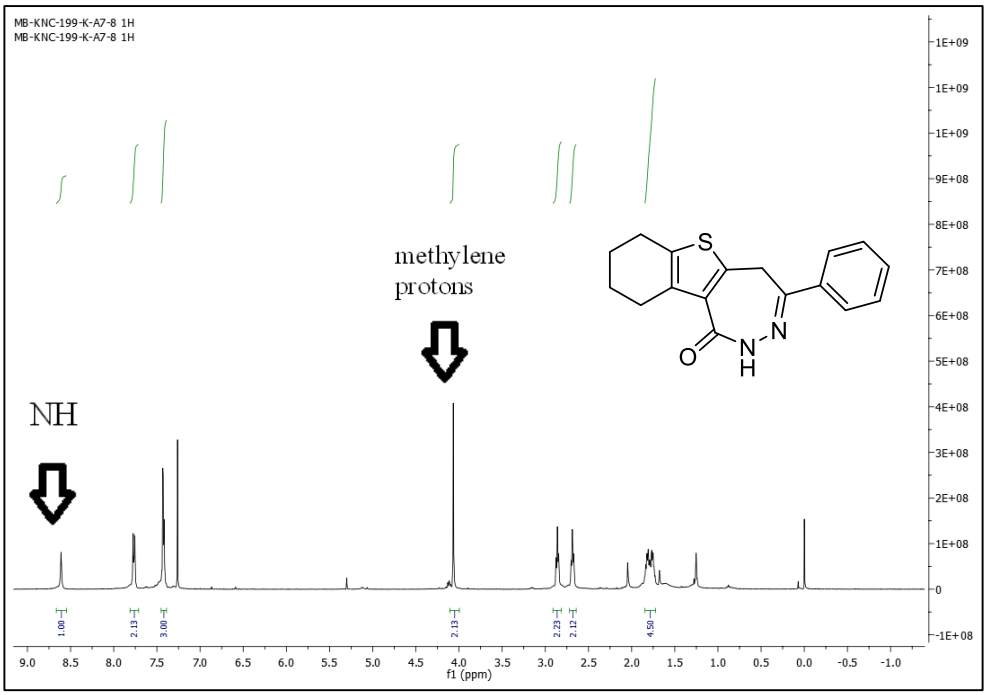

Figure 20. ^{1}H-NMR spectrum of compound **47**

We utilized HSQC and HMBC spectra for exact structure determination. First, we used the HSQC spectrum (Figure 21) to determine the methylene carbon atom. If we draw a perpendicular line from the methylene protons at 4.07 ppm to other axis, the line intersects cross peak indicating that these protons bear the carbon resonating at 30.2 ppm.

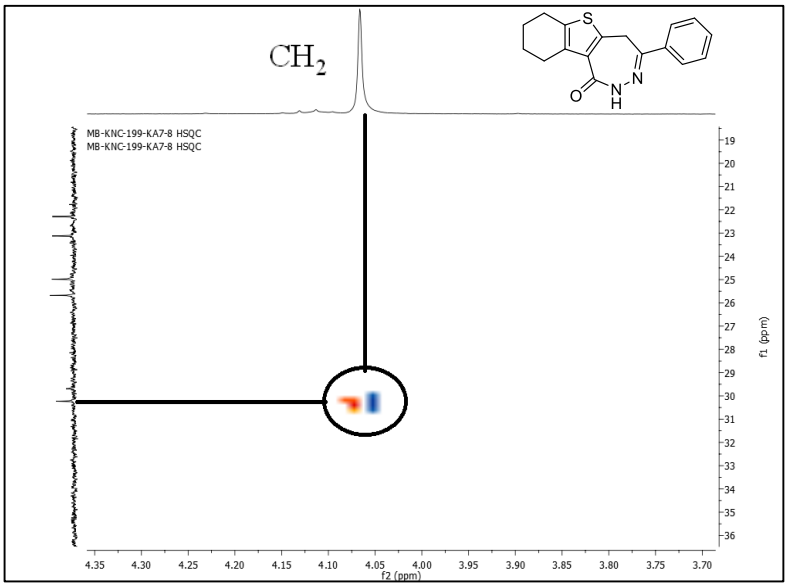

Figure 21. HSQC spectrum of compound **47**

Long-range heteronuclear correlation is observed in HMBC spectra which provides us very useful information about the structure. Since, it gives a correlation between proton and carbon peaks separated by multiple bonds (usually two or three), this spectrum suggests indirect way of information for the carbon and hydrogen connectivities. In the case of structure **77** we should observe a strong correlation between the methylene carbon atom and the aromatic protons. However, careful inspection of the HMBC spectrum doesn't show any correlation between the relevant atoms. Therefore, we can exclude the structure **77** because of the absence of a correlation between CH carbons of phenyl group and the CH_2 protons (Figure 22 and Figure 23).

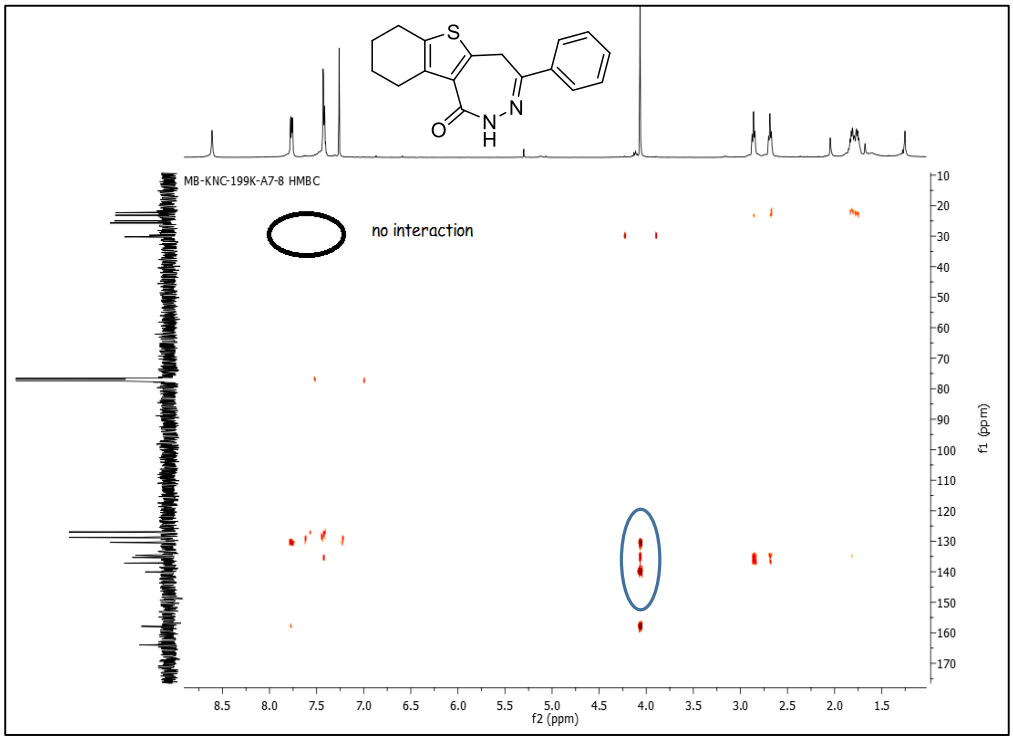

Figure 22. HMBC spectrum of compound **47**

On the other hand, the strong correlation between the methylene protons and thiophene carbon atoms strongly supports the presence of a seven-membered ring.

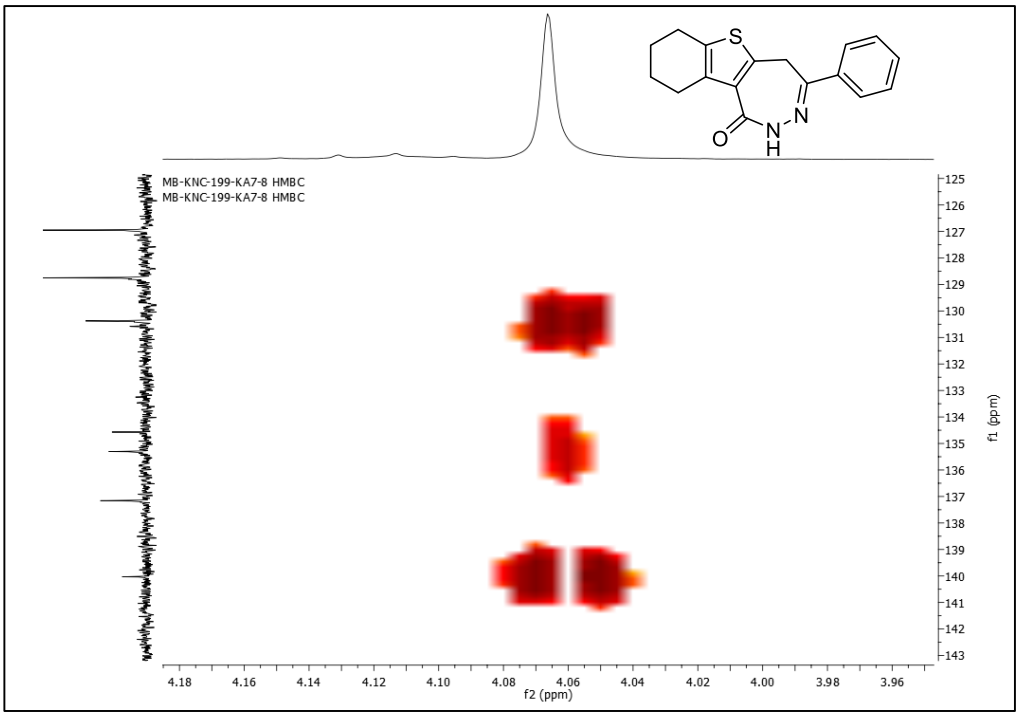

Figure 23. Expanded HMBC spectrum of compound **47**

1.2.6.4 Cyclization of ethyl 2-(hept-1-yn-1-yl)-4,5,6,7-tetrahydrobenzo [*b*]thiophene-3-carboxylate (45b) and ethyl 2-(hex-1-yn-1-yl)-4,5,6,7-tetrahydrobenzo[*b*]thiophene-3-carboxylate (45c) with hydrazine monohydrate

Reaction of **45b** and **45c** with hydrazine monohydrate in methanol under reflux condition, contrary to the result obtained with **45a**, resulted in the formation of cyclization products with six-membered ring (Scheme 29). The reaction was proceeded with excellent regioselectivity between 5-*exo*-dig and 6-*endo*-dig ring closure. The 6-*endo*-dig cyclization products **46b** and **46c** were exclusively formed.

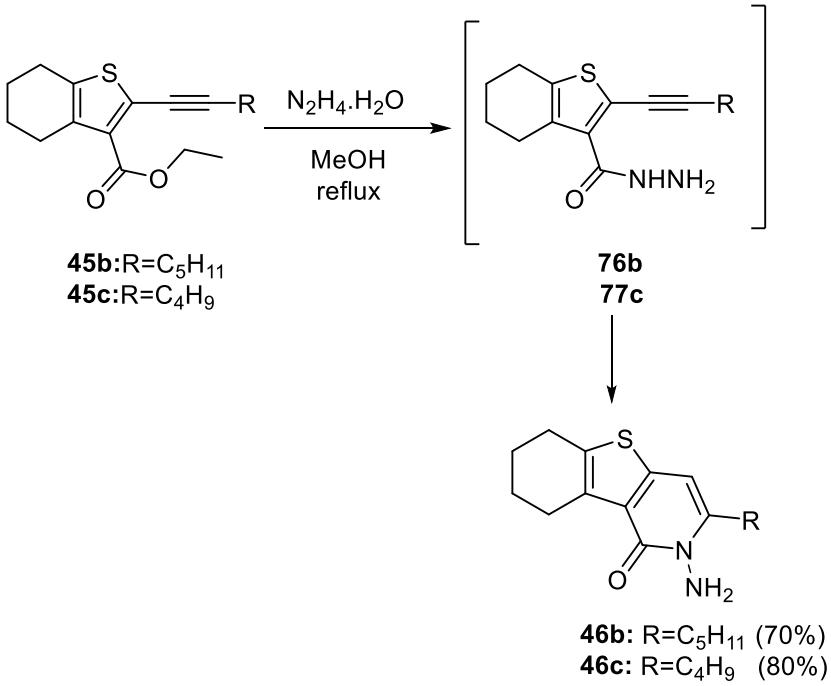

Scheme 29. 6-*endo*-dig cyclization product **46b** and **46c** formation

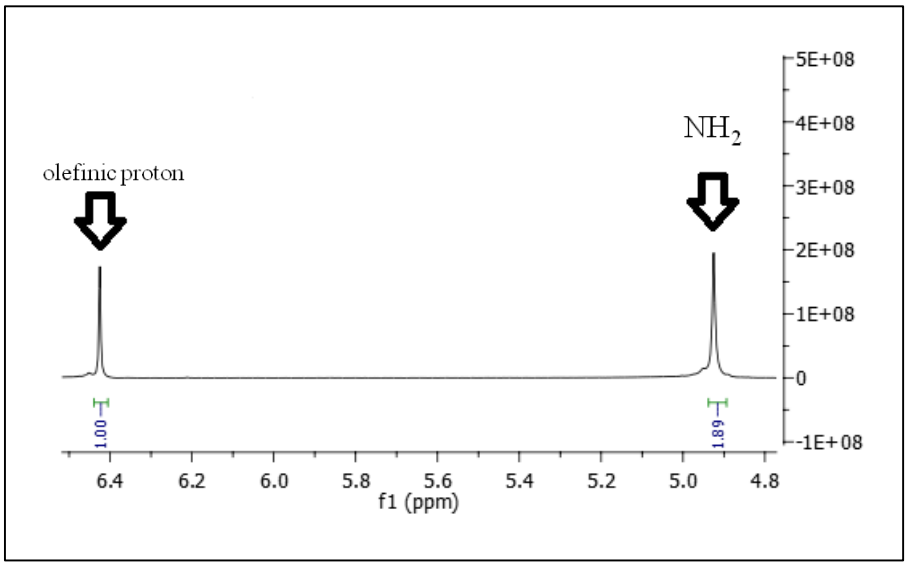

Figure 24. Expanded ^{1}H-NMR spectrum of compound **46c**

It was seen in the expanded ^{1}H-NMR spectrum of **46c** (Figure 24) that there were no methylene proton resonances which was a strong evidence for the formation of six-membered ring product, thienopyridinones **46b** and **46c**.

CHAPTER 2

DEVELOPMENT OF A SYNTHETIC METHODOLOGY FOR THE SYNTHESIS OF BENZIMIDAZO-OXAZEPINES

2.1 INTRODUCTION

Heterocyclic compounds are the cyclic organic compounds which contain at least one heteroatom in their structures. They play significant roles in the metabolism of all living cells; a great number of them are five- and six-membered rings. Those structures have received considerable attention due to the fact that they have an important role as pharmaceuticals in medical chemistry and also they are frequently found in a wide variety of biomolecules such as enzyme, vitamins, and natural products. Moreover, they can be used as antifungal, antiinflammatory, antibacterial, antioxidant, anticonvulsant, antiallergic, anti-HIV, antidiabetic, anticancer, insecticidal agents, and enzyme inhibitors.[57] In addition, biological molecules such as DNA, RNA, hemoglobin, vitamins and many more contain a heterocyclic ring in their major skeletons. There is a great number of pharmacologically active heterocyclic compounds, many of which can be used in clinical applications.[58]

Wahbi *et al*.[59] synthesized heterocyclic compounds having pyrrole, furan, and thiophene skeletons. They used some theoretical calculations in order to show their activities as antifungal agents. The structures of these compounds showing most promising results are given in Figure 25.

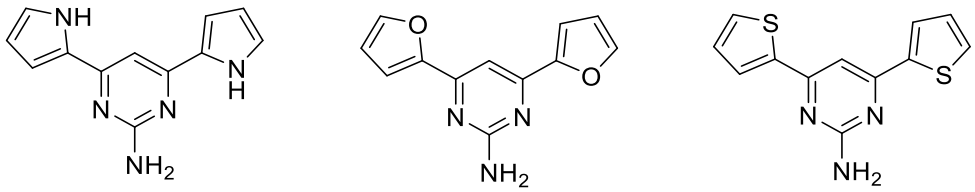

78 79 80

Figure 25. Antifungal agents

2.1.1 Imidazole

Imidazole is a five-membered heterocycle that contains two nitrogen atoms on the ring. Imidazole is generally regarded as being aromatic. The electrons on sp^3 hybridized nitrogen atom are delocalized through π-orbitals so the lone pairs are contributed to resonance stabilization. As a consequence, it is a cyclic, conjugated system with six π-electrons being an aromatic compound. Dewar *et al.*[60] calculated the resonance energy of imidazole as 15.4 kcal/mol. In order to compare this value with those of well-known aromatic compounds like benzene, pyridine, and pyrrole, they also calculated the resonance energies for those compounds and found the values of 20.0, 20.9, and 8.5 kcal/mol, respectively, which are close to that of imidazole. Similarly, the resonance energies of benzimidazole and naphthalene were also calculated as 30.9 kcal/mol and 30.5 kcal/mol, respectively.

Imidazole derivatives have attracted considerable attention due to their biological properties as therapeutics. In addition to this, they are involved in the inhibition of some enzymes. Young *et al.*[61] found how SB203580 (**81**) (Figure 26) binds to the ATP binding site and subsequently inhibits p38 kinase catalytic activity. They synthesized pyridinyl imidazoles and evaluated their inhibition properties on p38 mitogenactivated protein kinase.

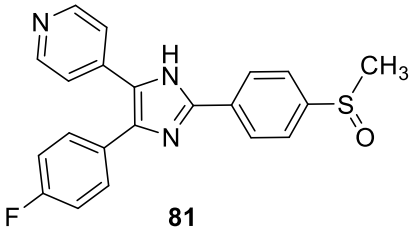

81

Figure 26. Structure of SB203580

2.1.2 Benzimidazole

Benzimidazole is a heterocyclic compound consisting of a fused benzene and imidazole ring and its derivatives have drawn considerable attention due to their diverse biological activities. They are well known compounds with their enzyme inhibition properties. Benzimidazole is a class of a heterocyclic compound that exhibit a wide range of biological activities such as antimicrobial, antiviral, antidiabetic, anticancer activity, numerous antioxidant, antiparasitic, antihelmintics, antiproliferative, anti-HIV, anticonvulsant, antiinflammatory, antihypertensive, antineoplastic, proton pump inhibitor, and antitrichinellosis.[62]

Hepatitis B virus (HBV) has become one of the most important diseases in the world because there have been two billion people being effected worldwide[63] and 0.5-1.2 million people died annually from the resulting cirrhosis, liver failure, and hepatocellular carcinoma.[64] The remarkable biological activity of imidazole skeleton has inspired the development of new imidazole derivatives. Benzimidazoles are regarded as being used in inhibition of HIV DNA synthesis. Li *et al.*[65] proposed an efficient and concise synthetic way to a series of new class of benzimidazole derivatives and evaluated them for their antihepatitis B virus (HBV) activity and cytotoxicity. Compounds **82** and **83** (Figure 27) demonstrated high activity against HIV replication with high antiviral potency (IC_{50}=0.9 and 0.7 μM, respectively).

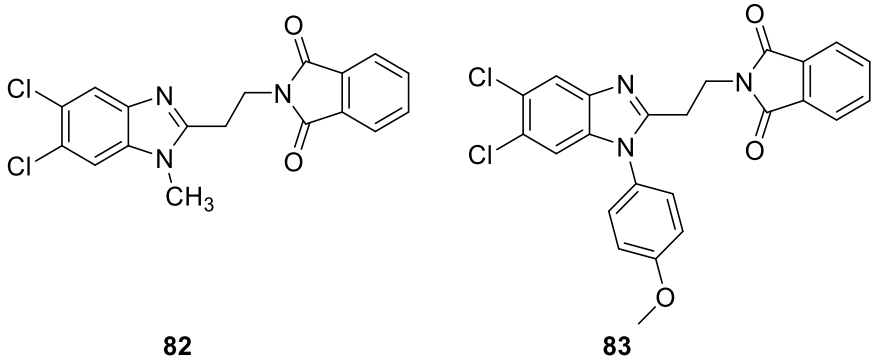

Figure 27. The structures against HIV replication

In recent years, bacteria gained high resistance to antibiotics that brought organic chemists to synthesize a new generation of antibacterial agents. Benzimidazole derivatives are well known compounds as being employed in drug discovery

particularly as used for antibacterial, antiviral, and antifungal activities[62] that's why they focused on the synthesis of novel benzimidazole derivatives structurally different from existing antibacterial agents. Kumar *et al.*[66] proposed a synthetic pathway for novel 2-(6-fluorochroman-2-yl)-1*H*-benzimidazole (**84**) (Figure 28) which show promising antibacterial activity against Salmonella typhimurium.

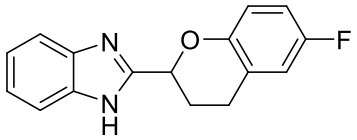

84

Figure 28. The structure against Salmonella thphimurium

Malaria has been a vital disease caused 350-500 million clinical events in a year and led to over one million deaths. Children under 5 years old in sub Saharan Africa were affected from this disease. Malaria is as serious disease as HIV/AIDS and tuberculosis.[62] Camacho *et al.*[67] reported a series of *N*-substituted-2-(5-nitrofuran or 5-nitrothiophen-2-yl)-3*H*-benzo[*d*]imidazole-5-carbohydrazide derivatives **85** as shown in Figure 29 and screened for their antimalarial activity in rodent Plasmodium berghei.

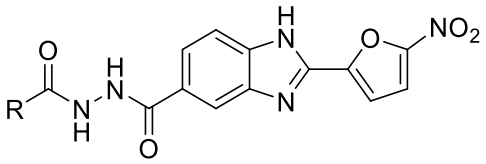

85

	R
1	H
2	Ph
3	3-ClPh
4	4-ClPh
5	3-MeOPh
6	3,4-MeOPh
7	3,4,5-MeOPh
8	3-PhOPh
9	3-OH-2-Naphtyl

Figure 29. Antimalarial agents **85**

2.1.3 Synthesis of benzimidazole derivatives

As mentioned, since bacteria have gained high resistance to existing antimicrobial drugs, design and the synthesis of novel antibacterial agents received considerable

attention. Benzimidazole moiety plays a significant role in drug synthesis so the search for efficient approach to synthesize new class of benzimidazoles with different substituents became the most important issue for medicinal chemistry. Padalkar *et al.*[68] proposed a class of benzimidazole derivatives acting as antibacterial agents.

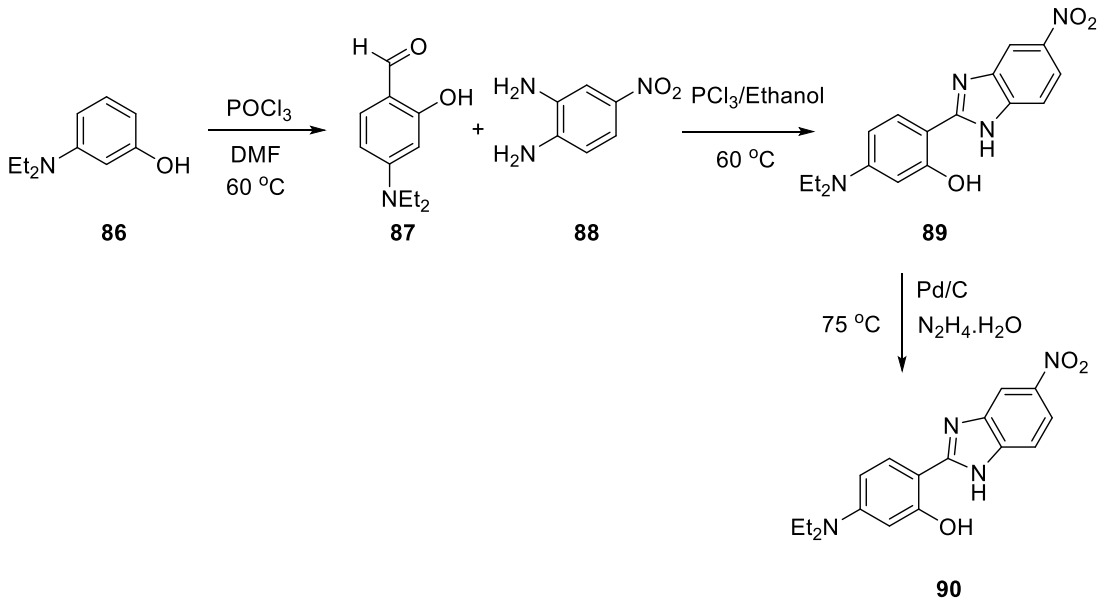

Scheme 30. Synthesis of compound **90**

Starting with 3(diethylamino)phenol (**86**), they achieved the synthesis of 4-(diethylamino)-2-hydroxybenzaldehyde (**87**) by using Vilsmeier–Haack reaction with DMF:$POCl_3$ at 60 °C which was then treated with substituted *o*-phenylenediamine in ethanol and PCl_3 at 60 °C to obtain the corresponding 5-(diethylamino)-2-(5-nitro-1*H*-benzo[*d*]imidazol-2-yl)phenol (**89**). Reduction of **89** by using 10% Pd/C in ethanol and hydrazine hydrate afforded targeted benzimidazole **90** (Scheme 30).

Mariappaz *et al.*[69] suggested a concise and efficient way for the synthesis of 2-substituted benzimidazole derivatives for subsequent anti-inflammatory and analgesic activity testing (Scheme 31). The compounds they synthesized had promising results for the use of those purposes. A mixture of *o*-phenylenediamine (**91**) and monochloroacetic acid was heated at the reflux temperature in 4 N hydrochloric acid. After treatment of compound **92** with substituted amine and KI in ethanol, resulting mixture was heated to its reflux temperature to provide benzimidazole derivatives **93a-e** (Scheme 31).

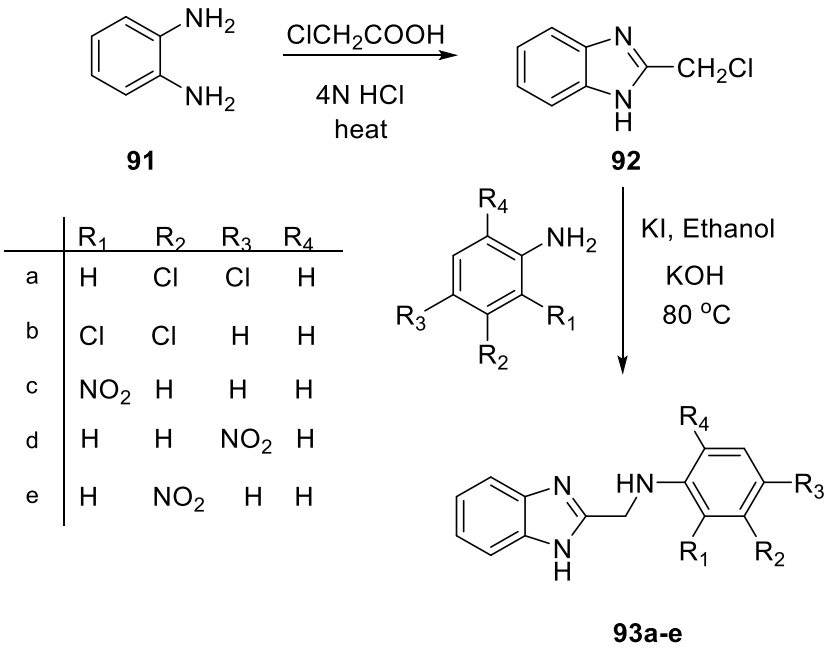

	R_1	R_2	R_3	R_4
a	H	Cl	Cl	H
b	Cl	Cl	H	H
c	NO_2	H	H	H
d	H	H	NO_2	H
e	H	NO_2	H	H

Scheme 31. Synthesis of **93a-e**

2.1.4 Oxazepine

Oxazepine is an unsaturated seven-membered heterocycle with a nitrogen replacing a carbon at one position and with an oxygen replacing a carbon at one position. The scientists have drawn attention to the synthesis of this moiety with different substituents due to their wide range of biological activities. This skeleton is involved in synthesis of various drugs used as antithrombotic, antiepileptic, anticonvulsant, antiinflammatory, antifungal, progesterone agonist, antipsychotic, antagonist, analgesic, antihistaminic, and anxiolytics agents.

There are several oxazepine derivatives reported in the literature having a significant role in inhibition of some enzymes (e.g. tyrosine kinase inhibitory).[70] Due to their structural importance in biological science, incorporation of new substituents to this skeleton has received considerable interest from medicinal and organic chemists.

Caba *et al.*[71] reported a set of synthesis of novel benzoxazepine derivatives and suggested their antiproliferative activity results against the MCF-7 adenocarcinoma cell. The most promising result was obtained from the structure **94** (Figure 30) with its inhibitory effect on cancerous breast cancer cell.

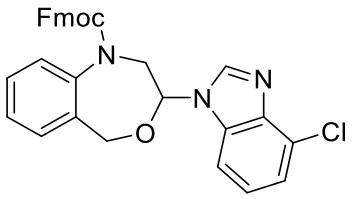

94

Figure 30. Antiproliferatively active compound **94**

Oxazepine derivatives with different moieties were proven to show high anticonvulsant activity. Scientists working on improvement of this effect have drawn attention to synthesis of this scaffold with different substituents. For instance, Deng *et al.*[72] synthesized a series of triazalo-benzoxazepines and proposed their anticonvulsant test results. The structure **95** (Figure 31) gave the best result among the triazalo-benzoxazepine derivatives.

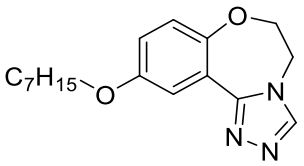

95

Figure 31. Anticonvulsantly active benzoxazepine **95**

2.1.5 Synthesis of oxazepine derivatives

Oxazepines, their aryl-annelated (benzoxazepines) and structural analogues diazepines and thiazepines are very important compounds for synthetic organic chemistry as they are responsible for biological activities of several drugs. Drugs having those skeletons can be used as antidepressant,[73] anticonvulsant,[74] antiviral,[75] antimicrobial,[76] and antifungal[77] agents.

Present methods for the synthesis of thioxo-oxazepine derivatives employ often expensive starting materials giving to low yield and provide compounds of limited diversity. Badru *et al.*[78] proposed an efficient approach to synthesize thioxo-oxazepines in high yield (Scheme 32).

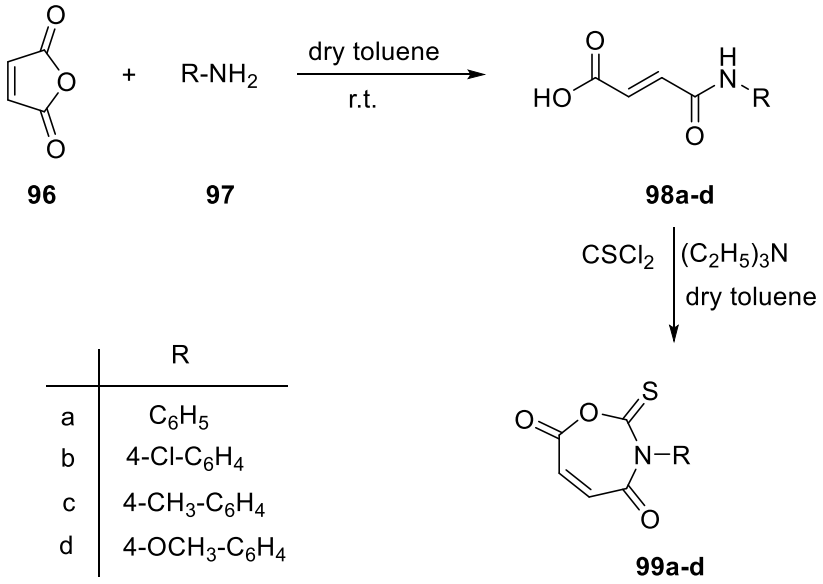

Scheme 32. Synthesis of **99a-d**

Maleic anhydride (**96**) was reacted with primary amine **97** derivatives in dry toluene to afford compound **98**. Triethylamine-catalyzed condensation of maleamic acids **98** with thiophosgene under anhydrous conditions gave cyclization product 2-thioxo-1,3-oxazepine-4,7-diones (**99**) accompanied by nucleophilic attack of O and N of maleamic acid to thiophosgene.

2.1.6 Benzoxazepine and benzimidazo-oxazepine

The benzoxazepines are privileged scaffolds that are present in natural compounds,[79-80] pharmaceuticals,[81,82] and functionalized materials.[83,84,85,86] In addition to this, benzoxazepine skeleton plays a significant role in regulation of central nervous system, in the synthesis of anti-breast cancer agents, and HIV inhibition.[87,88] To exemplify, there are several biologically important compounds constructed from benzoxazepine scaffold like Sintamilv, an antidepressant agent, **100**,[89] H1 receptor antagonist (antihistaminic agent) (**101**),[90] and Sintamil (**102**) (Figure 32).[91,92,93,94]

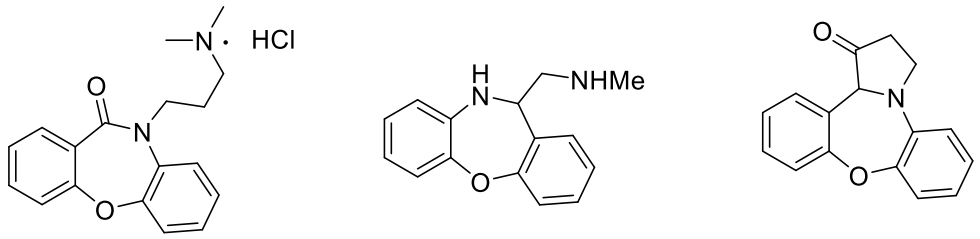

100 **101** **102**

Figure 32. Biologically active benzoxapine derivatives **100-102**

5,6-dihydrobenzo[*f*]imidazo[1,2*d*][1,4]oxazepine (**103**) and compound **104** (Figure 33) show biological activity as therapeutics. Benzimidazo-oxazepine scaffold is also present in several drugs used for the cancer treatment.[95]

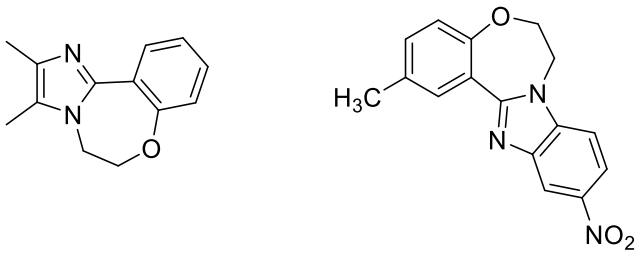

103 **104**

Figure 33. Structure of **103** and **104**

Phosphoinositide 3-kinases (PI3Ks) are key components which play essential roles in several cellular activities, they are lipid kinases that responsible for the conversion of membrane-bound 4,5-phosphatidylinositolbisphosphate (PIP2) into 3,4,5-phosphatidylinositol trisphosphate. Yin *et al.*[96] synthesized various benzimidazo-oxazepine derivatives and evaluated their activities for P13K inhibition and the best selectivity was obtained from compound **104**.

2.1.7 Synthesis of benzoxazepine and benzimidazo-oxazepine

Yin *et al.*[96] synthesized different derivatives of benzimidazo-oxazepine as P13K inhibitor. They evaluated them against human tumor cell lines and a great number of them exhibited antiproliferative activity. The most promising result was observed for the compound **104** (Scheme 33).

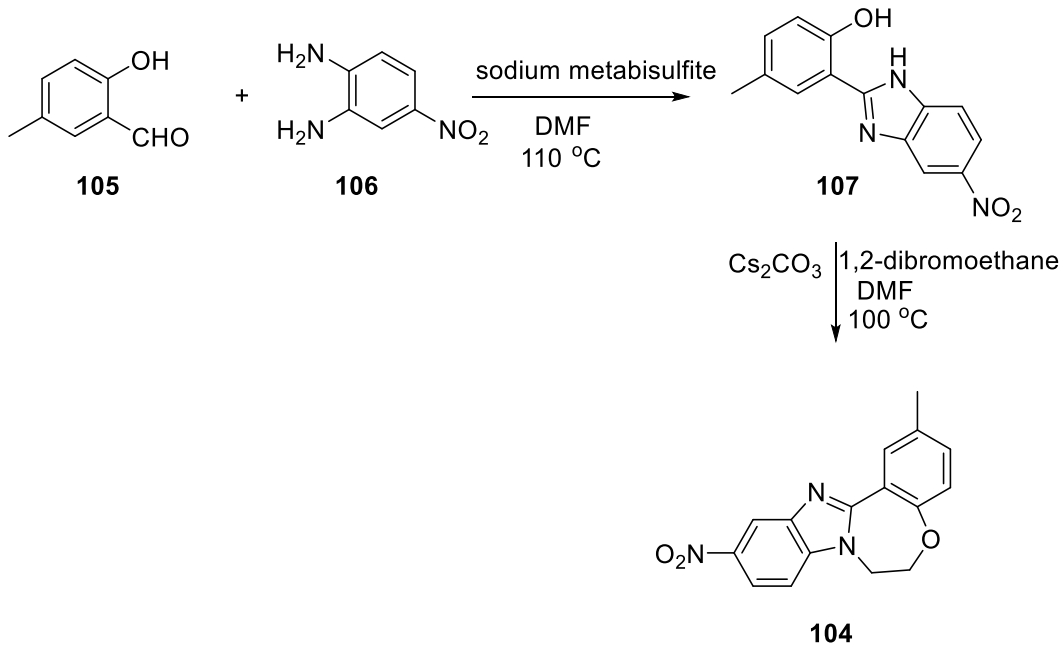

Scheme 33. Synthesis of antiproliferatively active compound **104**

Zhao *et al.*[97] developed a new methodology for the synthesis of benzo-1,4-oxazepines (Scheme 34). For this reaction, 2-(2-dimethylamino-vinyl)-1*H*-inden-1-ol derivatives were used as a ligand.

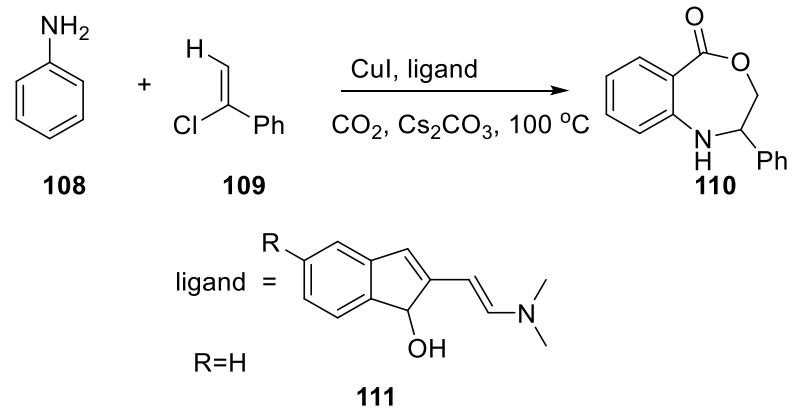

Scheme 34. Synthesis of benzoxazepine **110**

CuI exhibited superior catalytic efficiency for this transformation. Aniline (**108**) and (1-chloro-vinyl)-benzene (**109**) were reacted in the presence of cupper catalyst and indenol based ligand. According to the reaction mechanism, the first step is that ligand coordinates to cupper to form cupper(I) complex (Scheme 35).

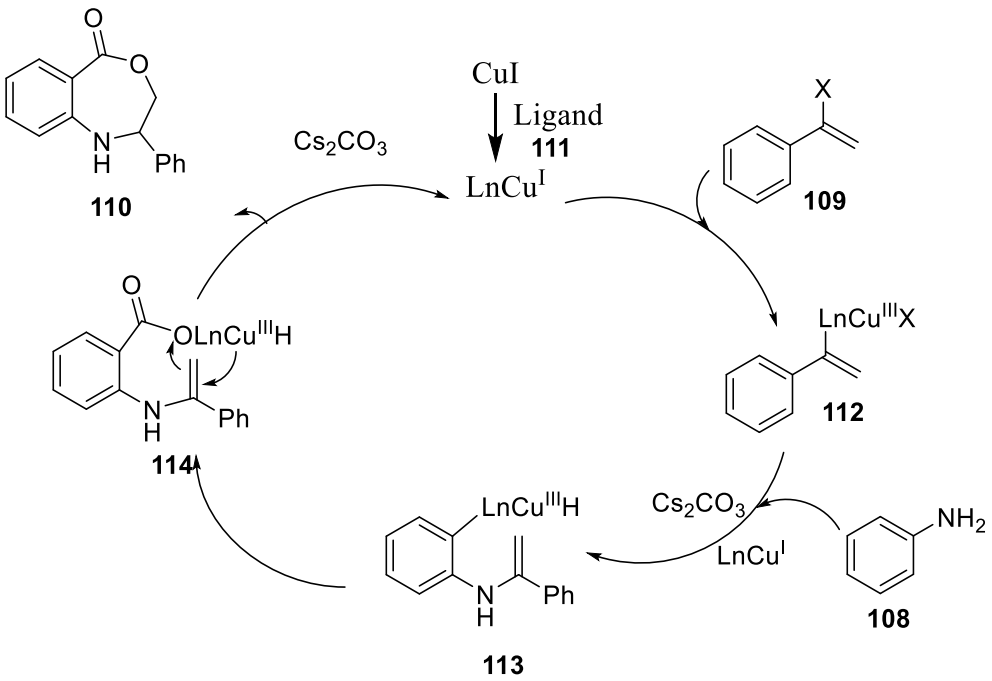

Scheme 35. Proposed mechanism for formation of compound **110**

After oxidative addition of vinylhalide **109**, cupper (III) complex **112** is formed. Subsequent reaction of **112** with aniline generates a new complex **113**. The key step is the ortho-carbonylation of the the lastly formed complex **114** followed by reductive elimination to afford **110**. It was discovered that this ligand was the ideal choice for this transformation when compared to other derivatives with different R groups as -Cl and -CH_3.

2.1.8 Aim of the study

In this part, our goal was to develop a new synthetic methodology for the synthesis of benzofuropyrroloimidazolone **118**. Starting with the methyl acetoacetate (**115**), our intention was to generate first a furan system **116** having a methyl group at the α-position. Subsequent oxidation followed by condensation reaction with *o*-phenylenediamine would give us benzimidazole skeleton **117**. Base-mediated cyclization reaction of **117** would afford **118** (Scheme 36).

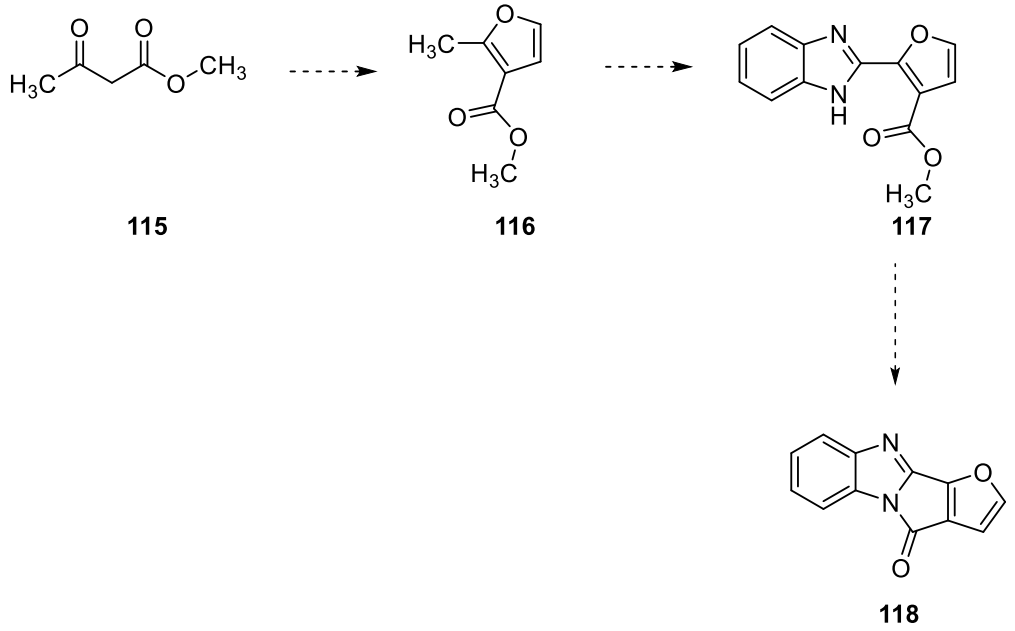

Scheme 36. Schematic pathway for the formation of benzimidazole-fused cyclization product **118**

In the second part, our aim was to develop a new methodology for the synthesis of benzimidazole derivatives fused to oxazepine scaffold. For this purpose, **119** was planned to be used as a starting material to generate alkyne substituted aldehyde **120** to be used for the synthesis of benzimidazol derivatives **121** (Scheme 37).

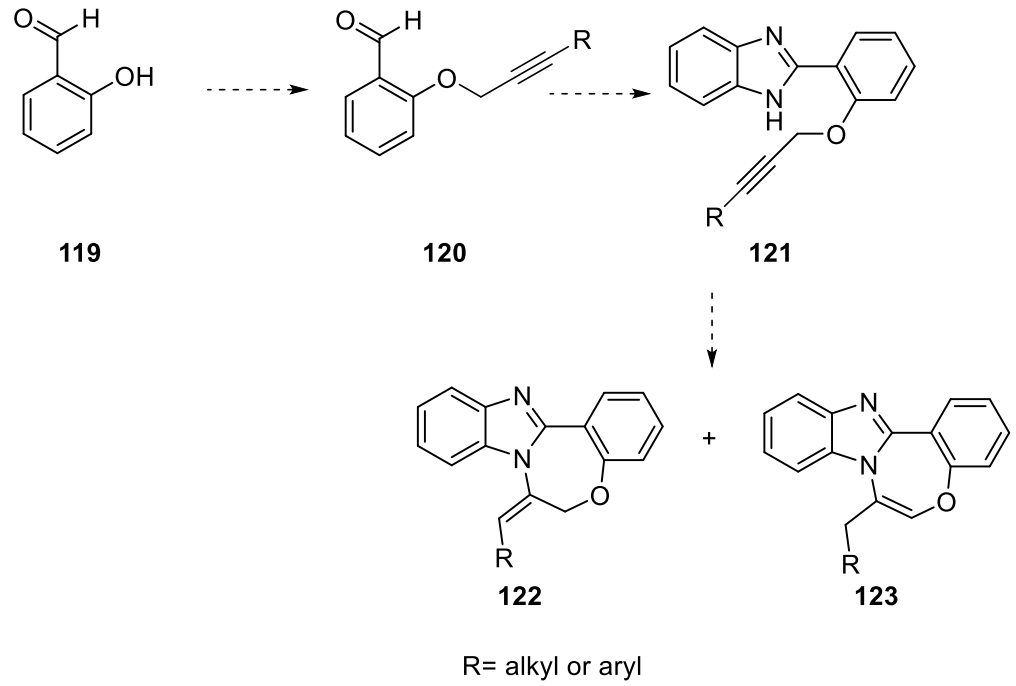

Scheme 37. Synthetic plan for the formation of **122** and **123**

Base-mediated cyclization reaction of **121** would result in the formation of **122** and **123**.

2.2 RESULTS AND DISCUSSION

2.2.1 Synthesis of methyl 2-methylfuran-3-carboxylate (116)

Methyl acetoacetate (**115**) was used as the starting material to construct a furan system with methyl group at its α-position. For this purpose, Feist-Benary furan synthesis reaction was used as the critical step (Scheme 38).[98]

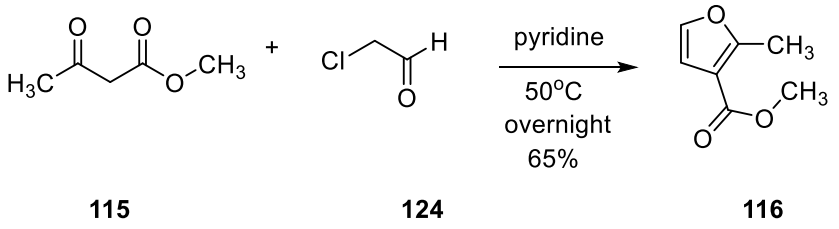

115 **124** **116**

Scheme 38. Synthesis of substituted furane **116**

Methyl acetoacetate (**115**) has a ketone and an ester functionality whose activities are quite different toward nucleophilic reagents. Delocalization of π-electrons of ester group decreases the reactivity of ester carbonyl carbon.

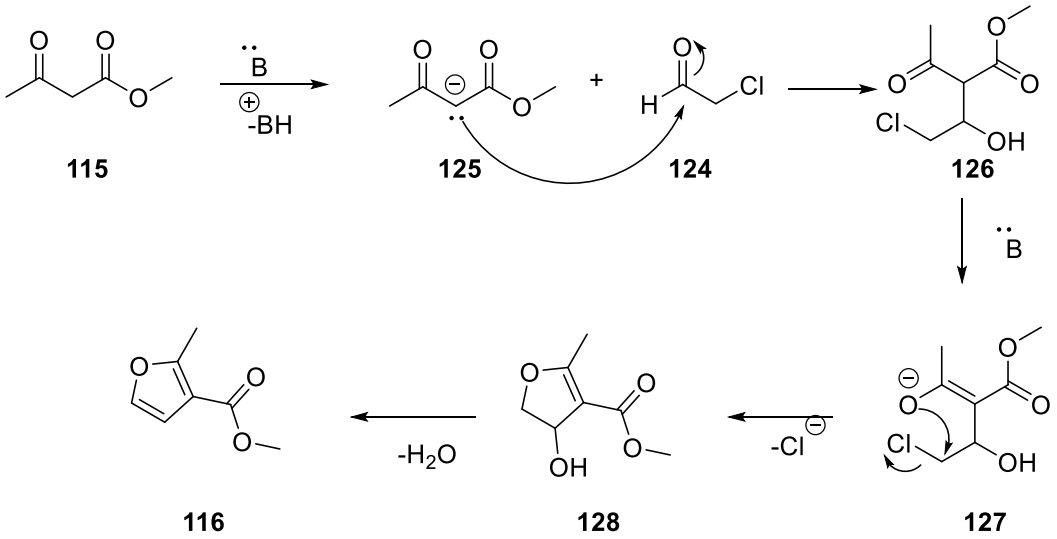

115 **125** **124** **126** **127** **128** **116**

Scheme 39. The reaction mechanism for the formation of **116**

The pKa value of methylene protons is quite low than those of other protons which leads to deprotection of methylene group. Resulting anion **125** attacks the electropositive carbon of **124** to afford **126** as an intermediate. Second proton abstraction from middle carbon forms enolate **127** which undergoes nucleophilic substitution reaction to generate **128** *via* intramolecular cyclization reaction. Water elimination affords **116** (Scheme 39).

The formation of **116** was verified by ^{1}H- and ^{13}C-NMR spectra. In the ^{1}H-NMR spectrum of **116**, there are two doublets that appear at 7.23 and 6.63 ppm with a coupling constant of J = 1.9 Hz which is a characteristic value for adjacent protons at 2,3-position in furan. It is quite less than those of benzene and thiophene adjacent protons.

2.2.2 Synthesis of methyl 2-formylfuran-3-carboxylate (129)

For further benzimidazole formation reactions it was necessary to convert the methyl group attached to the furan ring into an aldehyde. We utilized oxidation ability of selenium dioxide to afford desired compound **129** (Scheme 40).[98]

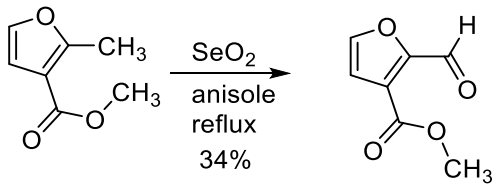

116 **129**

Scheme 40. Oxidation to aldehyde **129**

We used anisole as reaction solvent due to its high boiling point. We achieved the synthesis of compound **129** in 34% yield. In the ^{1}H-NMR spectrum of **129**, the signal at 10.24 ppm was a strong evidence for the formation of an aldehyde functionality. Moreover, the ^{13}C-NMR spectrum also supported this formation with the signal of aldehyde carbon at 178.7 ppm.

2.2.3 Synthesis of methyl 2-(1*H*-benzo[d]imidazol-2-yl)furan-3-carboxylate (117)

Aldehyde **129** and *o*-phenylenediamine (**91**) were mixed in DMF, then *p*-TsOH (20% mol) was added. The solution was heated to 80 °C and stirred at this temperature for appropriate time (monitored by TLC) to afford compound **117** (Scheme 41). By using this methodology, a novel substituted benzimidazole derivative **117** was synthesized with simple and one-pot reaction according to literature procedure.[99]

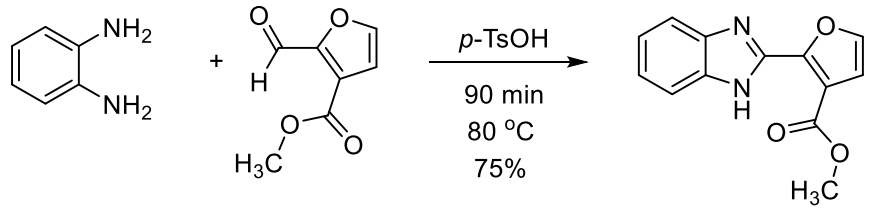

91 **129** **117**

Scheme 41. Synthesis of furane-substituted benzimidazole **117**

The ^{1}H- and ^{13}C-NMR spectra are consistent with the proposed structure **117**. In the ^{1}H-NMR spectrum, the broad signal at 12.65 ppm belongs to NH proton that is the strong evidence for the formation of imidazole skeleton. In addition to this, two adjacent furan protons resonating at 7.61 and 6.92 as distinct doublets with the coupling constant of J = 1.8 Hz are also in agreement with the proposed structure. In the ^{13}C-NMR spetrum, disappearance of the signal at 178.8 belonging to aldehyde carbon atom clearly shows occurrence of condensation reaction.

According to the proposed mechanism, one of the amine groups adds to the aldehyde carbonyl group in the presence of a catalytic amount of *p*-TSOH. Intramolecular cyclization reaction generates benzimidazole ring. The oxidation of the intermediate with air oxygen afforded substituted imidazole skeletons (Scheme 42).

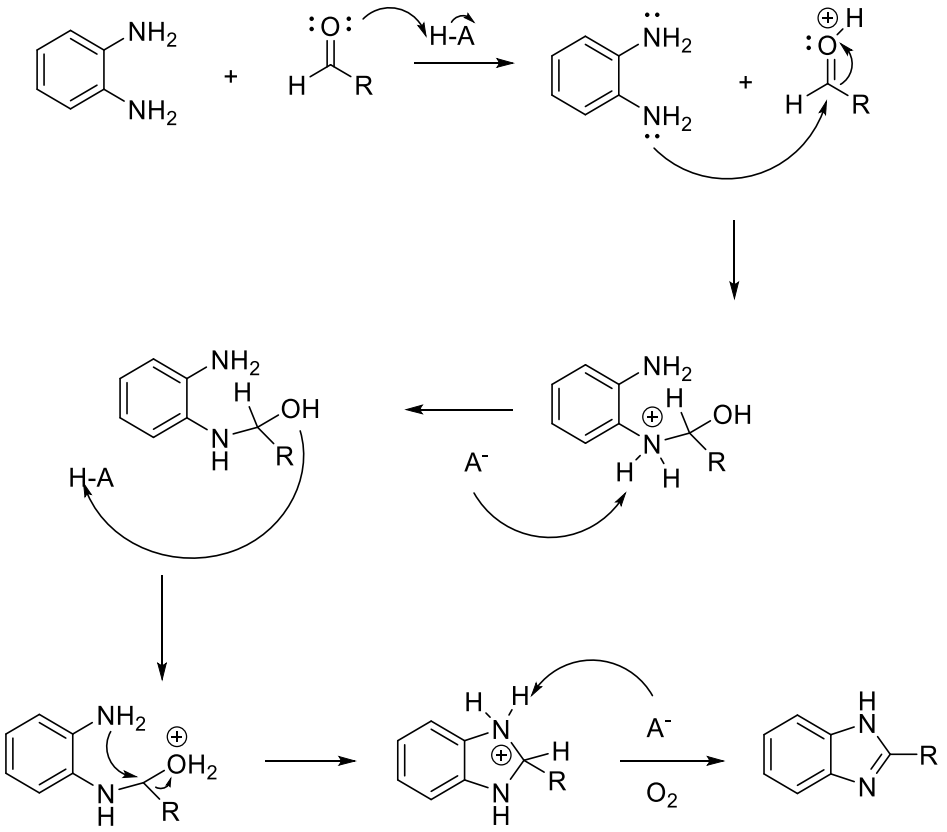

Scheme 42. Proposed mechanism for the formation of benzimidazole skeleton

2.2.4 Attempted incorporation of an alkyne functionality to benzimidazole 117 and synthesis of 118

First we intented to introduce an alkyne functionality to the carbonyl group as shown in the structure **132**. For the formation of **130**, first **117** should be hydrolyzed to the corresponding acid **130** followed by acylchloride formation using oxalyl chloride. Subsequent Sonogashira cross-coupling reaction would give us corresponding alkyne **132**. Reaction of **117** with K_2CO_3 did not form the expected hydrolysis product **130** (Scheme 43). The structure of the formed product was determined by IR and HRMS analysis. After analysis of IR and HRMS spectra, we concluded that during hydrolysis reaction, cyclization occurred to afford compound **118**. As expected, ^{1}H-NMR spectra of **118** and **130** are so similar so that information obtained from NMR spectra was not enough for exact structure determination.

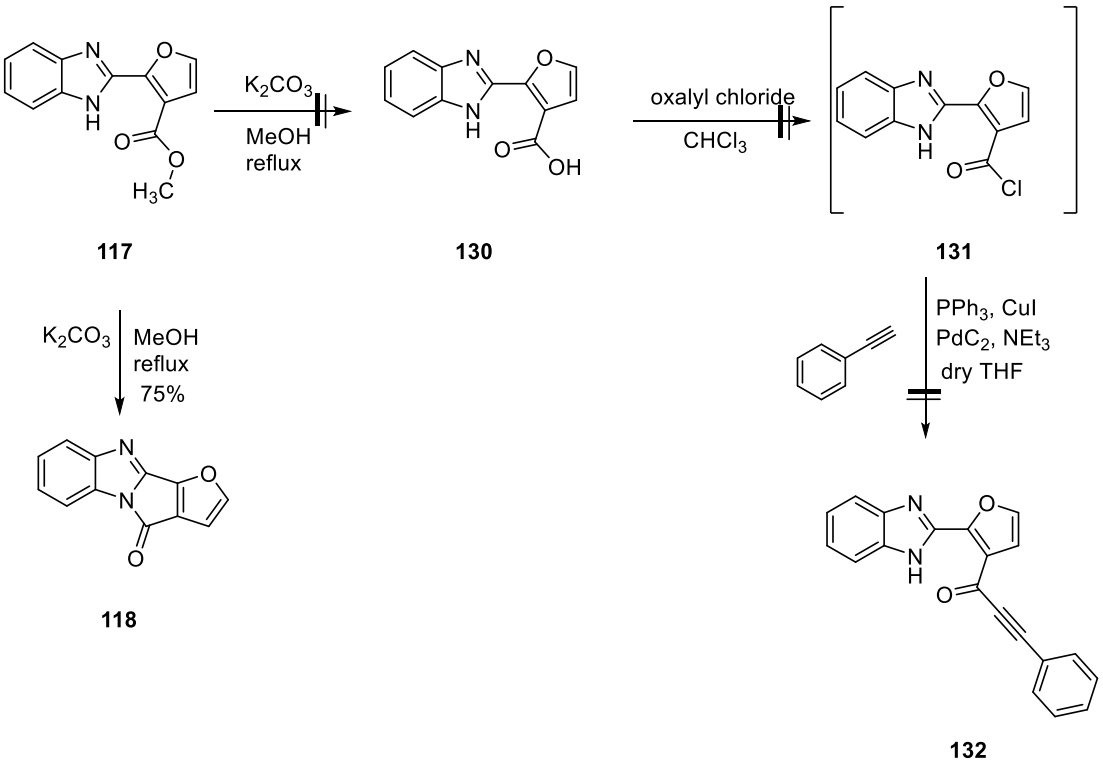

Scheme 43. Cyclization product **118** formation

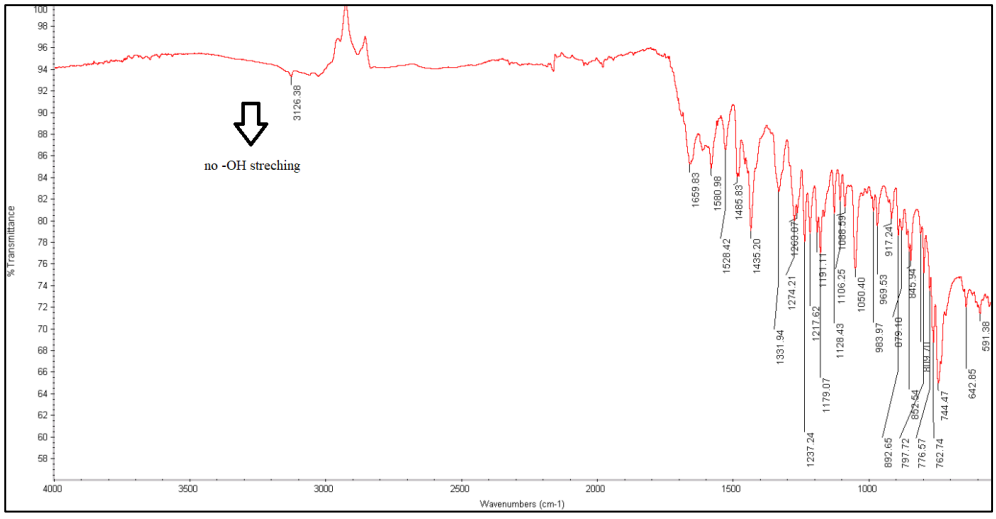

Figure 34. IR spectrum of compound **118**

In the IR spectrum of compound **118** (Figure 34) there is no –OH peak at around 3500 cm^{-1} supported the formation of cyclization product **118**. Furthermore, the HRMS spectrum also supported the formation of the product **118**.

2.2.5 Synthesis of *O*-propargylated salicyl aldehydes

For the construction of different benzimidazole skeletons, we synthesized *O*-propargylated salicyl aldehyde **120a** starting from salicyl aldehyde (**119a**). Treatment of **119a** with propargyl bromide in presence of potassium carbonate afforded desired product **120a** according to literature procedure (Scheme 44).[100]

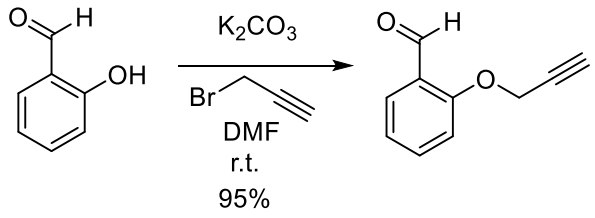

Scheme 44. Synthesis of *O*-propargylated salicyl aldehyde **120a**

For derivatization, we used substituted salicyl aldehydes **119b** and **119c** to synthesize further alkynyl compounds such as **120b** and **120c** by applying the same reaction procedure as described for the synthesis of **120a** (Scheme 45).[100]

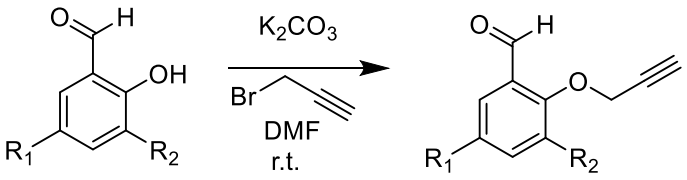

Scheme 45. *O*-propargylation of substituted salicyl aldehydes **119b** and **119c**

The ^{1}H- and ^{13}C-NMR spectra verified the formation of the compounds **120b** and **120c**. In the ^{1}H-NMR spectrum of compound **120b** shown in Figure 35, phenyl protons resonate at 7.91, 7.63 and 7.04 ppm. The signal at 7.91 ppm appears as doublet and split by the *m*-proton with a coupling constant of J = 2.5 Hz. The proton located between the bromine atom and aldehyde group resonates at 7.63 ppm as doublet of doublets with the coupling constants of J = 8.9 Hz and 2.5 Hz. The other phenyl proton at 7.04 ppm gave distinct doublet with a coupling constant of J = 8.9 Hz. The singlet

at 10.4 ppm belongs to the aldehyde proton. The peak at 4.83 ppm is arising from the methylene protons of the propargyl group. During the analysis of resonances of the methylene protons and alkyne protons, we realized that there is a long-range coupling between these protons. Methylene protons' signal splits into doublet by the terminal proton of triple bond with a coupling constant of J = 2.4 Hz. The terminal alkyne proton gave a triplet at 2.58 ppm with the same coupling constant of J = 2.4 Hz.

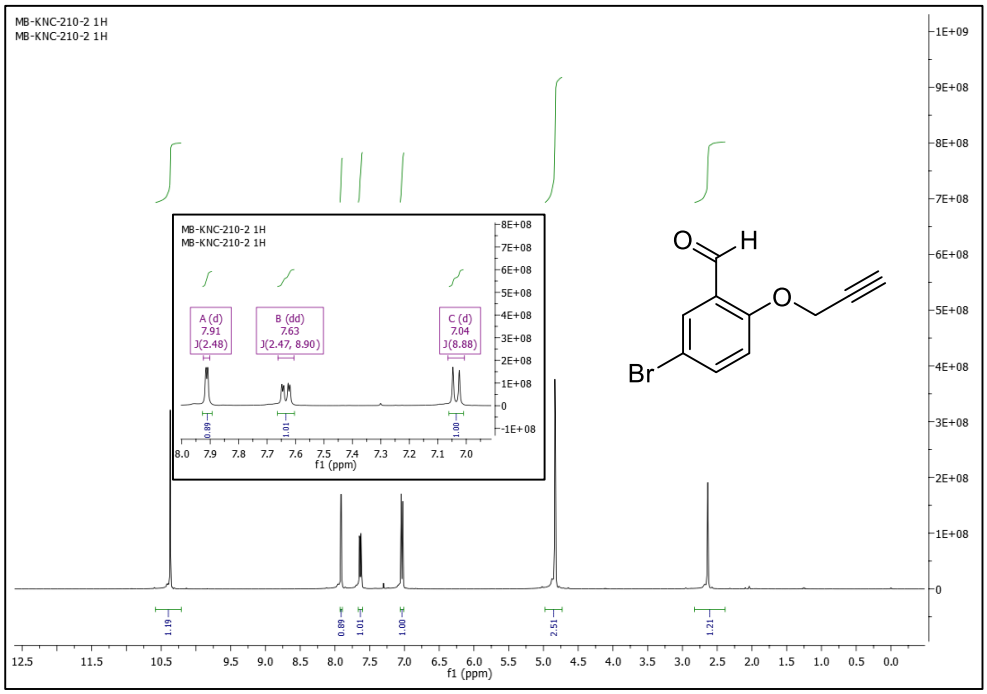

Figure 35. ^{1}H-NMR spectrum of the compound **120b**

2.2.6 Derivatization of 120a with Sonogashira cross-coupling reaction

We attached aryl substituents to acetylene group in **120a** by Sonogashira cross coupling reaction according to literature procedure (Scheme 46). Treatment of compound **120a** with the Sonogashira reagents in presence of iodobenzene and *o*-nitroiodobenzene gave us targeted molecules **120d**[100] and **120e**.

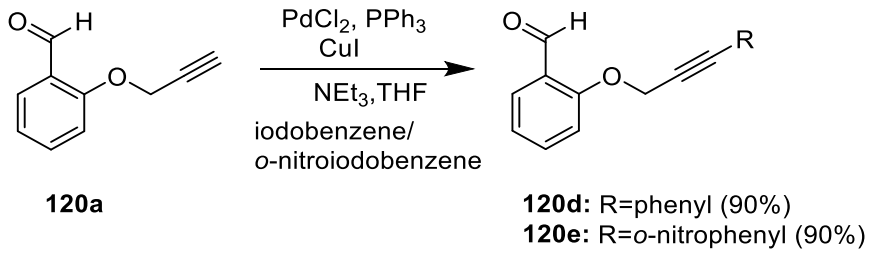

Scheme 46. Sonogashira cross-coupling reactions of compound **120a**

The formation of compound **120d** and **120e** was confirmed by ^{1}H- and ^{13}C-NMR spectra. In the ^{1}H-NMR spectrum of **120d**, the aldehyde proton resonates at 10.54 ppm as a singlet. Resonances between 7.88-7.09 ppm are arising from the phenyl protons. The methylene protons appear as a singlet at 4.93 ppm. In the ^{13}C-NMR spectrum of **120d**, triple bond carbons give rise to two separate peaks at 88.2 and 82.9 ppm. The ^{1}H-NMR spectrum of **120d** is similar to that of **120e** with the exception that there is an additional proton in the aromatic region.

2.2.7 Synthesis of *O*-substituted salicyl aldehydes 120f and 120g

After incorporation of aryl substituents to compound **120**, we introduced 2-butyne and choloroacetonitrile to the system **119a** for the formation of 1**20f**[100] and **120g**[101] (Scheme 47).

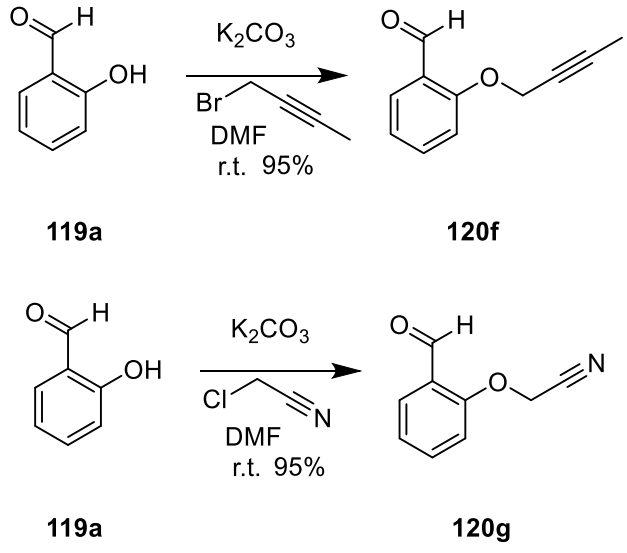

Scheme 47. Synthesis of *O*-substituted salicyl aldehydes

Characterization of these compounds was done by ^{1}H- and ^{13}C-NMR spectra analyses. It is obviously seen in the ^{1}H-NMR spectrum of **120f** (Figure 36) that there is a long range coupling between methylene protons and methyl protons. Methyl protons and methylene protons resonate at 1.86 ppm as triplet and 4.79 ppm as quartet, respectively with a coupling constant of J = 2.2 Hz. Moreover, the aldehyde proton gives a singlet at 10.49 ppm. In the ^{13}C-NMR spectrum of **120f** (Figure 37), the methyl carbon resonates at 3.6 ppm. The high field shift is due to the presence of the methyl group in the shielding zone of acetylene group. There are two carbon peaks at 84.7 and 73.3 ppm which belongs to the triple bond.

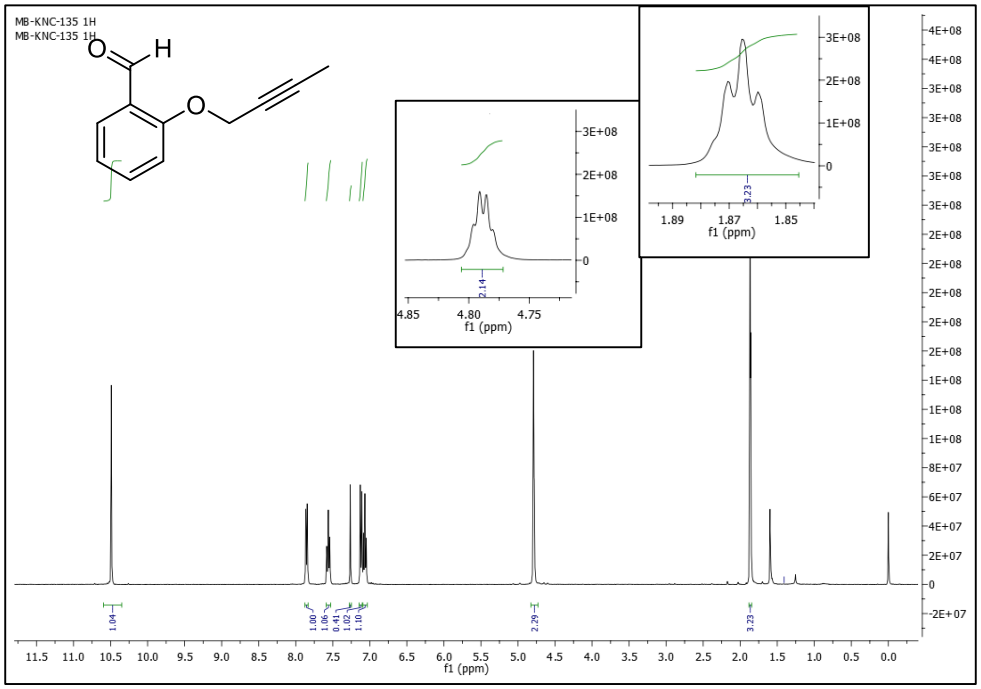

Figure 36. ^{1}H-NMR spectrum of compound **120f**

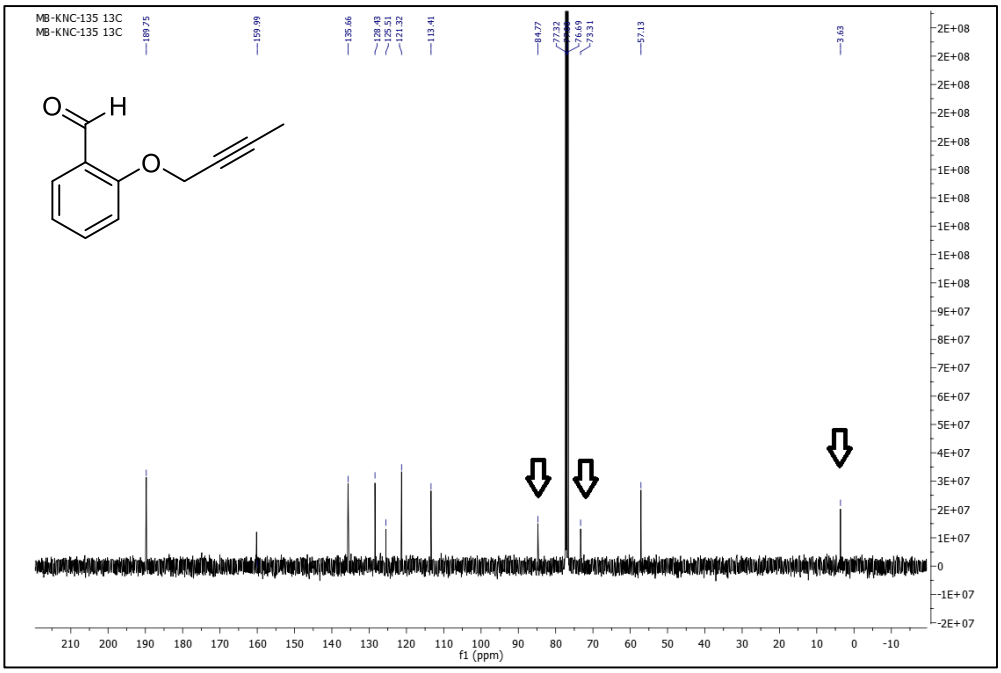

Figure 37. ^{13}C-NMR spectrum of the compound **120f**

2.2.8 Condensation reaction of salicyl aldehyde derivatives

After successful synthesis of salicyl aldehyde derivatives **120**, we constructed different benzimidazole skeletons **121** according to literature procedure[99] as shown in Scheme 48.

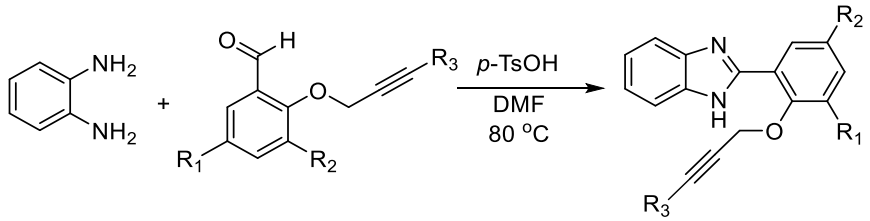

91

120a
120b
120c
120d
120f

121a: R_1=H, R_2=H, R_3=H (65%)
121b: R_1=Br, R_2=H, R_3=H (50%)
121c: R_1=OMe, R_2=H, R_3=H (60%)
121d: R_1=H, R_2=H, R_3=phenyl(30%)
121f: R_1=H, R_2=H, R_3=CH_3 (60%)

Scheme 48. Synthesis of substituted benzimidazoles **121**

The structures were confirmed by ^{1}H- and ^{13}C-NMR spectra. In the ^{1}H-NMR spectrum of **120c**, two phenyl protons resonances at 8.14 and 7.02 ppm arising from *o*- and *p*-protons of methoxy group with the coupling constants of J = 1.5 and 8.1 Hz. As it can

be seen in the ^{1}H-NMR spectrum (Figure 38), there are two aromatic protons which resonate as a broad singlet. Methoxy protons give a sharp singlet at 4.90 ppm. Furthermore, the IR spectrum of **121c** confirms the presence of NH-proton.

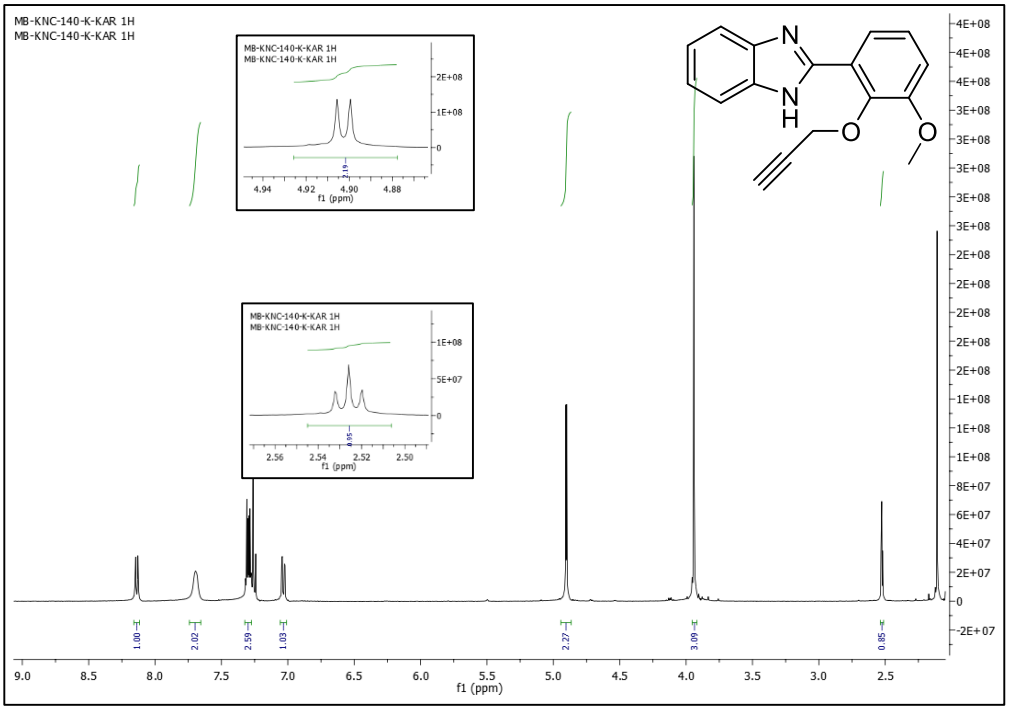

Figure 38. ^{1}H-NMR spectrum of compound **121c**

In the ^{13}C-NMR spectrum of **121c** there are two acetylene carbons resonating at 78.3 and 77.0 ppm. There is only one aliphatic carbon resonance at 57.3 ppm belonging to the methylene carbon. Other carbons resonate in the sp^2 region arising from benzimidazole and benzene carbons (Figure 39).

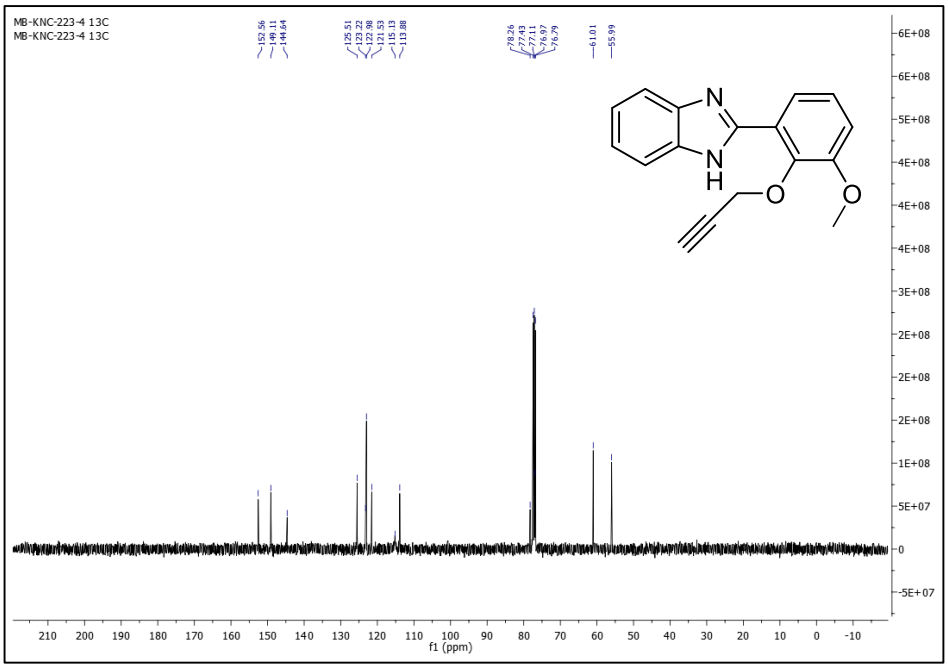

Figure 39. ^{13}C-NMR spectrum of compound **121c**

2.2.9 Cyclization reactions of salicyl aldeyde derivatives 120e, 120g and 120d

Treatment of compound **121d** with NaH at room temprature furnished both *Z*- and *E*-isomers, **122d-*Z*** and **122d-*E***.

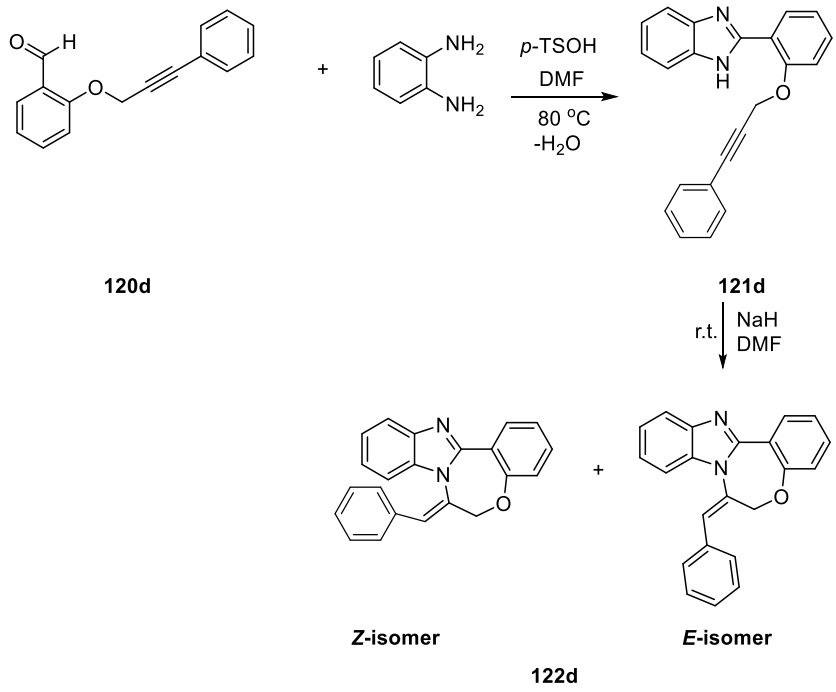

Scheme 49. Cyclization reaction of **121d** with NaH

However, in the case of **120e** and **120g**, during the formation of benzimidazole skeleton, intramolecular cyclization reaction spontaneously occurred to provide **122e** and **122g** without isolation of corresponding benzimidazoles (Scheme 50 and Scheme 51). The ^{13}C-NMR spectrum of **122e** was consistent with the proposed structure. The dissapparance of triple bond was the strong evidence for the formation of **122e**. Moreover, the chemical shift of methylene carbons is shifted to low field compared to that of starting materials where methylene groups are connected to acetylene group. We assume that the methylene protons in **122e** are located in the deshielding zone of the benzene ring.

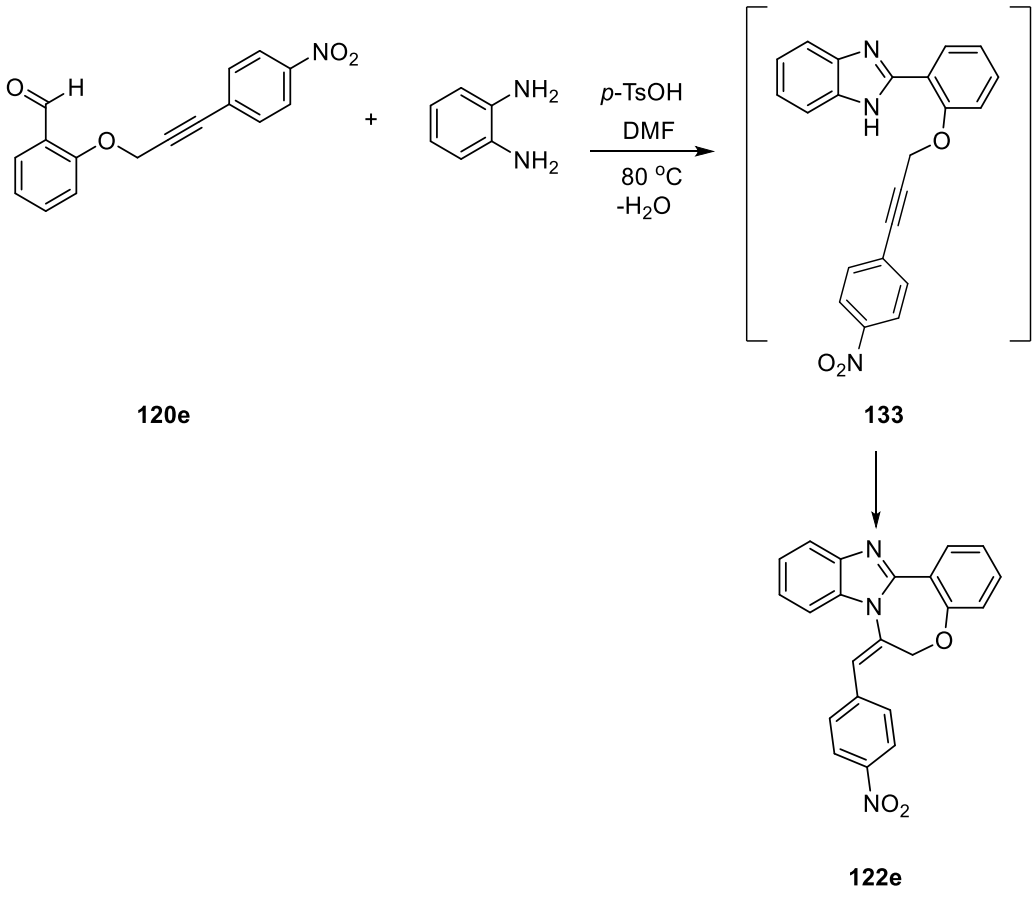

Scheme 50. Cyclization reaction of **120e**

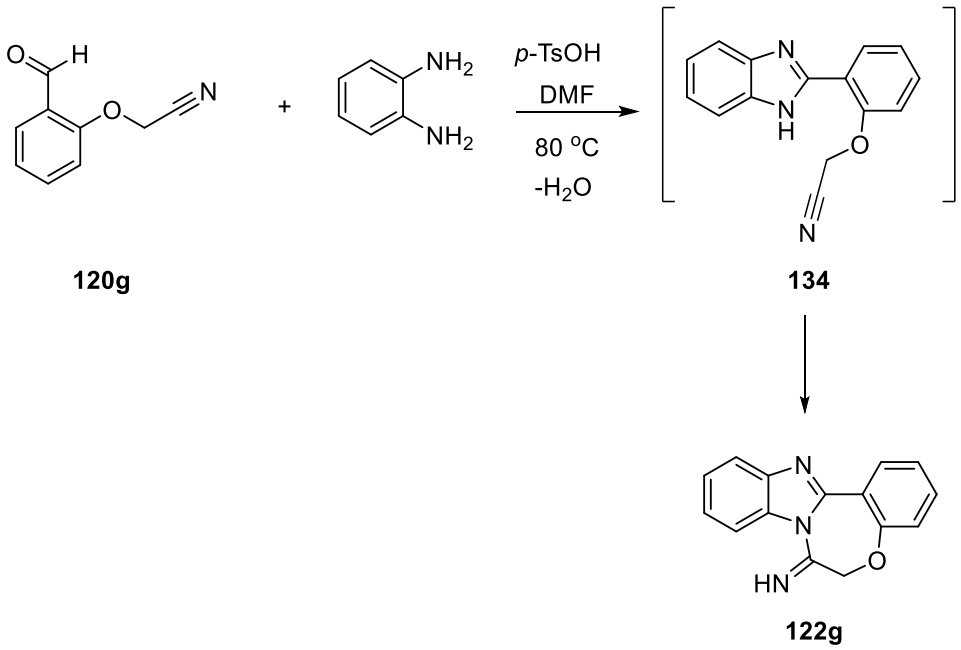

Scheme 51. Cyclization reaction of **120g**

In the ^{1}H-NMR spectrum of the compound **122e**, there is one additional proton at sp^{2}-region which can be easily assigned to the olefinic proton in **122e** (Figure 40).

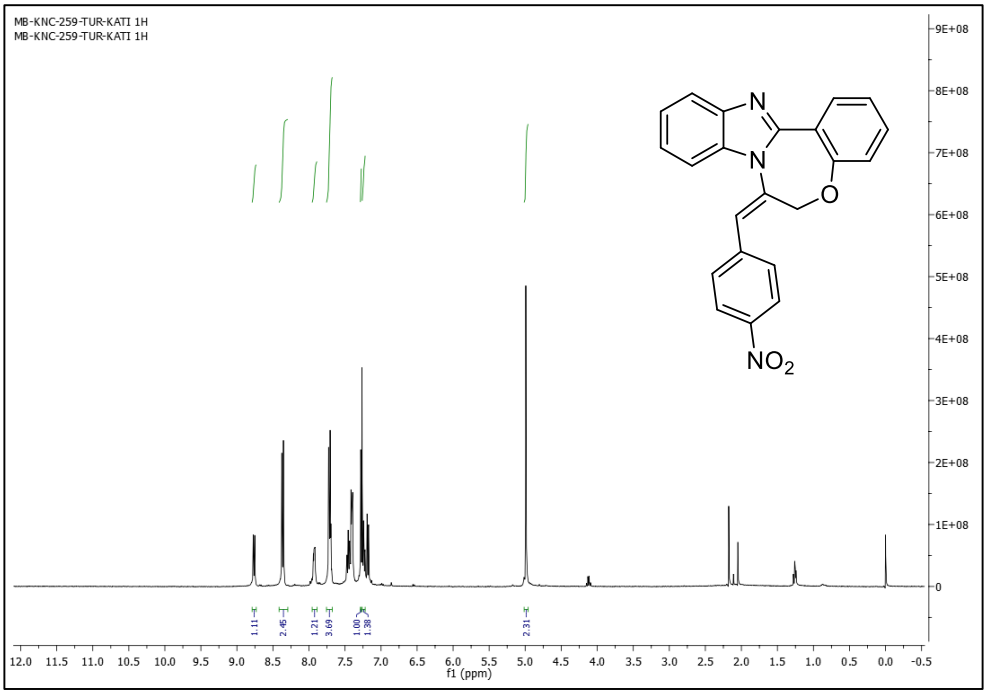

Figure 40. ^{1}H-NMR spectrum of compound **122e**

The plausible mechanism involves first the formation of benzimidazole as an intermediate. It was considered that *o*-nitro group on phenyl definitely has a significant influence on the reaction. Once the resonance structures of this molecule is analyzed, it can be obviously seen that there is a positive charge on one of the alkyne carbon atom which efficiently activated for an attack from a nucleophile (Scheme 52). The non-bonding electrons on nitrogen atom of benzimidazole skeleton can easily attack the alkyne unit to generate **122e**.

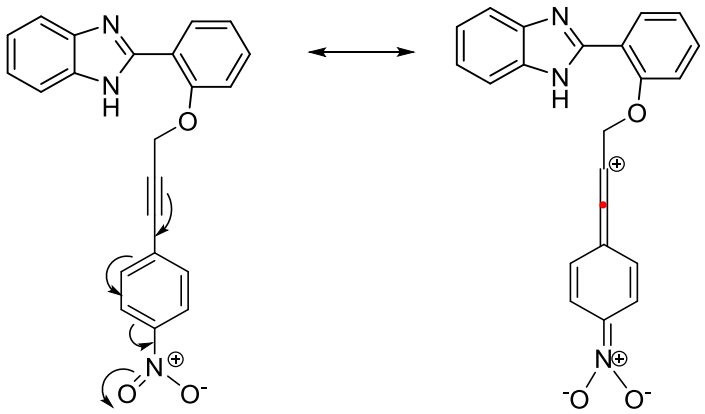

Scheme 52. Resonance form of intermediate **133**

The similar case was observed during the reaction of **120g**. Intramolecular cyclization reaction involving nitrogen attack to electropositive carbon on cyano group resulted in the formation of **122g**. The structure was confirmed by ^{1}H-, ^{13}C-NMR and IR spectra as well. As known that triple bond stretching at around 2200 cm^{-1} can be easily detected in the IR spectrum (Figure 41). Disappearence of nitrile peak supported the formation of cyclization product **122g**.

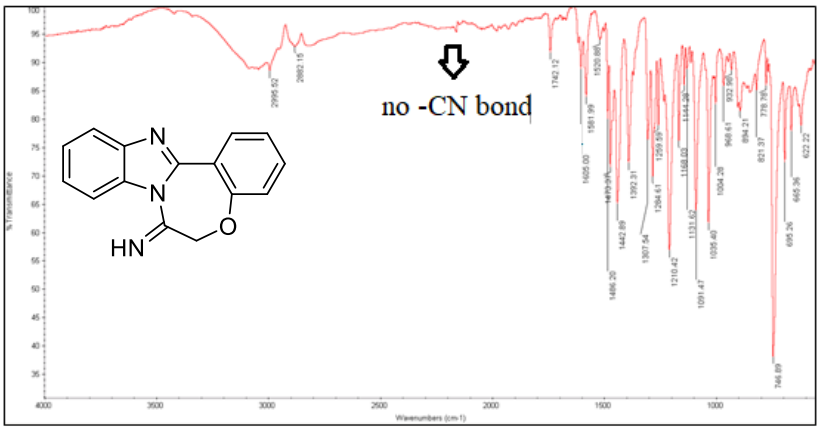

Figure 41. IR spectrum of compound **122g**

2.2.10 NaH Mediated cyclization reactions of phenyl-substituted benzimidazoles

NaH-mediated intramolecular cyclization of *O*-propargylated benzimidazole derivatives were established in this section. Treatment of **121c** with excess NaH at room temperature gave a mixture of three products **122c**, **135a**, and **135b** in a ratio of 2:1:2 (Scheme 53). The ratio of the products was determined by the analysis of the ^{1}H-NMR spectrum.

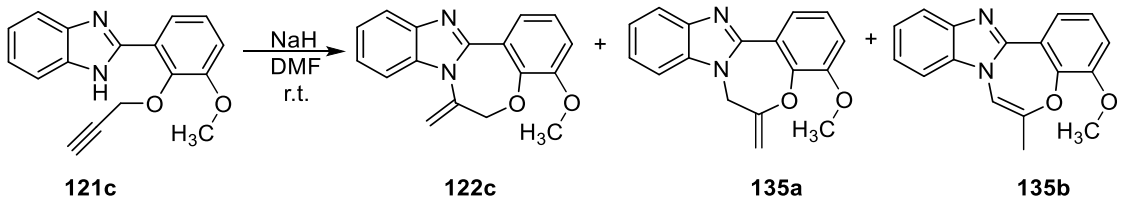

Scheme 53. Cyclization reactions of **121c** and formation of **122c**, **135a**, and **135b**

Exo-configurated products **122c** and **135a** were succesfully separated by coloumn chromatography. The analytically pure *exo*-configurated product **135a** was obtained after recrystallization using slow vapor deposition technique (chloroform/hexane).

The ^{1}H-NMR spectra of the *exo*-configurated products **122c** and **135a** are consistent with the proposed structures. It is clear from the spectra that there is a significant difference in geminal protons' resonances of the structures **122c** and **135a**. As shown in Figure 42, **135a** possesses methylene geminal protons resonate at 4.87 and 4.59 ppm with the coupling constant of J = 1.8 Hz. Additionally, the singlet peak at 4.81 ppm belongs to methylenic protons of compound **135a**. In the ^{1}H-NMR spectrum of the compound **122c**, ethylene geminal protons resonate at lower field compared to those of compound **135a** with distinct broad singlets at 5.69 and 5.52 ppm. The reason behind this observation is the infuence of the deshielding effect of the aromatic benzimidazole ring. The singlet resonating at 4.93 ppm is arising from the methylenic protons of **122c** (Figure 43).

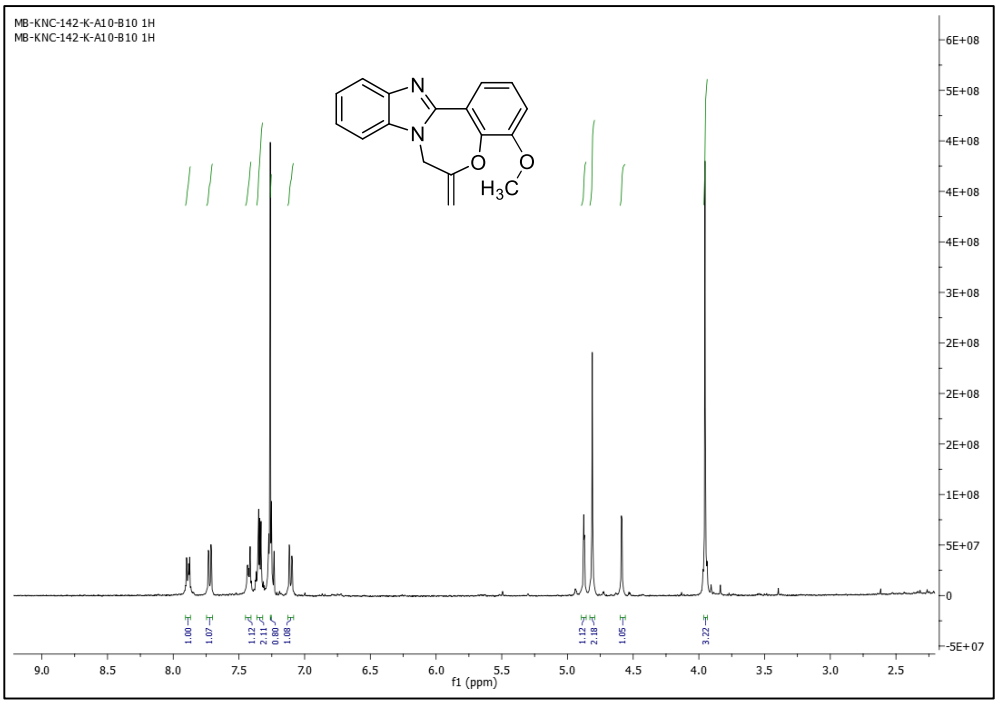

Figure 42. [1]H-NMR spectrum of compound **135a**

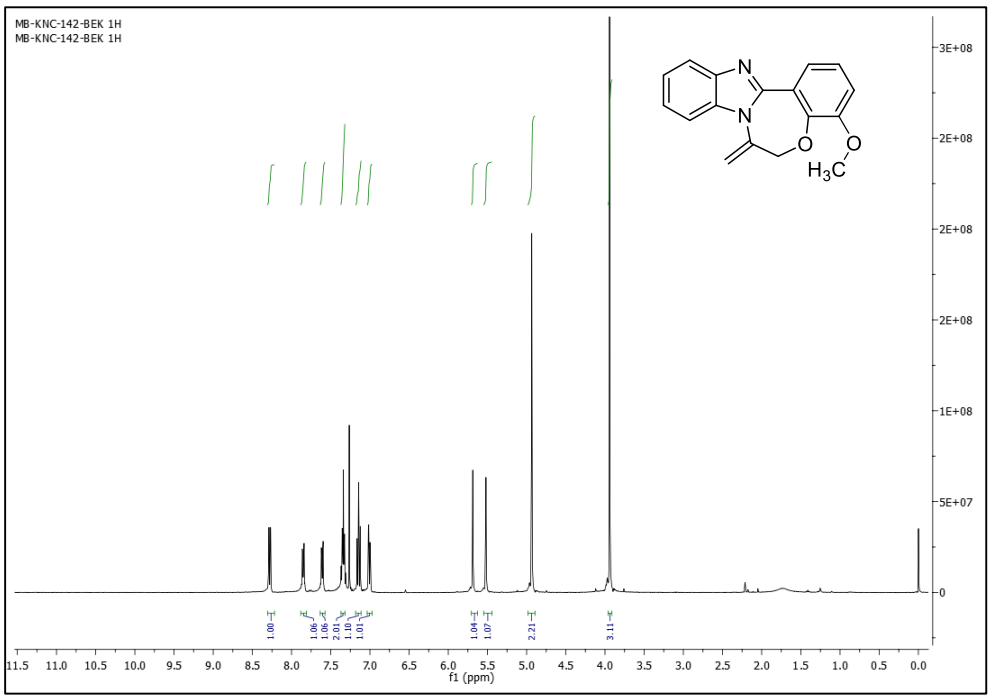

Figure 43. [1]H-NMR spectrum of compound **122c**

These findings were further supported by the single crystal X-ray analysis of **135a** (Figure 44).

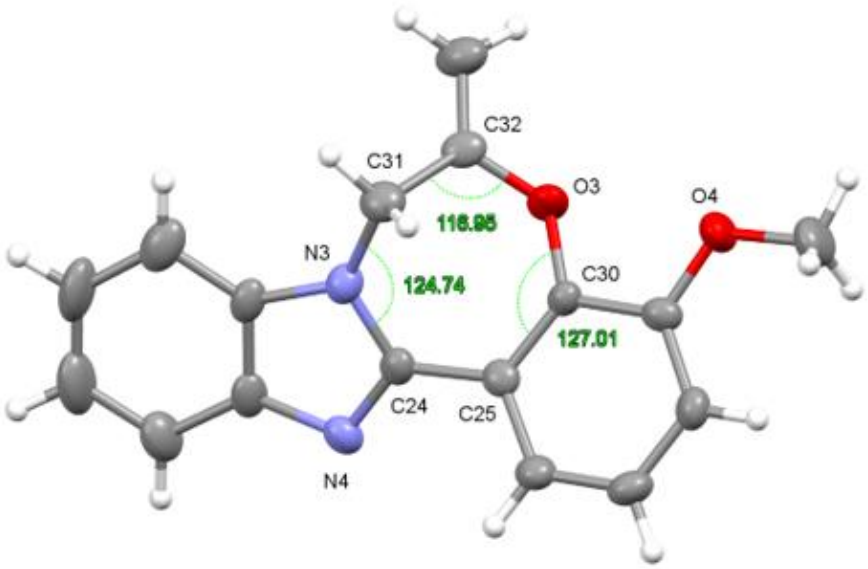

Figure 44. The molecular structure of compound **135a** determined by single crystal X-ray analysis

The formation of **122c** starts with the initial base-mediated alkyne-allene isomerization in **121c** to form **136** as the intermediate. It is well-established that the central carbon atom in allene **136** is much more electropositive than the terminal carbon atoms. Therefore, the nucleophile exclusively attacks the central carbon atom resulting in the formation of 7-*exo*-dig cyclization product **122c** (Scheme 54).

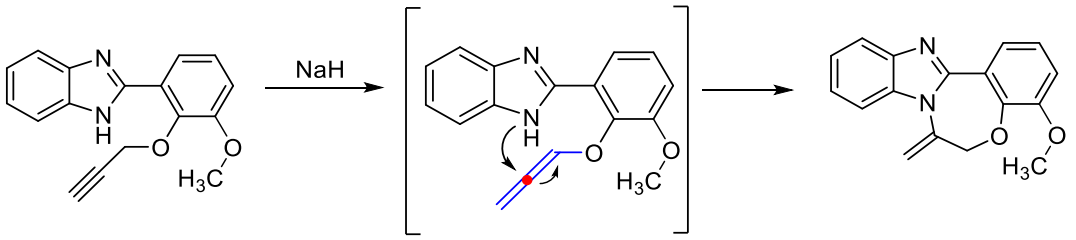

Scheme 54. Tentative reaction mechanism for the formation of **122c**

However, the formation of the isomeric products **135a** and **135b** is unusual at first glance. Herein, we propose the following reaction mechanism for their formation (Scheme 55). Abstraction of acidic NH proton generates a carbanion on nitrogen atom of **137** which can undergo a nucleophilic substitution reaction by attacking the methylene group which transfers the propargyl group from the oxygen atom to the

nitrogen atom to form **138**. Formation of allene **139** followed by cyclization reaction where the nucleophile exclusively attacks the central carbon atom, results in the formation of **135a** and **135b** as depicted in Scheme 55. To the best of our knowledge, the reported propargyl transformation is unprecedented in the literature. We assume that the conformational factors are responsible for this interesting transformation. The reaction mechanism will be further investigated with follow-up experiments as well as with theoretical calculations.

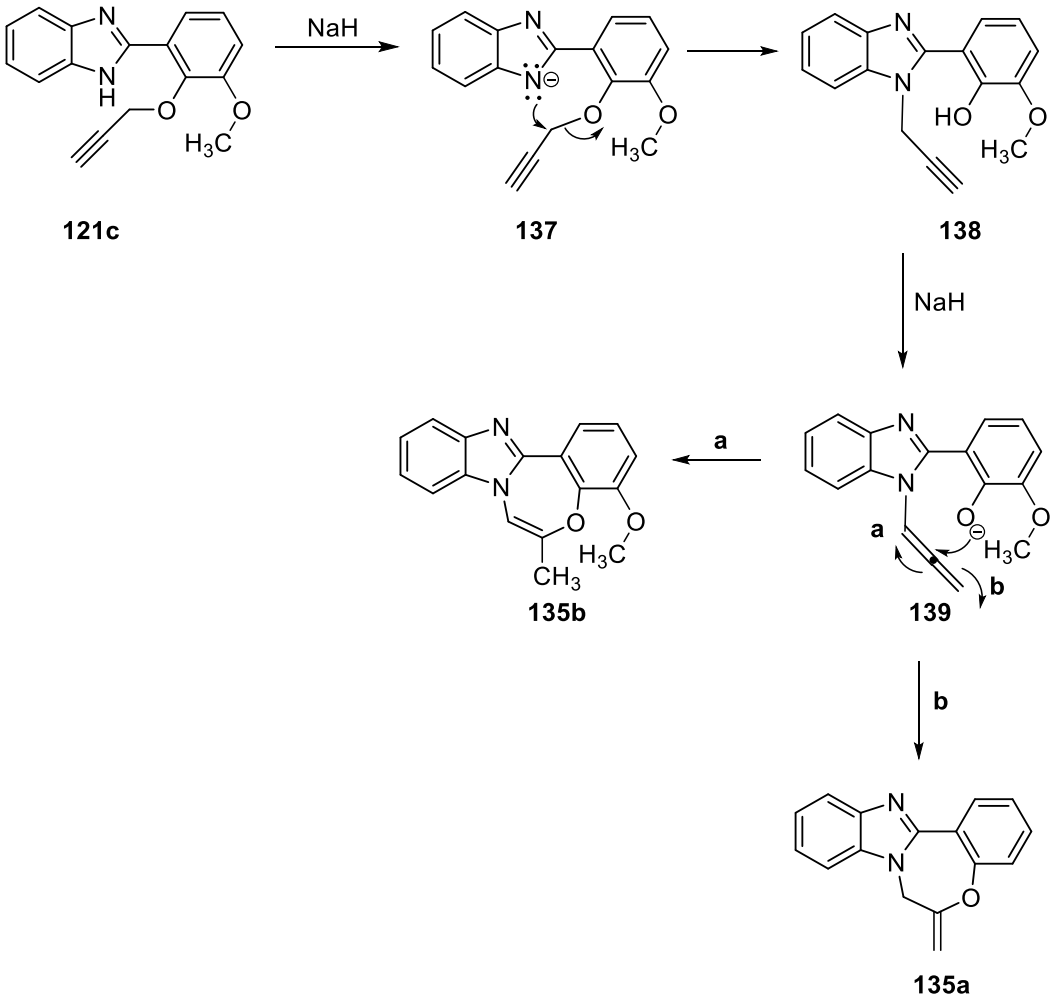

Scheme 55. Formation mechanism of the products **135a** and **135b**

As the next, treatment of **121c** with NaH at 85 °C exclusively resulted in the formation of **123c** and **135b** (Scheme 56).

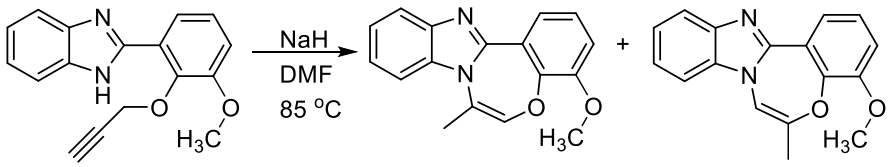

Scheme 56. NaH-supported cyclization reaction of **121c** at 85 °C

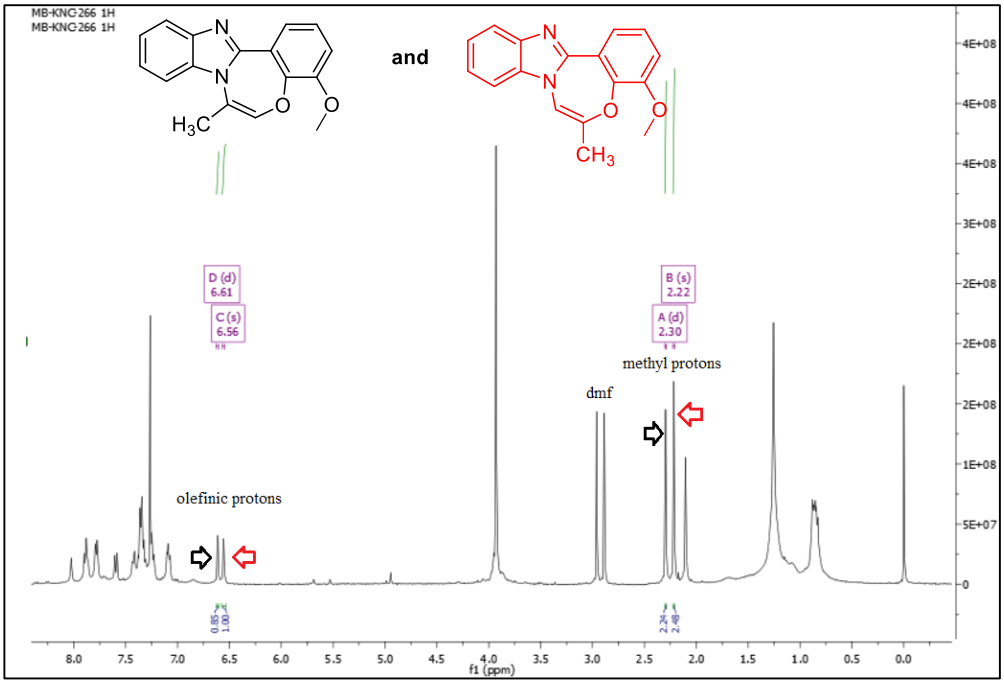

Figure 45. ^{1}H-NMR spectrum of a mixture of **123c** and **135b**.

Unfortunately, the crude reaction could not be purified by coloumn chromatography. The ^{1}H-NMR spectrum of the mixture showed the formation of proposed structures **123c** and **135b** (Figure 45). The olefinic and methyl protons resonating at 6.56 ppm and 2.22 ppm, respectively, correspond the compound **135b**. These signals resonate at higher field compared to those of structure **123c**. In compound **135b**, oxygen in the oxazepine skeleton pushes electrons mesomerically toward the olefin due to close distance. Thus, the chemical shift of olefinic proton resonates at lower ppm than that of compound **123c**. Proposed reaction mechanism for the formation of **123c** is shown in Scheme 57.

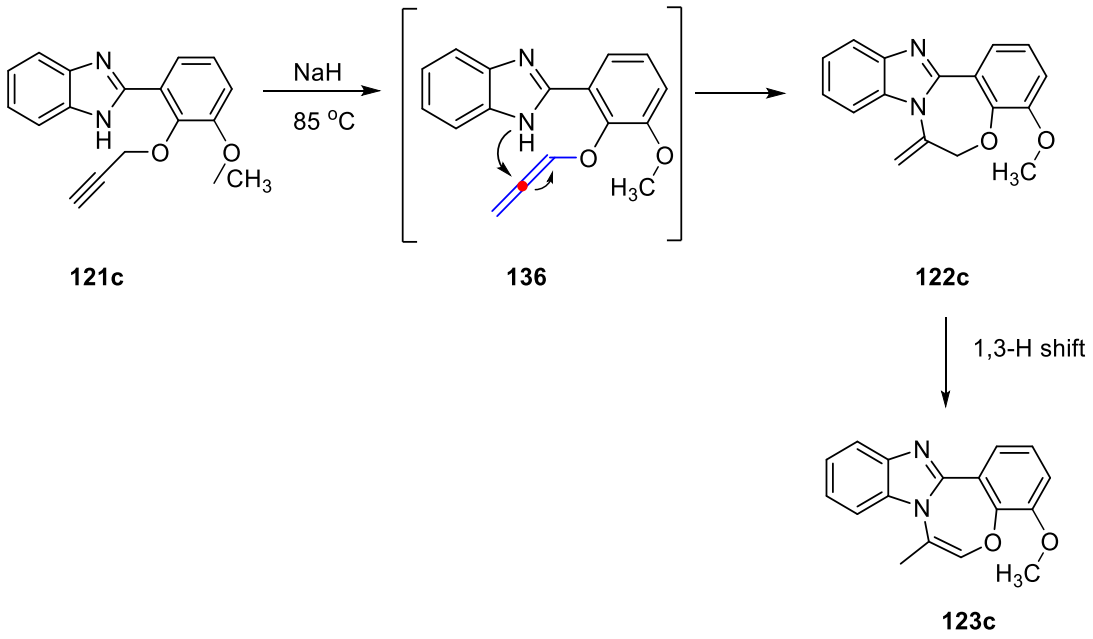

Scheme 57. Tentative mechanism for the formation of **123c**

After the formation of **122c** as discussed in Scheme 54, it undergoes isomerization *via* 1,3-H shift that afforded **123c**.

To evaluate the possible substituent effect on the reaction, unsubstituted derivative **121a** was submitted to the above mentioned cyclization reaction. Similar to the reaction of **121c**, treatment of compound **121a** with NaH in DMF at room temperature afforded three isomeric products; *exo*-configurated **122a** and **140a** and the *endo*-configurated **140b** in a ratio of 7:1:3 (Scheme 58).The ratio of the products was determined by the analysis of the ^{1}H-NMR spectrum. **122a** and **140b** were separated by column chromatography and characterized as the cyclization products with the *exo*- and *endo*-configuration of the double bonds. **140a** could not be isolated but characterized as the *exo*-configurated product by the help of the crude NMR analysis (Figure 46).

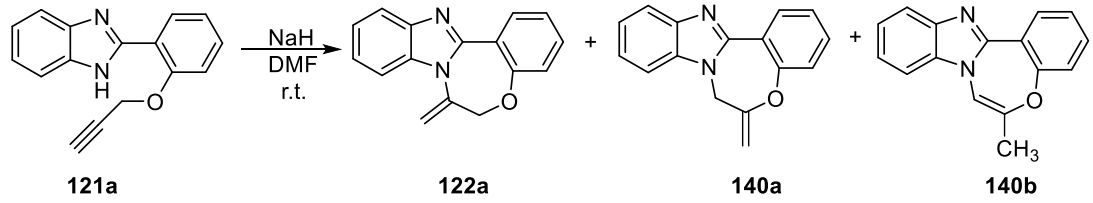

Scheme 58. Cyclization reactions of **121a** and formation of **122a**, **140a**, and **140b**

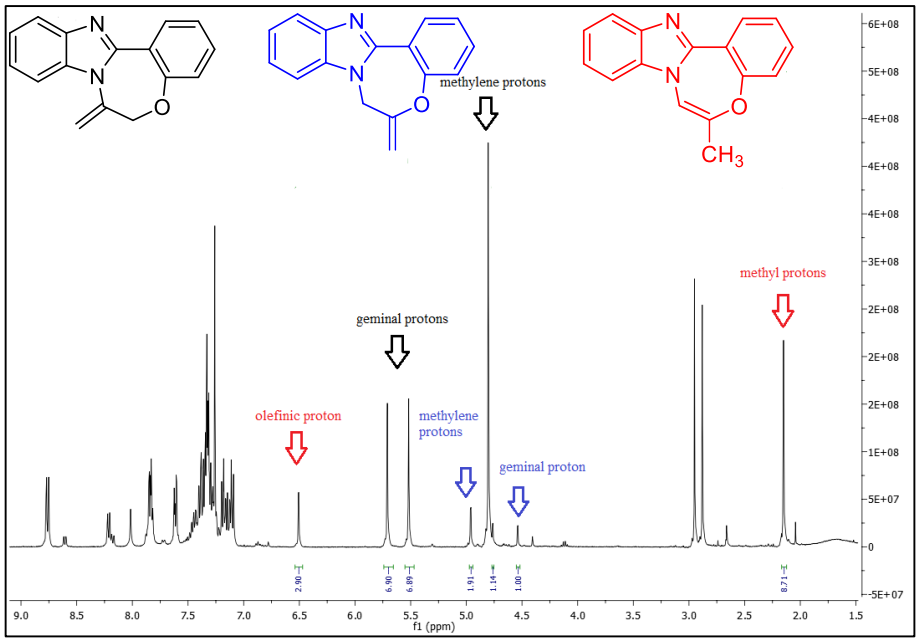

Figure 46. The crude ^{1}H-NMR of a mixture of cyclization reaction of **121a** in DMF

The structures of **122a** and **140a** were determined by comparison of the ^{1}H-NMR spectra with those of compounds **122c** and **135a**. Ethylene geminal protons of **122a** resonate at 5.64 and 5.45 ppm as distinct singlets which are similar to the ones observed in the ^{1}H-NMR spectrum of **122c**. The singlet observed at 4.73 ppm corresponds to methylenic protons adjacent to the oxygen atom (Figure 47).

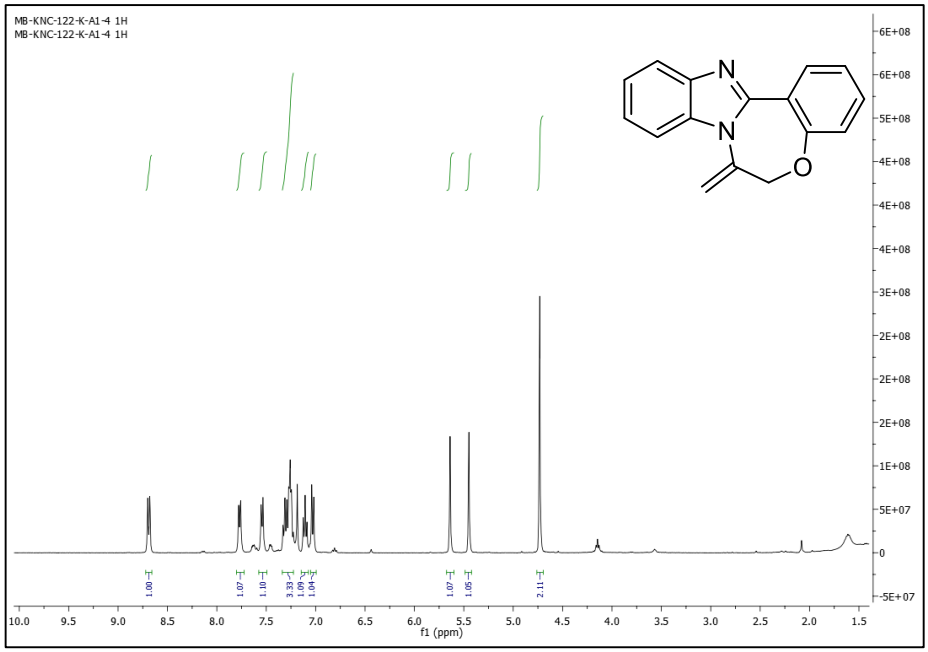

Figure 47. ^{1}H-NMR spectrum of compound **122a**.

With the pure **122a** in hand, we investigated isomerization of the double bond upon termal treatment (Scheme 59). The ^{1}H-NMR spectrum of the crude material demonstrated the full conversion of the *exo*-configurated product **122a** into the *endo*-product **123a** *via* 1,3-H shift.

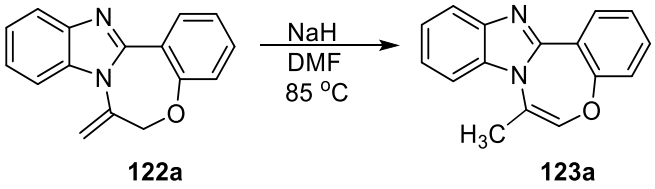

122a **123a**

Scheme 59. Conversion of **122a** to **123a** *via* NaH.

Both **123a** and **140b** have very similar ^{1}H-NMR spectrum. To obtain conclusive evidence that the structures of the compounds **123a** and **140b** are not identical, we mixed the pure **123a** and **140b**. In the ^{1}H-NMR spectrum of **123a** and **140b**, there were two sets of signals confirming that these two compounds are not identical. Methyl protons of **123a** resonate as doublet at 2.30 ppm whereas that of **140b** resonates at 2.16 ppm (Figure 48).

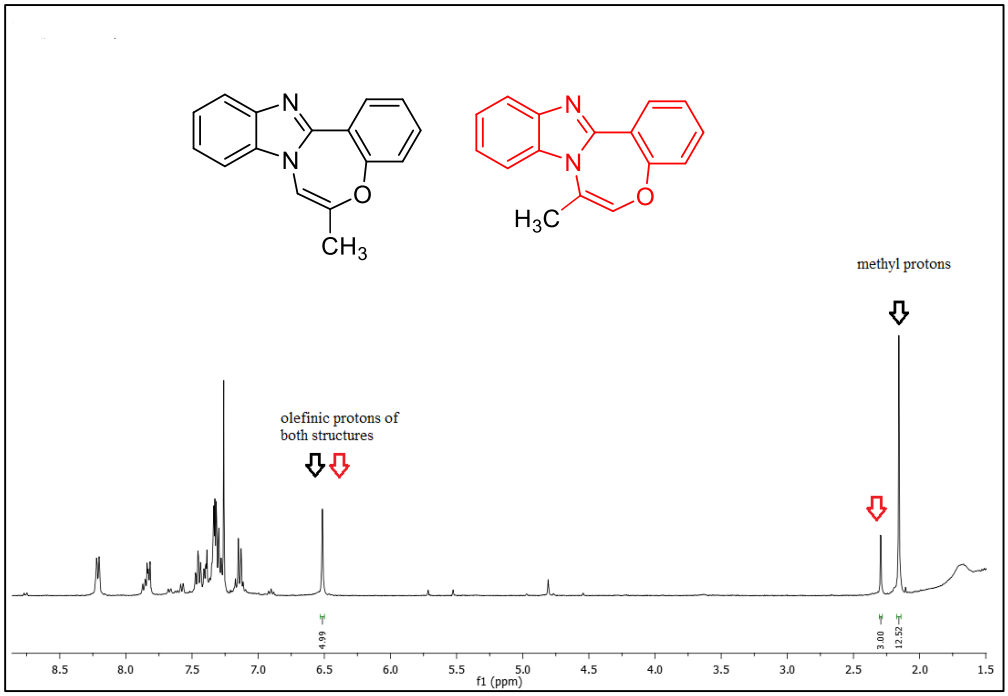

Figure 48. ^{1}H-NMR spectrum of a mixture of **123a** and **140b**

Finally, the brominated derivative **121b** was also submitted to the cyclization reaction (Scheme 60). Treatment of **121b** with NaH in DMF at room temperature over night afforded three isomeric products **122b**, **141a**, and **141b** with the *exo*- and *endo*-configuration of the double bonds in a ratio of 2:1:7. The ratio of the products was determined by the analysis of the ^{1}H-NMR spectrum similar to the previous case (Figure 49).

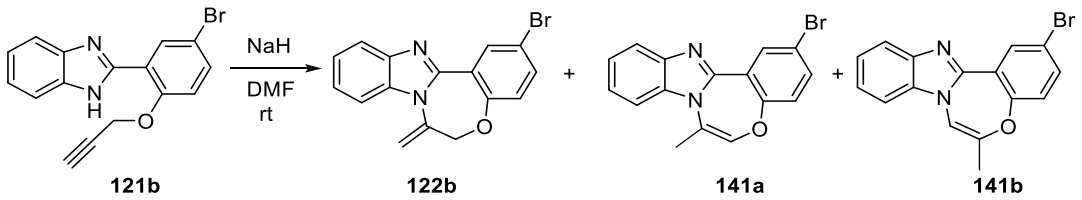

Scheme 60. Cyclization reactions of **121b** and formation of **122b**, **141a**, and **141b**

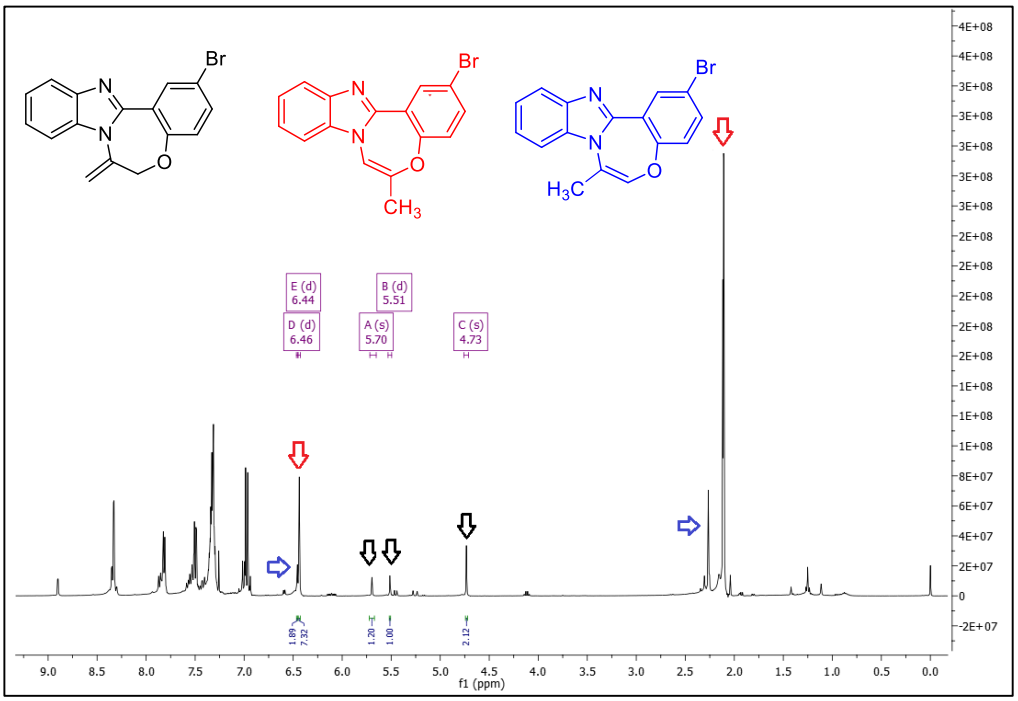

Figure 49. The crude ^{1}H-NMR spectrum of the products formed by cyclization reaction of **121b**

122b and **141b** were seperated by column chromatography. The characterization of the compounds **122b**, **141a** and **141b** was done by comparison of the ^{1}H-NMR spectra with those of compounds **122a**, **123a**, and **140b**. The ^{1}H-NMR spectrum of **141b** is shown in Figure 50. The aromatic protons of brom-substituted benzene ring resonate

at 8.36, 7.45 and 7.01 ppm. It is obviously seen that the proton H-1 is split into doublet due to the coupling with *m*-proton H-2 with a coupling constant of J = 2.5 Hz and the proton H-3 couples only with the proton H-2 with a coupling constant of J = 8.6 Hz. Olefinic proton resonates as quartet at 6.50 ppm and methyl protons resonate at 2.14 ppm as doublet due to the long-range coupling.

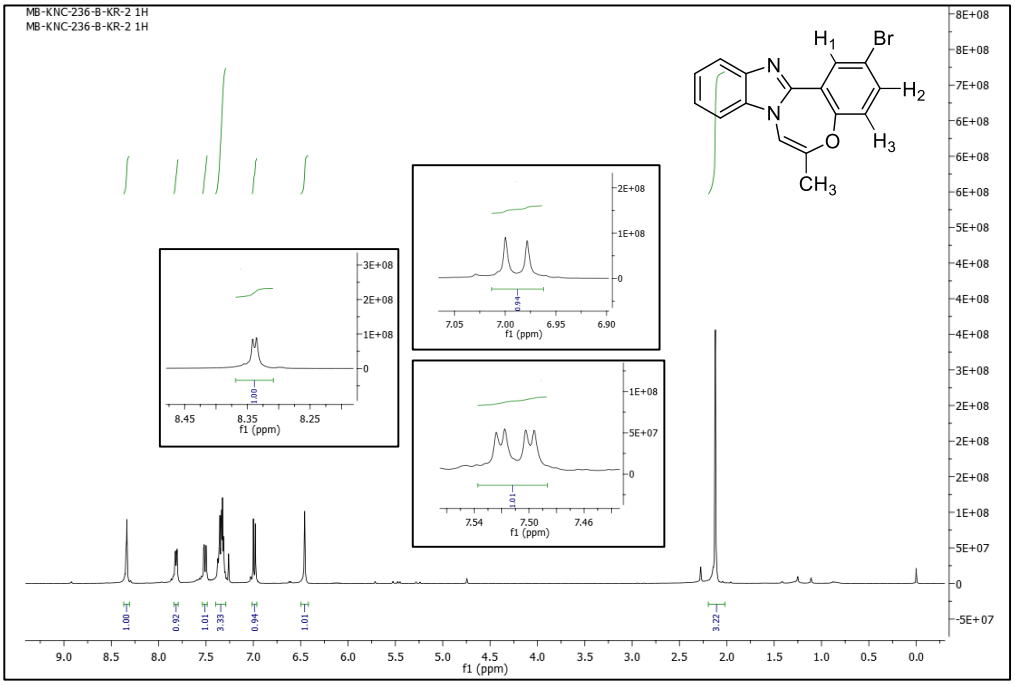

Figure 50. ^{1}H-NMR spectrum of compound **141b**

2.2.11 Synthesis of 1-(2-oxopropyl)-1*H*-pyrrole-2-carbaldehyde (143) and 1-(prop-2-yn-1-yl)-1*H*-pyrrole-2-carbaldehyde (144)

After successful synthesis of *O*-propargylated salicylaldehydes and substituted benzimidazoles, our aim was to show general applicability of this reaction. Starting with pyrrole aldehyde, we carried out a similar reaction and synthesized pyrrole substituted benzimidazoles. The first step was to generate *N*-substituted pyrole aldehydes. NaH was added to a solution of 1*H*-pyrrole-2-carbaldehyde (**142**) in DMF. After observation of hydrogen gas evolution, 1-chloropropan-2-one was added to the reaction mixture and stirred at room temperature to afford **143**. Treatment of **142** with proargyl bromide in presence of potassium carbonate in DMF afforded **144** (Scheme 61).[102]

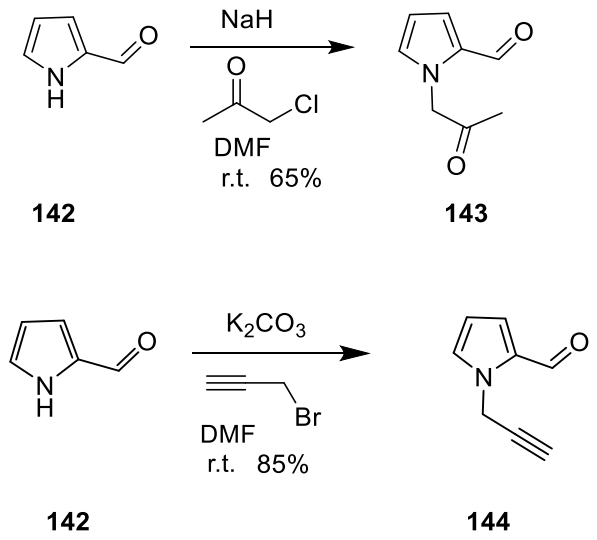

Scheme 61. *N*-propargylation of pyrrolealdehyde

2.2.12 Reaction of 144 and 143 with *o*-diaminobenzene followed by NaH-mediated cyclization reaction

Pyrrole substituted benzimidazole **145** was formed by the reaction of *o*-diaminobenzene and compound **144** as described in the literature.[99] The formed product **145** was treated with NaH at room temperature and afforded cyclization product **146** (Scheme 62).

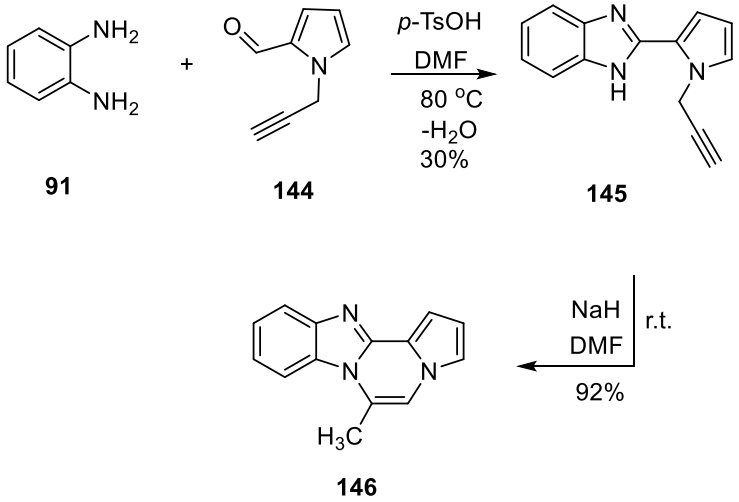

Scheme 62. Reaction pathway for the formation of **146**

For the synthesis of **146** we developed another synthetic way. According to this methodology we first reacted **143** with *o*-diaminobenzene and obtained the corresponding condensation product benzimidazole **147** as the intermediate. The formed benzimidazole **147** underwent cyclization reaction under the same reaction condition to provide **146**. (Scheme 63).

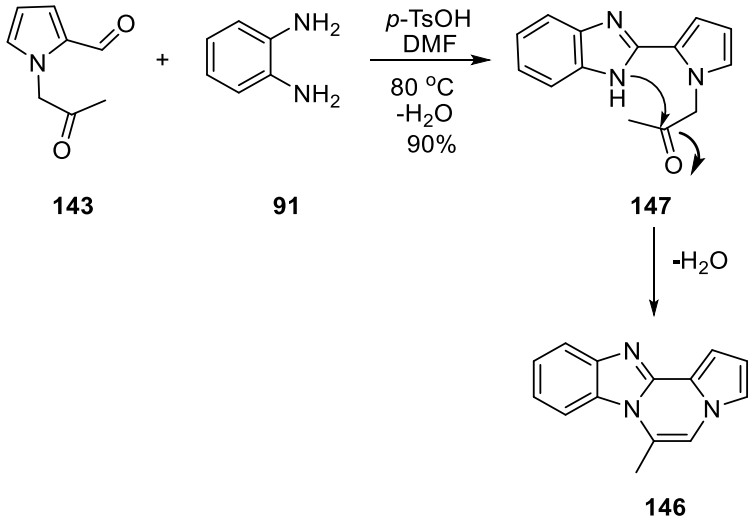

Scheme 63. One-pot synthesis of benzimidazo-pyrrolo-pyrazine **146**

CHAPTER 3

CONCLUSION

The aim of this thesis was to develop methodologies for the synthesis of organic compounds having potential activities in biological science. In the first part, we developed synthetic methodologies for the formation of thienopyridinone and thienodiazepinone derivatives. Firstly, dithiane **36** was used as the starting material to form thiophene ring **37** having an amine functionality at its α-position using the Gewald type reaction (Scheme 64).

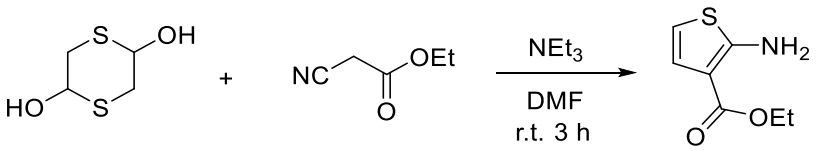

36 **48** **37**

Scheme 64. Synthesis of **37**

After the synthesis of the unsubstituted aminothiophene **37**, 4,5-substitued aminothiophene derivatives **40** and **59** were formed successfully by using the Gewald type reaction (Scheme 65).

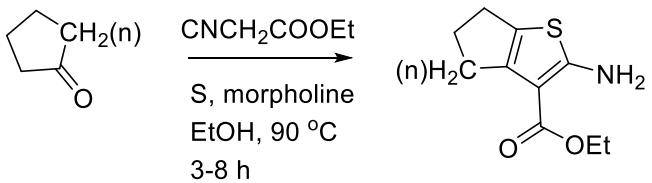

n=2
n=1

40
59

Scheme 65. Synthesis of **40** and **59**

Compound **37** was converted into iodo-thiophene **38** in presence of CuI and *tert*-butyl

nitrite *via* modified Sandmayer reaction. Treatment of **37** with $CuBr_2$ in the presence of *tert*-butyl nitrite afforded compound **63** while **40** formed corresponding bromothiophene **41** (Scheme 66).

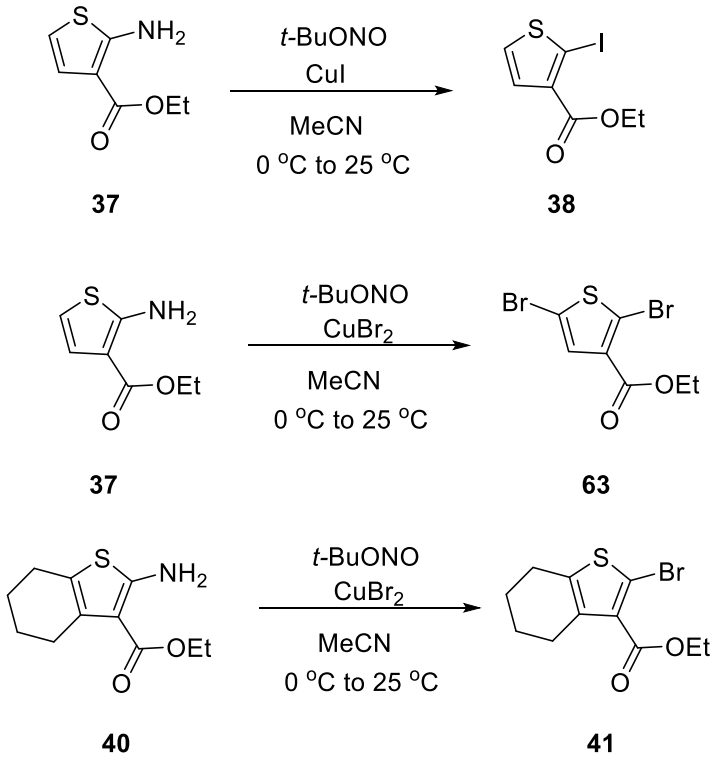

Scheme 66. Halothiophene formation

Sonogashira cross-coupling reaction was used to generate carbon-carbon single bond between the thiophene ring and alkyne derivatives to generate **42** and **45** (Scheme 67).

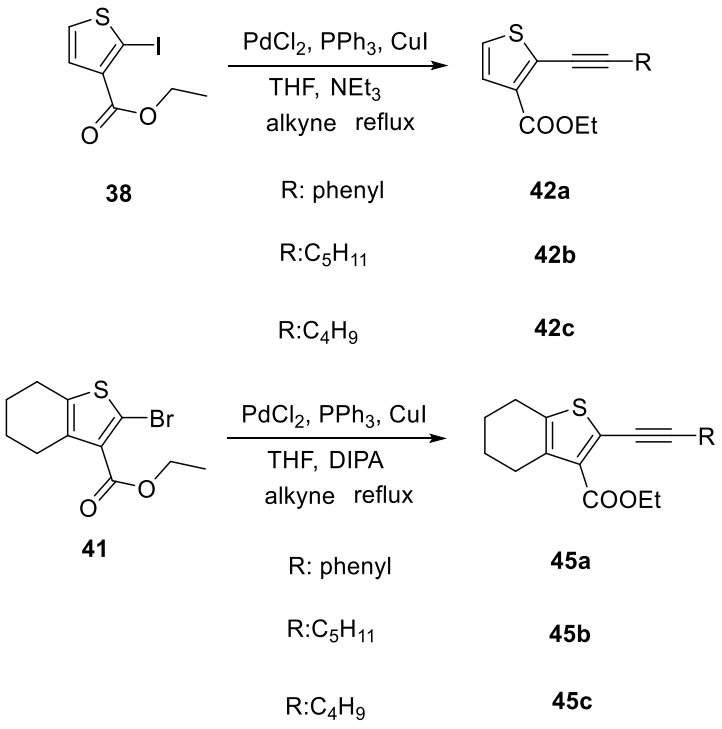

Scheme 67. Alkyne-substituted thiophene synthesis

Hydrazines are very useful compounds for organic synthesis used for the construction of important heterocyclic compounds. The obtained compounds were cyclized in the presence of hydrazine hydrate to give corresponding thienopyridinone and thienodiazepinone derivatives (Scheme 68).

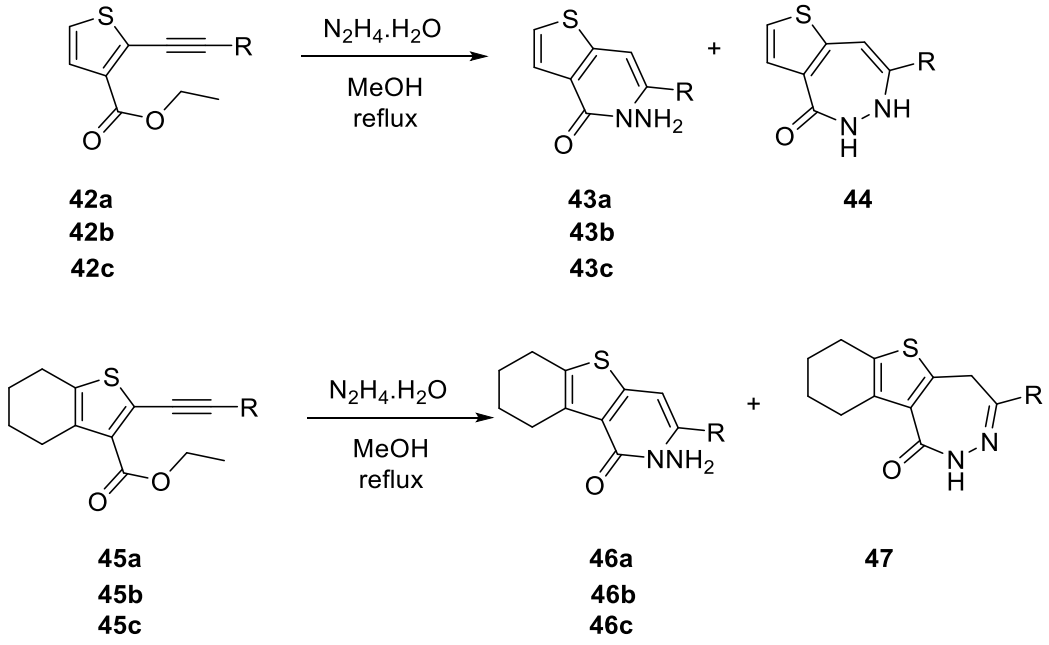

Scheme 68. Cyclization reaction with hydrazine hydrate

In the second part, we developed a new synthetic methodology for benzimidazo-oxazepine derivatives and benzimidazo-pyrrolo-pyrazine. Feist-Benary furan synthesis reaction was used for the formation of the compound **116** which was oxidized to **129** in the presence of SeO_2. Subsequent imidazole formation was achieved with *o*-phenylenediamine (**91**) to afford **117**. Hydrolysis of compound **117** under the basic condition gave cyclization product **118** (Scheme 69).

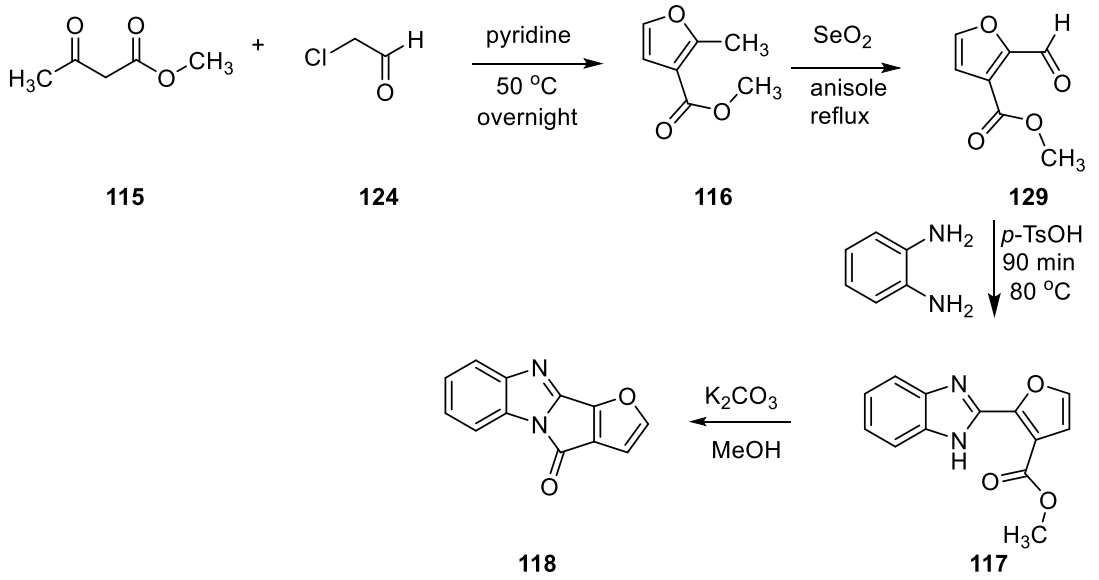

Scheme 69. Synthesis of **118**

Starting with **119**, *O*-propargylated salicylaldehyde derivatives **120** were synthesized in the presence of propargyl bromide under the basic condition. Incorporation of substituents into the alkyne functionality by Sonogashira cross-coupling reaction furnished compound **120d** and **120e** (Scheme 70).

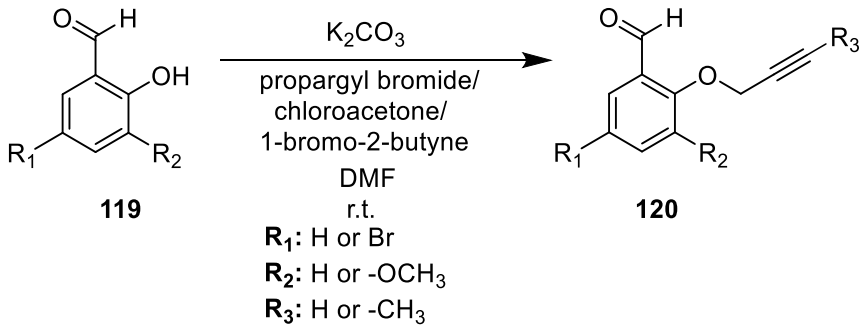

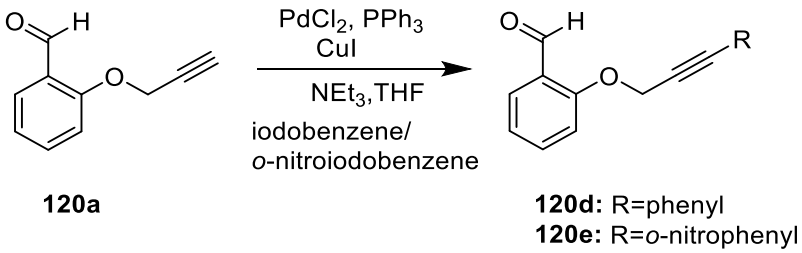

Scheme 70. Synthesis of *O*-propargylated salicylaldehyde derivatives

Benzimidazole skeleton formation was achieved with the reaction of *o*-phenylenediamine **91**. This particular reaction included condensation and oxidation steps respectively to generate **121** (Scheme 71).

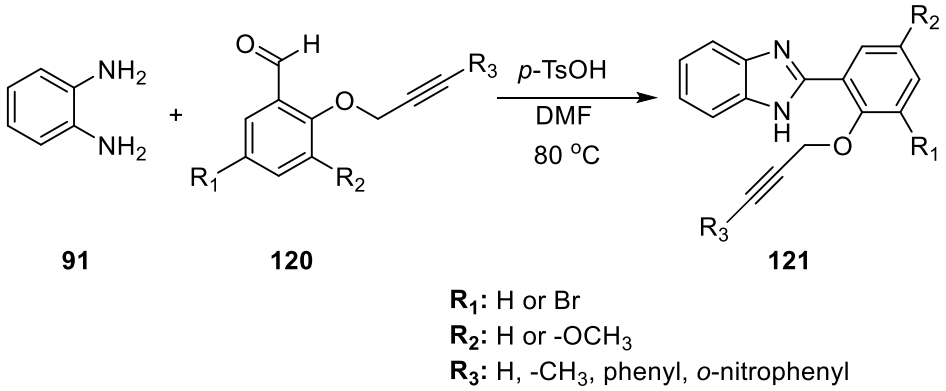

Scheme 71. Benzimidazole formation

Intramolecular NaH-mediated cyclization reaction gave benzimidazo-oxazepine derivatives **122**,**123**, **135**, **140**, and **141** (Scheme 72).

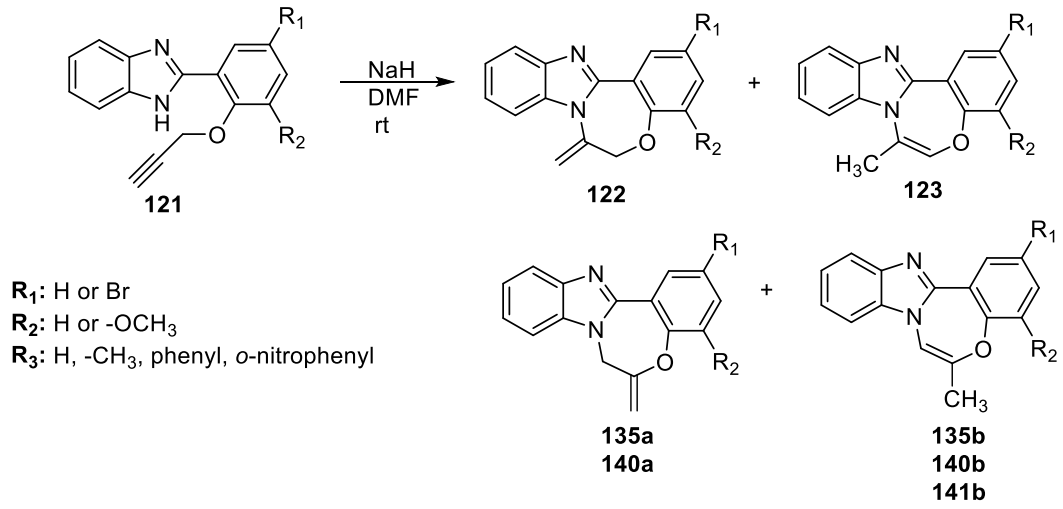

Scheme 72. NaH-mediated cyclization reaction of **121**

Benzimidazo-pyrrolo-pyrazine **146** was synthesized *via* NaH-mediated cyclization reaction of compound **145**. On the other hand, when **143** was reacted with **91** in presence of catalytic amount of acid, it undergoes the cyclization reaction accompanied by attack of nitrogen to ketone carbon atom followed by water elimination that results in the formation of **146** (Scheme 73).

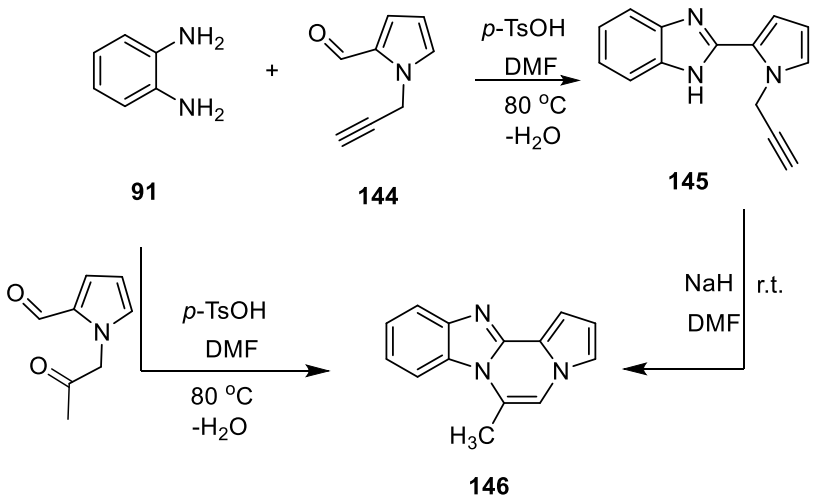

Scheme 73. Benzimidazo-pyrrolo-pyrazine formation

CHAPTER 4

EXPERIMENTAL

4.1 General

Nuclear Magnetic Resonance (^{1}H-NMR, ^{13}C-NMR and 2D-NMR) spectra were recorded on a Bruker Instrument Avance Series-Spectrospin DPX-400 Ultrashield instrument in $CDCl_3$, CD_3OD, CD_3COCD_3 and DMSO-d_6 with TMS as internal reference. Chemical shifts (δ) were expressed in unit parts per million (ppm). Spin multiplicities were specified as singlet (s), doublet (d), doublet of doublets (dd), triplet (t) and multiplet (m) and coupling constants (J) were reported in Hertz (Hz).

Infrared spectra were recorded on a Bruker Platinum ATR FT-IR spectrometer and Thermo Scientific Nicolet IS10 ATR FT-IR spectrometer. Band positions were reported in reciprocal centimeters (cm-1).

Gallenkamp electronic melting point apparatus was used to obtain melting points.

HRMS data were recorded by Agilent Technologies, 6224 TOF LC/MS-T1200 Series applying the electrospray technique. GC-MS data were recorded by Agilent Technology 7890A using Agilent J&W GC HP-5MS, 30m x 0,250mm x 0,25µm (190915-433:325 °C) column.

Column chromatographic separations were performed by using Merck Silica Gel 60 plates with a particle size of 0.063–0.200 mm. Thin layer chromatography (TLC) was performed by using 0.25 mm silica gel plates purchased from Merck.

Compounds were named by using ChemDraw Ultra 11.0 and ACD NMR. Solvents were purified as reported in the literature.

4.1.1 Synthesis of ethyl 2-aminothiophene-3-carboxylate (37)

NEt_3 (2.5 g, 25 mmol) was added dropwise to a mixture of 1,4-dithiane-2,5-diol (3.8 g, 25 mmol) and ethyl cyanoacetate (5.65 g, 50 mmol) in DMF (10 mL) at 0 °C and the resulting mixture was stirred at room temperature for 3 h. After completion of the reaction, water (100 mL) was added to the mixture and extracted with (4 x 20 mL) CH_2Cl_2. Collected organic phases were washed with (2 x 20 mL) water and dried over $MgSO_4$. Evaporation of solvent gave yellow residue which was purified by coloumn chromotography eluting with hexane/EtOAc (5:1) to give **37** (5.9 g, 70%) as a colorless crystal from hexane/ethylacetate, mp 47-49 °C. (lit. mp = 47-48 °C[1]).

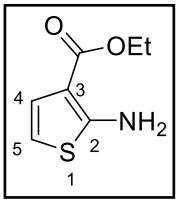

^{1}H-NMR (400 MHz, $CDCl_3$) δ 6.98 (d, J = 5.7 Hz, H5), 6.18 (d, J = 5.7 Hz, H4), 5.93 (br s, 2H, NH_2), 4.28 (q, J = 7.1 Hz, 2H, OCH_2), 1.34 (t, J = 7.1 Hz, 3H, CH_3); **^{13}C-NMR** (100 MHz, $CDCl_3$) δ 165.5, 162.8, 125.9, 107.0, 106.9, 59.7, 14.5; **IR** (cm^{-1}) 3409, 3299, 3172, 2984, 1651, 1266, 1025, 676.

4.2 General procedure for the synthesis of substituted 2-amino-3-carboxylate

A mixture of cyclopentanone/cyclohexanone (11.9 mmol), ethyl cyanoacetate (1.36 mL, 11.9 mmol), morpholine (1.07 mL, 11.9 mmol), and sulphur (0.38 g, 11.9 mmol) in ethanol (15 mL) was heated to reflux temperature and stirred for overnight. After completion of the reaction, solvent was removed under vacuum and the crude solid was washed with cold ethanol and filtered through funnel, dried under vacuum. The crude product was dissolved in dichloromethane (20 mL) and washed with brine (2 x 20 mL). The organic layer was collected, dried over $MgSO_4$ and concentrated under vacuum to give the desired product.

4.2.1 Synthesis of ethyl-2-amino-5,6-dihydro-4*H*-cyclopenta[*b*]thiophene-3-carboxylate (59)

Cyclopentanone (1.05 mL, 11.9 mmol) was reacted with ethyl cyanoacetate (1.36 mL, 11.9 mmol), morpholine (1.07 mL, 11.9 mmol) and sulphur (0.38 g, 11.9 mmol) as

described in general procedure to give the product **59** (0.75 g, 30%) as a brown solid, mp 182-184 °C. (lit. mp = 182.5-183.5 °C[1]).

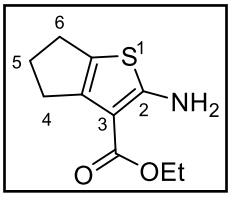

^{1}H-NMR (400 MHz, $CDCl_3$) δ 5.84 (br s, 2H, NH_2), 4.24 (q, J = 7.1 Hz, 2H, OCH_2), 2.81 (m, 2H, H6), 2.72 (m, 2H, H4), 2.31 (m, 2H, H5), 1.33 (t, J = 7.1 Hz, 3H, CH_3); **^{13}C-NMR** (100 MHz, $CDCl_3$) δ 166.3, 165.8, 142.7, 121.3, 102.9, 59.4, 30.7, 28.9, 27.2, 14.4; **IR** (cm^{-1}) 3410, 3292, 3170, 2985, 2903, 2855, 1641, 1490, 1257, 1037, 780.

4.2.2 Synthesis of ethyl 2-amino-4,5,6,7-tetrahydrobenzo[*b*]thiophene-3-carboxylate (40)

Cyclohexanone (1.26 mL, 11.9 mmol) was reacted with ethyl cyanoacetate (1.96 mL, 11.9 mmol), morpholine (1.07 mL, 11.9 mmol) and sulphur (0.38 g, 11.9 mmol) as described in general procedure to give the desired product **40** (1.68 g, 63%) as a light brown solid, mp 116-117 °C. (lit. mp = 116.2-117.2 °C[1]).

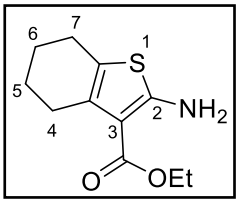

^{1}H-NMR (400 MHz, $CDCl_3$) δ 5.95 (br s, 2H, NH_2), 4.25 (q, J = 7.1 Hz, 2H, OCH_2), 2.70 (m, 2H, H7), 2.49 (m, 2H, H4), 1.75 (m, 4H, H5 and H6), 1.34 (t, J = 7.1 Hz, 3H, CH_3). **^{13}C-NMR** (100 MHz, $CDCl_3$) δ 166.0, 161.7, 132.5, 117.6, 105.9, 59.4, 26.9, 24.5, 23.3, 22.8, 14.5; **IR** (cm^{-1}) 3399, 3293, 3167, 2987, 2938, 2896, 2840, 1644, 1574, 1488, 1290, 1026, 780.

4.3 Synthesis of ethyl 2-iodothiophene-3-carboxylate (38)

CuI (0.84 g, 4.44 mmol) was dissolved in CH_3CN (10 mL) and the resulting mixture was placed into an ice-bath. *Tert*-butyl nitrite (0.83 mL, 7.1 mmol) was added dropwise into the mixture and the resulting mixture was allowed to stir for 10 minute. Aminothiophene **37** (0.76 g, 4.44 mmol) was dissolved in (5 mL) acetonitrile and added dropwise into the reaction mixture and allowed to stir at room temperature. Reaction was followed by TLC. After completion of the reaction, the mixture was filtered through celite then solvent was removed under vacuum. Water (25 mL) was added to the residue and then extracted with EtOAc (2 x 25 mL). Organic phases were

collected and was washed with brine and then dried over $MgSO_4$. After removal of solvent, the residue was purified over silicagel eluting with hexane/ethylacetate (50:1) to give the product **38** as a light brown liquid (120 mg, 10%).[1]

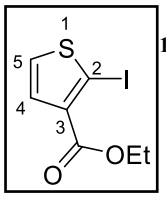

^{1}H-NMR (400 MHz, $CDCl_3$) δ 7.41 (d, J = 5.6 Hz, H5), 7.33 (d, J = 5.6 Hz, H4), 4.35 (q, J = 7.1 Hz, 2H, OCH_2), 1.40 (t, J = 7.1 Hz, 3H, CH_3); **^{13}C-NMR** (100 MHz, $CDCl_3$) δ 162.1, 135.5, 131.3, 129.4, 82.3, 61.0, 14.3; **IR (**cm^{-1}**)** 2917, 1710, 1637, 1242, 1148, 1024, 703.

4.4 General procedure for the synthesis of bromo thiophene

Tert-butyl nitrite (1.55 mL, 13.2 mmol) was added dropwise to a stirred solution of the $CuBr_2$ (1.94 g, 8.83 mmol) in CH_3CN (15 mL)at 0 °C. A solution of aminothiophene (8.83 mmol) in CH_3CN (10 mL) was added to this mixture and stirred at room temperature. The reaction was followed by TLC. After reaction completion, the mixture was filtered through celite and then solvent was removed under vacuum. 25 mL of 10% HCl solution was added to the mixture and then extracted with EtOAc (2 x 25 mL). Combined organic phases were washed with brine and then dried over $MgSO_4$. After removal of solvent, the residue was purified over silicagel eluting with hexane/ethylacetate (10:1) to give the desired compound.[44]

4.4.1 Synthesis of ethyl 2,5-dibromothiophene-3-carboxylate (63)

Tert-butyl nitrite (1.55 mL, 13.2 mmol), $CuBr_2$ (1.94 g, 8.83 mmol) and aminothiophene **37** (1.5 g, 8.83 mmol) were reacted as described in general procedure. The crude product was purified over silicagel eluting with hexane/ethylacetate (10:1) to give the compound **63** as light orange crystals (1.189 g, 43%) from hexane/ethylacetate, mp 35-37 °C.

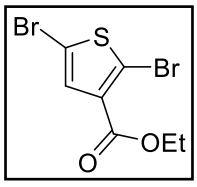

^{1}H-NMR (400 MHz, $CDCl_3$) δ 7.36 (s, 1H), 4.33 (q, J = 7.1 Hz, 2H, OCH_2), 1.37 (t, J = 7.1 Hz, 3H, CH_3); **^{13}C-NMR** (100 MHz, $CDCl_3$) δ 160.8, 131.9, 131.7, 119.0, 111.3, 61.2, 14.2; **IR** (cm^{-1}) 3100, 1716, 1425, 1227, 1148, 1005, 768.

4.4.2 Synthesis of ethyl 2-bromo-4,5,6,7-tetrahydrobenzo[*b*]thiophene-3-carboxylate (41) and ethyl 4,5,6,7-tetrahydrobenzo[*b*]thiophene-3-carboxylate (70)

Tert-butyl nitrite (1.61 mL, 13.8 mmol), $CuBr_2$ (2.02 g, 9.2 mmol) and aminothiophene **37** (2.1 g, 9.2 mmol) were reacted as described in general procedure. The crude product was purified over silicagel eluting with hexane/ethylacetate (15:1) gave the compound **41** as colorless liquid (1.84 g, 70%) and compound **70** as a colorless liquid (0.27 g, 15%).

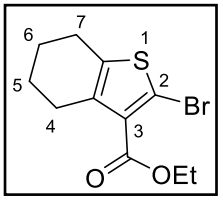

^{1}H-NMR (400 MHz, $CDCl_3$) δ 4.33 (q, J = 7.1 Hz, 2H, OCH_2), 2.75 (m, 2H, H7), 2.63 (m, 2H, H4), 1.78 (m, 4H, H5 and H6), 1.38 (t, J = 7.1 Hz, 3H, CH_3); **^{13}C-NMR** (100 MHz, $CDCl_3$) δ 162.9, 137.3, 136.1, 130.9, 115.3, 60.7, 26.2, 25.0, 22.8, 22.5, 14.3; **IR (**cm^{-1}**)** 2980, 2935, 2858, 1708, 1446, 1217, 1145,1031.

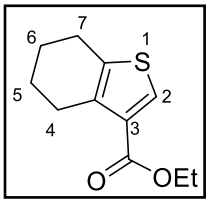

^{1}H-NMR (400 MHz, $CDCl_3$) δ 7.90 (s, H2), 4.29 (q, J = 7.1 Hz, 2H, OCH_2), 2.89 (qt, 2H, H7), 2.75 (qt, 2H, H4), 1.81 (m, 4H, H5 and H6), 1.35 (t, J = 7.1 Hz, 3H, CH_3); **^{13}C-NMR** (100 MHz, $CDCl_3$) δ 163.4, 135.8, 131.5, 130.3, 115.3, 60.1, 25.9, 25.4, 23.0, 22.5, 14.3; **IR** (cm^{-1}) 2927, 2854, 1709, 1456, 1212, 1114,1034, 735.

4.5 General procedure of Sonogashira cross-coupling reaction to iodothiophene

$PdCl_2$ (0.0026 g, 0.015 mmol), CuI (0.0085 g, 0.045mmol) and PPh_3 (0.015 g, 0.06 mmol) in THF (15 mL) were put into two-necked round bottom flask and allowed to stir for 10 minute under nitrogen atmosphere. NEt_3 (0.15 mL, 1.11 mmol) and alkyne (0.81 mmol) were added subsequently into reaction vessel. After stirring for 5 minute, iodothiophene (0.2 g, 0.744 mmol) was added and the resulting mixture was heated to reflux temperature and stirred for 4 h. After completion of the reaction, the mixture was cooled to room temperature, filtered through celite bed and the filtrate was concentrated under vacuum. Water (30 mL) was added to crude mass and then extracted with ethyl acetate (3 x 30 mL). The organic layers were collected, combined, washed with brine (2 x 25 mL), and dried over anhydrous $MgSO_4$. The crude product was purified by column chromatography on silica gel to afford the desired product.

4.5.1 Synthesis of ethyl 2-(phenylethynyl)thiophene-3-carboxylate (42a)

$PdCl_2$ (0.0026 g, 0.015 mmol), CuI (0.0085 g, 0.045mmol) and PPh_3 (0.015 g, 0.06 mmol), NEt_3 (0.15 mL, 1.11 mmol), phenylacetylene (0.088 mL, 0.81 mmol), iodothiophene (0.2 g, 0.744 mmol) in THF (15 mL) were reacted as described in general procedure. The crude product was purified by column chromatography on silica gel using 10:1 hexane/ethyl acetate to afford the desired product **42a** as a light green liquid (0.08 g, 45%).

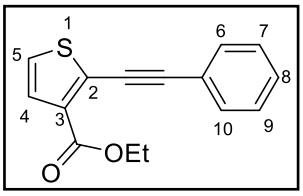

^{1}H-NMR (400 MHz, $CDCl_3$) δ 7.57 (m, 2H, H6 and H10), 7.47 (d, J = 5.3 Hz, H5), 7.37 (m, 3H, H7, H8, and H9), 7.20 (d, J = 5.3 Hz, H4), 4.39 (q, J = 7.1 Hz, 2H, OCH_2), 1.42 (t, J = 7.1 Hz, 3H, CH_3); **^{13}C-NMR** δ (100 MHz, $CDCl_3$) 162.1, 134.4, 131.6, 129.3, 129.0, 128.9, 128.4, 125.7, 122.7, 98.9, 81.8, 61.0, 14.3; **IR** (cm^{-1}) 2980, 2206, 1704, 1238, 1151, 1024, 688.[1]

4.5.2 Synthesis of ethyl 2-(hept-1-yn-1-yl)thiophene-3-carboxylate (42b)

$PdCl_2$ (0.0027 g, 0.017 mmol), CuI (0.0096 g, 0.053 mmol), PPh_3 (0.017 g, 0.071 mmol) NEt_3 (0.18 mL, 1.35 mmol), iodothiophene (0.25 g, 0.89 mmol) and 1-heptyne (0.13 mL, 0.97 mmol) in THF (15 mL) were reacted as described in general procedure. The crude product was purified by column chromatography on silica gel using 15:1 hexane/ethyl acetate to afford the desired compound **42b** as a light brown liquid (0.13 g, 57%).

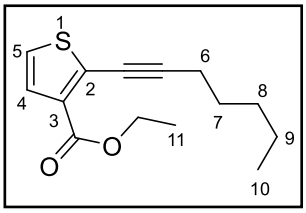

^{1}H-NMR (400 MHz, $CDCl_3$) δ 7.38 (d, J = 5.4 Hz, H5), 7.08 (d, J = 5.4 Hz, H4), 4.34 (q, J = 7.1 Hz, 2H, OCH_2), 2.50 (t, J = 7.1 Hz, 2H, H6), 1.65 (m, 2H, H7), 1.45 (m, 2H, H8), 1.37 (m, 5H, H9 and H11), 0.9 (t, J = 7.3 Hz, 3H, H10); **^{13}C-NMR** (100 MHz, $CDCl_3$) δ 162.5, 133.6, 130.6, 128.6, 124.4, 101.4, 72.9, 60.6, 31.1, 28.1, 22.2, 20.1, 14.3, 13.9; **IR** (cm^{-1}) 2956, 2930, 2859, 2226, 1704, 1267, 1146, 1025, 708; **HRMS-TOF [M + H]+** Calcd for $C_{14}H_{18}SO_2$ 251.11003, found: 251.11125.

4.5.3 Synthesis of ethyl 2-(hex-1-yn-1-yl)thiophene-3-carboxylate (42c)

$PdCl_2$ (0.0018 g, 0.011 mmol), CuI (0.0058 g, 0.033 mmol), PPh_3 (0.011 g, 0.044 mmol) NEt_3 (0.11 mL, 0.85 mmol), iodothiophene (0.16 g, 0.57 mmol) and 1-hexyne (0.072 mL, 0.63 mmol) in THF (10 mL) were reacted as described in general procedure. The crude compound was purified by column chromatography on silica gel using 10:1 hexane/ethyl acetate to afford the desired compound **42c** as a yellow liquid (0.08 g, 60%).

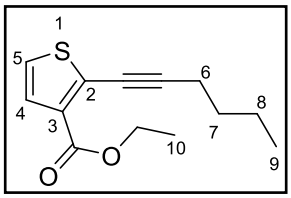

^{1}H-NMR (400 MHz, $CDCl_3$) δ 7.38 (d, J = 5.4 Hz, H5), 7.08 (d, J = 5.4 Hz, H4), 4.34 (q, J = 7.1 Hz, 2H, OCH_2), 2.51 (t, J = 7.1 Hz, 2H, H6), 1.63 (m, 2H, H7), 1.49 (m, 2H, H8), 1.38 (t, J = 7.1 Hz, 3H, H10), 0.9 (t, J = 7.3 Hz, 3H, H9); **^{13}C-NMR** (100 MHz, $CDCl_3$) δ 162.5, 133.5, 130.4, 128.6, 124.4, 101.1, 72.4, 60.6, 30.5, 22.1, 19.8, 14.3, 13.6; **IR** (cm^{-1}) 2957, 2932, 2871, 2224, 1704, 1269, 1146, 1025, 70; **HRMS-TOF [M + H]+** Calcd for $C_{13}H_{16}SO_2$ 237.09560, found: 237.09438.

4.6 General procedure of Sonogashira cross-coupling reaction to bromothiophene 41 and 63

$PdCl_2$ (0.0026 g, 0.015 mmol), CuI (0.0085 g, 0.045mmol) and PPh_3 (0.015 g, 0.06 mmol) in THF (15 mL) were put into two-necked round bottom flask and allowed to stir for 10 minute under nitrogen atmosphere. DIPA (0.15 mL, 1.11 mmol) and alkyne (0.81 mmol) were added subsequently into reaction vessel. After stirring for 5 minute, bromothiophene (0.744 mmol) was added and the resulting mixture was heated to reflux temperature. Reaction was controlled by TLC. After completion of the reaction, the mixture was cooled to room temperature, filtered through celite bed and the filtrate was concentrated under vacuum. Water (20 mL) was added to crude mass and then extracted with ethyl acetate (3 x 20 mL). The organic layers were collected, combined, washed with brine (2 x 25 mL), and dried over anhydrous $MgSO_4$. The crude product was purified by column chromatography on silica gel to afford the desired product.

4.6.1 Synthesis of ethyl 2-(phenylethynyl)-4,5,6,7-tetrahydrobenzo[*b*]thiophene -3-carboxylate (45a)

$PdCl_2$ (0.0026 g, 0.015 mmol), CuI (0.0085 g, 0.045mmol) and PPh_3 (0.015 g, 0.06 mmol), DIPA (0.15 mL, 1.11 mmol), bromothiophene **41** (0.21 g, 0.744 mmol) and phenylacetylene (0.088 mL, 0.81 mmol) in THF (15 mL) were reacted as described in general procedure. The crude product was purified by column chromatography on silica gel using 15:1 hexane/ethyl acetate to afford the desired compound **45a** as an pale yellow crystal from hexane/ethylacetate (0.14 g, 60%), mp 82-84 °C. (lit. mp = 88.5-89.5 °C[1]).

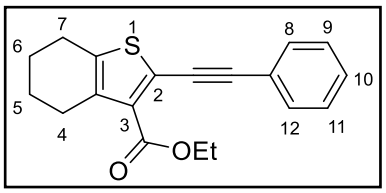

^{1}H-NMR (400 MHz, $CDCl_3$) δ 7.52 (m, 2H, H8 and H12), 7.34 (m, 3H, H9, H10, and H11), 4.36 (q, J = 7.1 Hz, 2H, OCH_2), 2.83 (qt, 2H, H7), 2.73 (qt, 2H, H4), 1.81, m, 4H, H6 and H5), 1.39 (t, J = 7.1 Hz, 3H, CH_3); **^{13}C-NMR** (100 MHz, $CDCl_3$) δ 163.2, 138.0, 136.3, 133.1, 131.4, 128.5, 128.4, 125.7, 123.1, 97.6, 82.9, 60.5, 26.2, 25.4, 22.8, 22.4, 14.4; **IR** (cm^{-1}) 2946, 2905, 2196, 1697, 1224, 1158, 753, 690.[1]

4.6.2 Synthesis of ethyl 2-(hept-1-yn-1-yl)-4,5,6,7-tetrahydrobenzo[*b*]thiophene-3-carboxylate (45b)

$PdCl_2$ (0.0026 g, 0.015 mmol), CuI (0.0085 g, 0.045mmol), PPh_3 (0.015 g, 0.06 mmol), DIPA (0.15 mL, 1.11 mmol), bromothiophene **41** (0.21 g, 0.744 mmol) and 1-heptyne (0.11 mL, 0.81 mmol) in THF (15 mL) were reacted as described in general procedure. The crude product was purified by column chromatography on silica gel using 15:1 hexane/ethyl acetate to afford the desired compound **45b** as a yellow solid (0.15 g, 72%), mp 204-206 °C.

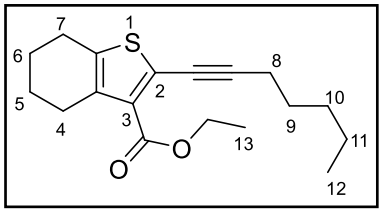

^{1}H-NMR (400 MHz, $CDCl_3$) δ 4.32 (q, J = 7.1 Hz, 2H, OCH_2, 2.78 (qt, 2H, H7), 2.68 (qt, 2H, H4), 2.47 (t, J = 7.1 Hz, 2H, H8), 1.79 (m, 4H, H5 and H6), 1.62 (m, 2H, H9), 1.42 (m, 2H, H10), 1.37 (m, 5H, H11 and H13) , 0.91 (t, J = 7.1 Hz, 3H, H12); **^{13}C-NMR** (100 MHz, $CDCl_3$) δ 163.4, 136.4,

135.7, 132.4, 127.0, 99.8, 73.7, 60.3, 31.1, 28.2, 26.1, 25.2, 22.8, 22.5, 22.2, 20.1 14.3, 13.9; **IR** (cm^{-1}) 2945, 1608, 1555, 1436, 1272, 1233,1047, 945, 746; **HRMS-TOF [M + H]+** Calcd for $C_{18}H_{24}SO_2$ 305.16011, found: 305.15698.

4.6.3 Synthesis of ethyl 2-(hex-1-yn-1-yl)-4,5,6,7-tetrahydrobenzo[*b*]thiophene-3-carboxylate (45c)

$PdCl_2$ (0.0035 g, 0.02 mmol), CuI (0.011 g, 0.06mmol), PPh_3 (0.02 g, 0.08 mmol), DIPA (0.21 mL, 1.57 mmol), bromothiophene **41** (0.30 g, 1.06 mmol) and 1-hexyne (0.13 mL, 1.17 mmol) in THF (15 mL) were reacted as described in general procedure. The crude product was purified by column chromatography on silica gel using 20:1 hexane/ethyl acetate to afford the desired compound **45c** as a brown liquid (0.14 g, 45%).

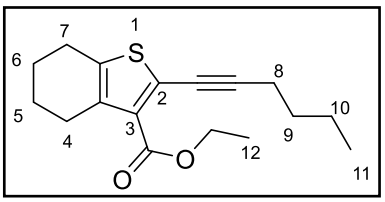

^{1}H-NMR (400 MHz, $CDCl_3$) δ 4.31 (q, J = 7.2 Hz, 2H, OCH_2), 2.78 (qt, 2H, H7), 2.68 (qt, 2H, H4), 2.47 (t, J = 7.1 Hz, 2H, H8), 1.79 (m, 4H, H5 and H6), 1.61 (m, 2H, H9), 1.47 (m, 2H, H10), 1.37 (t, J = 7.1 Hz, 3H, H12), 0.91 (t, J = 7.2 Hz, 3H, H11); **^{13}C-NMR** (100 MHz, $CDCl_3$) δ 163.4, 136.4, 135.7, 132.4, 127.0, 99.8, 73.7, 60.3, 30.6, 26.1, 25.2, 22.8, 22.5, 22.1, 19.8 14.3, 13.6; **IR** (cm^{-1}) 2928, 2859, 2196, 1704, 1634, 1271, 1183, 1032, 753, 703; **HRMS-TOF [M + H]+** Calcd for $C_{17}H_{22}SO_2$ 291.14380, found: 291.14133.

4.6.4 Synthesis of ethyl 2,5-bis(phenylethynyl)thiophene-3-carboxylate (74)

$PdCl_2$ (0.0031 g, 0.018 mmol), CuI (0.010 g, 0.05 mmol), PPh_3 (0.018 g, 0.072 mmol), DIPA (0.18 mL, 1.32 mmol), bromothiophene **63** (0.16 g, 0.45 mmol) and phenylacetylene (0.11 mL, 1.00 mmol) in THF (15 mL) were reacted as described in general procedure. The crude mass was purified by column chromatography on silica gel using 20:1 hexane/ethyl acetate to afford the desired compound **74** as a yellow solid (0.07 g, 45%), mp 72-74 °C.

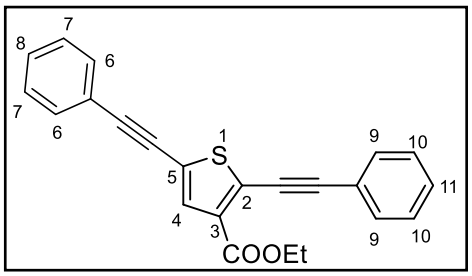

^{1}H-NMR (400 MHz, $CDCl_3$) δ 7.60 (s, H4), 7.58 (m, 2H, H9), 7.52 (m, 2H, H6), 7.38 (m, 6H, H7, H8, H10, and H11), 4.38 (q, J =7.1 Hz, 2H, OCH_2), 1.40 (t, J = 7.1 Hz, 3H, CH_3); **^{13}C-NMR** (100 MHz, $CDCl_3$) δ 161.6, 133.1, 131.7, 131.7, 131.6, 129.2, 129.2, 129.0, 128.5, 123.1, 122.5, 122.2, 99.6, 94.5, 81.6, 61.0, 14.3; **IR** (cm^{-1}) 3055, 2955, 2915, 2847, 2204, 1708, 1214, 1024, 729, 687; **HRMS-TOF [M + H]+** Calcd for $C_{23}H_{16}SO_2$ 357.09777, found: 357.09438.

4.7 General procedure of cyclization reaction

Alkyne-subsituted thiophene (0.5 mmol) was dissolved in MeOH (5 mL) and allowed to stir for 5 min under nitrogen atmosphere. Hydrazine monohydrate (0.23 mL, 5 mmol) was added into reaction vessel and the resulting mixture was heated at the reflux temperature. Reaction was controlled by TLC. Removal of the solvent under vacuum gave residue which was then purified by coloumn chromotography on silica gel.

4.7.1 Synthesis of 5-amino-6-phenylthieno[3,2-*c*]pyridin-4(5*H*)-one (43a)

A solution of compound **42a** (0.13 g, 0.5 mmol) in MeOH (5 mL) was reacted with hydrazine monohydrate (0.23 mL, 5 mmol) as described in general procedure to give the cyclization product **43a** as a yellow solid (0.06 g, 55%), mp 126-128 °C and **44** as a pale yellow solid, (0.016 g, 15%), mp 214-216 °C.

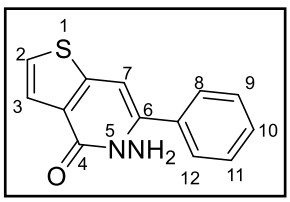

^{1}H-NMR (400 MHz, $CDCl_3$) δ 7.61 (d, J = 5.4 Hz, H2), 7.46, (m, 2H, H8 and H12), 7.40 (m, 3H, H9, H10, and H11), 7.24 (d, J = 5.4 Hz, H3), 6.64 (s, H7), 5.03 (bs, 2H, NH_2); **^{13}C-NMR** (100 MHz, $CDCl_3$) δ 159.7, 146.5, 134.5, 133.5, 129.2, 129.1, 128.7, 125.0, 124.8, 111.1, 102.7; **IR** (cm^{-1}) 3303, 3187, 3303, 2917, 2849, 1610, 1553, 1494, 1310, 767, 696; **HRMS-TOF**; [M + H]+ Calcd for $C_{13}H_{10}N_2SO$ 243.05954, found: 243.05866.

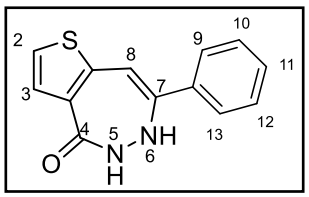

^{1}H-NMR (400 MHz, $CDCl_3$) δ 10.05 (s, NH), 7.67 (m, 2H, H9 and H13), 7.55-7.45 (m, 5H, H2, H8, H10, H11, and H12), 7.31(d, J = 5.3 Hz, H3), 6.99 (s, NH); **IR** (cm^{-1}) 3090, 2981, 1621, 11497, 1272, 1169, 986, 755, 680, 632; **HRMS-TOF**; [M + H]+ Calcd for $C_{13}H_{10}N_2SO$ 243.05985, found: 243.05866.

4.7.2 Synthesis of 5-amino-6-pentylthieno[3,2-*c*]pyridin-4(5*H*)-one (43b)

Compound **42b** (0.12 g, 0.48 mmol) in MeOH (5 mL) was reacted with hydrazine monohydrate (0.23 mL, 5 mmol) as described in general procedure to give the cyclization product **43b** as pale yellow crystals (0.09 g, 80%), mp 30-32 °C.

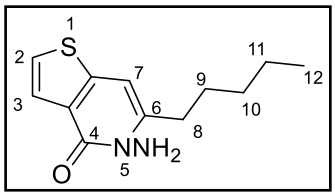

^{1}H-NMR (400 MHz, $CDCl_3$) δ 7.59 (d, J = 5.4 Hz, H2), 7.20 (d, J = 5.4 Hz, H3), 6.56 (s, H7), 4.96 (s, 2H, NH_2), 2.85 (t, J = 7.7 Hz, 2H, H8), 1.68 (m, 2H, H9), 1.40 (m, 4H, H10 and H11), 0.98 (t, J = 7.3 Hz, 3H, H12); **^{13}C-NMR** (100 MHz, $CDCl_3$) δ 158.1, 146.1, 144.4, 126.4, 123.7, 122.5, 99.0, 31.7, 30.4, 27.0, 21.4, 12.9; **IR** (cm^{-1}) 3301, 2927, 2857, 1637, 1558, 724, 703; **HRMS-TOF**; [M + H]+ Calcd for $C_{12}H_{16}N_2SO$ 237.10844, found: 237.10561.

4.7.3 Synthesis of 5-amino-6-butylthieno[3,2-*c*]pyridin-4(5*H*)-one (43c)

Compound **42c** (0.06 g, 0.26 mmol) in MeOH (2.5 mL) was reacted with hydrazine monohydrate (0.12 mL, 2.5 mmol) as described in general procedure to give the cyclization product **43c** as a pale yellow solid (0.05 g, 95%), mp > 300 °C.

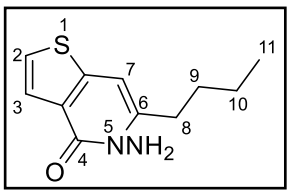

^{1}H-NMR (400 MHz, $CDCl_3$) δ 7.59 (d, J = 5.4 Hz, H2), 7.20 (d, J = 5.4 Hz, H3), 6.56 (s, H7), 4.96 (s, 2H, NH_2), 2.85 (t, J = 7.7 Hz, 2H, H8), 1.68 (m, 2H, H9), 1.45 (m, 2H, H10), 0.98 (t, J = 7.3 Hz, 3H, H11); **^{13}C-NMR** (100 MHz, $CDCl_3$) δ 159.2, 147.1, 145.4, 127.4, 124.7, 123.5, 99.9, 32.4, 30.5, 22.4, 13.9; **IR** (cm^{-1}) 3184, 3079, 2949, 2929, 2870, 1644, 1054, 715; **HRMS-TOF**; [M + H]+ Calcd for $C_{11}H_{14}N_2SO$ 223.09207, found: 223.08996.

4.7.4 Synthesis of 2-amino-3-phenyl-6,7,8,9-tetrahydrobenzo[4,5]thieno[3,2-*c*]pyridin-1(2*H*)-one (46a) and 4-phenyl-2,5,7,8,9,10-hexahydro-1*H*-benzo[4,5] thieno[3,2-*d*][1,2]diazepin-1-one (47)

Compound **45a** (0.2 g, 0.64 mmol) in MeOH (6.5 mL) was reacted with hydrazine monohydrate (0.31 mL, 6.5 mmol) as described in general procedure to give the cyclization products **46a** (0.07 g, 40%) as a pale yellow solid, mp 146-148 °C and **47** (0.66 g, 35%) as white tiny needles from hexane/EtOAc, mp 235-237 °C.

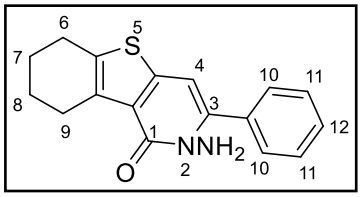

^{1}H-NMR (400 MHz, $CDCl_3$) δ 7.51 (m, 2H, H10), 7.45 (m, 3H, H11 and H12), 6.61 (s, H4), 5.11 (bs, 2H, NH_2), 3.16 (bs, 2H, H9), 2.80 (bs, 2H, H6), 1.88 (m, 4H, H8 and H7); **^{13}C-NMR** (100 MHz, $CDCl_3$) δ 158.2, 145.0, 142.4, 135.3, 134.0, 129.2, 128.9, 128.6, 128.1, 126.5, 102.9, 26.0, 25.5, 23.0, 22.4; **IR** (cm^{-1}) 3301, 3059, 2928, 2830, 1635, 1557, 769, 703. **HRMS-TOF**; [M + H]+ Calcd for $C_{17}H_{16}N_2SO$ 297.10850, found: 297.10561.

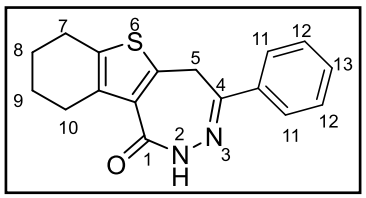

^{1}H-NMR (400 MHz, $CDCl_3$) δ 8.61 (s, NH), 7.77 (m, 2H, H11), 7.42 (m, 3H, H12 and H13), 4.07 (s, 2H, H5), 2.86 (t, J = 6.1 Hz, 2H, H7), 2.69 (t, J = 5.9 Hz, 2H, H10), 1.79 (m, 4H, H8 and H9); **^{13}C-NMR** (100 MHz, $CDCl_3$) δ 164.0, 158.0, 140.1, 137.2, 135.3, 134.5, 130.6, 130.4, 128.8, 127.0, 30.2, 25.7, 25.0, 23.1, 22.3; **IR** (cm^{-1}) 3162, 3050, 2919, 2850, 1636, 1432, 758, 687; **HRMS-TOF**; [M + H]+ Calcd for $C_{17}H_{16}N_2SO$ 297.10697, found: 297.10561.

4.7.5 Synthesis of 2-amino-3-pentyl-6,7,8,9-tetrahydrobenzo[4,5]thieno[3,2-*c*]pyridin-1(2*H*)-one (46b)

Compound **45b** (0.1 g, 0.35 mmol) in MeOH (4 mL) was reacted with hydrazine monohydrate (0.17 mL, 4 mmol) as described in general procedure to give the cyclization product **46b** (0.09 g, 90%) as a pale yellow solid, mp 69-71 °C.

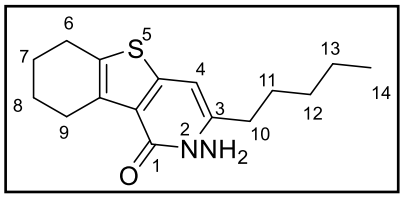

^{1}H-NMR (400 MHz, $CDCl_3$) δ 6.43 (s, H4), 4.95 (s, 2H, NH_2), 3.10 (m, 2H, H6), 2.77 (m, 4H, H9 and H10), 1.85 (m, 4H, H7 and H8), 1.65 (m, 2H, H11), 1.38 (m, 4H, H12 and H13), 0.96 (m, 3H, H14); **^{13}C-NMR** (100 MHz, $CDCl_3$) δ 159.3, 146.0, 144.3, 134.7, 133.7, 125.4, 100.1, 32.6, 31.4, 28.0, 26.0, 25.4, 23.1, 22.5, 22.4, 14.0; **IR** (cm^{-1}) 3268, 3196, 2916, 2856, 1625, 1575, 989; **HRMS-TOF**; [M + H]+ Calcd for $C_{16}H_{22}N_2SO$ 291.15540, found: 291.15256.

4.7.6 Synthesis of 2-amino-3-butyl-6,7,8,9-tetrahydrobenzo[4,5]thieno[3,2-*c*]pyridin-1(2*H*)-one (46c)

Compound **45c** (0.07 g, 0.26 mmol) in MeOH (3 mL) was reacted with excess hydrazine monohydrate (0.14 mL, 3 mmol) as described in general procedure to give the cyclization product **46c** (0.06 g, 80%) as white tiny needles from hexane/EtOAc, mp 64-66°C.

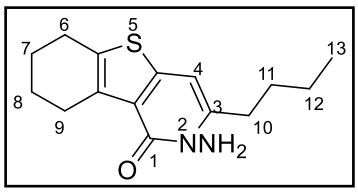

^{1}H-NMR (400 MHz, $CDCl_3$) δ 6.43 (s, H4), 4.93 (s, 2H, NH_2), 3.1 (t, J = 4.8 Hz, 2H, H6), 2.78 (m, 4H, H9 and H10), 1.85 (m, 4H, H7 and H8), 1.65 (m, 2H, H11), 1.43 (m, 2H, H12), 0.96 (t, J = 7.3 Hz, 3H, H13); **^{13}C-NMR** (100 MHz, $CDCl_3$) δ 159.3, 145.8, 144.3, 133.8, 125.4, 100.1, 32.3, 30.5, 25.9, 25.4, 23.1, 22.4, 22.3, 13.9; **IR** (cm^{-1}) 3292, 3192, 2929, 2856, 1636, 1568, 1455, 769; **HRMS-TOF**; [M + H]+ Calcd for $C_{15}H_{20}N_2SO$ 277.13975, found: 277.13691.

4.8 Synthesis of methyl 2-methylfuran-3-carboxylate (116)

Methyl acetoacetate **115** (10.0 g, 86.1 mmol) was dissolved in pyridine (50 mL). To the resulting mixture, a solution of chloroacetaldehyde **124** (45%, 15.5 mL, 107.6 mmol) was added dropwise at room temperature and then stirred at 50 °C for 16 h. The reaction was controlled by TLC. After the completion of the reaction, the mixture was extracted with water (100 mL) and ethyl acetate (3 x 100 mL). The combined organic extracts were washed with 2M of HCl (100 mL), 5% $NaHCO_3$ (100 mL), 10% NaOH

(100 mL) and brine (100 mL) one by one, dried over $MgSO_4$. Removal of the solvent gave the crude product, which was then purified by column chromatography eluting with hexane/EtOAc (5:1). Eluted solvent was evaporated to yield ester **116** as an oily colorless liquid (7.8 g, 65%).[98]

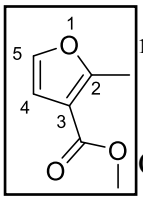

^{1}H-NMR (400 MHz, CDCl3) δ 7.22 (d, J = 2.0 Hz, H5), 6.63 (d, J =2.0 Hz, H4), 3.82 (s, 3H, OCH_3), 2.57 (s, 3H, CH_3); **^{13}C- NMR** (100 MHz, $CDCl_3$) δ 164.5, 159.3, 140.3, 113.2, 110.6, 51.2, 13.6; **IR** (cm^{-1}) 2954, 1819, 1720, 1668, 1438, 1383, 1302, 1120, 1044, 967, 835, 757.

4.9 Synthesis of methyl 2-formylfuran-3-carboxylate (129)

The ester **116** (1.0 g, 7.14 mmol) was dissolved in anisole (15 mL). To this solution, SeO_2 (1.58 g, 14.28 mmol) was added and the mixture was stirred overnight at 160 °C. The reaction was controlled by TLC. After the completion of the reaction, the reaction mixture filtered and extracted with water (50 mL) and ethyl acetate (3 x 70 mL). Then the combined organic extracts were dried over Mg_2SO_4. Removal of the solvent gave the crude product, which was then purified by column chromatography eluting with hexane/EtOAc (5:1). Eluted solvent was evaporated to yield aldehyde **129** as yellow crystals from hexane/EtOAc (0.38 g, 34%), mp 77-79 °C. (lit.mp = 77-78 °C[98]).

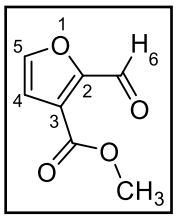

^{1} H-NMR (400 MHz, $CDCl_3$) δ: 10.24 (s, H6), 7.64 (d, J = 1.8 Hz, H5), 6.89 (d, J = 1.8 Hz, H4), 3.95 (s, 3H, OCH_3); **^{13}C-NMR** (100 MHz, $CDCl_3$) δ 178.8, 162.0, 152.4, 146.7, 126.2, 112.9, 52.5; **IR** (cm^{-1}) 3155, 3131, 1714, 1672, 1577, 1481, 1435, 1403, 1365, 1305, 1266, 1213, 1072, 1044, 891, 807, 756.

4.10 General procedure for the synthesis of substituted imidazoles

Aldehyde (2.66 mmol) was dissolved in DMF (8 mL). To this solution, *o*-phenylenediamine (**91**) (2.66 mmol) and *p*-TsOH (0.53 mmol) were added at room temperature and the resulting mixture was heated at 80 ºC for 2-3 hours. The reaction was controlled by TLC. After the completion of the reaction, Na_2CO_3 (0.53 mmol) was dissolved in water (100 mL) and was added to this solution dropwise. EtOAc (20 mL)

was added and then extracted with water (2 x 20 mL). The combined organic extracts were dried over $MgSO_4$. Removal of the solvent gave the crude product which was then purified by column chromatography eluting with hexane/EtOAc (3:1) to give the product.[99]

4.10.1 Synthesis of methyl 2-(1*H*-benzo[*d*]imidazol-2-yl)furan-3-carboxylate (117)

Compound **129** (2.66 mmol, 0.41 g), *o*-phenylenediamine (**91**) (2.66 mmol, 0.28 g) and *p*-TsOH (0.53 mmol, 0.09 g) in DMF (8 mL) were reacted as described in general procedure. The resulting residue was purified by column chromatography eluting with hexane/EtOAc (5:1). Eluted solvent was evaporated to yield furane-substituted imidazole **117** as a brown solid (0.48 g, 75%), mp 164-168 ºC.

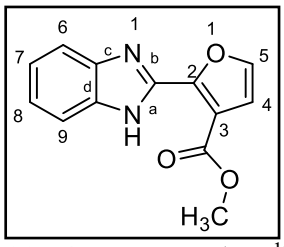

^{1}H-NMR (400 MHz, $CDCl_3$) δ 12.65 (s, NH), 7.88 (m, H6), 7.61 (d, J = 1.8 Hz, H5), 7.58 (m, H9), 7.34, (m, 2H, H7 and H8), 6.92 (d, J =1.8 Hz, H4), 4.01 (s, 3H, CH_3); **^{13}C-NMR** (100 MHz, $CDCl_3$) δ 165.4, 148.8, 143.4, 142.1, 123.7, 123.7, 116.1, 112.4, 52.7; **IR** (cm^{-1}) 2954, 2669, 1727, 1615, 1418, 1296, 1282, 1067, 1039, 743; **HRMS-TOF**; [M + H]+ Calcd for $C_{13}H_{10}N_2O_3$ 243.07677, found: 243.07642.

4.11 Synthesis of 4*H*-benzo[*d*]furo[2',3':3,4]pyrrolo[1,2-*a*]imidazol-4-one (118)

Compound **117** (0.15 g, 0.62 mmol) was dissolved in methanol (10 mL) and to this solution, K_2CO_3 (0.1 g, 0.68 mmol) was added and this solution was heated to reflux temperature and stirred for overnight. After the completion of the reaction, it was cooled to room temperature and the solvent was evaporated under vacuum. The residue was dissolved in CH_2Cl_2 (20 mL) and washed with 1N HCl (20 mL) solution. The organic phase was washed with water (20 mL) and brine (20 mL). Collected organic phases were dried over $MgSO_4$ and removal of the solvent gave the product **118** as a brown solid (0.1 g, 75%), mp>300 ºC.

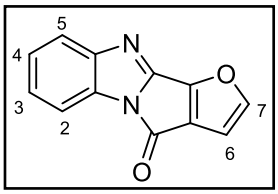

^{1}H-NMR (400 MHz, DMSO-d_6) δ 7.97 (d, J = 1.8 Hz, H7), 7.78 (dd, J = 3.1 and 6.2 Hz, 2H, H2 and H5), 7.51 (m, 2H, H3 and H4), 7.13 (d, J = 1.8 Hz, H6); **^{13}C-NMR** (100 MHz, DMSO -d_6) δ 166.0, 147.2, 135.6, 126.8, 116.0, 115.5, 111.7; **IR** (cm^{-1}) 3126, 1659, 1580, 1485, 1435, 1331, 1260, 1050, 744; **HRMS-TOF**; [M + H]+ Calcd for $C_{12}H_6N_2O_2$ 211.04944, found: 211.0502.

4.12 General procedure of *O*-propargylation

Aromatic hydroxyaldehyde (10 mmol) was dissolved in DMF (10 mL) and anhydrous K_2CO_3 (15.0 mmol) was added to this solution at rt. After stirring for 20 min, propargyl bromide (11.0 mmol) was added and the resulting mixture was stirred overnight at room temperature. After the completion of the reaction, ethyl acetate (30 mL) was added and the organic phase was washed with water (3 × 50 mL) and then dried over $MgSO_4$. Removal of solvent gave the product.

4.12.1 Synthesis of 2-(prop-2-yn-1-yloxy)benzaldehyde (120a)

Salicylaldehyde (**119a**) (1.0 g, 8.19 mmol) was reacted with anhydrous K_2CO_3 (1.7 g, 12.3 mmol) and propargyl bromide (1.05 mL, 9.82 mmol) as described in general procedure to give the product **120a** as colorless cubic crystals from chloroform (1.1 g, 84%), mp 68-70 ºC. (lit. mp = 68-69 °C[100]).

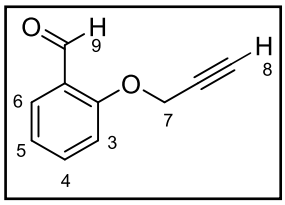

^{1}H-NMR (400 MHz, $CDCl_3$) δ 10.49 (s, H9), 7.87 (dd, J =7.5 and 1.8 Hz, H6), 7.57 (ddd, J = 8.6, 7.5 and 1.8 Hz, H4), 7.12 (d, J = 8.6 Hz, H3), 7.09 (t, J = 7.5, H5), 4.83 (d, J = 2.3 Hz, 2H, H7), 2.57 (t, J = 2.3 Hz, H8); **^{13}C-NMR** (100 MHz, $CDCl_3$) δ: 189.6, 159.7, 135.8, 128.6, 125.6, 121.8, 113.3, 77.8, 76.6, 56.4; **IR** (cm^{-1}) 3268, 2117, 1729, 1681, 1597, 1449, 1284, 1207, 1166, 1066, 924, 832, 742, 610.

4.12.2 Synthesis of 5-bromo-2-(prop-2-yn-1-yloxy)benzaldehyde (120b)

5-bromo-salicylaldehyde (**119b**) (2.0 g, 9.95 mmol), K_2CO_3 (2.1 g, 14.9 mmol) and propargyl bromide (1.3 mL g, 11.9 mmol) were reacted as described in general

procedure to give the product **120b** as white needles from chloroform/hexane (2.13 g, 90%), mp 94-96 ºC. (lit. mp = 94-96 °C[100]).

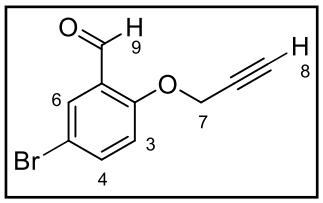

^{1}H-NMR (400 MHz, $CDCl_3$) δ 10.40 (s, H9), 7.91 (d, J = 2.5 Hz, H6), 7.63 (dd, J = 8.9 and 2.5 Hz, H4), 7.04 (d, J = 8.9 Hz, H3), 4.83 (d, J = 2.4 Hz, 2H, H7), 2.58 (t, J = 2.4 Hz, H8); **^{13}C-NMR** (100 MHz, $CDCl_3$) δ 188.2, 158.7, 138.2, 131.3, 126.9, 115.5, 114.7, 77.3, 77.1, 56.8; **IR** (cm^{-1}) 3233, 2981, 2882, 2117, 1681, 1589, 1478, 1454, 1395, 1291, 1275, 1218, 1183, 1124, 1001, 879, 810, 732, 654, 630, 581.

4.12.3 Synthesis of 3-methoxy-2-(prop-2-yn-1-yloxy)benzaldehyde (120c)

3-Methoxy-salicylaldehyde (**119c**) (2.0 g, 13.1 mmol), K_2CO_3 (2.7 g, 19.7 mmol), and propargyl bromide (1.7 mL, 15.8 mmol) were reacted as described in general procedure to yield the product **120c** as colorless cubic crystals from EtOAc/hexane (2.3 g, 92%), mp 49-51 ºC. (lit. mp = 49-51 °C[100]).

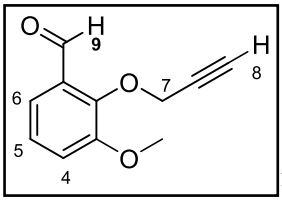

^{1}H-NMR (400 MHz, $CDCl_3$) δ 10.50 (s, H9), 7.44 (dd, J = 6.0 and 3.4 Hz, H6), 7.22 – 7.13 (m, 2H, H4 and H5), 4.88 (d, J = 2.4 Hz, 2H, H7), 3.89 (s, 3H, OCH_3), 2.52 (t, J = 2.4 Hz, H8); **^{13}C-NMR** (100 MHz, $CDCl_3$) δ 190.6, 152.9, 149.5, 131.1, 124.9, 118.9, 117.8, 77.3, 77.11, 60.8, 56.1; **IR** (cm^{-1}) 3265, 2889, 2837, 2118, 1681, 1583, 1477, 1249, 1179, 983, 911, 749, 651.

4.12.4 Synthesis of 2-(but-2-yn-1-yloxy)benzaldehyde (120f)

Salicylaldehyde (**119a**) (0.5 g, 4.1 mmol), 1-bromobut-2-yne (0.66 mL, 6.14 mmol), and K_2CO_3 (0.68 g, 4.9 mmol) in DMF (5 mL) were reacted as described in general procedure to give the product **120f** as a colorless oil (0.68 g, 95%).

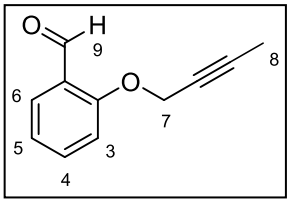

^{1}H-NMR (400 MHz, $CDCl_3$) δ 10.49 (s, H9), 7.85 (dd, J = 7.7 and 1.7 Hz, H6), 7.56 (ddd, J = 8.4, 7.7 and 1.7 Hz, H4), 7.11-7.06 (m, 2H, H3 and H5), 4.79 (q, J = 2.1 Hz, 2H, H7), 1.86 (t, J = 2.1 Hz, 3H, H8); **^{13}C-NMR** (100 MHz, $CDCl_3$) δ 189.7, 160.1, 135.7, 128.2, 125.3, 121.2, 113.3, 84.7, 73.4, 57.0, 3.6; **IR** (cm^{-1}) 2917, 2864, 2231, 1686, 1597, 1480, 1458, 1397, 1369, 1286, 1261, 1217, 1190, 1162, 1102, 1042, 995, 831, 755, 645, 595.[100]

4.12.5 Synthesis of 2-(2-formylphenoxy)acetonitrile (120g)

Salicylaldehyde (**119a**) (0.5 g, 4.1 mmol), chloroacetonitrile (0.46 g, 6.14 mmol), and K_2CO_3 (0.68 g, 4.9 mmol) in DMF (5 mL) were reacted as described in general procedure to give the product **120g** as an orange crystal (0.63 g, 95%) mp 63-65 °C. (lit. mp =78-80 °C)[101]

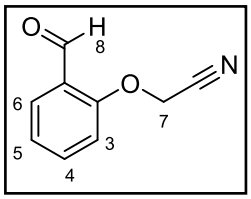

^{1}H-NMR (400 MHz, $CDCl_3$) δ 10.42 (s, H8), 7.88 (dd, J = 7.6 and 1.6 Hz, H6), 7.63 (m, H4), 7.19 (qt, H3), 7.08 (d, J = 8.4 Hz, H5), 4.93 (s, 2H, H7); **^{13}C-NMR** (100 MHz, $CDCl_3$) δ 188.8, 158.3, 136.1, 129.5, 125.6, 123.3, 114.6, 112.7 53.8; **IR** (cm^{-1}) 3100, 2117**,** 1676, 1597, 1483, 1455, 1283, 1231, 1033, 842, 757, 652.

4.12.6 Synthesis of 2-((3-phenylprop-2-yn-1-yl)oxy)benzaldehyde (120d)

$PdCl_2$ (0.009 g, 0.052 mmol), CuI (0.028 g, 0.15 mmol) and PPh_3 (0.05 g, 0.21 mmol), NEt_3 (0.52 mL, 3.9 mmol), iodophenyl (0.26 mL, 2.36 mmol) and compound **120a** (0.42 g, 2.6 mmol) in THF (10 mL) were reacted as described in section 4.6. The residue was purified by column chromatography on silica gel using 15:1 hexane/ethyl acetate to afford the desired compound **120d** as a pale yellow solid (0.61 g, 90%), mp 83-84 °C. (lit. mp = 79-80 °C[100])

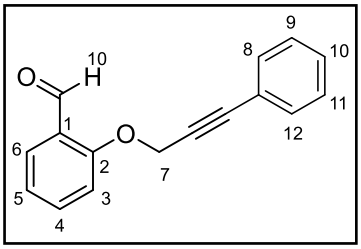

^{1}H-NMR (400 MHz, $CDCl_3$) δ 10.54 (s, H10), 7.88 (dd, J = 7.5 and 1.8 Hz, H6), 7.58 (ddd, J = 8.4, 7.5 and 1.8 Hz, H4), 7.43 (m, 2H, H8 and H12), 7.32 (m, 3H, H9, H10 and H11), 7.21 (d, J = 8.4 Hz, H3), 7.09 (t, J = 7.5 Hz, H5), 5.05 (s, 2H, H7); **^{13}C-NMR** (100 MHz, $CDCl_3$) δ 189.7, 160.2, 135.5, 131.8, 128.9, 128.5, 128.4 128.4, 121.9, 121.5, 113.5, 88.2, 82.9, 57.2; **IR** (cm^{-1}) 3257, 3106, 2861, 2239, 1681, 1598, 1509, 1372, 1205, 1044, 748.

4.12.7 Synthesis of 2-((3-(4-nitrophenyl)prop-2-yn-1-yl)oxy)benzaldehyde (120e)

$PdCl_2$ (0.155 mmol, 0.026 g), CuI (0.466 mmol, 0.081 g) and PPh_3 (0.62 mmol, 0.16 g), NEt_3 (1.05 mL, 7.78 mmol), *p*-nitroiodophenyl (2.33 g, 7.7 mmol) and compound **120a** (1.34 g, 8.4 mmol) in THF (15 mL) were reacted as described in section 4.6. The crude product was purified by column chromatography on silica gel using 5:1 hexane/ethyl acetate to afford the desired compound **120e** as orange crystals (1.9 g, 90%), mp 110-111 °C.

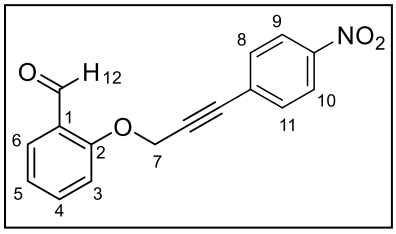

^{1}H-NMR (400 MHz, $CDCl_3$) δ 10.53 (s, H12), 8.19 (m, 2H, H8 and H11), 7.89 (dd, J = 7.6 and 1.8 Hz, H6), 7.62-7.55 (m, 3H, H4, H9, and H10), 7.17 (d, J = 8.3 Hz, H3), 7.13 (bt, J = 7.6 Hz, H5), 5.10 (s, 2H, H7); **^{13}C-NMR** (100 MHz, $CDCl_3$) δ 189.4, 159.8, 147.5, 135.7, 132.6, 128.8, 128.6, 125.7, 123.6, 121.9, 113.3, 88.1, 86.0, 57.1; **IR** (cm^{-1}) 3257, 3106, 2860, 2239, 1682, 1589, 1509, 1370, 1339, 1295, 1222, 1204, 759, 747.

4.13 Synthesis of 2-(2-(prop-2-yn-1-yloxy)phenyl)-1*H*-benzo[*d*]imidazole (121a)

Compound **120a** (1.56 g, 9.72 mmol), *o*-phenylenediamine (**91**) (1.048 g, 9.72 mmol) and *p*-TsOH (1.94 mmol) in DMF (15 mL) were reacted as described in section 4.10. The resulting residue was purified by column chromatography eluting with hexane/EtOAc (4:1). Eluted solvent was evaporated to yield imidazole **121a**[95] as a brown crystal (1.56 g, 65%) from hexane/ethylacetate, mp 164-168 ºC.

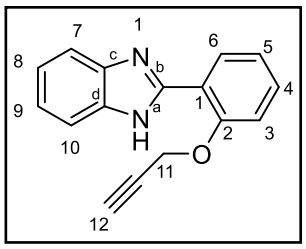

^{1}H-NMR (400 MHz, DMSO-d_6) δ 8.22 (dd, J = 1.5 and 7.7 Hz, H6), 7.68 (d, J = 3.1 and 6.1 Hz, 2H, H7 and H10), 7.53 (m, H4), 7.38 (bd, J = 8.3 Hz, H3), 7.31 (dd, J = 3.1 and 6.1 Hz, 2H, H8 and H9), 7.20 (bt, J = 7.7 Hz H5), 5.08 (d, J = 2.3 Hz, 2H, H11), 3.07 (t, J = 2.3 Hz, H12); **^{13}C-NMR** (100 MHz, DMSO-d_6) δ 156.7, 150.2, 138.2, 133.2, 131.2, 124.5, 123.1, 118.4, 115.7, 114.9, 79.3, 78.0, 57.3; **IR** (cm^{-1}) 3301, 3288, 2119, 1684, 1603, 1581, 1462, 1438, 1216, 1091, 1006, 793, 667, 623.

4.14 Synthesis of 2-(5-bromo-2-(prop-2-yn-1-yloxy)phenyl)-1*H*-benzo[*d*] imidazole (121b)

Compound **120b** (0.71 g, 3.0 mmol), *o*-phenylenediamine (**91**) (0.33 g, 3.0 mmol) and *p*-TsOH (0.114 g, 0.6 mmol) in DMF (10 mL) were reacted as described in section 4.10. The resulting residue was purified by column chromatography eluting with hexane/EtOAc (5:1). Eluted solvent was evaporated to yield imidazole **121b**[95] as white crystals (0.49 g, 50%), mp 130-131 ºC

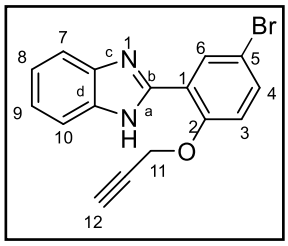

^{1}H-NMR (400 MHz, $CDCl_3$) δ 10.50 (s, NH), 8.76 (d, J = 2.5 Hz, H6), 7.83 (bs, H7), 7.53 (dd, J = 8.8 and 2.5 Hz, H4), 7.53 (bs, H10), 7.29 (dd, J = 3.0 and 6.1 Hz, H8 and H9), 7.04 (d, J = 8.8 Hz, H3), 4.95 (d, J = 2.4 Hz, 2H, H11), 2.67 (t, J = 2.4 Hz, H12); **^{13}C-NMR** (100 MHz, $CDCl_3$) δ 153.8, 147.9, 133.5, 132.8, 123.3, 122.9, 120.6, 119.6, 115.4, 114.8, 110.9, 77.2, 77.1, 57.2; **IR** (cm^{-1}) 3294, 2122, 1471, 1443, 1269, 1213, 1085, 1015, 800, 736.

4.15 Synthesis of 2-(3-methoxy-2-(prop-2-yn-1-yloxy)phenyl)-1*H*-benzo[*d*]imi dazole (121c)

Compound **120c** (1.75 g, 9.2 mmol), *o*-phenylenediamine (**91**) (0.99 g, 9.2 mmol) and *p*-TsOH (0.35 g, 1.84 mmol) in DMF (20 mL) were reacted as described in section 4.10. The resulting residue was purified by column chromatography eluting with hexane/EtOAc (5:1). Eluted solvent was evaporated to yield imidazole **121c**[95] as white crystals (1.50 g, 60%), mp 135-137 ºC.

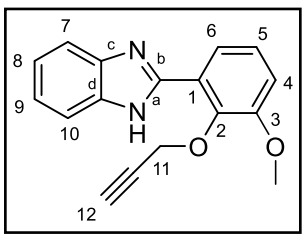

^{1}H-NMR (400 MHz, $CDCl_3$) δ 10.82 (s, NH), 8.13 (d, J = 1.2 and 8.1 Hz, H6), 7.77 (bs, H7), 7.58 (bs, H10), 7.27 (m, 3H, H8, H9 and H5), 7.02 (dd, J = 1.2 and 8.1 Hz, H4), 4.90 (d, J = 2.4 Hz, 2H, H11), 3.94 (s, 3H, OCH_3), 2.53 (t, J = 2.4 Hz, H12); **^{13}C-NMR** (100 MHz, $CDCl_3$) δ 152.5, 151.1, 149.2, 144.6, 125.5, 123.6, 122.9, 121.7, 121.5, 115.1, 113.8, 113.5, 113.4, 78.2, 77.4, 61.0, 56.0; **IR** (cm^{-1}) 3278, 3260, 2938, 2836, 2117, 1478, 1428, 1277, 1124, 1059, 980, 745.

4.16 Synthesis of 2-(2-(but-2-yn-1-yloxy)phenyl)-1*H*-benzo[*d*]imidazole (121f)

Compound **120f** (1.6 g, 9.2 mmol), *o*-phenylenediamine (**91**) (0.99 g, 9.2 mmol) and *p*-TsOH (0.35 g, 1.84 mmol) in DMF (20 mL) were reacted as described in section 4.10. The resulting residue was purified by column chromatography eluting with hexane/EtOAc (5:1). Eluted solvent was evaporated to yield imidazole **121f** as a pale yellow solid (1.45 g, 60%), mp 156-158 ºC.

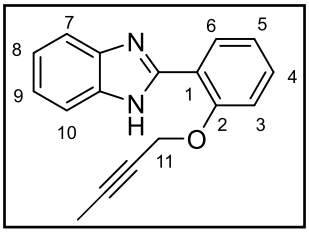

^{1}H-NMR (400 MHz, $CDCl_3$) δ 10.70 (s, NH), 8.60 (dd, J = 1.7 and 7.8 Hz, H6), 7.82 (bs, H9), 7.49 (bs, H7), 7.42 (m, H4), 7.26 (dd, J = 3.1 and 5.8 Hz, 2H, H8 and H10), 7.17 (m, 2H, H3 and H5), 4.90 (m, 2H, H11), 1.89 (qt, 3H, CH_3); **^{13}C-NMR** (100 MHz, $CDCl_3$) δ 155.2, 149.7, 131.0, 131.0, 130.3, 122.5, 122.5, 122.2, 118.5, 113.1, 85.2, 73.3, 57.4, 3.66; **IR** (cm^{-1}) 3202, 2919, 2851, 2161, 1587, 1488, 1471, 1259, 1224, 994, 737. **HRMS-TOF [M + H]+** Calcd for $C_{17}H_{14}N_2O$ 263.12055, found: 263.11789.

4.17 Synthesis of 2-(2-((3-phenylprop-2-yn-1-yl)oxy)phenyl)-1*H*-benzo[*d*] imidazole (121d)

Compound **120d** (0.64 g, 2.7 mmol), *o*-phenylenediamine (**91**) (0.29 g, 2.7 mmol) and *p*-TsOH (0.1 g, 0.52 mmol) in DMF (10 mL) were reacted as described in section 4.10. The resulting residue was purified by column chromatography eluting with hexane/EtOAc (7:1). Eluted solvent was evaporated to yield imidazole **121d** as white crystals (0.26 g, 30%), mp 178-180 ºC.

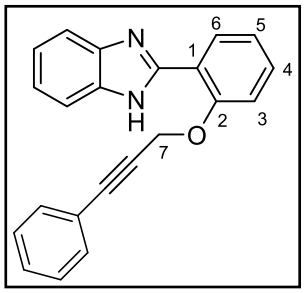

^{1}H-NMR (400 MHz, $CDCl_3$) δ 8.60 (s, NH), 8.60 (d, J = 1.6 and 7.8 Hz, H6), 7.68-7.15(m, other phenyl protons), 5.15 (m, 2H, H7); **^{13}C-NMR** (100 MHz, $CDCl_3$) δ 155.2, 149.4, 131.8, 131.8, 131.3, 130.4, 129.1, 128.4, 128.4, 122.8, 122.5, 121.7, 113.2, 88.5, 82.8, 57.8; **IR** (cm^{-1}) 3327, 3051, 2238, 1604, 1455, 1309, 1207, 1001, 744, 712; **HRMS-TOF [M + H]+** Calcd for $C_{22}H_{16}N_2O$ 325.13444, found: 325.13354.

4.18 Synthesis of 1-(2-oxopropyl)-1*H*-pyrrole-2-carbaldehyde (143)

To a solution of 1*H*-pyrrole-2-carbaldehyde (**142**) (0.50 g, 5.25 mmol) in DMF (10 mL) was added NaH (0.126 g, 5.25 mmol) at 0 ºC. After stirring for 20 min, chloroacetone (0.42 mL, 5.25 mmol) was added and the resulting mixture was stirred overnight at 50 ºC. After the completion of the reaction, ethyl acetate (30 mL) was added and the organic phase was washed with water (3 × 50 mL) and then dried over $MgSO_4$. Removal of solvent gave the product **143** as white needles (0.51 g, 65%) from chloroform/hexane, mp 60-62 ºC (lit. mp = 60-62 ºC[102]).

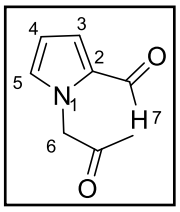

^{1}H-NMR (400 MHz, $CDCl_3$) δ 9.49 (s, H7), 7.00 (dd, J = 1.5 and 4.0 Hz, H3), 6.87 (bs, H5), 6.31 (dd, J = 2.6 and 4.0 Hz, H4), 5.10 (s, 2H, H6), 2.33 (s, CH_3); **^{13}C-NMR** (100 MHz, $CDCl_3$) δ 201.8, 179.8, 132.2, 131.4, 124.7, 110.3, 58.0, 27.0; **IR** (cm^{-1}) 2938, 2797, 1718, 1645, 1526, 1479, 1397, 1362, 1320, 1222, 1172, 1077.

4.19 Synthesis of 1-(prop-2-yn-1-yl)-1*H*-pyrrole-2-carbaldehyde (144)

To a solution of 1*H*-pyrrole-2-carbaldehyde (**142**) (1.00 g, 10.5 mmol) in DMF (10 mL) was added NaH (0.27 g, 10.5 mmol) at 0 ºC. After stirring for 20 min, propargyl bromide (1.17 mL, 11 mmol) was added and the resulting mixture was stirred overnight at rt. The residue was extracted with EtOAc and the organic phase was washed with water (3 × 50 mL) and then dried over $MgSO_4$.The crude product was purified by column chromatography eluting with hexane/EtOAc (5:1). Eluted solvent was evaporated to give **144** as a brown liquid (1.1 g, 85%).[102]

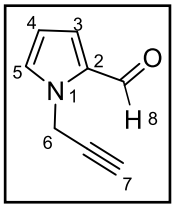

^{1}H-NMR (400 MHz, $CDCl_3$) δ 9.50 (d, J = 0.9 Hz, H8), 7.23 (m, H5), 6.92 (dd, J = 1.7 and 4.0 Hz, H3), 6.24 (dd, J = 2.6 and 4.0 Hz, H4), 5.15 (d, J = 2.6 Hz, 2H, H6), 2.33 (t, J = 2.6 Hz, H7); **^{13}C- NMR** (100 MHz, $CDCl_3$) δ 179.4, 131.0, 130.4, 124.8, 110.1, 77.7, 74.5, 38.0; **IR** (cm^{-1}) 3202, 2919, 2851, 2161, 1587, 1488, 1471, 1259, 1224, 994, 737.

4.20 Synthesis of 2-(1-(prop-2-yn-1-yl)-1*H*-pyrrol-2-yl)-1*H*-benzo[*d*]imidazole (145)

Compound **144** (1.3 g, 10.0 mmol), *o*-phenylenediamine (**91**) (1.08 g,10.0 mmol) and *p*-TsOH (0.34 g, 2.00 mmol) in DMF (10 mL) were reacted as described in general procedure. The resulting residue was purified by column chromatography eluting with hexane/EtOAc (10:1). Eluted solvent was evaporated to give benzimidazole **145** as as a brown solid (0.6 g, 30%), mp 160-162 ºC.

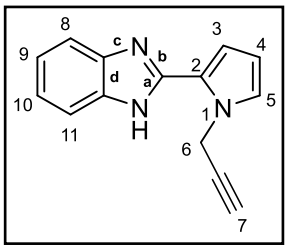

^{1}H-NMR (400 MHz, CD_3OD) δ 7.56 (br s, 2H, H8 and H11), 7.22 (m, 2H, H9 and H10), 7.15 (dd, J = 3.8 and 1.7 Hz H3), 6.81 (dd, J = 2.6 and 1.7 Hz, H5), 6.27 (m, H4), 5.43 (d, J = 2.5 Hz, 2H, H6), 2.75 (t, J = 2.5 Hz, H7); **^{13}C-NMR** (100 MHz, CD_3OD) δ 147.8, 126.6, 123.8, 123.5, 113.6, 110.0, 79.8, 74.6, 38.6; **IR** (cm^{-1}) 3296, 3284, 2162, 1583, 1452, 1397, 1284, 1096, 782, 729, 665; **HRMS-TOF [M + H]+** Calcd for $C_{14}H_{11}N_3$ 222.10171, found: 222.10257.

4.21 Synthesis of 7-(4-nitrobenzylidene)-6,7-dihydrobenzo[*f*]benzo[4,5]imidazo [1,2-*d*][1,4]oxazepine (122e)

Compound **120e** (2.2 g, 13.7 mmol), *o*-phenylenediamine (**91**) (1.48 g, 13.7 mmol) and *p*-TsOH (0.47 g, 2.74 mmol) in DMF (15 mL) were reacted as described in section 4.10. The resulting residue was purified by column chromatography eluting with hexane/EtOAc (10:1). Eluted solvent was evaporated to give benzimidazo-oxazepine **122e** as a pale yellow solid (1.51 g, 30%), mp 194-196 ºC.

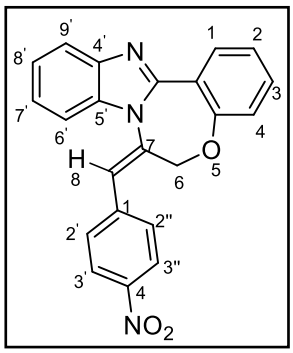

^{1}H-NMR (400 MHz, $CDCl_3$) δ 8.76 (d, J = 1.4 and 8.1 Hz, H1), 8.37 (d, J = 8.7 Hz, 2H, H2' and H2"), 7.93(m, H6'), 7.71(d, J = 8.7 Hz, 2H, H3" and H3'), 7.71 (bs, H9'), 7.45 (m, H3), 7.41 (m, 2H, H7' and H8'), 7.28 (s, H8), 7.23 (t, J = 8.1 Hz, H2), 7.18 (d, J = 8.3 Hz, H4), 4.99 (s, 2H, H6); **^{13}C-NMR** (100 MHz, $CDCl_3$) δ 156.5, 147.6, 143.8, 140.3, 140.1, 134.5, 132.2, 132.1, 130.0, 124.1, 123.9, 123.8, 123.1, 120.6, 120.2, 110.6, 68.3; **IR** (cm^{-1}) 3060, 1597, 1454, 1310, 1209, 1022, 753, 734, 700, 683; **HRMS-TOF [M + H]+** Calcd for $C_{22}H_{15}N_3O_3$ 370.12176, found: 370.11862.

4.22 Synthesis of benzo[*f*]benzo[4,5]imidazo[1,2-*d*][1,4]oxazepin-7(6*H*)-imine (122g)

Compound **120g** (1.01 g, 6.3 mmol) was dissolved in DMF (10 mL). To this solution *o*-phenylenediamine (**91**) (0.67 g, 6.3 mmol) and *p*-TsOH (0.24 g, 1.26 mmol) were added at room temperature and the resulting mixture was heated at 80 ºC for 2-3 hours. The reaction was controlled by TLC. When the reaction was finished, the solution was cooled to room temperature. The reaction mixture was added dropwise with vigorous stirring into a mixture of Na_2CO_3 (1.26 mmol) and H_2O (100 mL). The product was precipitated as a free flowing solid in the solution and it was collected by filtration, washed with H_2O and dried to give benzimidazo-oxazepine **122g** as a white solid (0.94 g, 60%), mp 178-180 ºC.

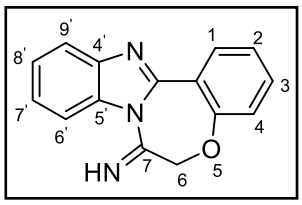

^{1}H-NMR (400 MHz, DMSO-d_6) δ 12.30 (bs, NH), 8.35 (dd, J = 1.6 and 7.6 Hz, H1), 7.64 (bs, 2H, H6' and H9'), 7.57 (m, H3), 7.41 (qd, J = 8.3 Hz, H4), 7.26 (t, J = 7.6 Hz, H2), 7.22 (dd, J = 3.1 and 6.0 Hz, 2H, H7' and H8'), 5.41 (s, 2H, H6); **^{13}C-NMR** (100 MHz, DMSO-d_6) δ 153.5, 148.1, 134.7, 131.2, 130.4, 122.7, 122.0, 119.2, 117.4, 116.5, 114.6, 113.1, 53.7; **IR** (cm^{-1}) 2995, 2882, 1742, 1581, 1470, 1442, 1392, 1210, 1091, 1035, 746; **HRMS-TOF [M + H]+** Calcd for $C_{15}H_{11}N_3O$ 250.10058, found: 250.09749.

4.23 General procedure of cyclization with NaH

To a solution of benzimidazole derivative (1.51 mmol) in DMF (10 mL) was added NaH (60% suspension in oil) (0.12 g, 3.02 mmol) and the resulting mixture was stirred at room temperature overnight. After completion of the reaction (controlled by TLC), the solvent was evaporated and water (10 mL) was added into reaction vessel. The mixture was extracted with EtOAc (2 × 10 mL), and organic extracts were washed with water (5 × 20 mL) and dried over $MgSO_4$ and evaporated. The residue was purified by column chromatography using hexane/ethylacetate.

4.23.1 Cyclization of 121a with NaH

To a solution of benzimidazole derivative (**121a**) (1.0 g, 4 mmol) in DMF (10 mL) was added NaH (60% suspension in oil) (0.32 g, 8 mmol) and the resulting mixture was reacted as described in general procedure. The residue was purified by column chromatography using hexane/ethylacetate (10:1) to give **122a**[95] as a white solid (NMR ratio: 64%, isolated yield 20%, 0.19 g) (mp 176-178 ºC) and **140b** as a white solid (NMR ratio: 27%, isolated yield 15%, 0.14 g) (mp 102-104 ºC).

4.23.2 Synthesis of 7-methylene-6,7-dihydrobenzo[*f*]benzo[4,5]imidazo[1,2-*d*][1,4]oxazepine (122a)

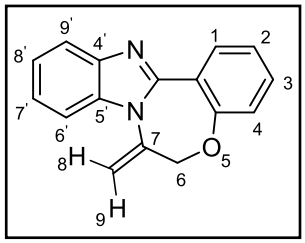

^{1}H-NMR (400 MHz, $CDCl_3$) δ 8.69 (d, J = 8.0 Hz, H1), 7.77 (d, J = 7.7 Hz, H9'), 7.54 (d, J = 7.5 Hz, H6'), 7.27 (m, 3H, H3, H7' and H8'), 7.11 (t, J = 8.0 Hz, H2), 7.03 (d, J = 8.2 Hz, H4), 5.64 (s, H8), 5.45 (s, H9), 4.73 (s, 2H, H6); **^{13}C-NMR** (100 MHz, $CDCl_3$) δ 156.2, 149.9, 143.6, 138.1, 134.6, 132.0, 132.7, 123.4, 123.4, 122.8, 120.6, 120.0, 117.6, 111.2, 110.1, 72.7; **IR** (cm^{-1}) 2918, 2849, 1652, 1606, 1452, 1387, 1213, 1044, 744.

4.23.3 Synthesis of 6-methylbenzo[*f*]benzo[4,5]imidazo[1,2-*d*][1,4]oxazepine (140b)

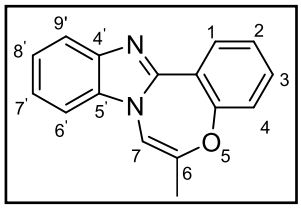

^{1}H-NMR (400 MHz, $CDCl_3$) δ 8.21 (dd, J = 8.1 and 1.6 Hz, H1), 7.83 (m, H9'), 7.45 (m, H3), 7.39 (m, H6'), 7.31 (m, 3H, H7', H8' and H2), 7.13 (d, J = 8.1 Hz, H4), 6.50 (s, H7), 2.15 (s, 3H, CH_3); **^{13}C-NMR** (100 MHz, $CDCl_3$) δ 157.9, 150.0, 148.8, 142.7, 134.4, 132.1, 130.7, 125.5, 123.4, 123.3, 122.9, 121.3, 120.0, 109.4, 108.3, 18.4; **IR** (cm^{-1}) 3300, 3287, 3047, 1684, 1439, 1394, 1216, 1091, 1006, 738, 622. **HRMS-TOF [M + H]+** Calcd for $C_{16}H_{12}N_2O$ 249.10288, found: 249.10224.

4.23.4 Cyclization of 121b with NaH

To a solution of benzimidazole derivative **121b** (1.3 g, 4 mmol) in DMF (10 mL) was added NaH (60% suspension in oil) (0.32 g, 8 mmol) and the resulting mixture was reacted as described in general procedure. The residue was purified by column chromatography using hexane/ethylacetate (15:1) to give **122b**[95] as a white crystal (NMR ratio: 10%, isolated yield 10%, 0.13 g) (mp 166-168 ºC) and **141b** as a white crystal (NMR ratio: 70%, isolated yield 15%, 0.19 g) (mp 143-145 ºC) from hexane/ethylacetate.

4.23.5 Synthesis of 2-bromo-7-methylene-6,7-dihydrobenzo[*f*] benzo[4,5]imidazo [1,2-*d*][1,4] oxazepine (122b)

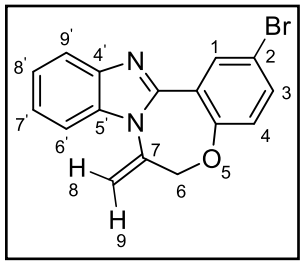

^{1}H-NMR (400 MHz, $CDCl_3$) δ 8.95 (d, J = 2.4 Hz, H1), 7.86 (m, H9'), 7.62 (m, H6'), 7.45 (dd, J = 2.4 and 8.7 Hz, H3), 7.36 (m, 2H, H7' and H8'), 6.98 (d, J = 8.7 Hz, H4), 5.75 (s, H8), 5.56 (s, H9), 4.73 (s, 2H, H6); **^{13}C-NMR** (100 MHz, $CDCl_3$) δ 155.3, 148.2, 143.3, 138.1, 134.6, 134.4, 134.0, 123.9, 123.7, 122.4, 120.2, 119.2, 115.3, 111.3, 110.6, 72.6; **IR** (cm^{-1}) 3062, 2986, 2914, 1490, 1444, 1409, 1309, 1007, 812, 726, 704.

4.23.6 Synthesis of 2-bromo-6-methylbenzo[*f*]benzo[4,5]imidazo[1,2-*d*][1,4] oxazepine (141b)

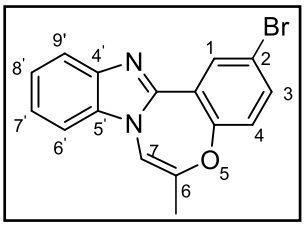

^{1}H-NMR (400 MHz, $CDCl_3$) δ 8.36 (d, J = 2.5 Hz, H1), 7.83 (m, H9'), 7.45 (dd, J = 2.5 and 8.6 Hz, H3), 7.40 (m, H6'), 7.35 (m, 2H, H7' and H8'), 7.01 (d, J = 8.6 Hz, H4), 6.50 (d, J = 0.9 Hz, H7), 2.14 (d, J = 0.9 Hz, 3H, CH_3); **^{13}C-NMR** (100 MHz, $CDCl_3$) δ 156.2, 148.6, 142.4, 134.8, 134.3, 133.0, 124.5, 123.8, 123.6, 123.0, 120.2, 118.3, 109.5, 108.3, 18.4; **IR** (cm^{-1}) 3300, 3287, 3047, 1704, 1521, 1427, 1333, 1221, 1197, 931, 727, 715. **HRMS-TOF [M + H]+** Calcd for $C_{16}H_{11}BrN_2O$ 327.01481, found: 327.01275.

4.23.7 Cyclization of 121c with NaH

1. To a solution of benzimidazole derivative **121c** (1.1 g, 4 mmol) in DMF (10 mL) was added NaH (60% suspension in oil) (0.32 g, 8 mmol) and the resulting mixture was reacted as described in general procedure. The residue was purified by column chromatography using hexane/ethylacetate (15:1) to give **122c**[95] as a pale yellow solid, mp 164-166 ºC (NMR ratio: 40%, isolated yield 30%, 0.32 g), **135a** as a pale yellow solid (NMR ratio: 20%, isolated yield 10%, 0.10 g), and **135b** as white solid (NMR ratio: 40%).

2. To a solution of benzimidazole derivative **121c** (1.1 g, 4 mmol) in DMF (10 mL) was added NaH (60% suspension in oil) (0.32 g, 8 mmol) and the resulting mixture was heated to 85 ºC and stirred over night to afford **135b** (NMR ratio: 50%) and **123c** (NMR ratio: 50%) as white solid mixture.

4.23.8 Synhtesis of 4-methoxy-7-methylene-6,7-dihydrobenzo[*f*]benzo[4,5] imidazo[1,2-*d*][1,4] oxazepine (122c) and 4-methoxy-6-methylene-6,7-dihydrobenzo [*f*]benzo [4,5] imidazo[1,2-*d*][1,4]oxazepine (135a)

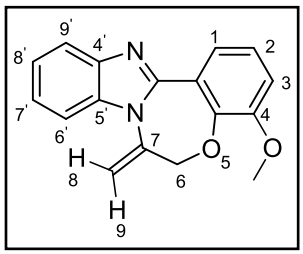

^{1}H-NMR (400 MHz, $CDCl_3$) δ 8.28 (dd, J = 8.1 and 1.5 Hz, H1), 7.85 (m, H9'), 7.61 (m, H6'), 7.34 (m, 2H, H8' and H7'), 7.14 (t, J = 8.1 Hz, H2), 7.03 (dd, J = 8.1 and 1.5 Hz, H3), 5.69 (s, H8), 5.52 (s, H9), 4.93 (s, 2H, H6), 3.94 (s, 3H, OCH_3); **^{13}C-NMR** (100 MHz, $CDCl_3$) δ 150.8, 149.7, 146.4, 143.2, 138.4, 134.6, 123.6, 123.4, 123.1, 122.8, 119.3, 120.1, 113.1, 111.2, 110.3, 73.6, 56.3.

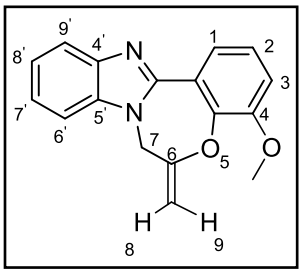

^{1}H-NMR (400 MHz, $CDCl_3$) δ 7.87 (m, H9'), 7.72 (dd, 8.28 (dd, J = 8.0 and 1.4 Hz, H1), 7.42 (m, H6'), 7.34 (m, 2H, H8' and H7'), 7.25 (t, J = 8.0 Hz, H2), 7.10 (dd, J = 8.0 and 1.4 Hz, H3), 4.87 (d, J = 1.8 Hz, H8), 4.81 (bs, 2H, H7), 4.59 (d, J = 1.8 Hz, H9), 3.95 (s, 3H, OCH_3); **^{13}C-NMR** (100 MHz, $CDCl_3$) δ 156.7, 151.9, 150.3, 142.1, 141.6, 134.1, 124.6, 123.1, 122.8, 122.2, 121.6, 120.1, 114.4, 108.6, 94. 2, 55.9, 44.7; **IR** (cm^{-1}) 3009, 2834, 1658, 1578, 1525, 1478, 1435, 1235, 1048, 851, 744, 732.

4.23.9 Synthesis of 4-methoxy-6-methylbenzo[*f*]benzo[4,5]imidazo[1,2-*d*][1,4] oxazepine and 4-methoxy-7-methylbenzo[*f*]benzo[4,5]imidazo[1,2-*d*][1,4]oxazepi ne (135b and 123c)

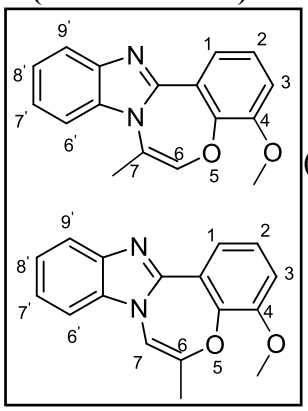

^{1}H-NMR (400 MHz, $CDCl_3$) δ 7.92 (m, H1), 7.81, 7.58, 7.40 (m, H8' and H7'), 7.35 (m, H6' and H9') 7.26 (m, H2), 7.09 (m, H3), 6.61, 6.55 (bd, H6 and H7,), 2.28 (d, J = 0.8 Hz, CH_3), 2.20 (d, J = 1.4 Hz, CH_3); **^{13}C-NMR** (100 MHz, $CDCl_3$) δ 151.4, 151.1, 150.7, 150.1, 149.3, 149.1, 147.3, 141.9, 140.1, 137.6, 133.7, 133.6, 125.9, 125.6, 125.5, 124.1, 124.0, 123.6, 123.5, 123.0, 122.1, 121.9, 115.3, 114.8, 112.9, 109.8, 108.8, 56.3, 56.3, 18.4, 14.9; **IR** (cm^{-1}) 2923, 1679, 1519, 1480, 1436, 1267, 1208, 1172, 1049, 739; **HRMS-TOF [M + H]+** Calcd for $C_{17}H_{14}N_2O_2$ 279.11541, found: 279.11280.

4.23.10 Cyclization of 121d with NaH

To a solution of benzimidazole derivative **121d** (1.05 g, 4 mmol) in DMF (10 mL) was added NaH (60% suspension in oil) (0.32 g, 8 mmol) and the resulting mixture was reacted as described in general procedure. The residue was purified by column chromatography using hexane/ethylacetate (20:1) to give **122d-*E*** as white crystals (NMR ratio: 50%, isolated yield 10%, 0.12 g) (mp 194-196 ºC) from hexane/ethylacetate and **122d-*Z*** as a pale yellow solid (NMR ratio: 50%).

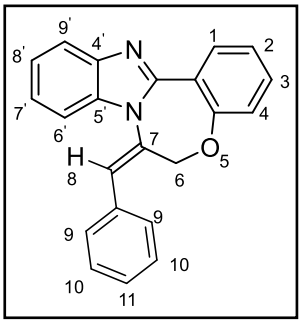

^{1}H-NMR (400 MHz, $CDCl_3$) δ 8.63 (dd, J = 8.0 and 1.6 Hz, H1), 7.82 (d, J = 8.0 Hz, H9'), 7.42 (m, H3), 7.20 (m, 2H, H7' and H8'), 7.12 (m, 4H, H10, H11, H6'), 6.97 (m, 3H, H2 and H9), 6.82 (s, H8), 6.66 (d, J = 8.2 Hz, H4), 5.12 (bs, 1H, H6), 4.67 (bs, 1H, H6); **^{13}C-NMR** (100 MHz, $CDCl_3$) δ 155.4, 150.5, 143.5, 133.1, 132.5, 132.0, 131.9, 129.3, 129.0, 128.8, 128.5, 127.4, 123.0, 122.8, 122.4, 120.8, 119.7, 116.9, 112.2, 99.8, 74.7; **IR** (cm^{-1}) 3202, 2919, 2851, 1587, 1488, 1471, 1259, 1224, 994, 737 **HRMS-TOF [M + H]+** Calcd for $C_{22}H_{16}N_2O$ 325.13392, found: 325.13354.

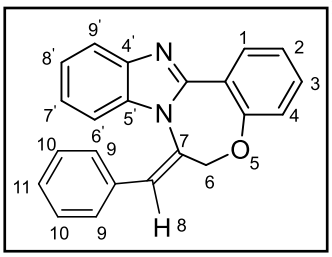

^{1}H-NMR (400 MHz, $CDCl_3$) δ 8.69 (dd, J = 8.1 and 1.6 Hz, H1), 7.88 (m, H9'), 7.71 (m, H6'), 7.50-7.39 (m, 5H, H9, H10, H11), 7.41 (m, H3) 7.36 (m, 2H, H7' and H8'), 7.22 (s, H8), 7.19 (m, 2H, H2 and H4), 5.03 (s, 2H, H6); **^{13}C-NMR** (100 MHz, $CDCl_3$) δ 156.1, 150.5, 143. 6, 134.6, 133.8, 131.9, 131.8, 131.7, 129.1, 128.8, 128.6, 127.3, 123.3, 122.7, 120.7, 120.1, 117.6, 110.7, 68.8.

4.23.11 Synthesis of 6-methylbenzo[4,5]imidazo[1,2-*a*]pyrrolo[2,1-*c*]pyrazine (146)

To a solution of benzomidazole derivative **145** (1.1 g, 5 mmol) in DMF (10 mL) was added NaH (60% suspension in oil) (0.4 g, 10 mmol) and the resulting mixture was reacted as described in general procedure. The residue was purified by column chromatography using hexane/ethylacetate (3:1) to give **146** as a brown crystal

(isolated yield: 92%, 1.02 g) from hexane/ethylacetate, (mp 147-149 ºC). (lit. mp = 158 ºC[103]).

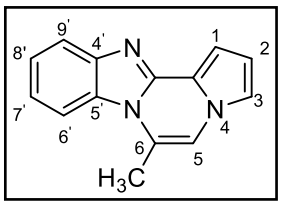

^{1}H-NMR (400 MHz, CD_3OD) δ 7.91 (m, 2H, H9' and H6'), 7.41 (td, J = 7.4 and 1.0 Hz, H8'), 7.37 (bs, H5), 7.30 (td, J = 1.0 and 7.4 Hz, H7'), 7.23 (dd, J = 1.3 and 2.5 Hz, H3), 7.14 (bs, H1), 6.71 (dd, J = 2.5 and 4.0 Hz, H2) 2.86 (d, J = 1.1 Hz, 3H, CH_3); **^{13}C-NMR** (100 MHz, CD_3OD) δ 144.0, 143.0, 131.1, 124.0, 122.0, 120.6, 120.2, 119.4, 117.2, 112.7, 109.9, 106.2, 17.7; **IR** (cm^{-1}) 3103, 1614, 1566, 1501, 1445, 1354, 1269, 1223, 1073, 737.

REFERENCES

[1] Nakhi, A. *Bioorg. Med. Chem. Lett.* **2012**, *22*, 4418-4427.

[2] Patel, K. V.; Sing. H. A.; Jain, D. K.; Patel, P.; Veerasamy, R.; Sharma, P. C.; Rajak, H. *J. Pharm. Sci,* **2017**, *3*, 71-78.

[3] Langfeld, M.; *The World Health Report*; Reducing Risks, Promoting Healthy Life; World Health Organization: Geneva, France, 2002; pp 1–14.

[4] Qu, D.; Ludwig, D. S.; Gammeltoft, S.; Piper, M.; Pelleymounter, M. A.; Cullen, M. J.; Mathes, W. F.; Przypek, J.; Kanarek, R.; Maratos-Flier, E. *Nature* **1996**, *380*, 243-247.

[5] Della-Zuana, O.; Presse, F.; Ortola, C.; Duhault, J.; Nahon, J. L.; Levens, N. *Int. J. Obes.* **2002**, *26*, 289-1295.

[6] McBriar, M. D.; Guzik, H.; Xu, R.; Paruchova, J.; Li, S.; Palani, A.; Clader, J. W.; Greenlee, W. J.; Hawes, B. E.; Kowalksi, T. J.; O'Neill, K.; Spar, B.; Weig, B. *J. Med. Chem*. **2005**, *48*, 2274-2277.

[7] Dyck, B.; Markison, S.; Zhao, L.; Tamiya, J.; Grey, J.; Rowbottom, M. W.; Zhang, M.; Vickers, T.; Sorensen, K.; Norton, C.; Wen, J.; Heise, C. E.; Saunders, J.; Conlon, P.; Madan, A.; Schwarz, D.; Goodfellow, V. S. *J. Med. Chem*. **2006**, *49*, 3754-3756.

[8] Finder, V. H. *J. Alzheimers. Dis.* **2010**, *22*, 1-5.

[9] Sahu, S. N.; Singh, S.; Shaw, R.; Ram, V. J.; Pratap, R. *RSC Adv*. **2016**, *6*, 85515-85520.

[10] Brouillette, Y.; Martinez, J.; Lisowski, V. *J. Org. Chem*. **2009**, *74*, 4975-4981.

[11] Sauve, A. A. *Biochim. Biophys. Acta*. **2010**, *1804*, 1591-1603.

[12] Longo, V. D.; Kennedy, B. K. *Cell* **2006**, *126*, 257-268.

[13] Galli, M.; Van Gool, F.; Leo, O. *Biochem. Pharmacol*. **2011**, *81*, 569-576.

[14] Choi, J. E. *Curr. Opin. Genet. Dev*. **2014**, *26*, 24-32.

[15] Jing, H.; Hu, J.; He, B.; Negron Abril, Y. L.; Stupinski, J.; Weiser, K.; Carbonaro, M.; Chiang, Y. L.; Southard, T.; Giannakakou, P.; Weiss, R. S.; Lin, H. *Cancer Cell* **2016**, *29*, 297-310.

[16] Sundriyal, S.; Moniot, S.; Mahmud, Z.; Yao, S.; Fruscia, P. D.; Reynolds, C. R.; Dexter, D. T.; Sternberg, M. J. E.; Lam, E. W. F.; Steegborn, C.; Fuchter, M. J. *J. Med. Chem.* **2017**, *60*, 1928-1945.

[17] Zhang, H. T. *Curr. Pharm. Des*. **2009**, *15*, 1688-1698.

[18] Press, N. J.; Banner, K. H. *Prog. Med. Chem*. **2009**, *47*, 37-74.

[19] DalPiaz, V.; Giovannoni, M. P.; Vergelli, C.; AguilarIzquierdo, Pyridazin-3(2h)-one derivatives as pde4 inhibitors. W.O. Patent 2003097613, November 27, 2003.

[20] Gràcia, J.; Buil, M. A.; Castro, J.; Eichhorn, P.; Ferrer, M.; Gavaldà, A.; Hernández, B.; Segarra, V.; Lehner, M. D.; Moreno, I.; Pagès, L.; Roberts, R. S.; Serrat, J.; Sevilla, S.; Taltavull, J.; Andrés, M.; Cabedo, J.; Vilella, D.; Calama, E.; Carcasona, C.; Miralpeix, M. *J. Med. Chem*. **2016**, *59*, 10479−10497.

[21] Borowsky, B.; Durkin, M. M.; Ogozalek, K.; Marzabadi, M. R.; DeLeon, J.; Lagu, B.; Heurich, R.; Lichtblau, H.; Shaposhnik, Z.; Daniewska, I.; Blackburn, T. P.; Branchek, T. A.; Gerald, C.; Vaysse, P. J.; Forray, C. *Nat. Med*. **2002**, *8*, 825-830.

[22] Chaki, S.; Funakoshi, T.; Hirota-Okuno, S.; Nishiguchi, M.; Shimazaki, T.; Iijima, M.; Grottick, A. J.; Kanuma, K.; Omodera, K.; Sekiguchi, Y.; Okuyama, S.; Tran, T.-A.; Semple, G.; Thomsen, W. *J. Pharmacol. Exp. Ther*. **2005**, *313*, 831-839.

[23] Chaki, S.; Yamaguchi, J.; Yamada, H.; Kanuma, K.; Sekiguchi, Y. *Drug Dev. Res*. **2005**, *65*, 278-290.

[24] Iden, H. S.; Lubel, W. D. *Org. Lett*. **2006**, *8*, 3425-3428.

[25] Evans, B. E.; Rittle, K. E.; Bock, M. G.; Dipardo, R. M.; Freidinger, R. M.; Whitter, W. L.; Lundell, G. F.; Veber, D. F.; Anderson, P. S.; Chang, R. S. L.; Lotti, V. J.; Cerino, D. J.; Chen, T. B.; Kling, P. J.; Kunkel, K. A.; Springer, J. P.; Hirshfield, J. *J. Med. Chem*. **1988**, *31*, 2235–2246.

[26] Patchett, A. A.; Nargund, R. P. *Annu. Rep. Med. Chem*. **2000**, *35*, 289–298.

[27] Pereillo, J. M.; Maftouh, M.; Andrieu, A.; Uzabiaga, M. F.; Fedeli, O.; Savi, P.; Pascal, M.; Herbert, J. M.; Maffrand, J. P.; Picard, C. *Drug Metab. Dispos*. **2002**, *30*, 1288–1295.

[28] Nakamoto, Y.; Ishizuka, Y.; Fujii, M. JPO 61172884 A 1986.

[29] Nakanishi, M.; Tahara, T.; Araki, K.; Shiroki, M.; Tsumagari, T.; Takigawa, Y. *J. Med. Chem*. **1973**, *16*, 214–219.

[30] Zhao, G.; Iyengar, R. R.; Judd, A. S.; Cool, B.; Chiou, W.; Kifle, L.; Frevert, E.; Sham, H.; Kym, P. R. *Bioorg. Med. Chem. Lett*. **2007**, *17*, 3254- 3257.

[31] Zhao, G.; Iyengar, R. R.; Judd, A. S.; Cool, B.; Chiou, W.; Kifle, L.; Frevert, E.; Sham, H.; Kym, P. R. *Bioorg. Med. Chem. Lett.* **2007**, *17*, 3254-3257.

[32] Terzioglu, N.; Gursoy, A. *Eur. J. Org. Chem.* **2003**, *38*, 781-786.

[33] Gadad, A. K.; Noolvi, M. N.; Karpoormath, R. K. *Bioorg. Med. Chem.* **2004**, *12*, 5651-5659.

[34] Andreani, A.; Granaiola, M.; Leoni, A.; Locatelli, A.; Morigi, R.; Rambaldi, R. G.; Fato, R.; Bergamini, C.; Farruggia, G. *J. Med. Chem*. **2005**, *48*, 3085-3089.

[35] Andreani, A.; Leoni, A.; Locatelli, A.; Morigi, R.; Rambaldi, R. G.; Recanatini, M.; Garaliene, V. *Bioorg. Med. Chem*. **2000**, *8*, 2359-2366.

[36] Kolavi, G.; Hegde, V.; Khazi, I. A. *Tetrahedron Lett.* **2006**, *47*, 2811-2814.

[37] Puterová, Z.; Krutošíkov, A.; Véghc, D. *ARKIVOC* **2010**, *2010*, 209-246.

[38] Hoffman, R. A.; Gronowitz, S. *Ark. Kemi* **1960**, *16*, 515-516.

[39] Stacy, G. W.; Eck, D. L. *Tetrahedron Lett*. **1967**, 5201-5204.

[40] Eck, D. L.; Stacy, G.W. *J. Heterocycl. Chem.* **1969**, *6*, 147-151.

[41] Elguero, J.; Marzin, C.; Katritzky, A. R.; Linda, P. *The Tautomerism of Heterocycles*, *in Advances in Heterocyclic Chemistry*, Academic Press: New York, 1976.

[42] Brandsma, L.; Vvedensky, V. Y.; Nedolya, N. A.; Tarasova, O. A.; Trofimov, B. A. *Tetrahedron Lett*. **1998**, *39*, 2433-2436.

[43] Doyle, M. P.; Siegfried, B.; Dellaria, J. F. *J. Org. Chem*. **1977**, *42*, 2426-2431.

[44] Iaroshenko, V. O.; Ali, S.; Mkrtchyan, S.; Gevorgyan, A.; Babar, T. M.; Semeniuchenko, V.; Hassan, Z.; Villinger, A.; Langer, P. *Tetrahedron Lett*. **2012**, *53*, 7135-7139.

[45] Zhang, H.; Yao, B.; Zhao, L.; Wang, D. X. B.; Xu, Q.; Wang, M. X. *J. Am. Chem. Soc*. **2014**, *136*, 6326-6332.

[46] King, A. E.; Huffman, L. M.; Casitas, A.; Costas, M.; Ribas, X.; Stahl, S. S. *J. Am*. *Chem. Soc*. **2010**, *132*, 12068-12073.

[47] Du, Z. J.; Gao, L. X.; Lin, Y. J.; Han, F. S. *Chem*. *Cat. Chem*. **2014**, *6*, 123-126.

[48] Ribas, X.; Calle, C.; Pouter, A.; Casitas, A.; Gómez, L.; Xifra, R.; Parella, T.; Benet-Buchholz, J.; Schweiger, A.; Mitrikas, G.; Solà, M.; Llobet, A.; Stack, D. P. *J. Am. Chem. Soc*. **2010**, *132*, 12299–12306.

[49] Phipps, R. J.; Gaunt, M. J. *Science*, **2009**, *323*, 1593–1597.

[50] Chinchilla, R.; Najera, C. *Chem. Rev*. **2007**, *107*, 874−922.

[51] Jenny, N. M.; Mayor, M.; Eaton, T. R. *Eur. J. Org. Chem*. **2011**, *2011*, 4965−4983.

[52] (a) Lauterbach, T.; Livendahl, M.; Rosellón, A.; Espinet, P.; Echavarren, A. M. *Org. Lett*. **2010**, *12*, 3006−3009. (b) Leadbeater, N. E. *Nature Chem*. **2010**, *2*, 1007−1009.

[53] Tykwinski, R. R. *Angew. Chem*. *Int. Ed.* **2003**, *42*, 1566-1568.

[54] Batey, R. A.; Shen, M.; Lough, A. *J. Org. Lett*. **2002**, *4*, 1411-1414.

[55] (a) Chow, H. F.; Wan, C. W.; Low, K. H.; Yeung, Y.Y. *J. Org. Chem*. **2001**, *66*, 1910-1913 (b) Rau, S.; Lamm, K.; Goerls, H.; Schoeffel, J.; Walther, D. *J. Organomet. Chem*. **2004**, *689*, 3582-3592. (c) Urgaonkar, S.; Verkade, J. G. *J. Org. Chem*. **2004**, *69*, 5752-5755.

[56] Chinchilla, R.; Nájera, C. *Chem. Soc. Rev.*, **2011**, *40*, 5084–5121.

[57] Mulla, A. A. *Der Pharma Chemica*. **2017**, *9*, 141-147.

[58] Mukhtyar. S. S.; Kumar, A.; Dwivedi, J.; Singh, R. *Int. J. Pharm. Sci. Res*. **2013**, *4*, 66-77.

[59] Wahbi, H. I.; Ishak, C.Y.; Khalid, A.; Adlan, T. *Int. J. Pharm. Phytopharmacol. Res*. **2014**, *4*, 13-19.

[60] Dewar, M. J. S.; Harget, A. J.; Trinajstié, N. *J. Am. Chem. Soc.* **1969**, *91*, 6321-6325.

[61] Young, P. T.; McLaughlin, M. M.; Kumari, S.; Kassisi, S.; Doyle, M. L.; McNulty, D.; Gallagher, T. F.; Fisher, S.; McDonnell, P. C.; Carr, A. S.; Huddleston, M. J.; Seibel, G.; Porter, T. G.; Livi, G. P.; Adams, J. L.; Lee, J. C. *J. Biol. Chem.* **1997**, *272*, 12116-12121.

[62] Singh, N.; Pandurangan, A.; Rana, K.; Anand, P.; Ahamad, A.; Kumar, A. *Int. J. Curr. Pharm.* **2012**, *1*, 119-127.

[63] Mast, E. E.; Alter, M. J.; Margolis, H. S. *Vaccine*, **1999**, *17*, 1730-1733.

[64] Lavanchy, D. *J. Viral Hepat*. **2004**, *11*, 97-107.

[65] Li, Y. F.; Wang, G. F.; He, P. L.; Huang, W. G.; Zhu, F. H.; Gao, H. Y.; Tang, W.; Luo, Y.; Feng, C. L.; Shi, L. P.; Ren, Y. D., Lu, W.; Zuo, J. P. *J. Med. Chem*. **2006**, *49*, 4790-4794.

[66] Kumar, B. V. S.; Vaidya, S. D.; Kumar, R. V.; Bhirud, S. B.; Mane, R. B. *Eur. J. Med. Chem*. **2006**, *41*, 599–604.

[67] Camacho, J.; Barazarte, A.; Gamboa, N.; Rodrigues, J.; Rojas, R.; Vaisberg, A.; Gilman, R.; Charris, *J. Bioorg. Med. Chem*. **2011**, *19*, 2023–2029.

[68] Padalkar, V. S.; Borse, B. N.; Gupta, V. D.; Phatangare, K. R.; Patil, V. S.; Umape, P. G.; Sekar, N. *Arab. J. Chem.* **2016**, *9*, 1125-1130.

[69] Mariappaz, G.; Hazarika, R.; Alam, F.; Karki, R.; Patangia, U.; Nath, S. *Arab. J. Chem.* **2015**, *8*, 715-719.

[70] Samir, A. H.; Rumez, R. M.; Fadhil, H. A. *Int. J. Appl. Chem*. **2017**, *13*, 393-407.

[71] Caba, O.; Gavilán, M. D.; Serrano, F. R.; Boulaiz, H.; Aránega, A.; Gallo, M. A.; Marchal, J. A.; Campos, J. M. *Eur. J. Med. Chem*. **2011**, *46*, 3802-3809.

[72] Deng, X. Q.; Wei, C. X.; Li, F. N.; Sun, G. Z.; Quan, Z. S. *Eur. J. Med. Chem*. **2010**, *45*, 3080-3086.

[73] Wilde, M. I.; Benfield, P. *Drugs* **1995**, *49*, 411-439.

[74] Sharma, G.; Park, J. Y.; Park, M. S. *Bioorg. Med. Chem. Lett.* **2008**, *18*, 3188-3191.

[75] Campiani, G.; Nacci, V.; Fiorini, I.; Filippis, M. P. D.; Garofalo, A.; Greco, G.; Novellino, E.; Altamura, S.; Renzo, L. D. *J. Med. Chem.* **1996**, *39*, 2672-2680.

[76] Kumar, R.; Joshi, Y. C. *J. Chem. Sci.* **2009**, *121*, 497-502.

[77] Serrano-Wu, M. H.; St. Laurent, D. R.; Chen, Y.; Huang, S.; Lam, K. R.; Matson, J. A.; Mazzucco, C. E.; Stickle, T. M.; Tully, T. P.; Wong, H. S.; Vyas, D. M.; Balasubramanian, B. N. *Bioorg. Med. Chem. Lett.* **2002**, *12*, 2757-2760.

[78] Badru, R.; Singh, B. *J. Heterocyclic Chem.* **2015**, *52*, 635-640.

[79] Maier, M. E. *Angew. Chem. Int. Ed*. **2000**, *39*, 2073-2077.

[80] Nubbemeyer, U. *Top*. *Curr. Chem*. **2001**, *216*, 125-196.

[81] Goutham, K.; Ashok Kumar, D.; Suresh, S.; Sridhar, B.; Narender, R.; Karunakar, G.V. *J. Org. Chem*. **2015**, *80*, 11162–11168.

[82] Karadeniz, E.; Zora, M. *Tetrahedron Lett*. **2016**, *57*, 4930-4934.

[83] Sanchez-Quesada, J.; Ghadiri, M. R.; Bayley, H.; Braha, O. *J. Am. Chem. Soc*. **2000**, *122*, 11757-11766.

[84] Bong, D.T.; Clark, T. D.; Granja, J. R.; Ghadiri, M. R. *Angew. Chem. Int. Ed*. **2001**, *40*, 988-1011.

[85] Jarvo, E. R.; Miller, S. J. *Tetrahedron* **2002**, *58*, 2481-2495.

[86] Mikušek, J.; Matouš, P.; Matoušová, E.; Janoušek, M.; Kuneš, J.; Pour, M. *Adv. Synth. Catal.* **2016**, *358*, 2912-2922.

[87] Díaz-Gavilán, M.; Rodríguez-Serrano, F.; Gómez-Vidal, J. A.; Marchal, J. A.; Aránega, A.; Gallo, M. A.; Espinosa, A.; Campos, A. M. *Tetrahedron* **2004**, *60*, 11547-11557.

[88] Shen, J. H.; Yang, X. F.; Wang, F. Y.; Wang, Y.; Cheng, G. L.; Cui, X. L. *RSC Adv*. **2016**, *6*, 48905-48909.

[89] Nagarajan, K.; David, J.; Kulkarni, Y. S.; Hendi, S. B.; Shenoy, S. J.; Upadhyaya, P. *Eur. J. Med. Chem.* **1986**, *21*, 21–26.

[90] Walther, G.; Daniel, H.; Bechtel, W. D.; Brandt, K. *Arzneim. Forsch*. **1990**, *40*, 440–446.

[91] Hadou, A.; Hamid, A.; Mathouet, H.; Deïda, M. F.; Daïch, A. *Heterocycles* **2008**, *76*, 1017–1022.

[92] Grunewald, G. L.; Dahanukar, V. H.; Ching, P.; Crisclone, K. R. *J. Med. Chem.* **1996**, *39*, 3539-3546.

[93] Steiner, G.; Franke, A.; Hädicke, E.; Lenke, D.; Teschendorf, H. J.; Hofmann, H. P.; Kreiskott, H.; Worstmann, W. J. *J. Med. Chem.* **1986**, *29*, 1877-1888.

[94] Liao, Y.; Venhuis, B. J.; Rodenhuis, N.; Timmerman, W.; Wikström, H.; Meier, E.; Bartoszyk, G. D.; Böttcher, H.; Seyfried, C. A.; Sundell, S. *J. Med. Chem.* **1999**, *42*, 2235-2244.

[95] Yavari, H.; Alinezhad, H.; Shafieeb, A. *J. Heterocyclic Chem*. **2017**, *54*, 2393-2396.

[96] Yin, Y.; Zhang, Y. Q.; Jin, B.; Sha, S.; Wu, X.; Sangani, C. B.; Wang, S. F. Qiao, F.; Lu, A. M.; Lv, P. C.; Zhu, H. L. *Bioorg. Med. Chem*. **2015**, *23*, 1231–1240.

[97] Zhao, X.; Zhang, J.; Zheng, Z.; Runsheng, X. *Molecules* **2017**, *22*, 53-65.

[98] Karahan, E.; Koza, G.; Balci, M. *Helv. Chim. Acta* **2014**, *97*, 1487-1496.

[99] Xiangming, H.; Huiqiang, M.; Yulu, W. *ARKIVOC*, **2007**, *13*, 150-154.

[100] Keskin, S.; Balci, M. *Org. Lett*. **2015**, *17*, 964–967.

[101] Hoplamaz, E.; Keskin, S.; Balci, M. *Eur. J. Org. Chem*. **2017**, *2017*, 1489-1497.

[102] Menges, N.; Sari, O.; Abdullayev, Y.; Sag Erdem, S.; Balci, M. *J. Org. Chem*. **2013**, *78*, 5184−5195.

[103] Ramesh, S.; Ghosh, S. K.; Nagarajan, R. *Org. Biomol. Chem.* **2013**, *11*, 7712-7720.

APPENDIX A

SPECTRAL DATA

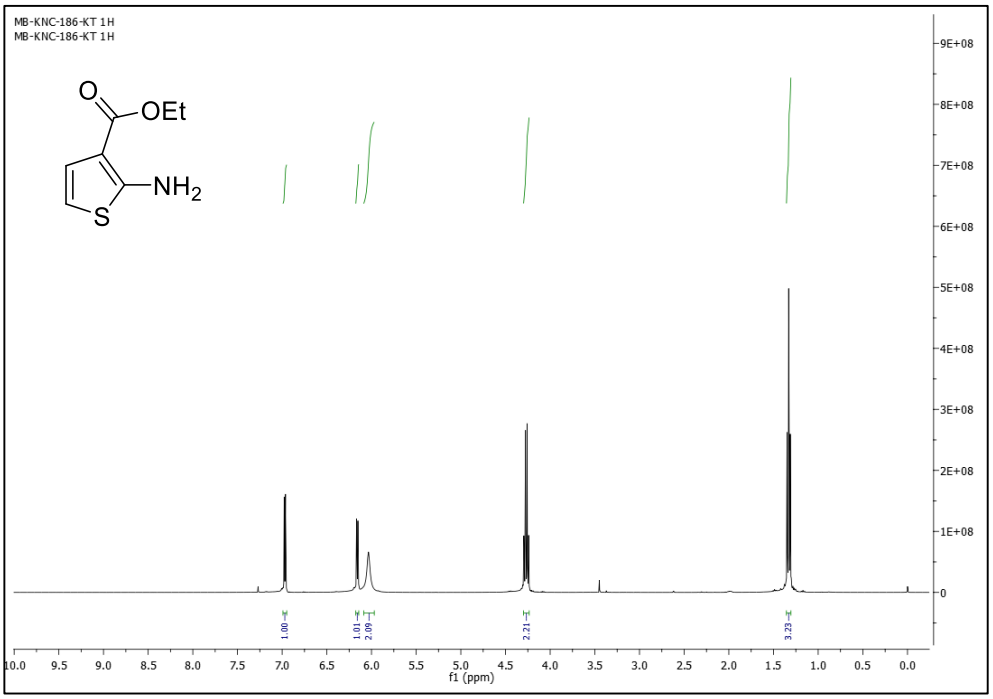

Figure 51. ^{1}H-NMR spectrum of compound **37**

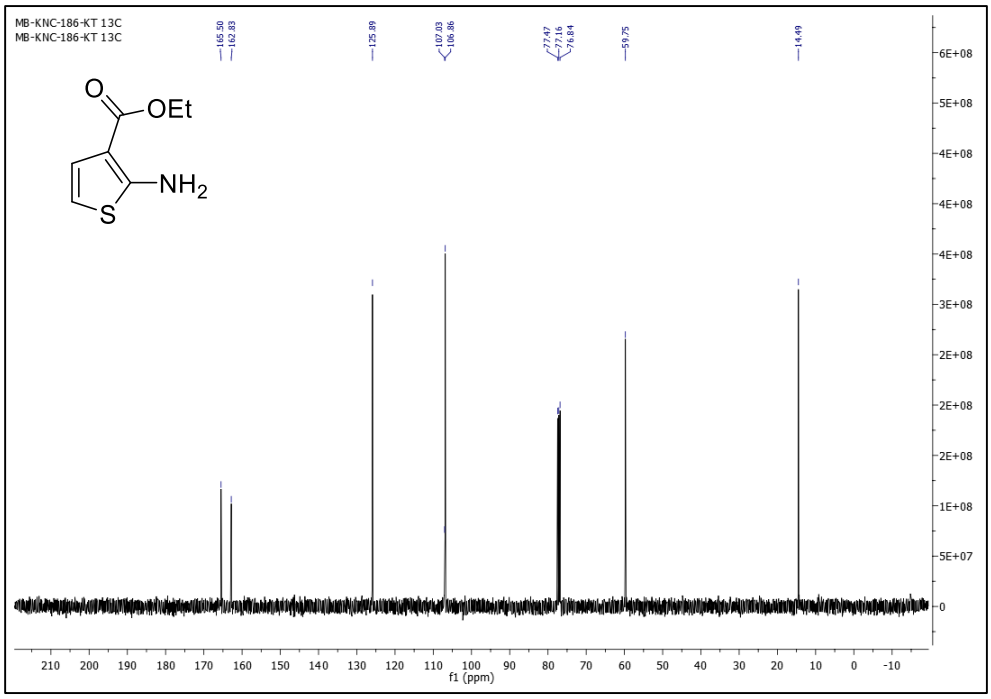

Figure 52. ^{13}C-NMR spectrum of compound **37**

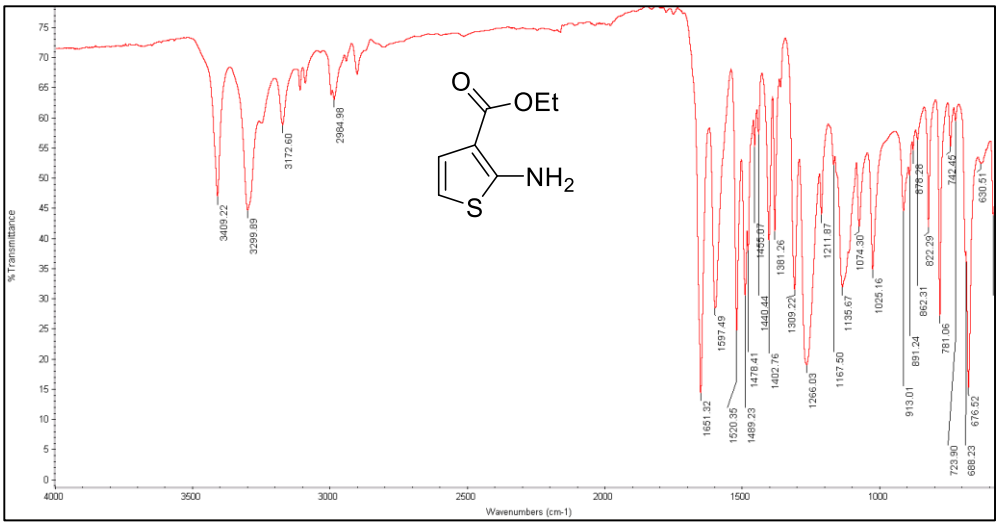

Figure 53. IR spectrum of compound **37**

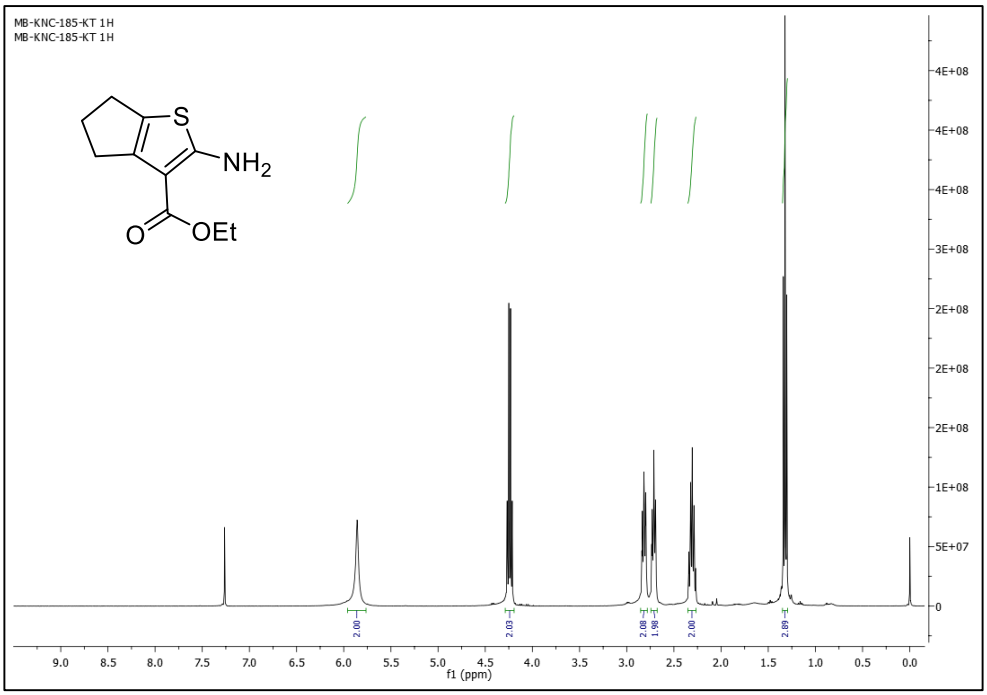

Figure 54. ^{1}H-NMR spectrum of compound **59**

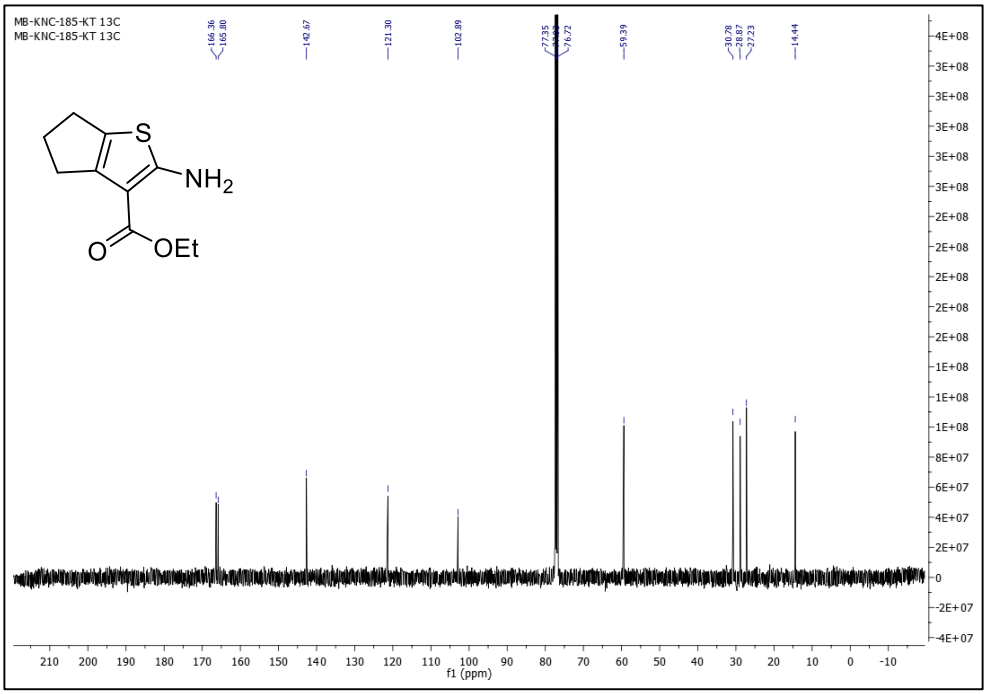

Figure 55. ^{13}C-NMR spectrum of compound **59**

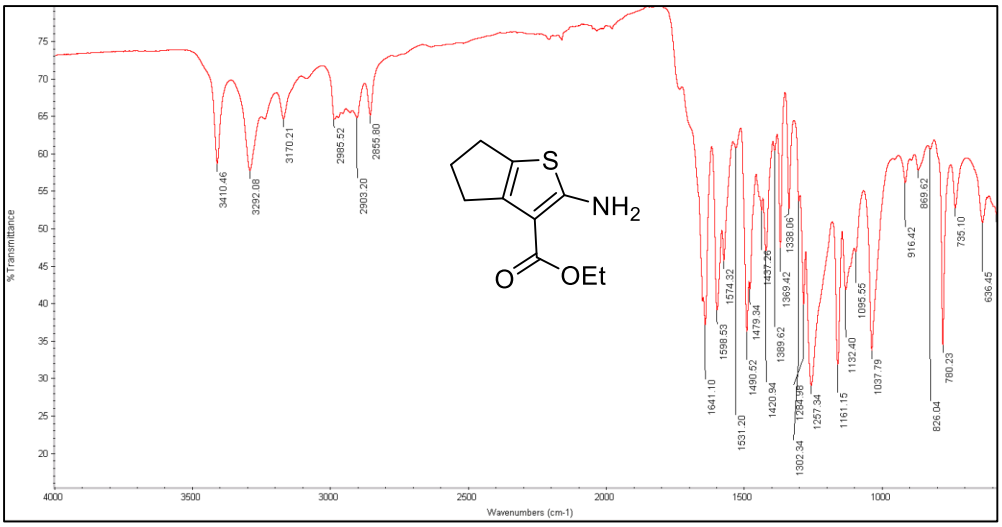

Figure 56. IR spectrum of compound **59**

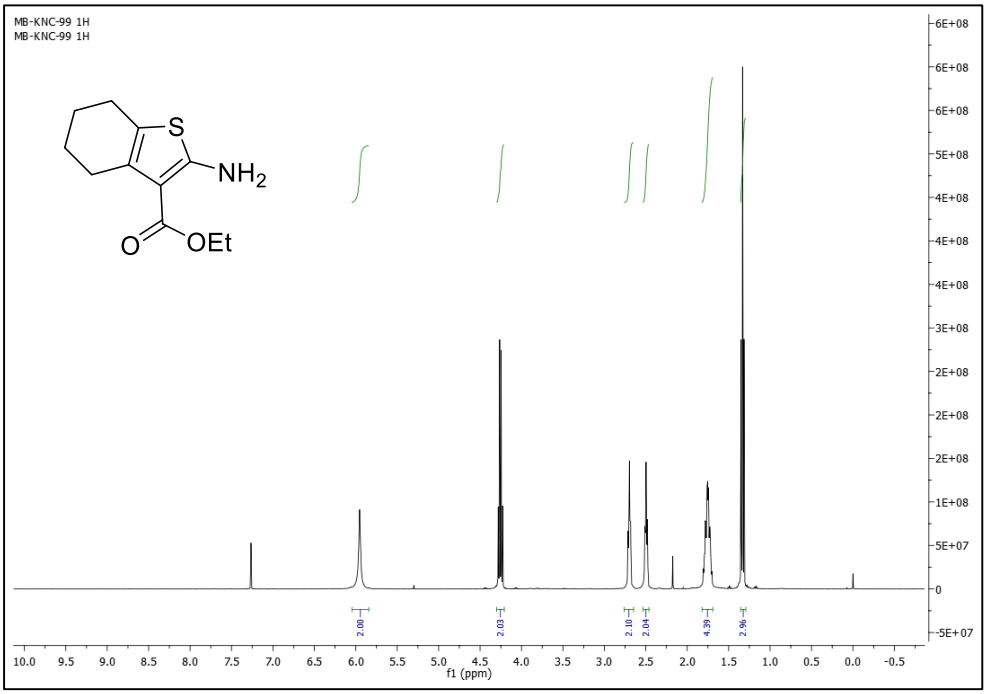

Figure 57. ^{1}H-NMR spectrum of compound **40**

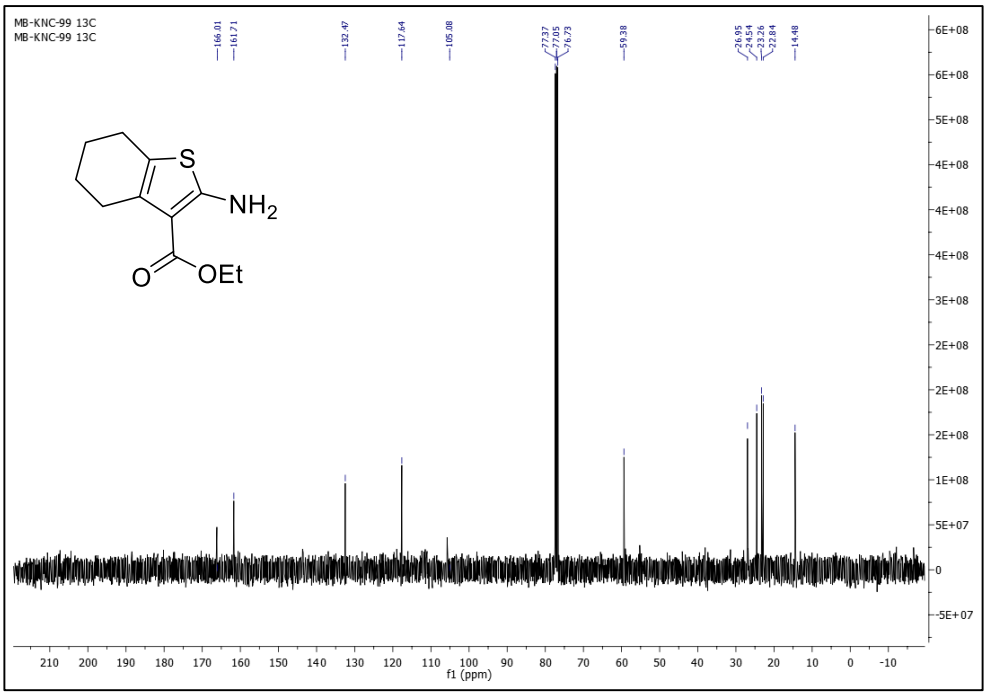

Figure 58. ^{13}C-NMR spectrum of compound **40**

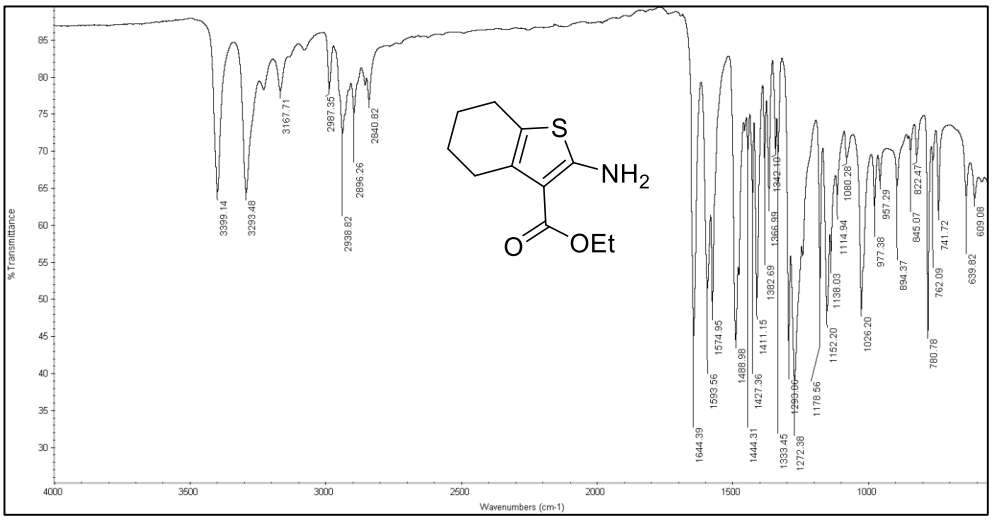

Figure 59. IR spectrum of compound **40**

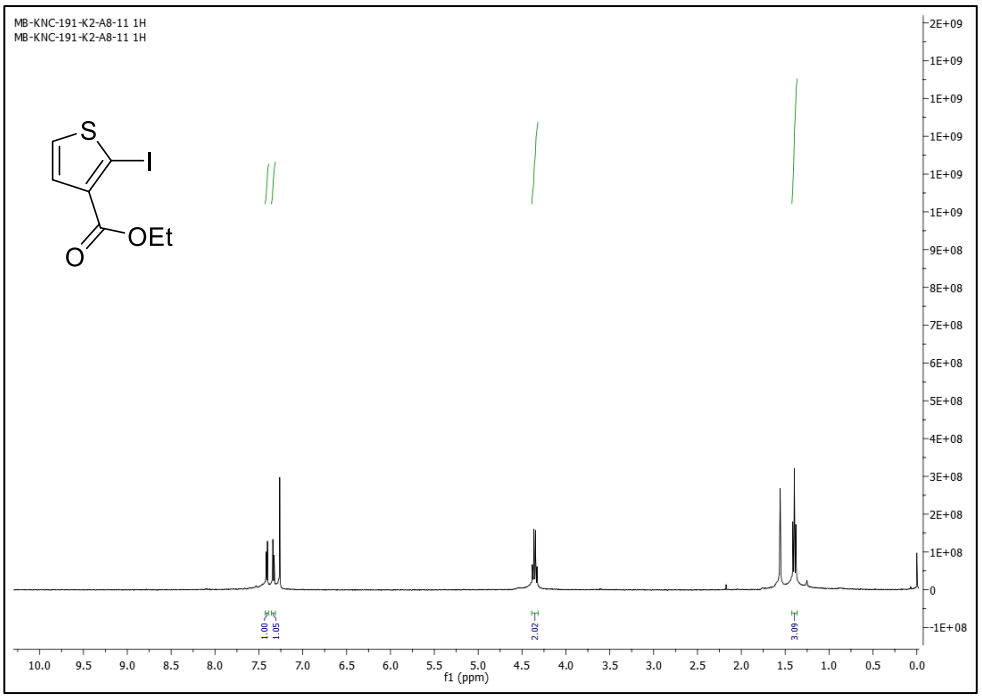

Figure 60. ^{1}H-NMR spectrum of compound **38**

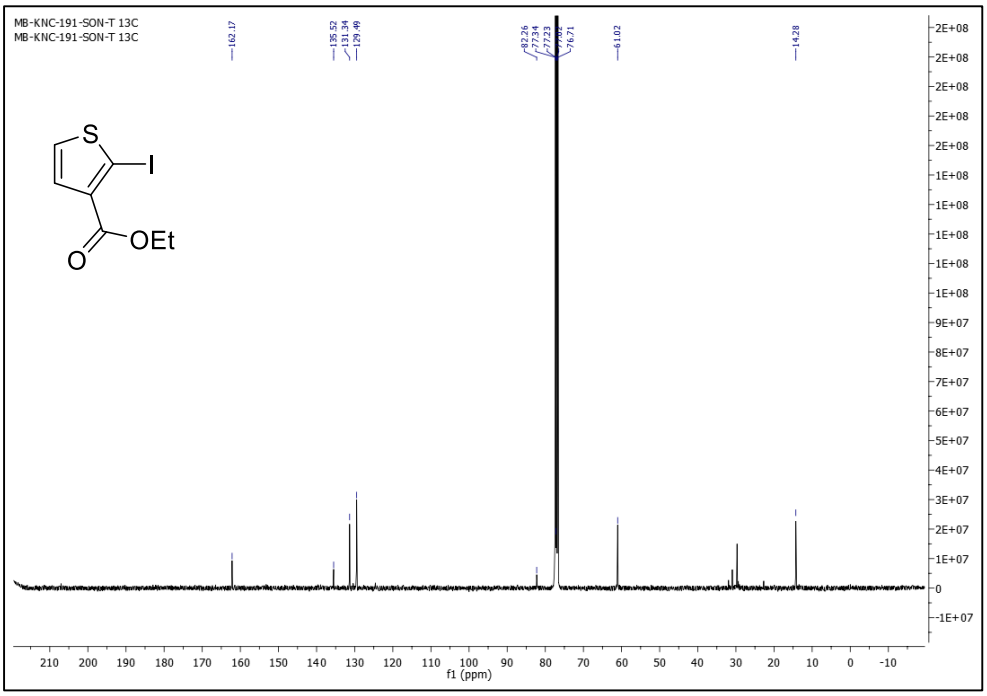

Figure 61. ^{13}C-NMR spectrum of compound **38**

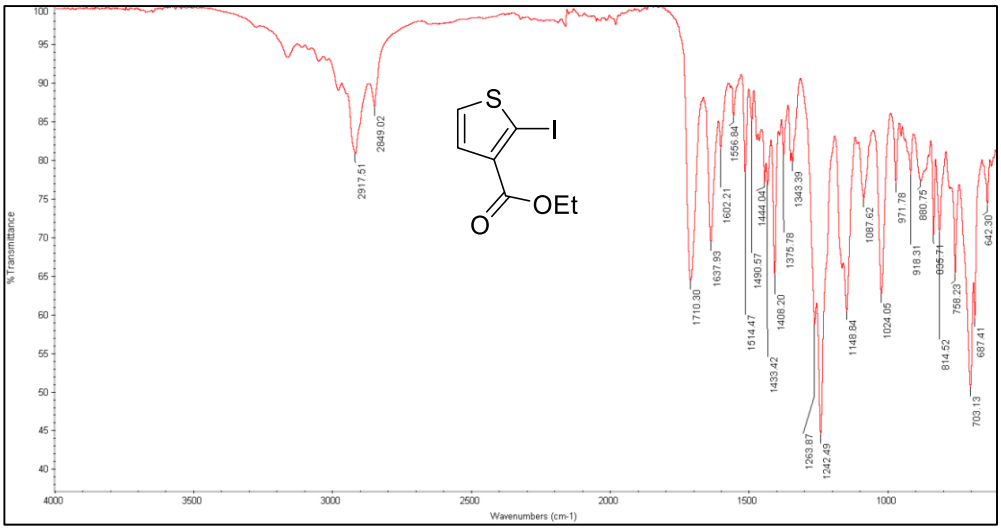

Figure 62. IR spectrum of compound **38**

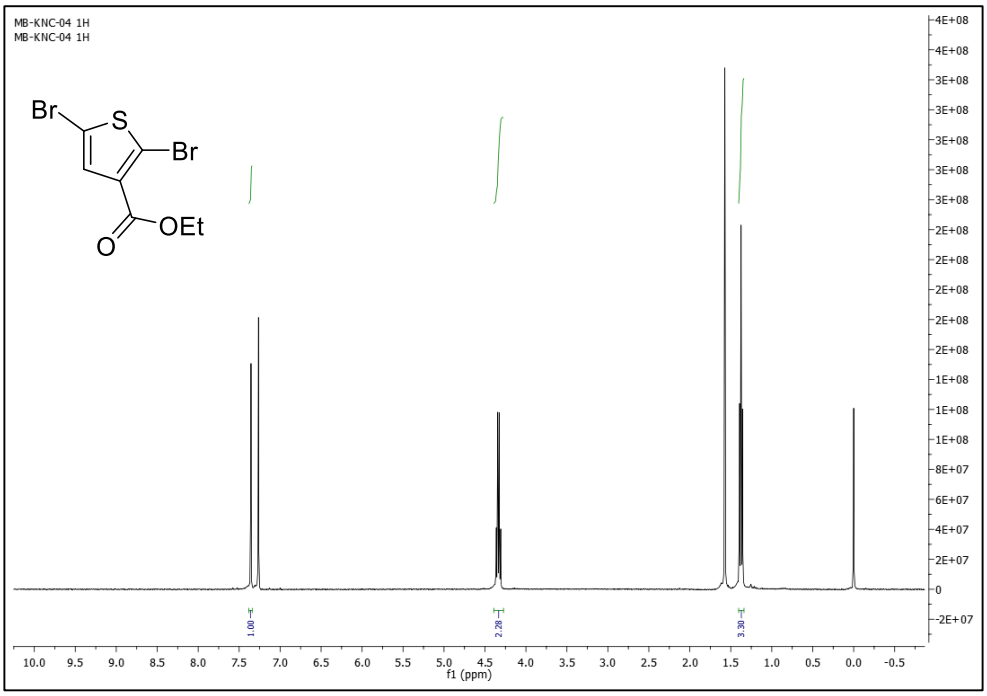

Figure 63. ^{1}H-NMR spectrum of compound **63**

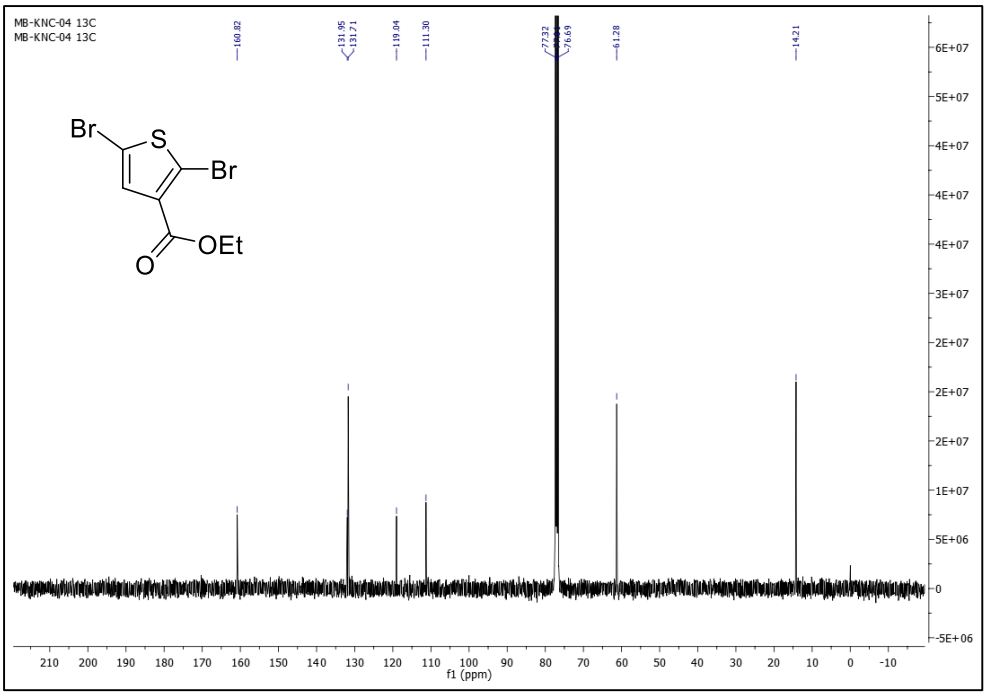

Figure 64. ^{13}C-NMR spectrum of compound **63**

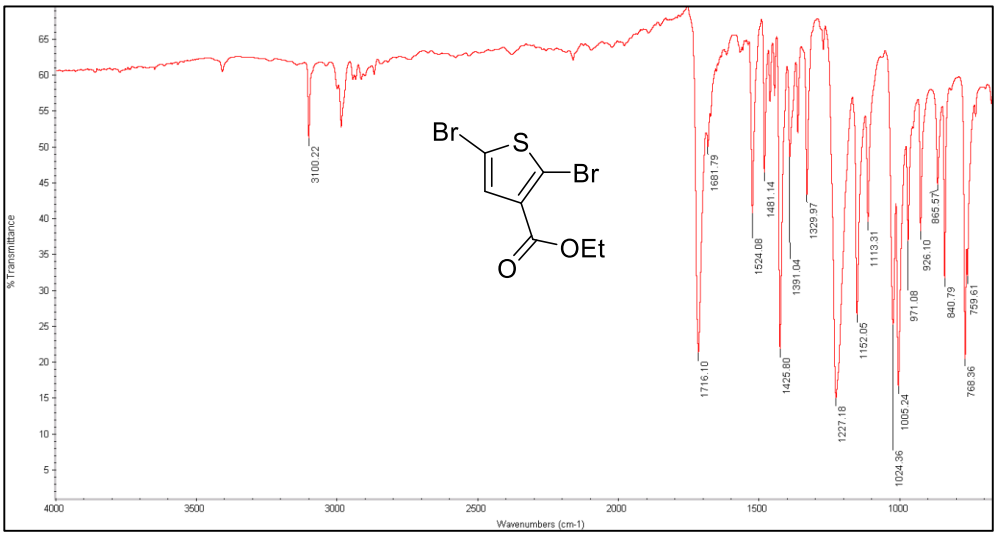

Figure 65. IR spectrum of compound **63**

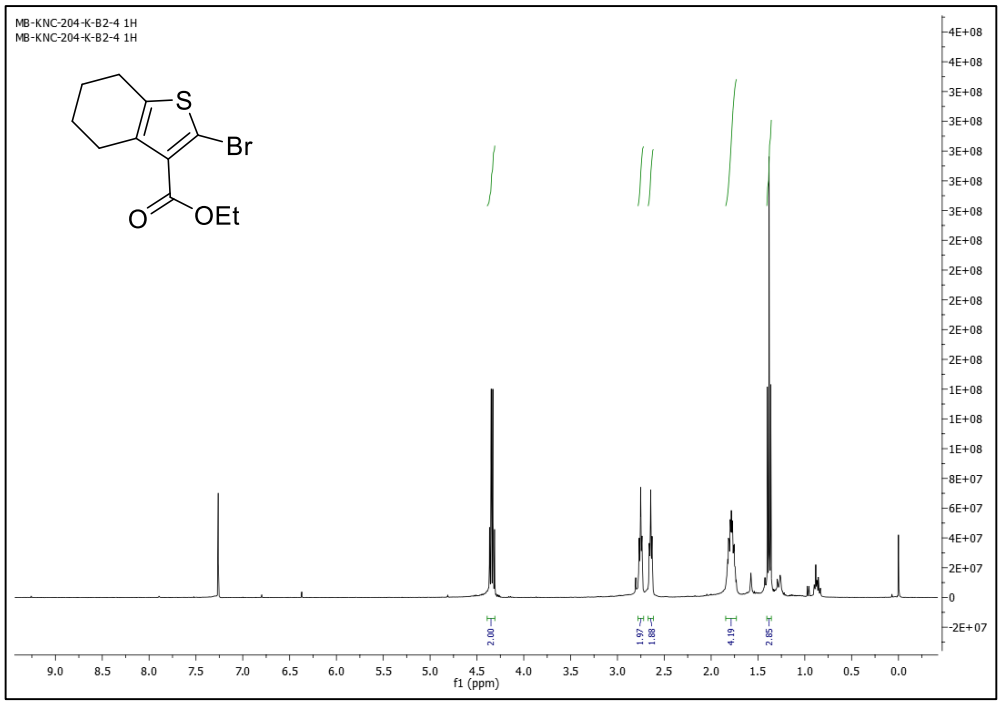

Figure 66. ^{1}H-NMR spectrum of compound **41**

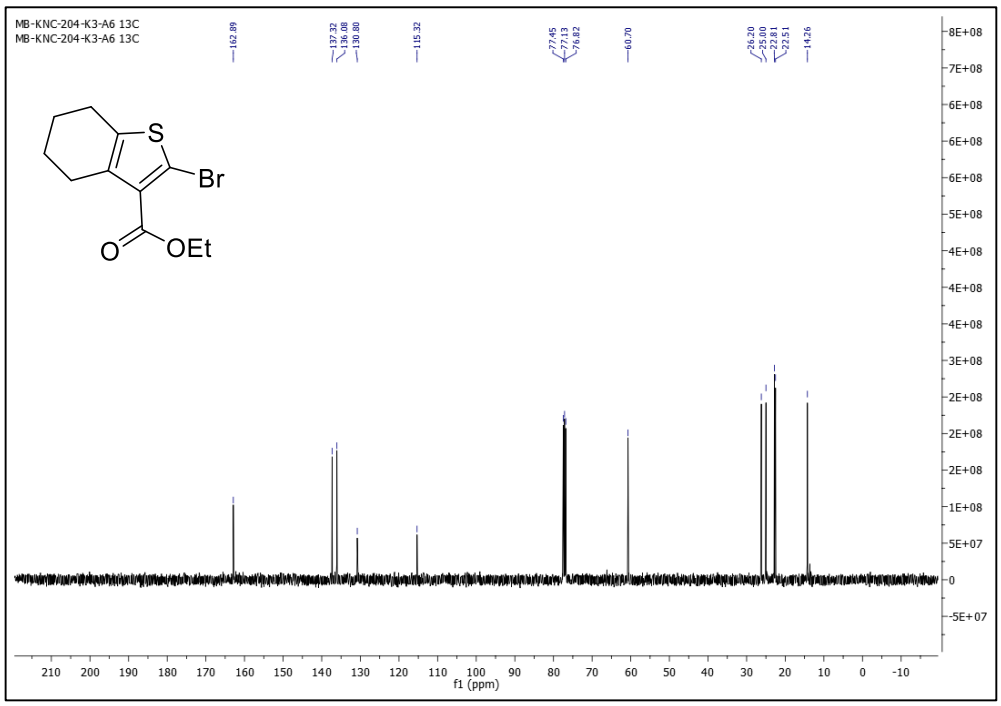

Figure 67. ^{13}C-NMR spectrum of compound **41**

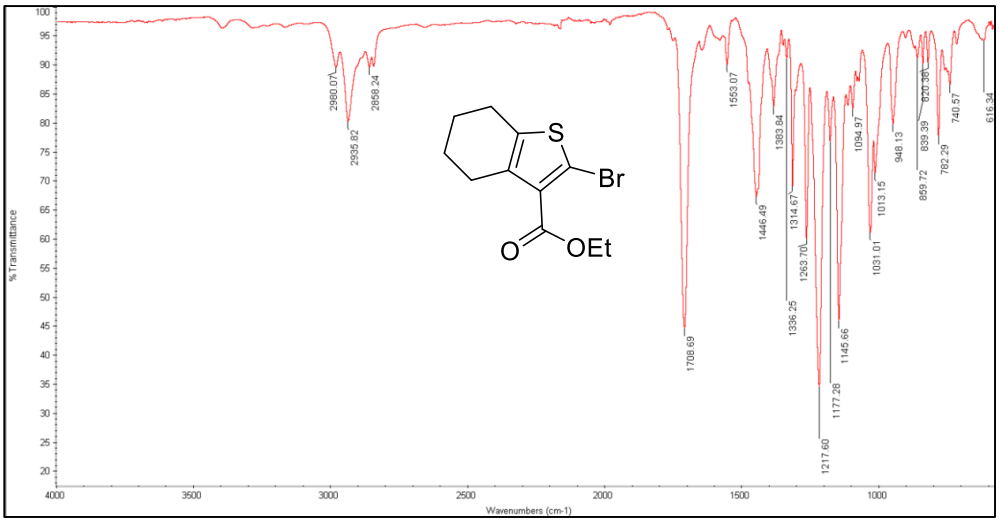

Figure 68. IR spectrum of compound **41**

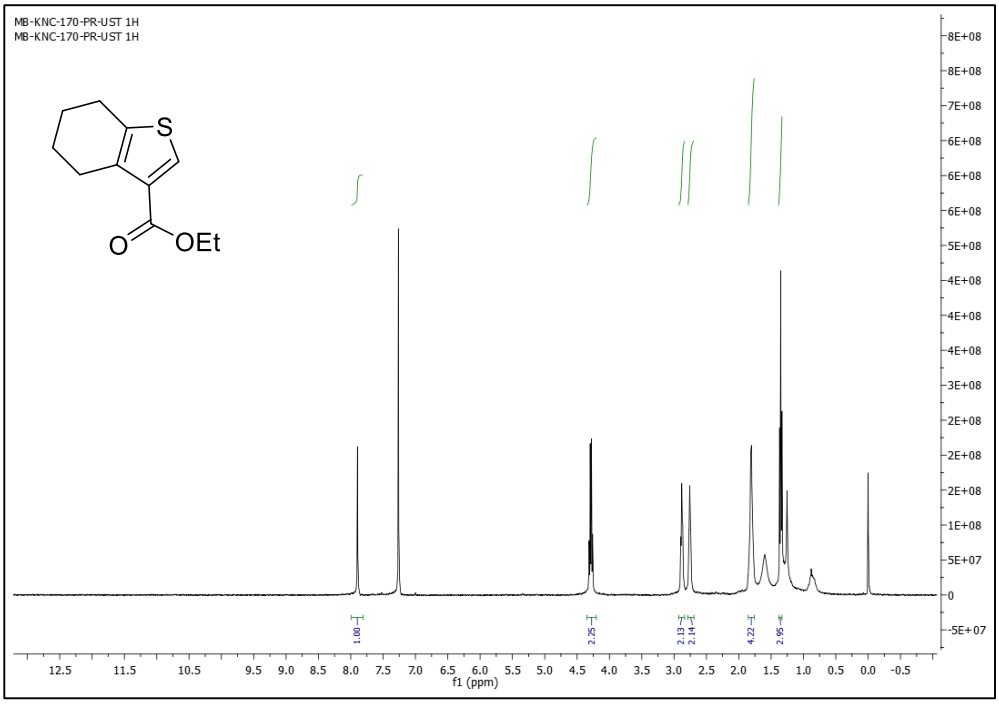

Figure 69. ^{1}H-NMR spectrum of compound **70**

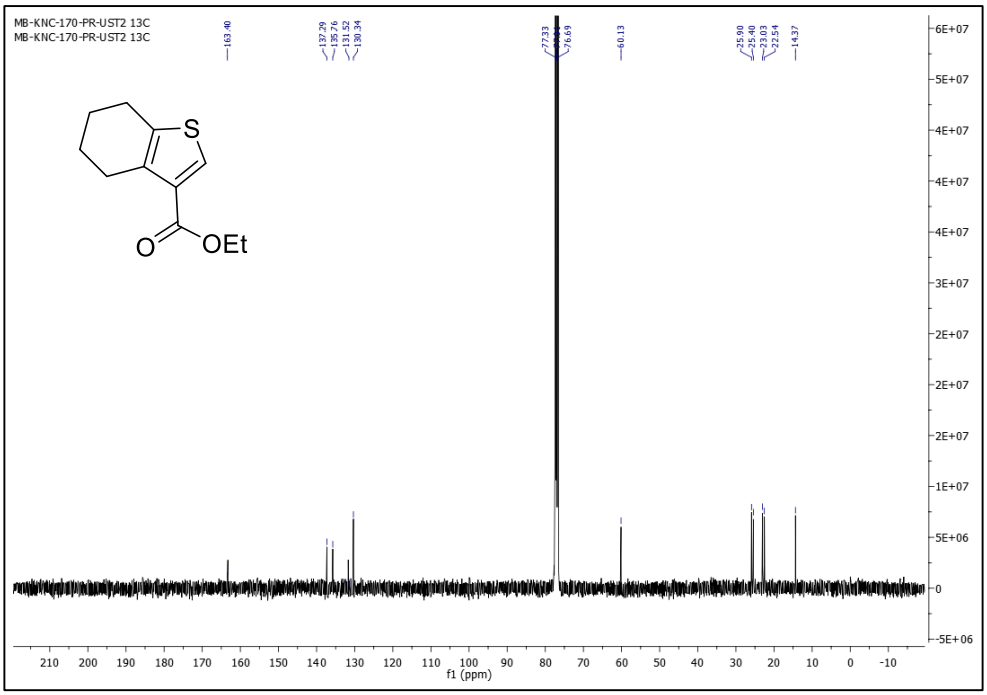

Figure 70. ^{13}C-NMR spectrum of compound **70**

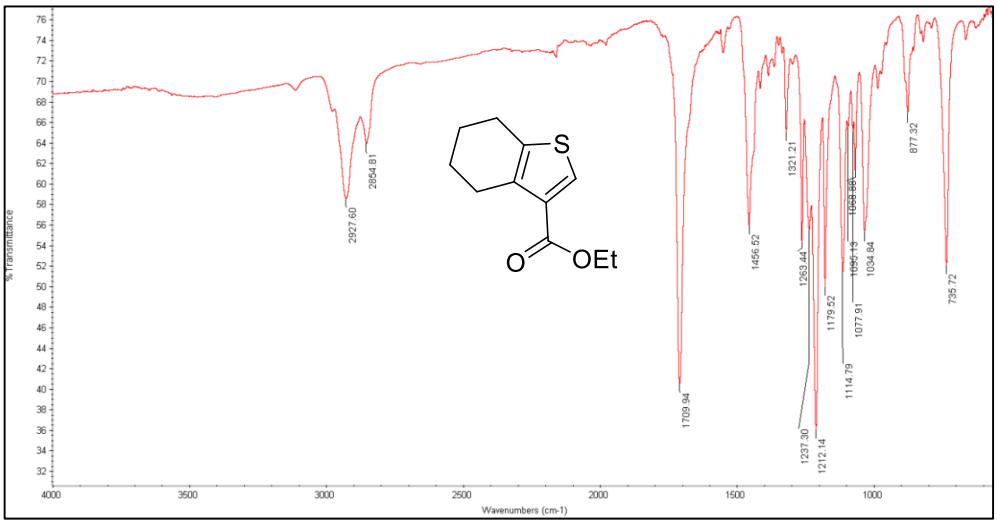

Figure 71. IR spectrum of compound **70**

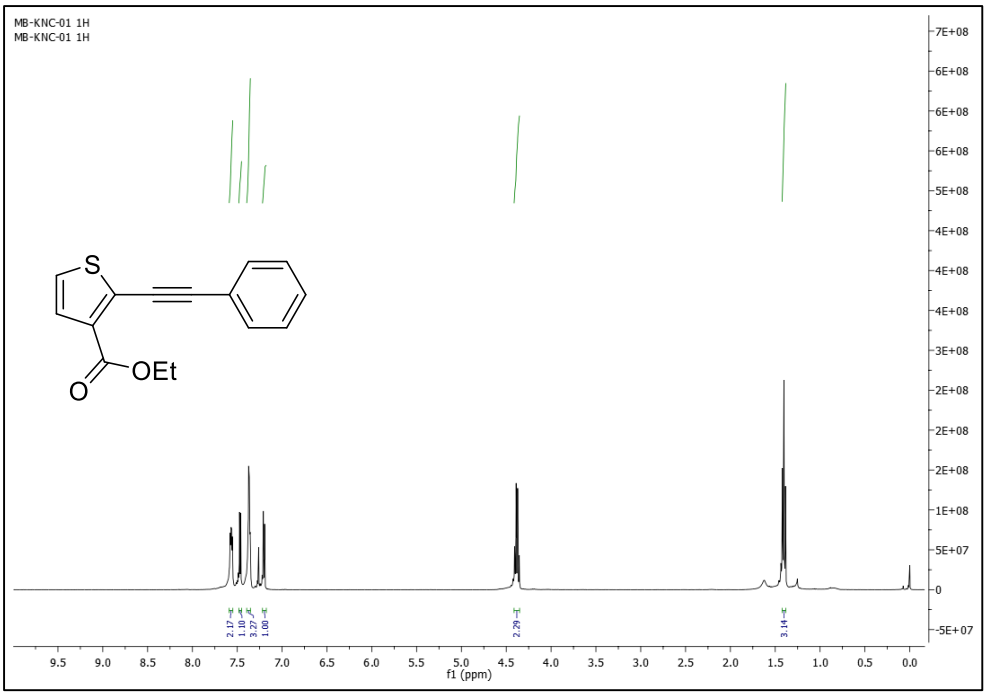

Figure 72. ^{1}H-NMR spectrum of compound **42a**

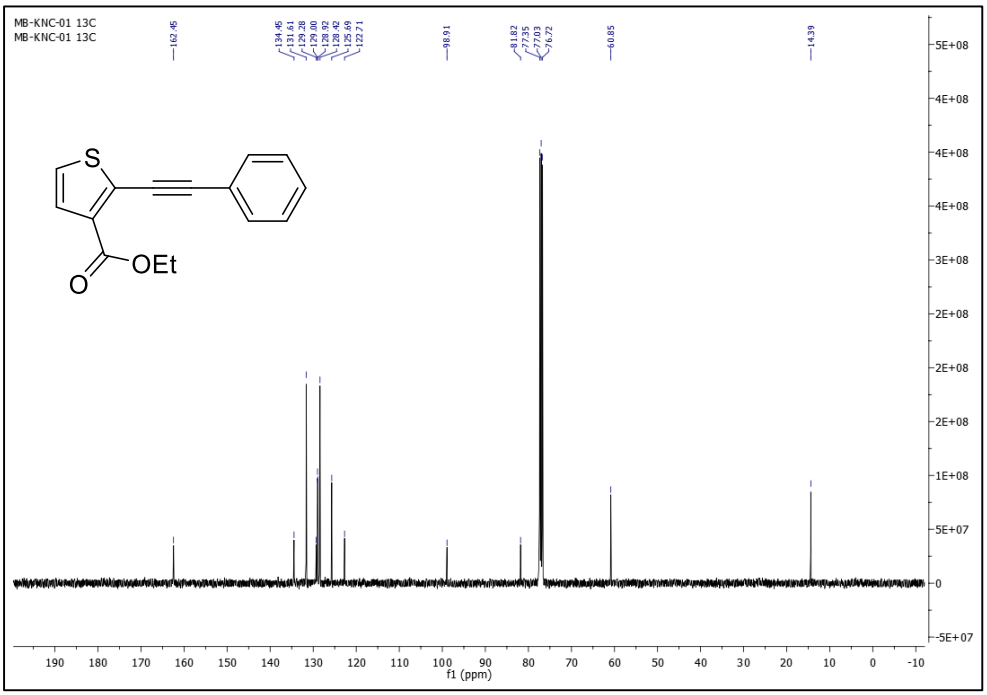

Figure 73. ^{13}C-NMR spectrum of compound **42a**

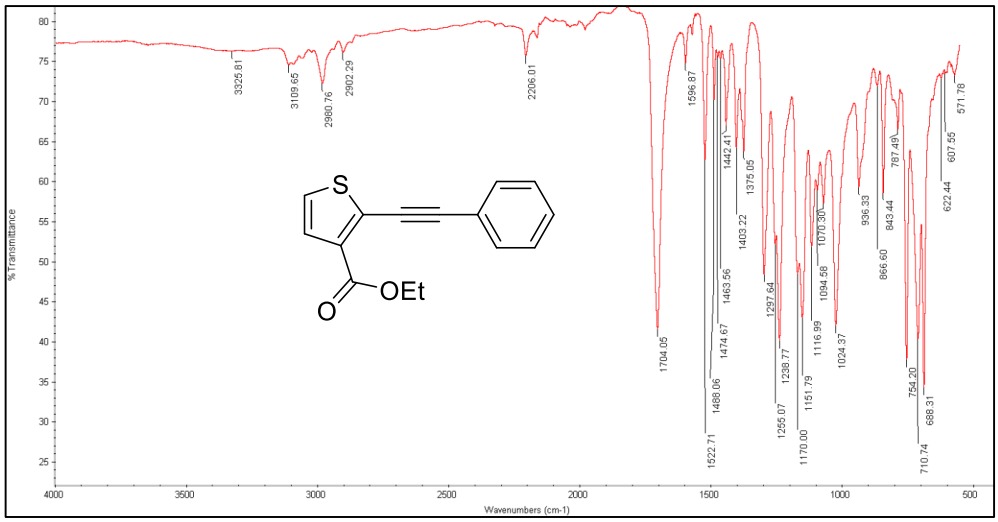

Figure 74. IR spectrum of compound **42a**

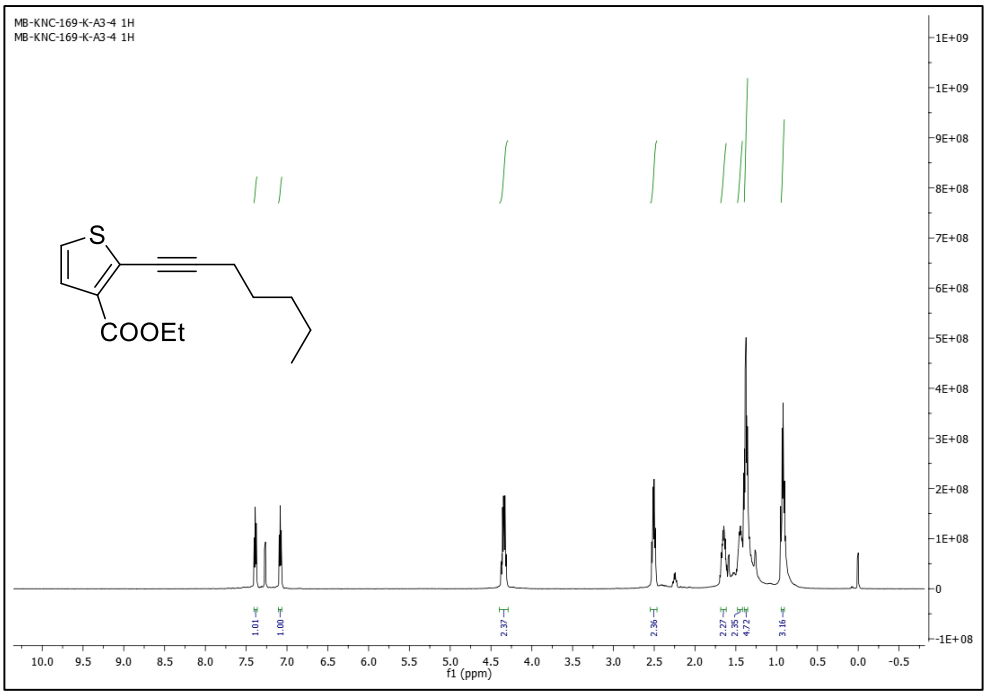

Figure 75. ^{1}H-NMR spectrum of compound **42b**

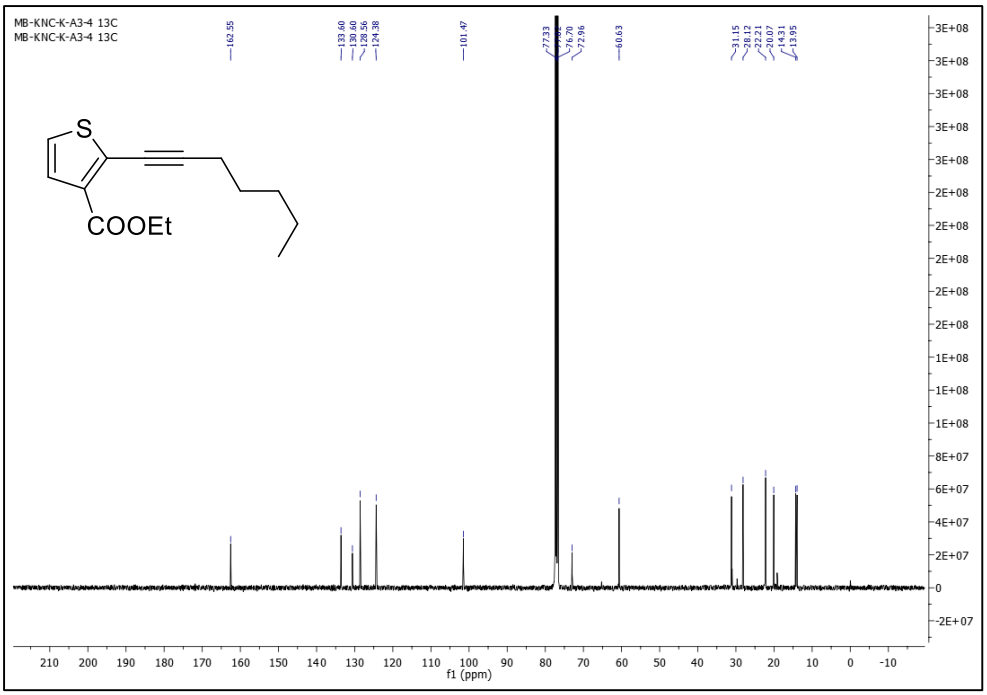

Figure 76. ^{13}C-NMR spectrum of compound **42b**

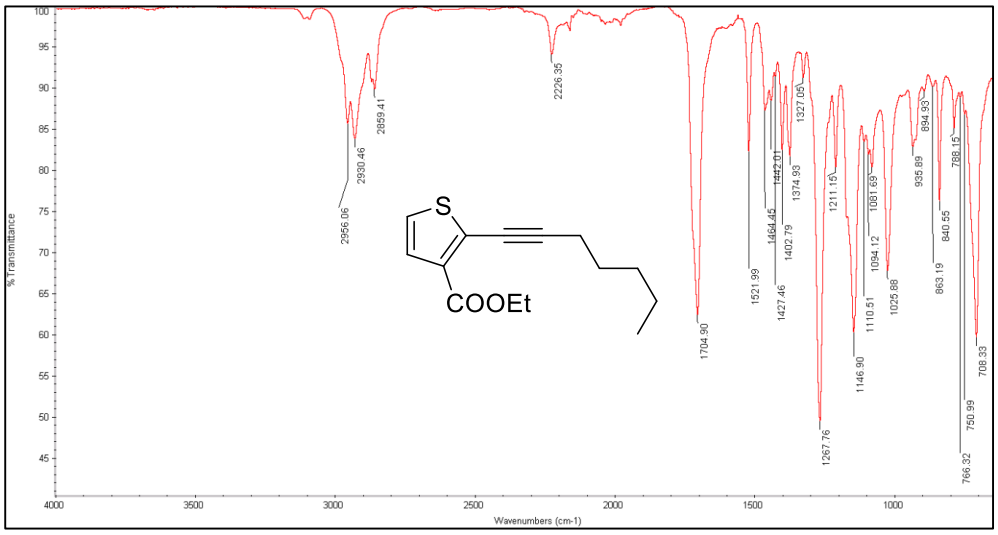

Figure 77. IR spectrum of compound **42b**

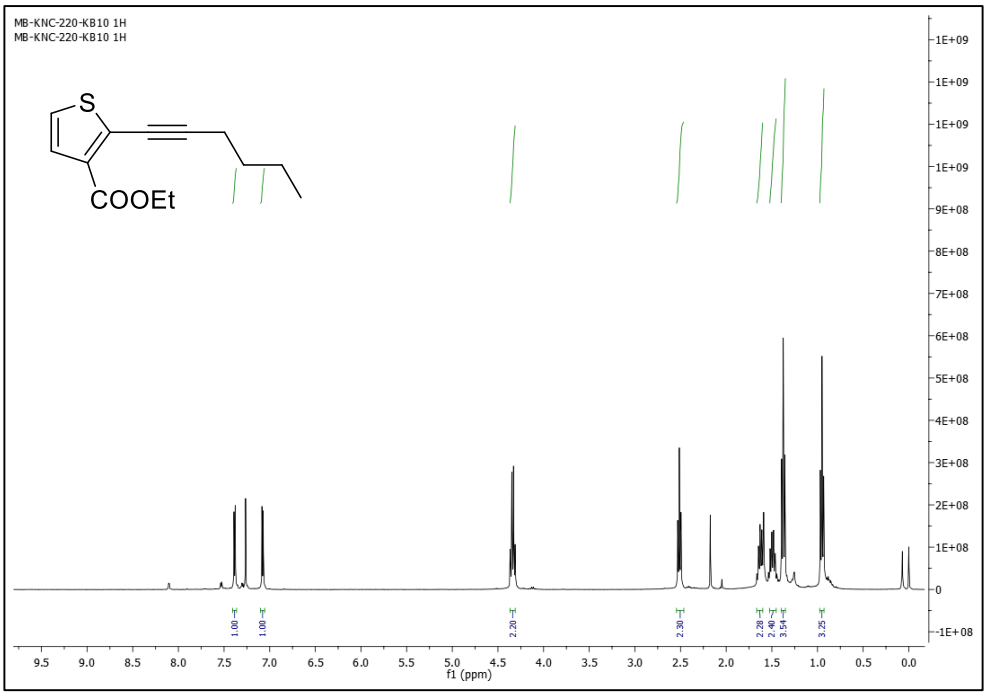

Figure 78. ^{1}H-NMR spectrum of compound **42c**

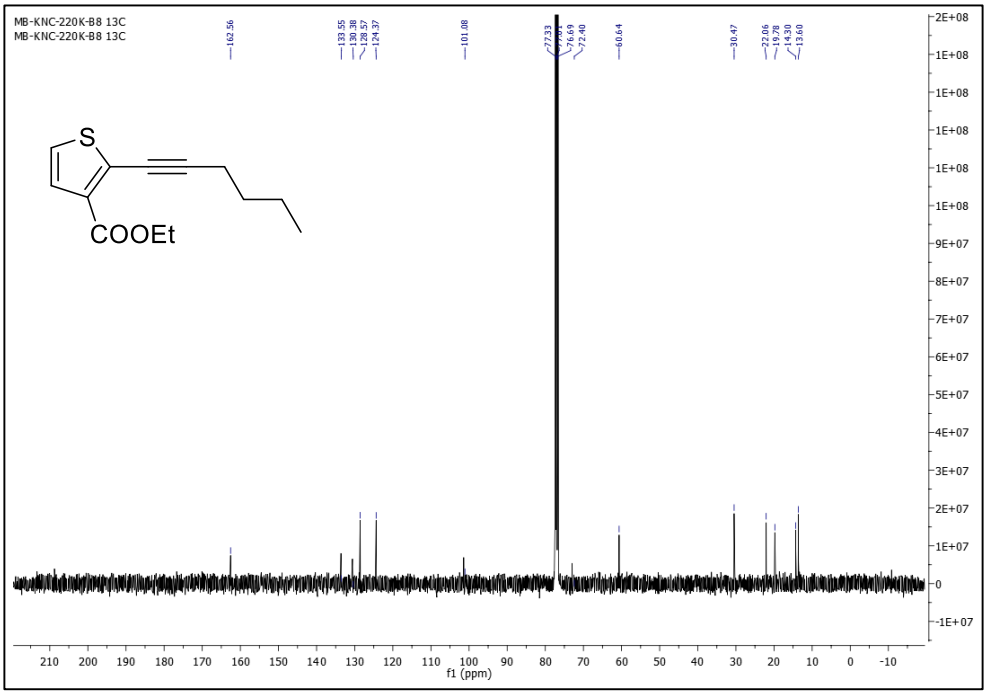

Figure 79. ^{13}C-NMR spectrum of compound **42c**

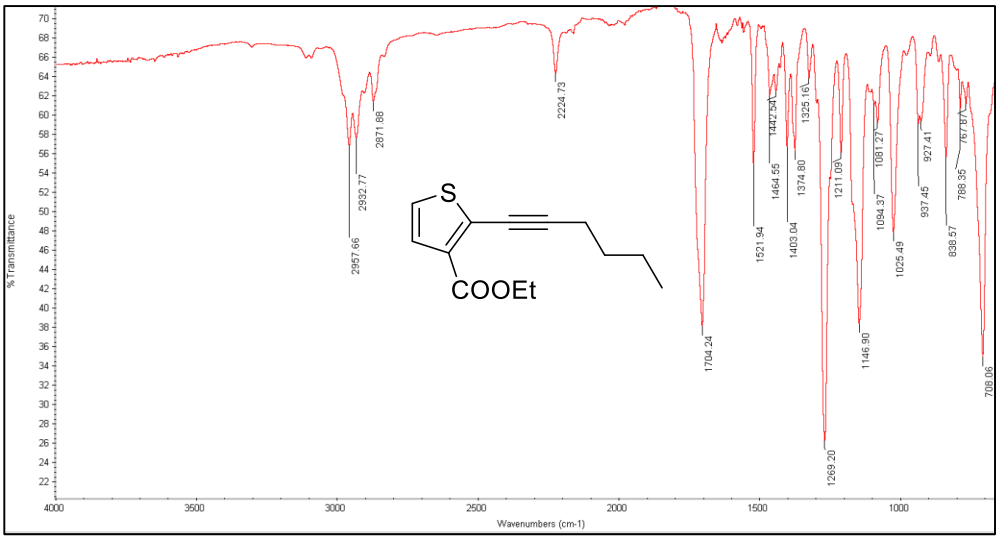

Figure 80. IR spectrum of compound **42c**

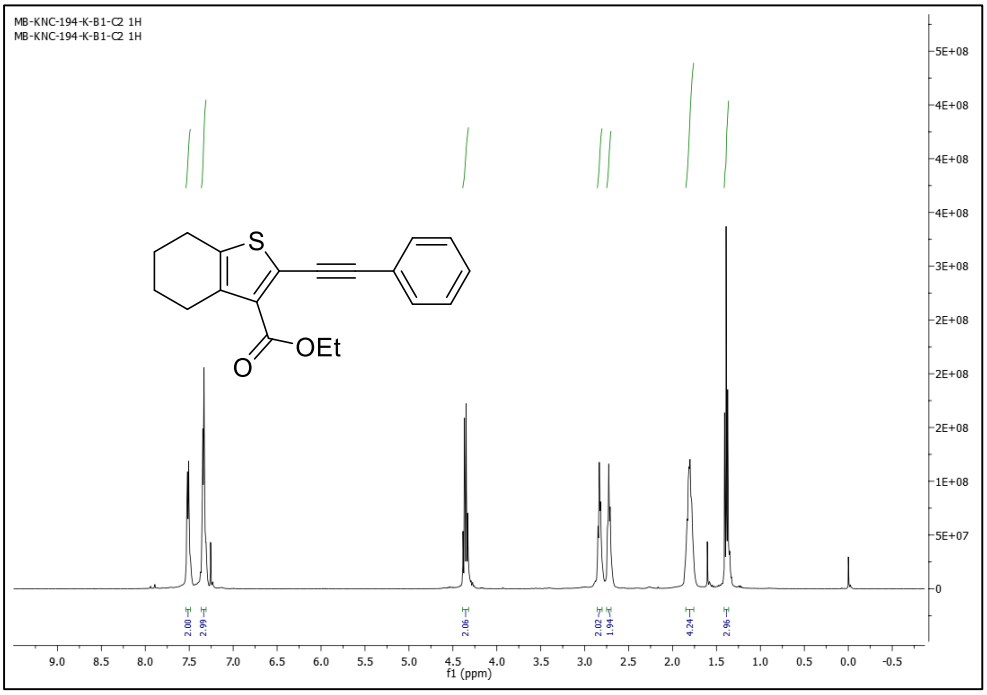

Figure 81. ^{1}H-NMR spectrum of compound **45a**

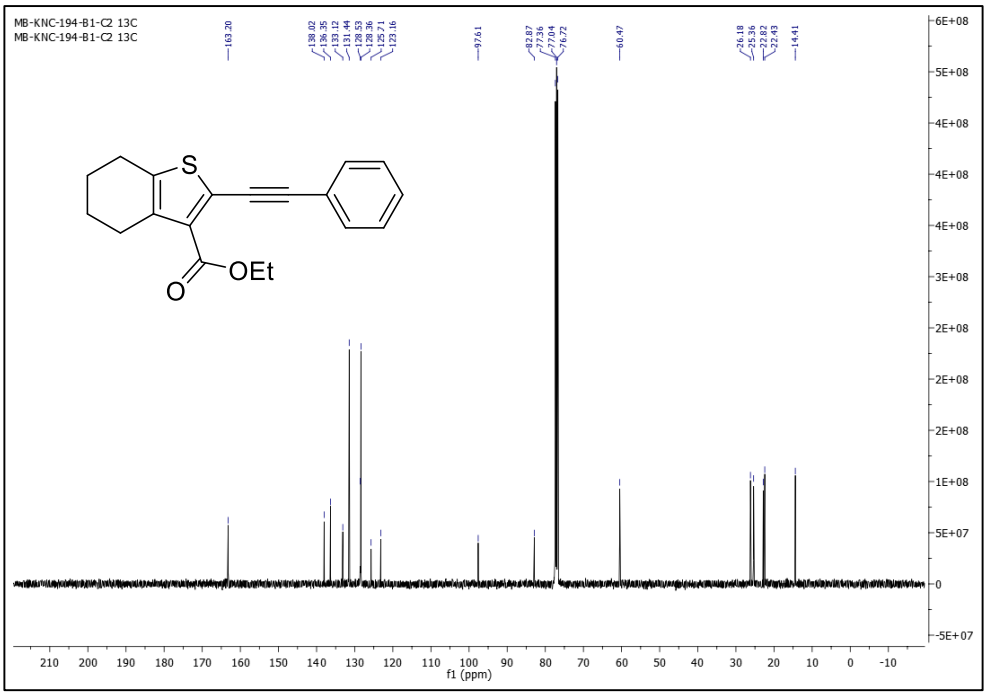

Figure 82. ^{13}C-NMR spectrum of compound **45a**

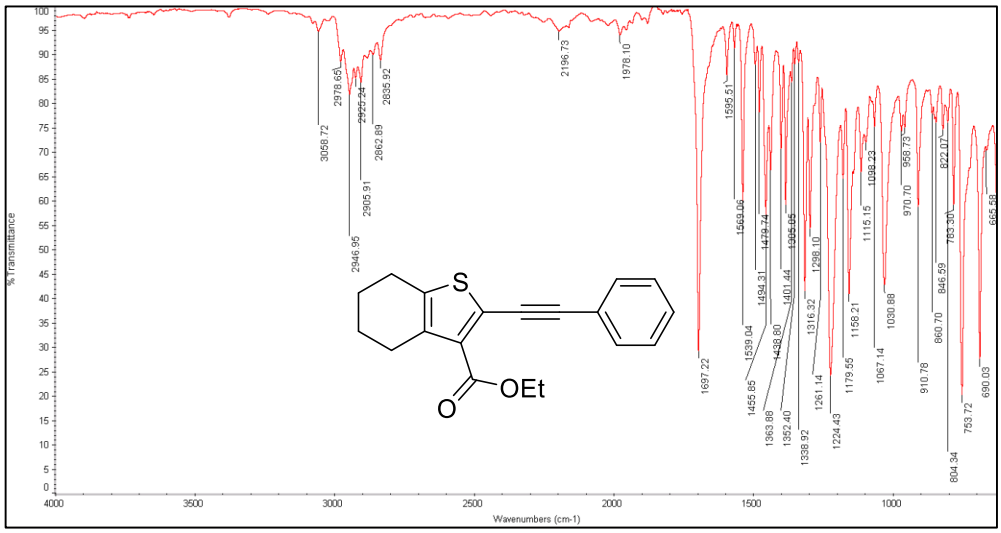

Figure 83. IR spectrum of compound **45a**

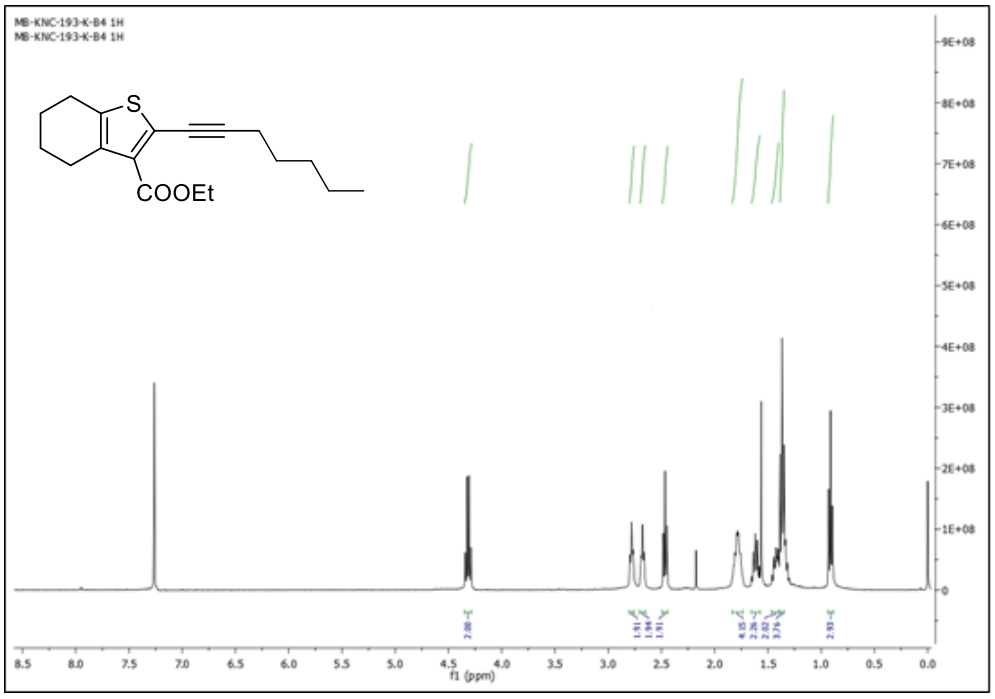

Figure 84. ^{1}H-NMR spectrum of compound **45b**

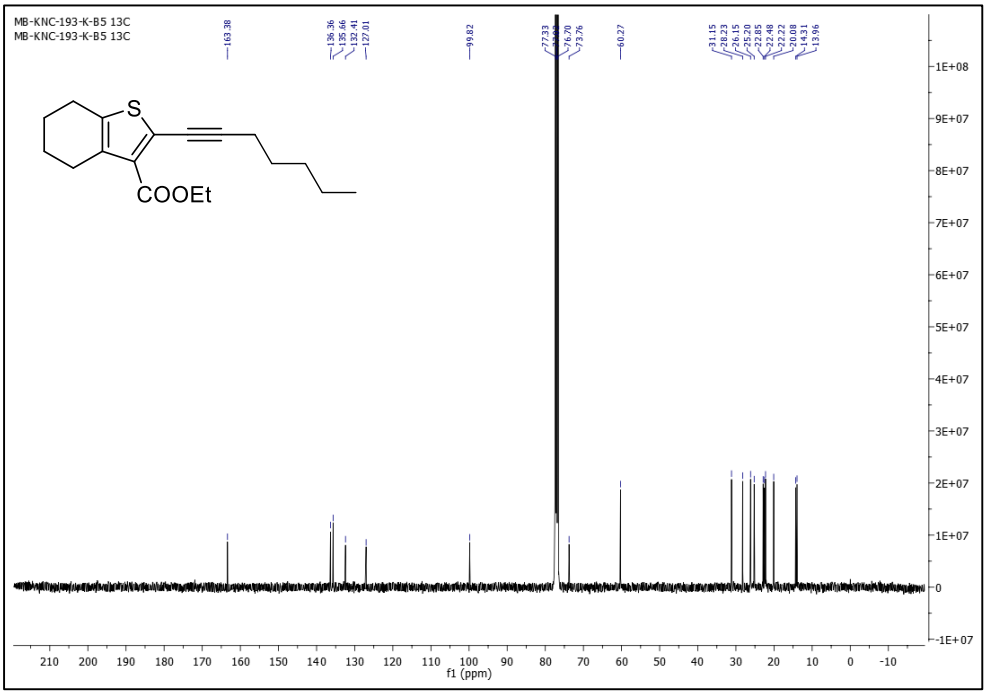

Figure 85. ^{13}C-NMR spectrum of compound **45b**

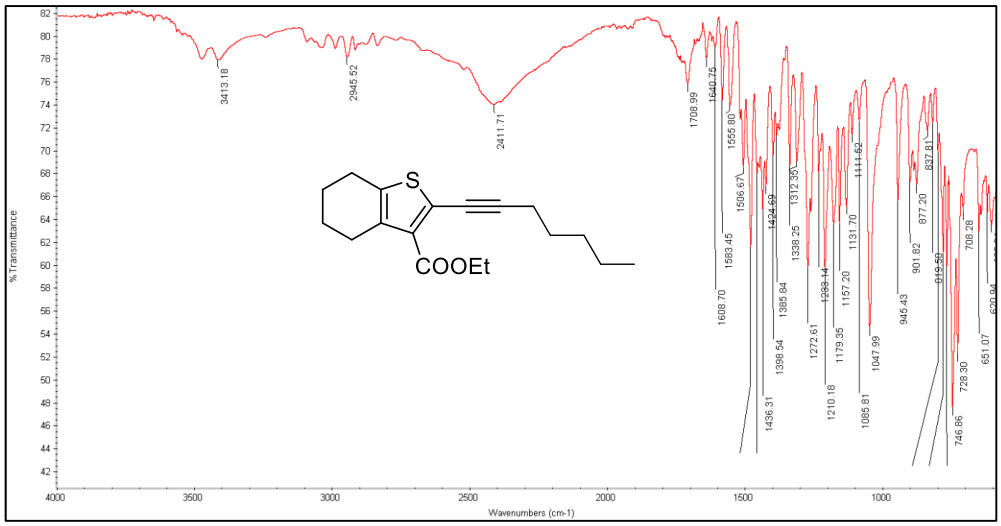

Figure 86. IR spectrum of compound **45b**

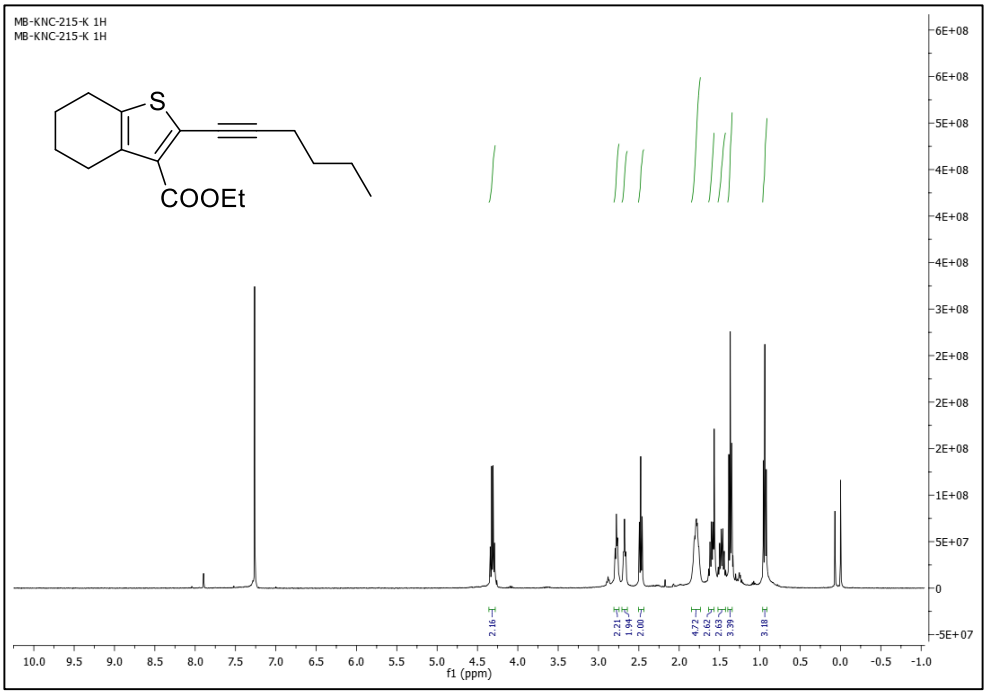

Figure 87. ^{1}H-NMR spectrum of compound **45c**

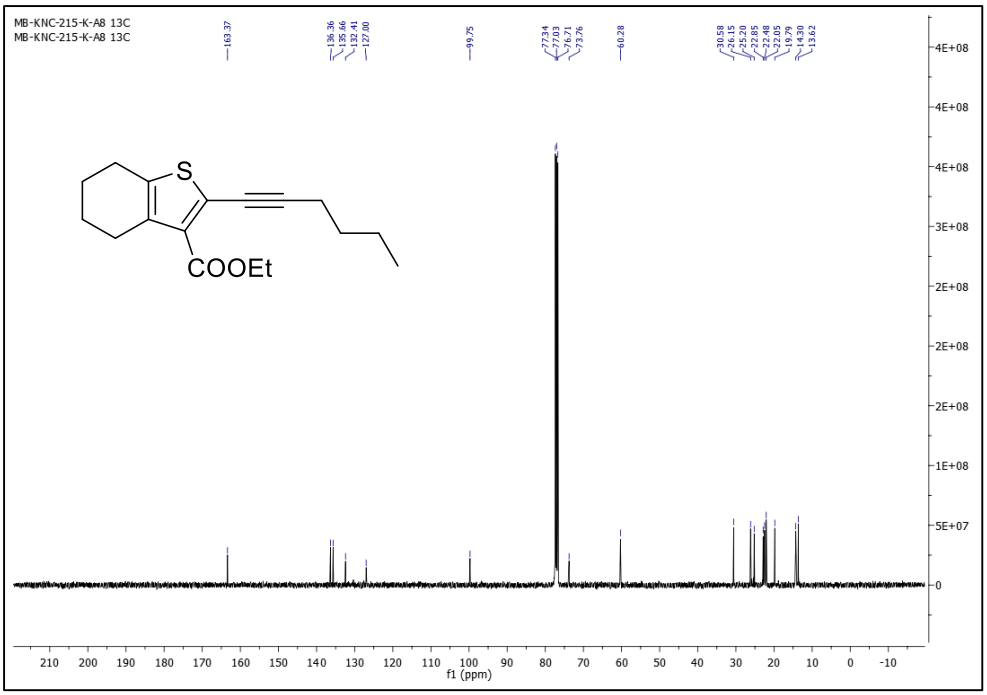

Figure 88. ^{13}C-NMR spectrum of compound **45c**

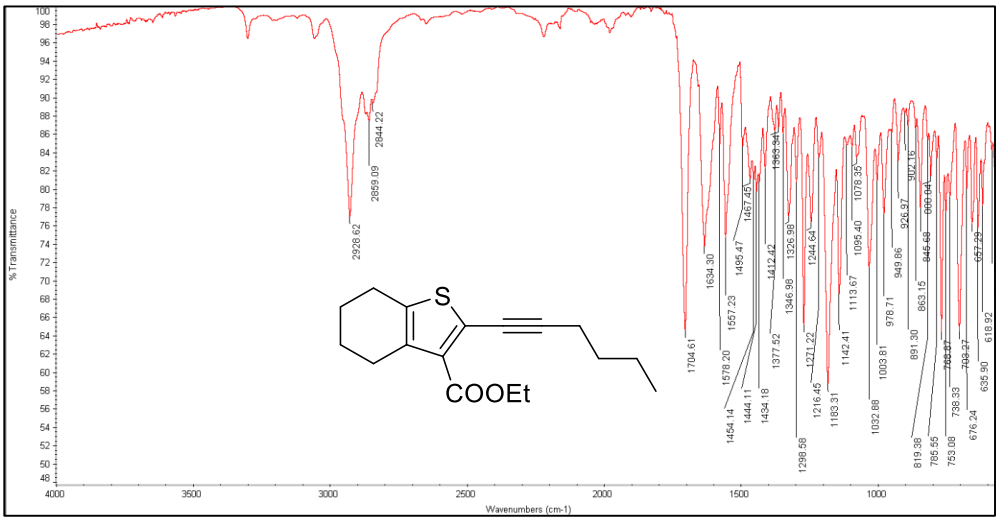

Figure 89 IR spectrum of compound **45c**

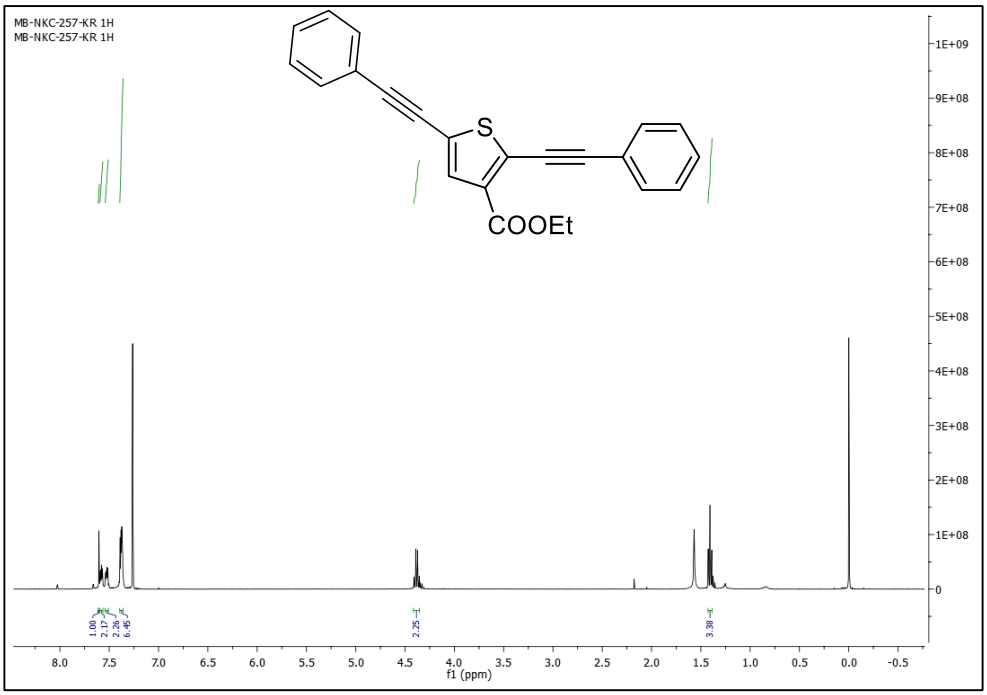

Figure 90. ^{1}H-NMR spectrum of compound **74**

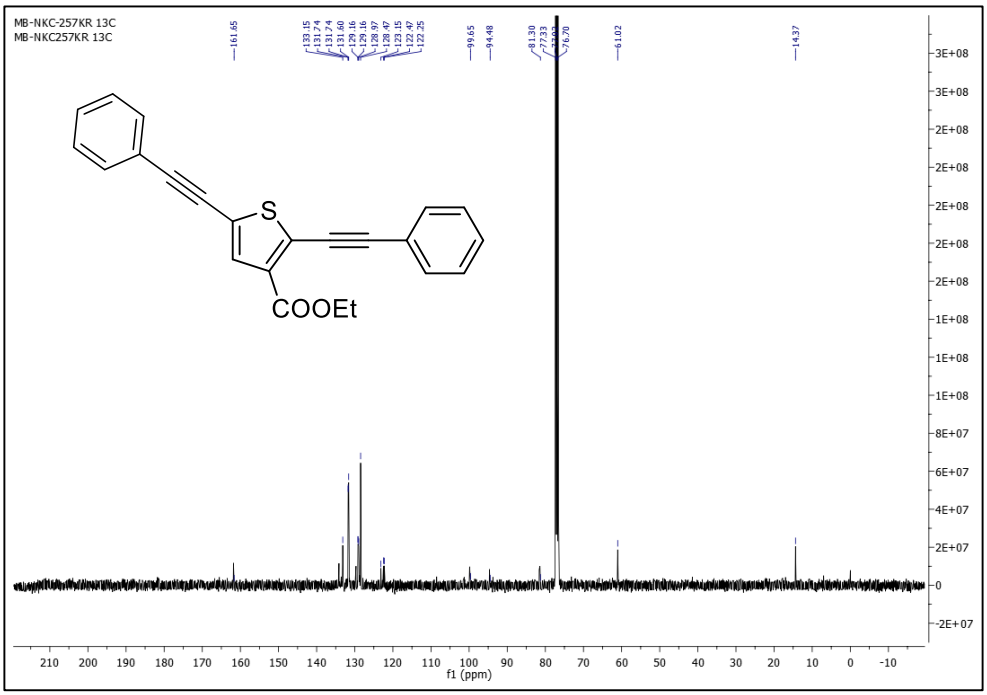

Figure 91. ^{13}C-NMR spectrum of compound **74**

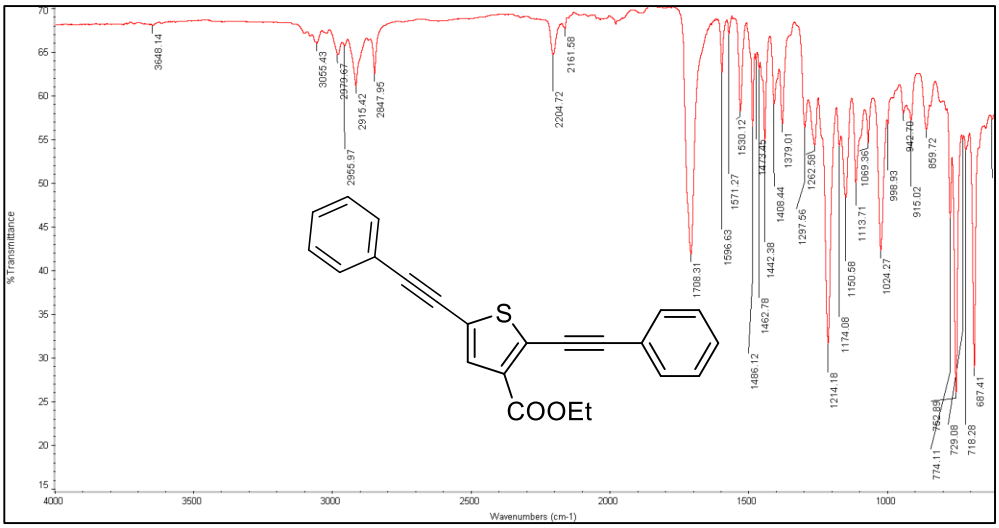

Figure 92. IR spectrum of compound **74**

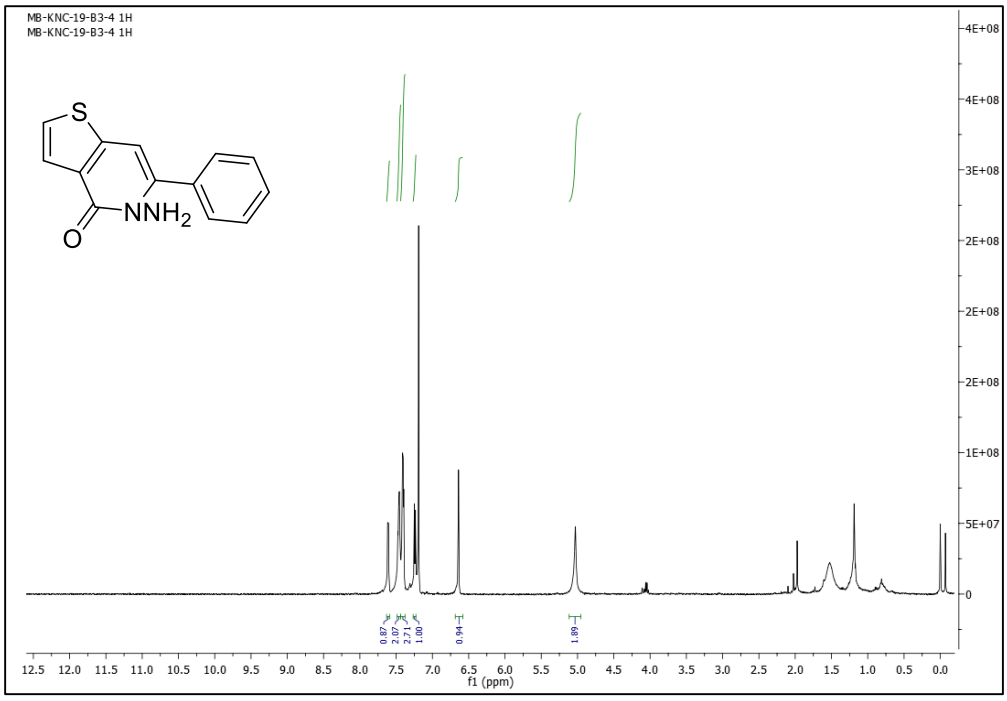

Figure 93. ^{1}H-NMR spectrum of compound **43a**

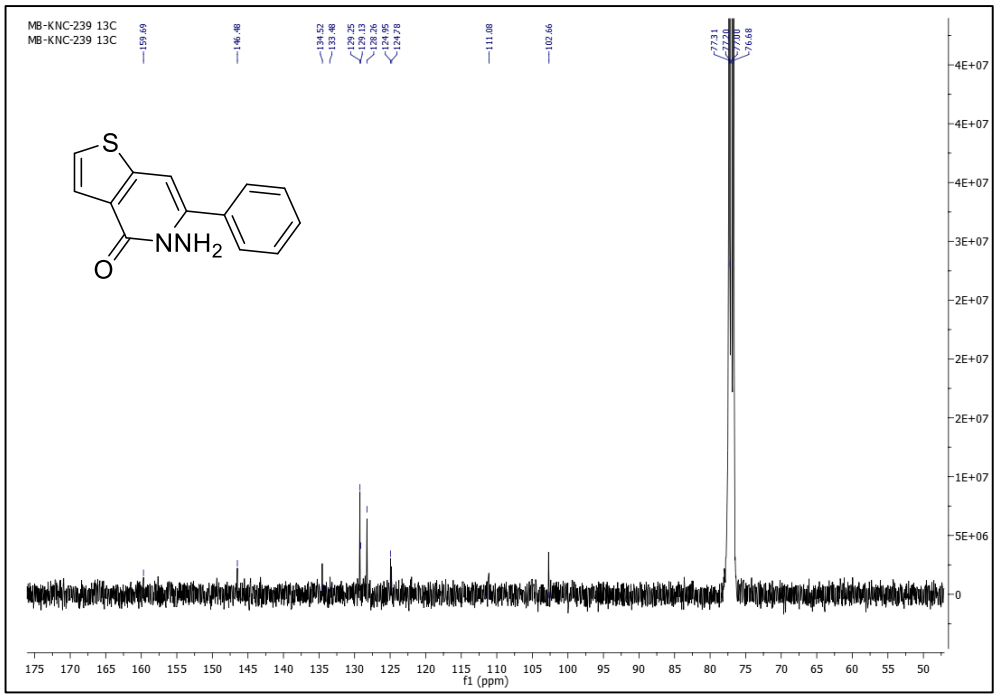

Figure 94. ^{13}C-NMR spectrum of compound **43a**

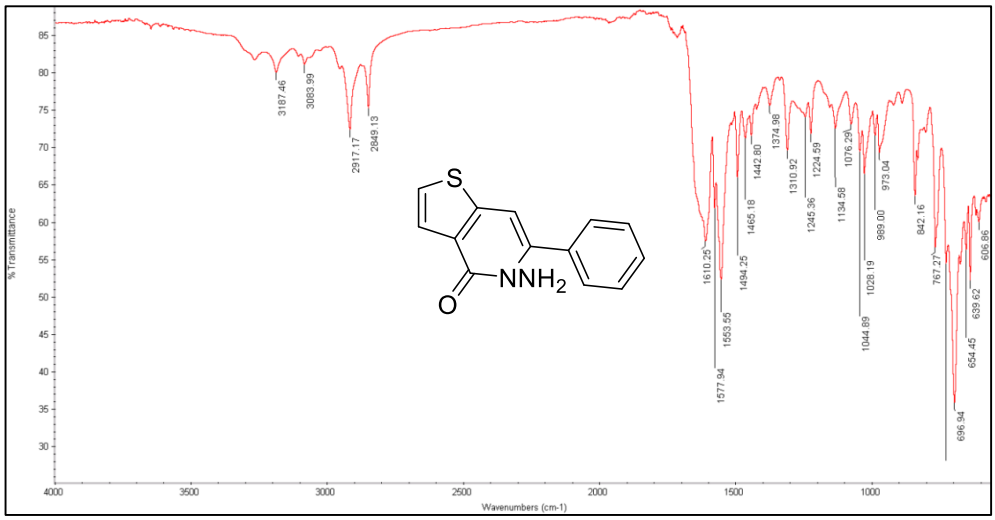

Figure 95. IR spectrum of compound **43a**

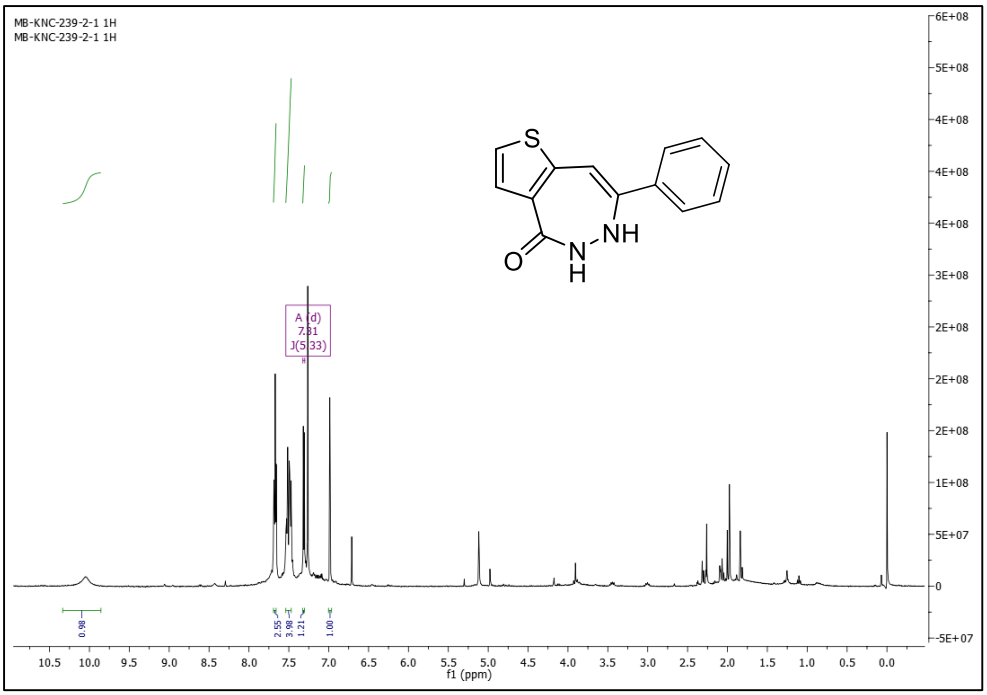

Figure 96. ^{1}H-NMR spectrum of compound **44**

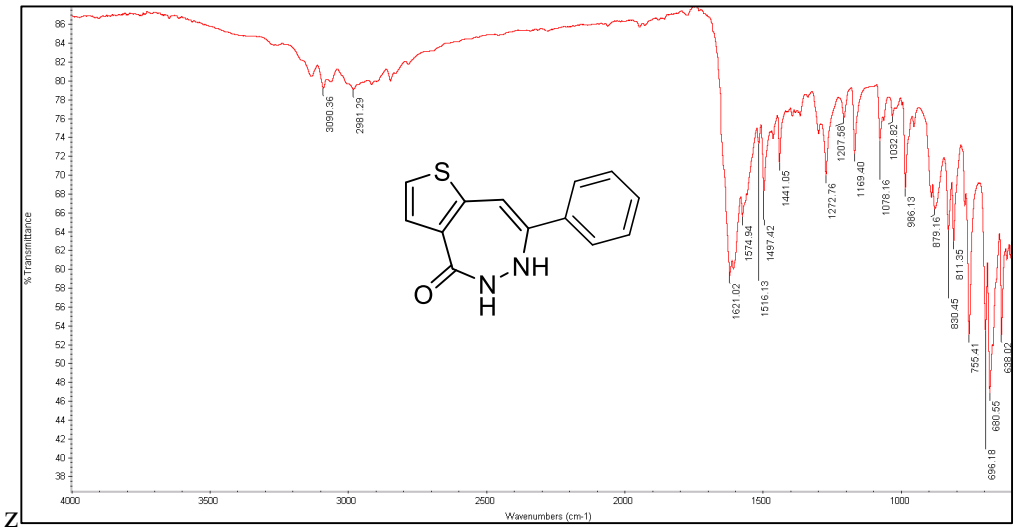

Z

Figure 97. IR spectrum of compound **44**

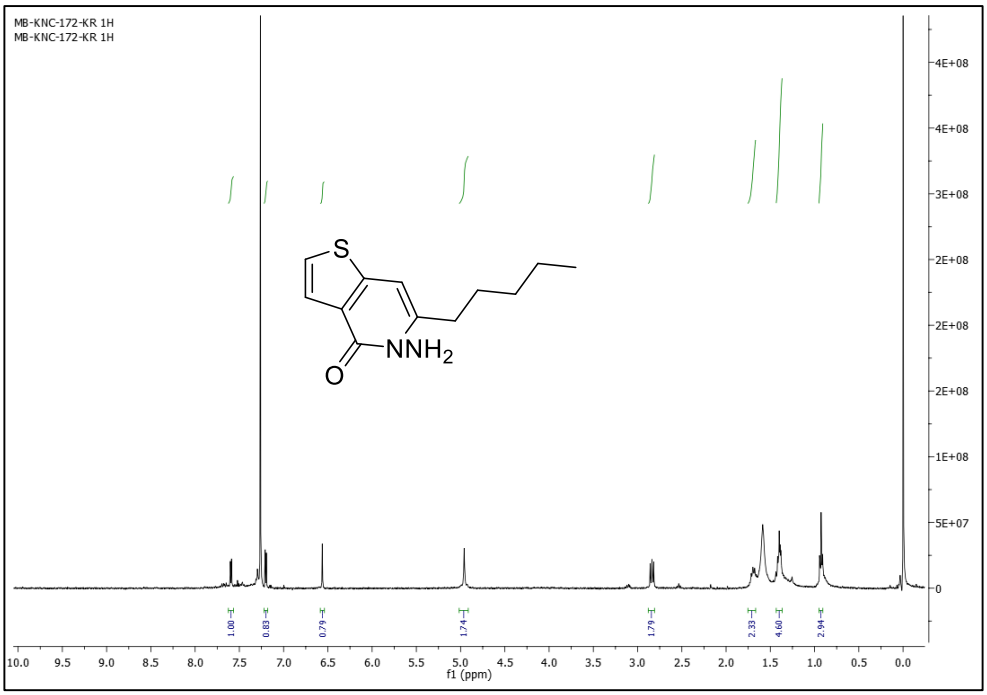

Figure 98. ^{1}H-NMR spectrum of compound **43b**

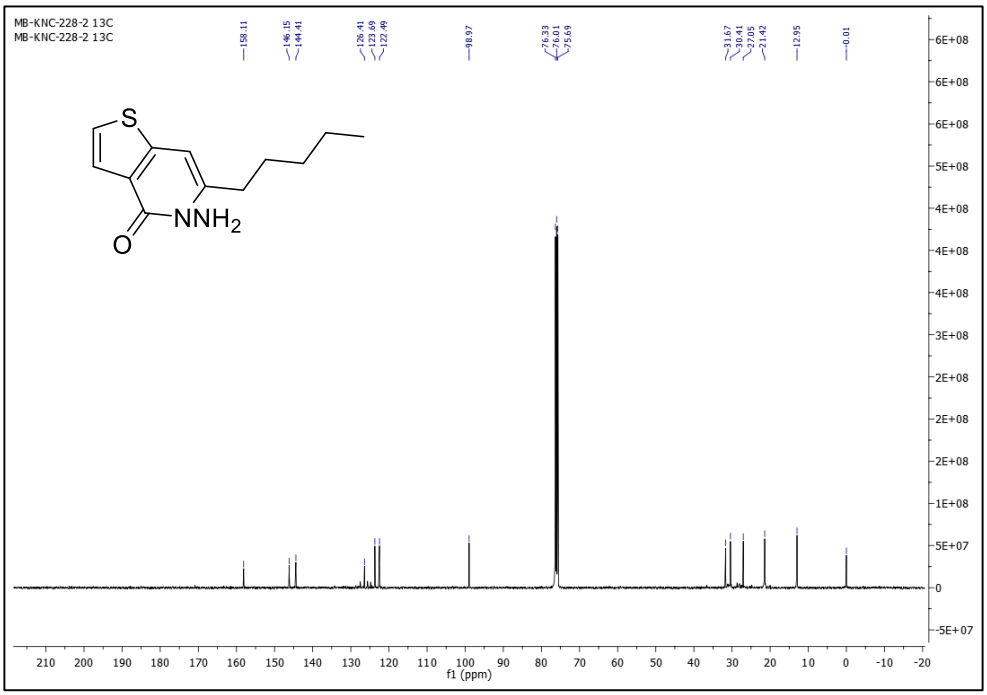

Figure 99. ^{13}C-NMR spectrum of compound **43b**

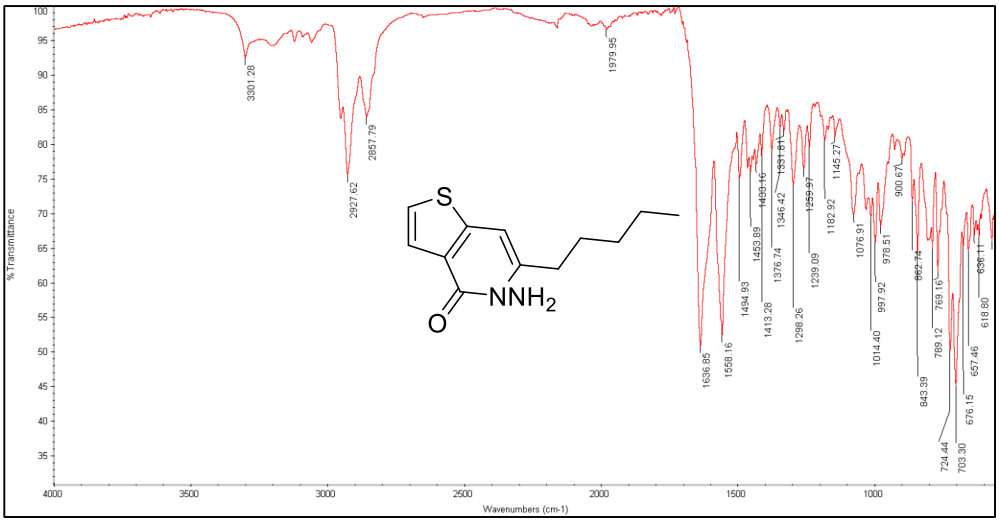

Figure 100. IR spectrum of compound **43b**

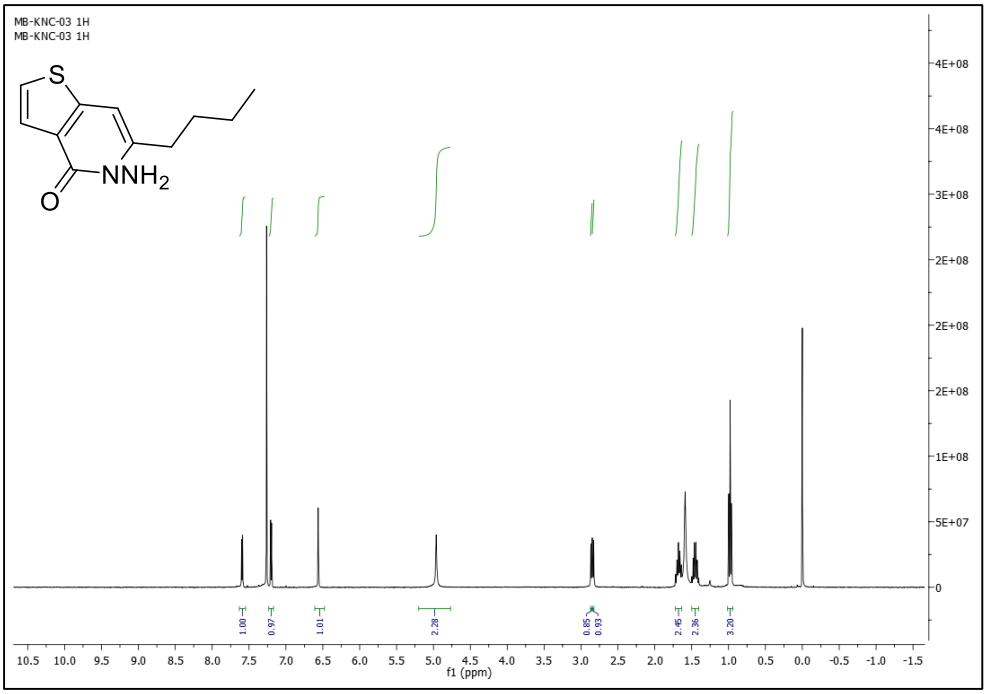

Figure 101. ^{1}H-NMR spectrum of compound **43c**

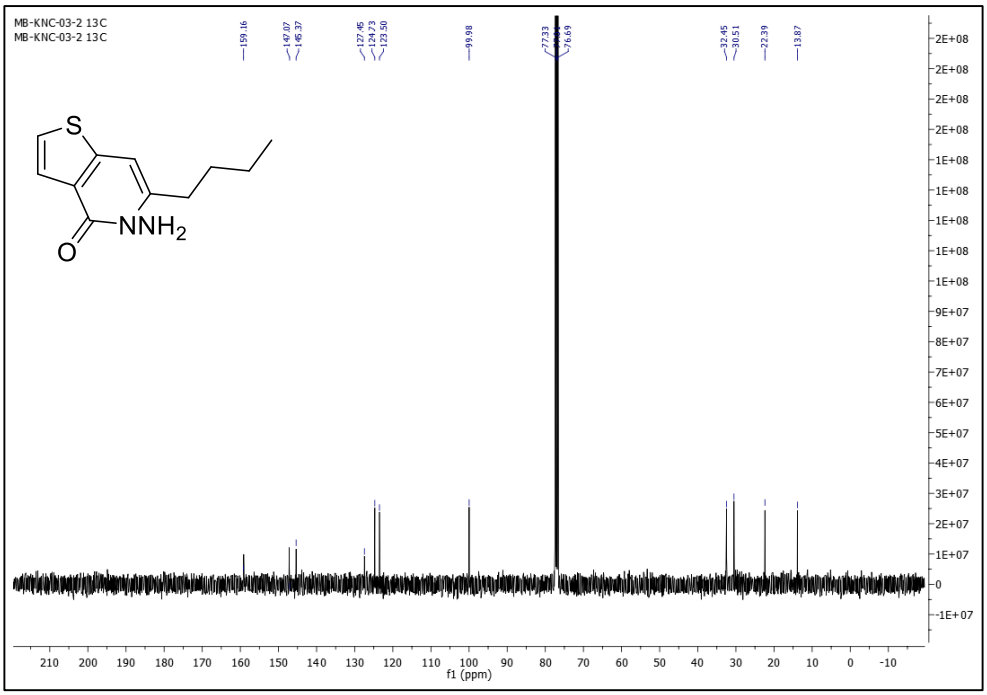

Figure 102. ^{13}C-NMR spectrum of compound **43c**

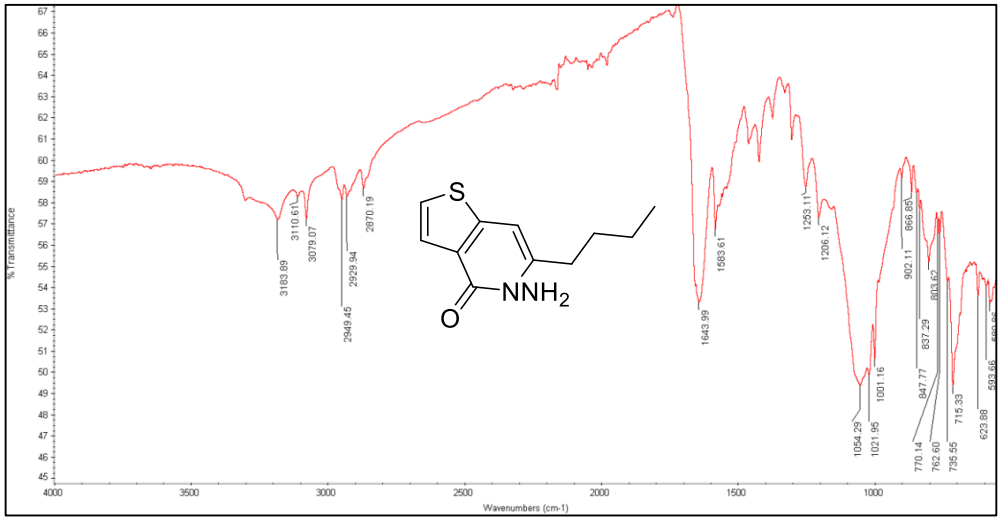

Figure 103. IR spectrum of compound **43c**

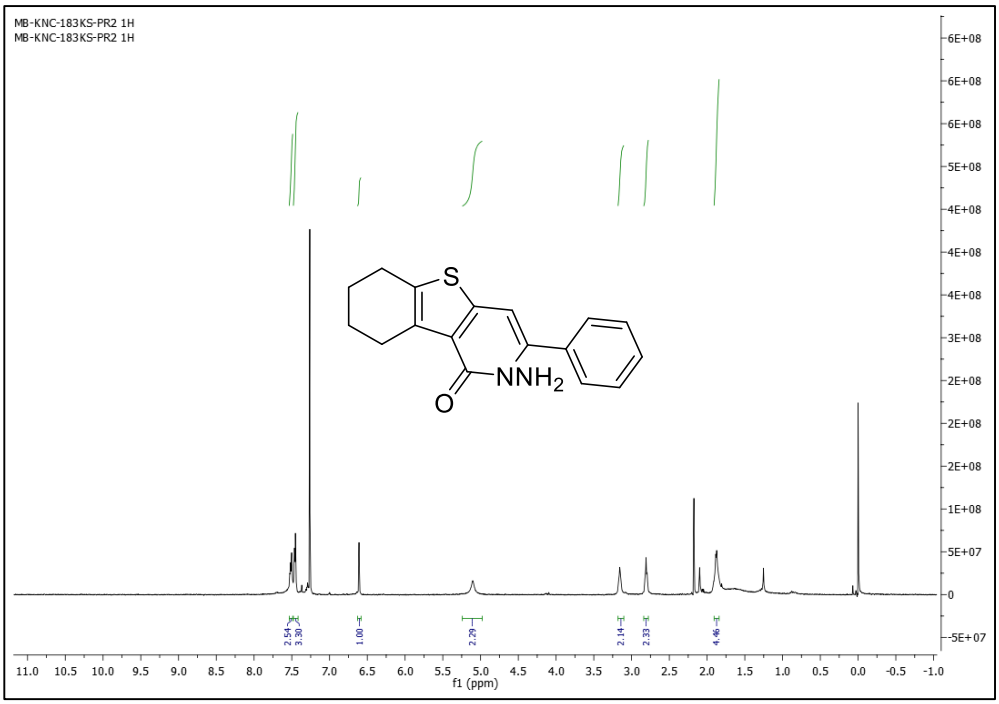

Figure 104. ^{1}H-NMR spectrum of compound **46a**

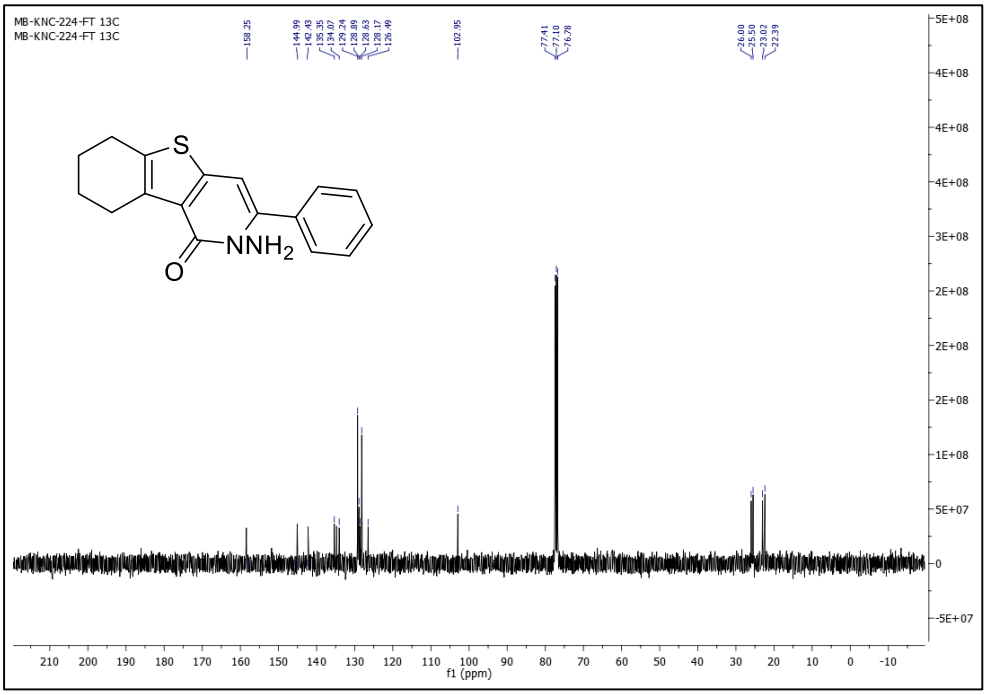

Figure 105. ^{13}C-NMR spectrum of compound **46a**

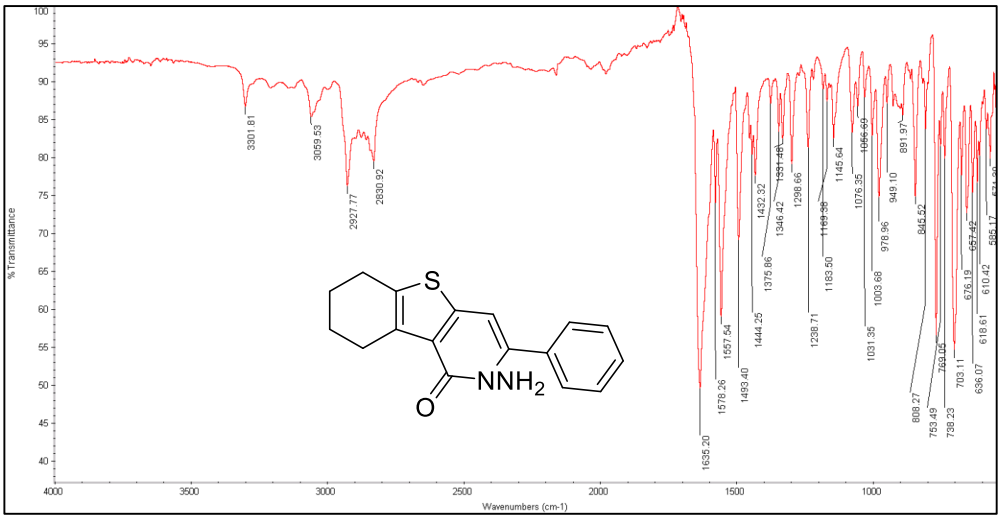

Figure 106. IR spectrum of compound **46a**

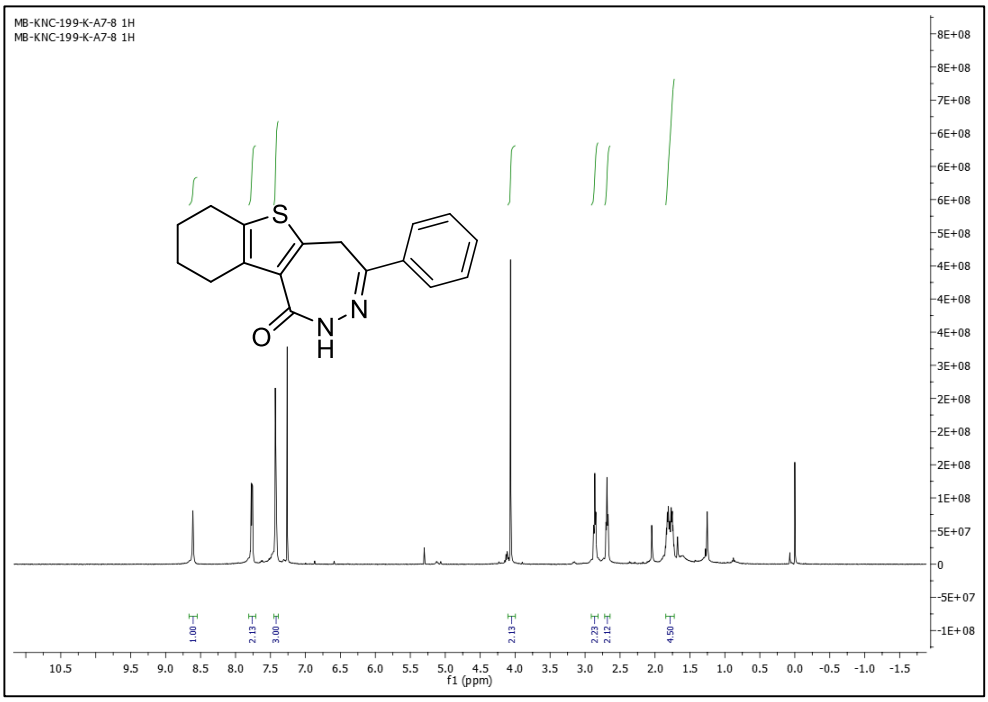

Figure 107. ^{1}H-NMR spectrum of compound **47**

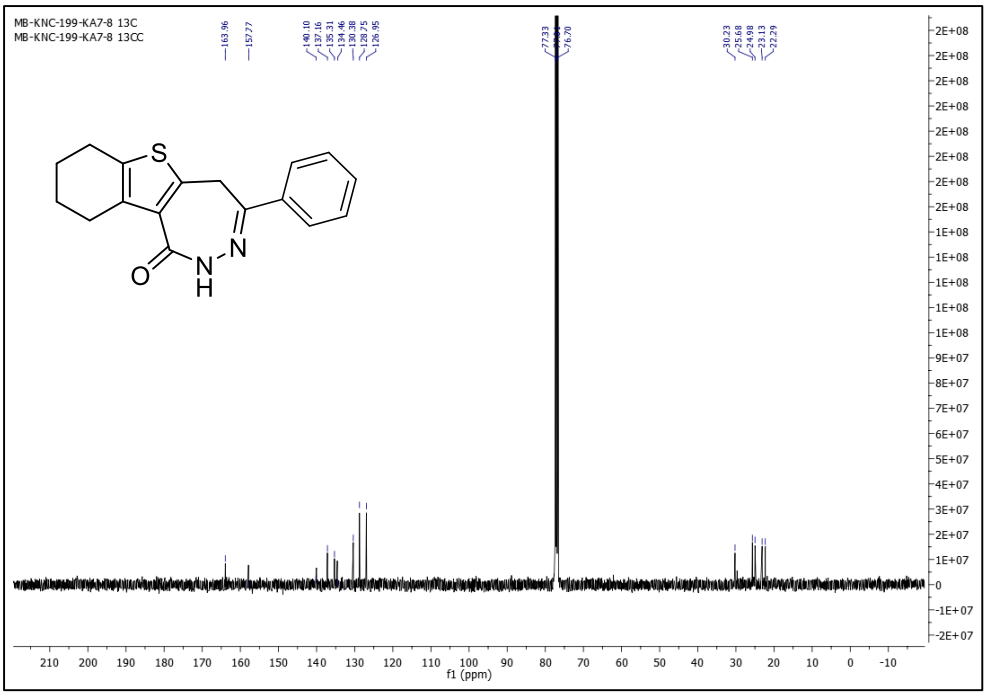

Figure 108. ^{13}C-NMR spectrum of compound **47**

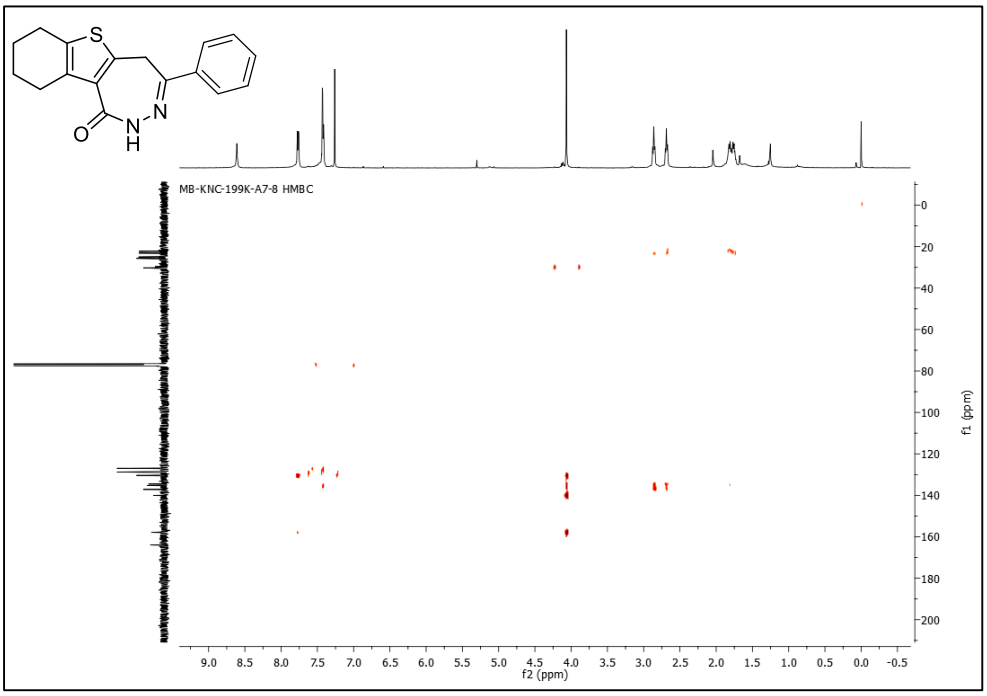

Figure 109. HMBC spectrum of compound **47**

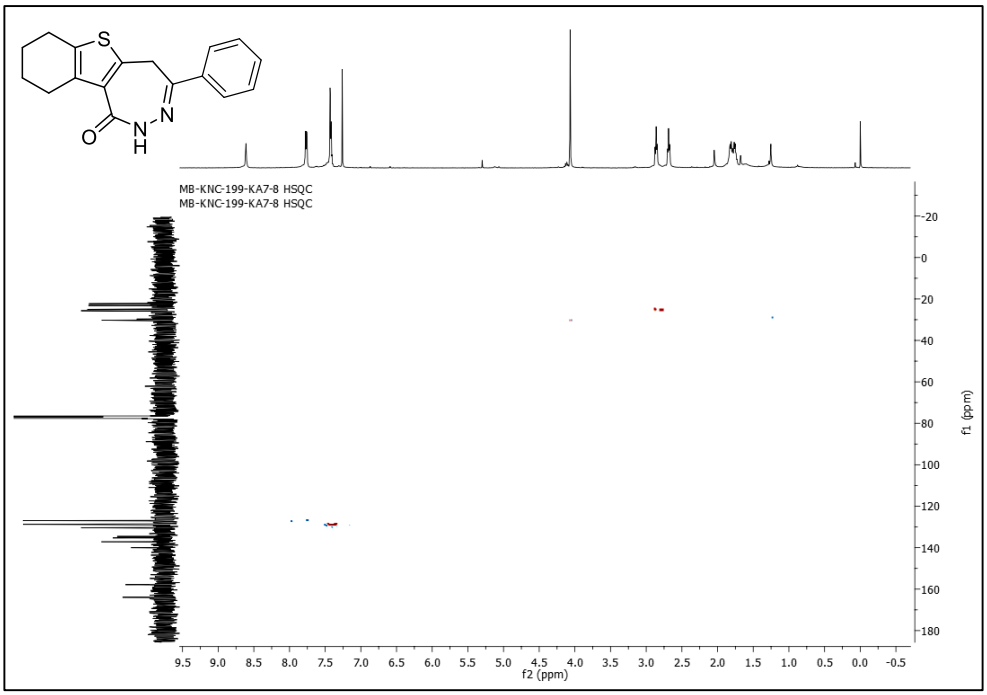

Figure 110. HSQC spectrum of compound **47**

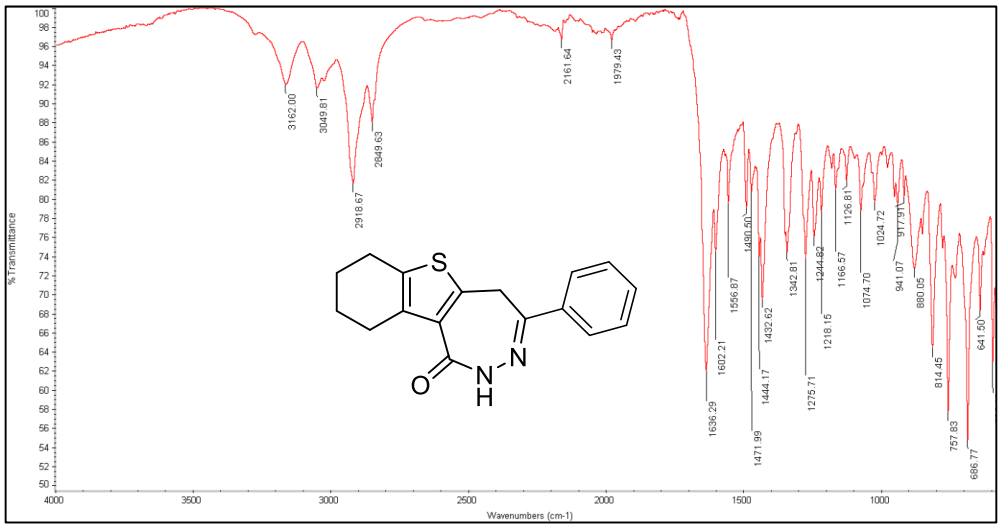

Figure 111. IR spectrum of compound **47**

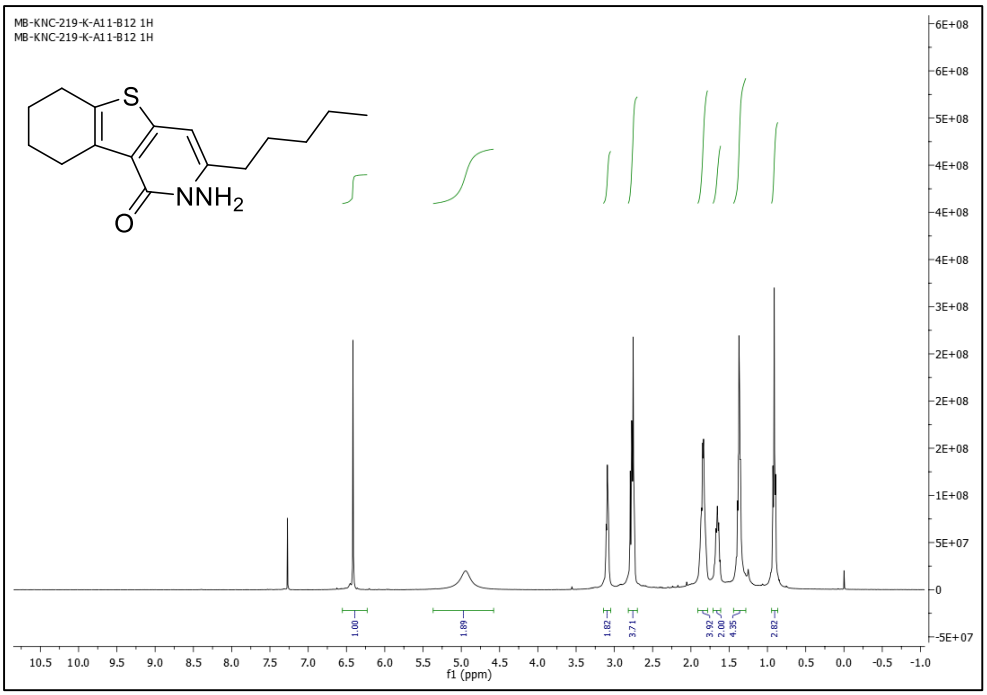

Figure 112. ^{1}H-NMR spectrum of compound **46b**

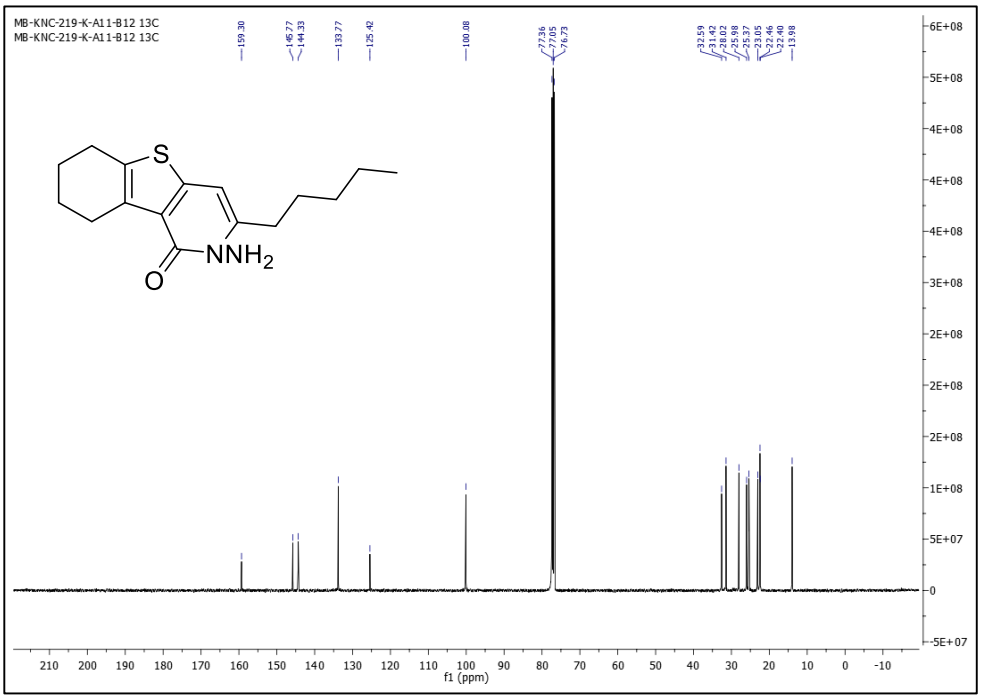

Figure 113. ^{13}C-NMR spectrum of compound **46b**

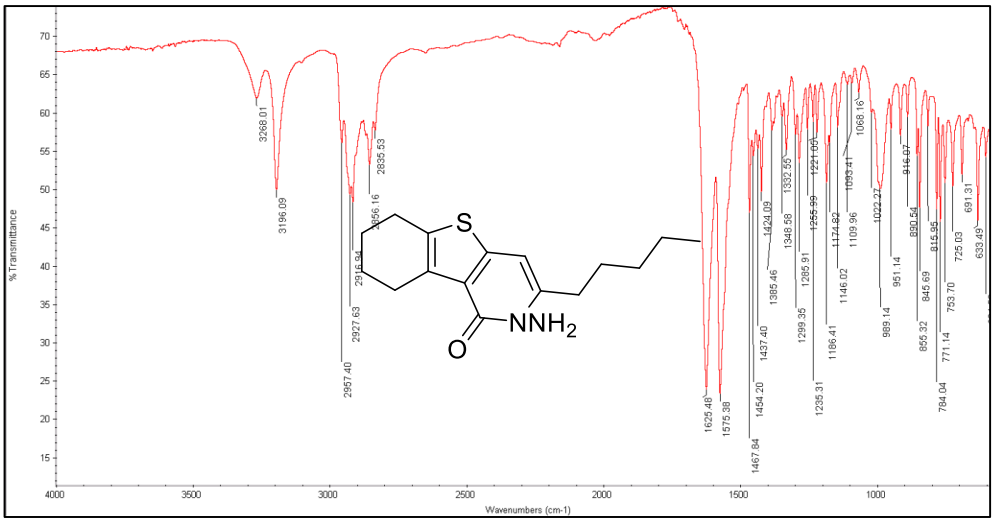

Figure 114. IR spectrum of compound **46b**

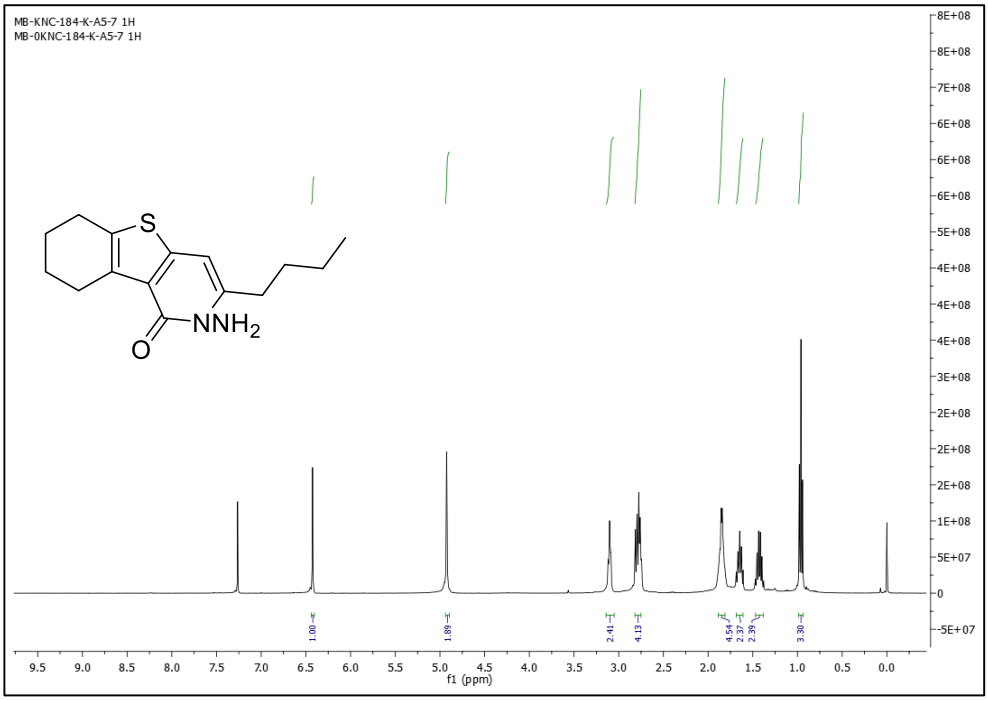

Figure 115. ^{1}H-NMR spectrum of compound **46c**

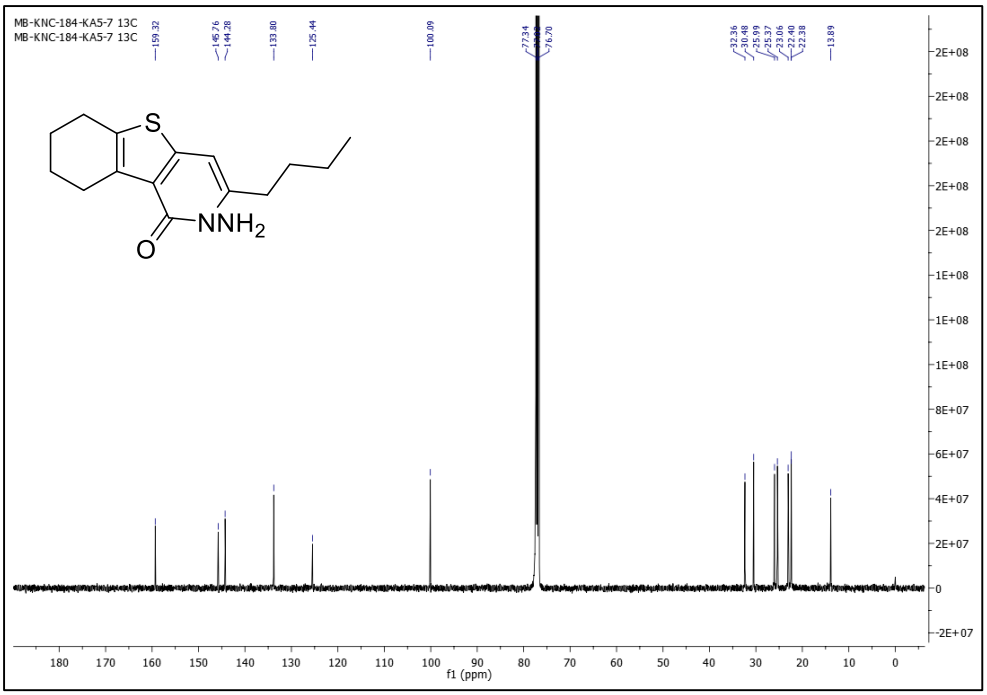

Figure 116. ^{13}C-NMR spectrum of compound **46c**

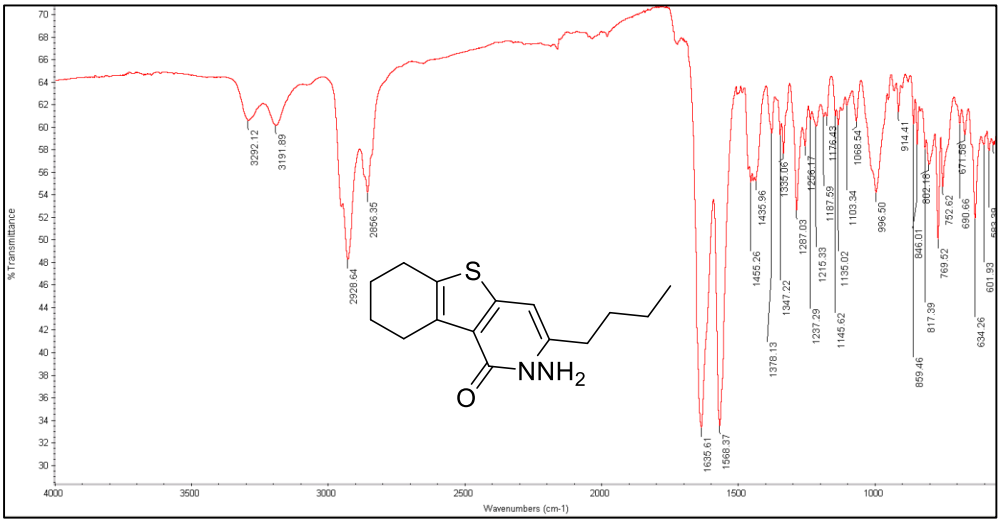

Figure 117. IR spectrum of compound **46c**

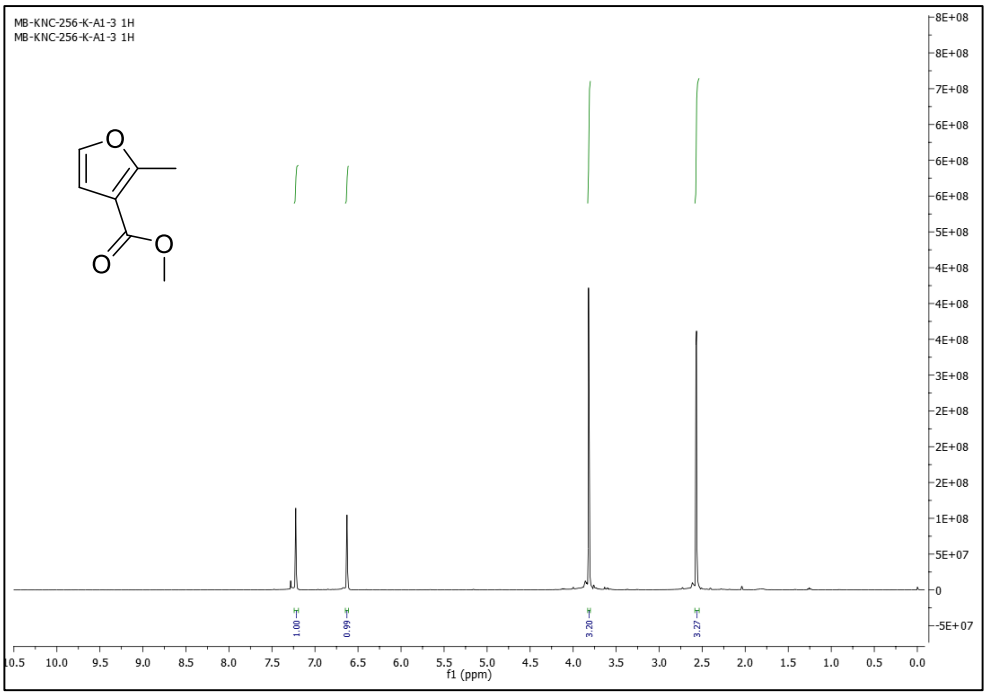

Figure 118. ^{1}H-NMR spectrum of compound **116**

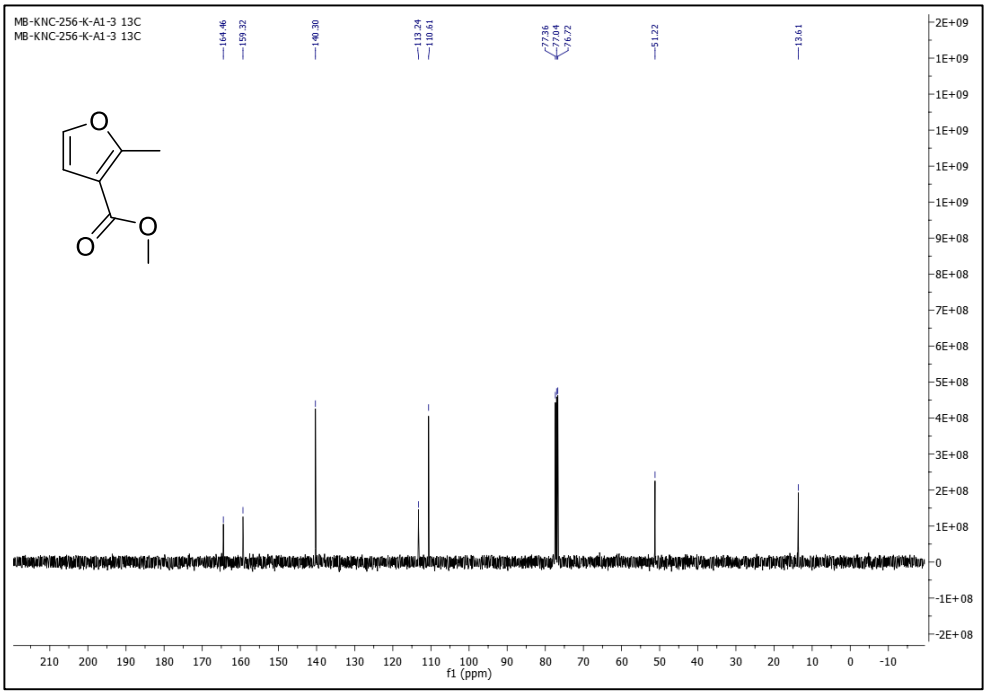

Figure 119. ^{13}C-NMR spectrum of compound **116**

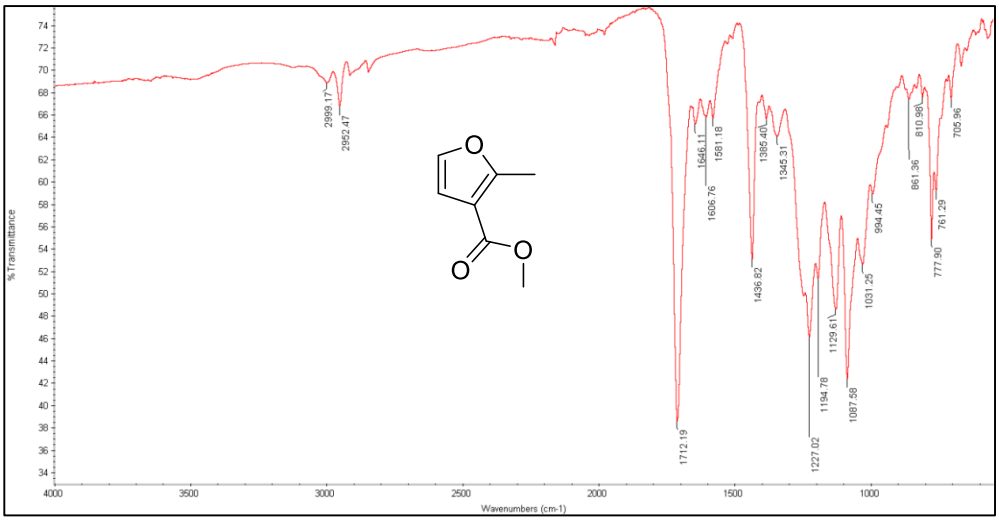

Figure 120. IR spectrum of compound **116**

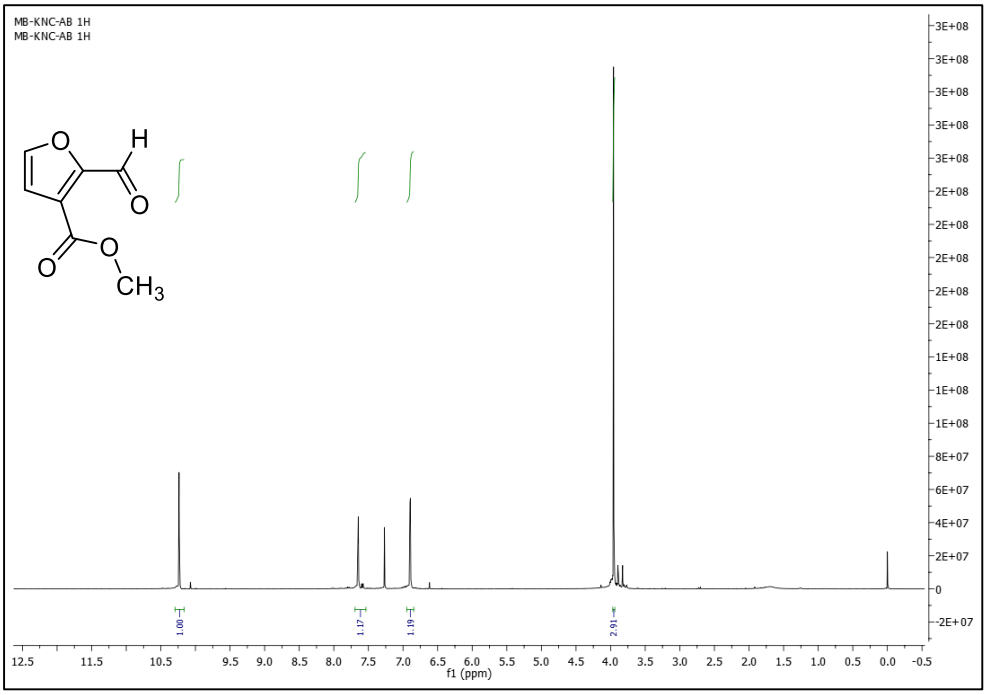

Figure 121. ^{1}H-NMR spectrum of compound **129**

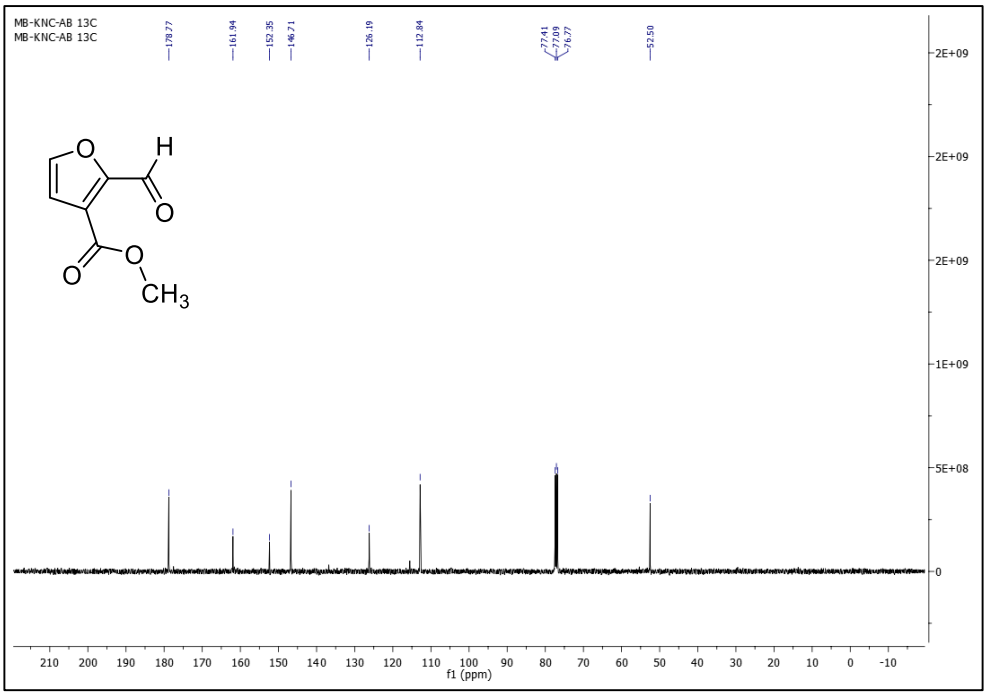

Figure 122. ^{13}C-NMR spectrum of compound **129**

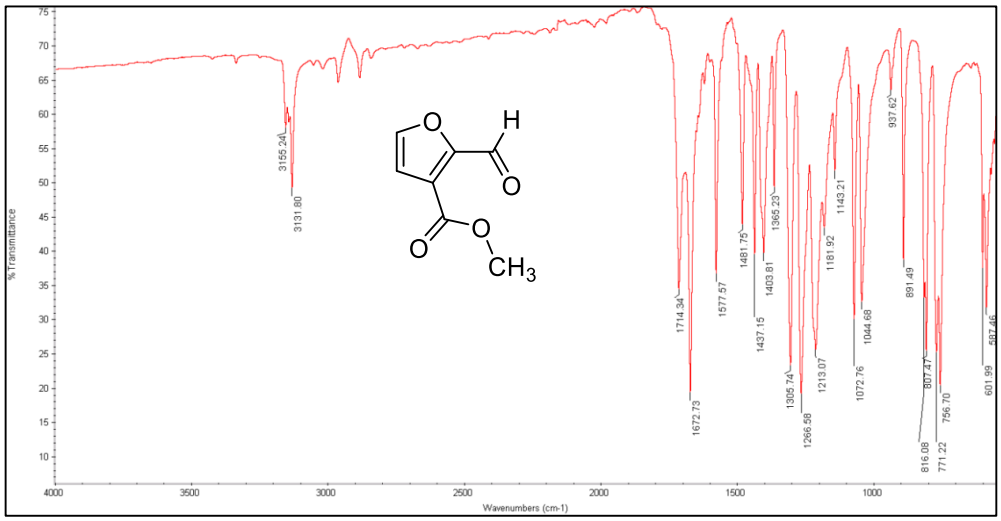

Figure 123. IR spectrum of compound **129**

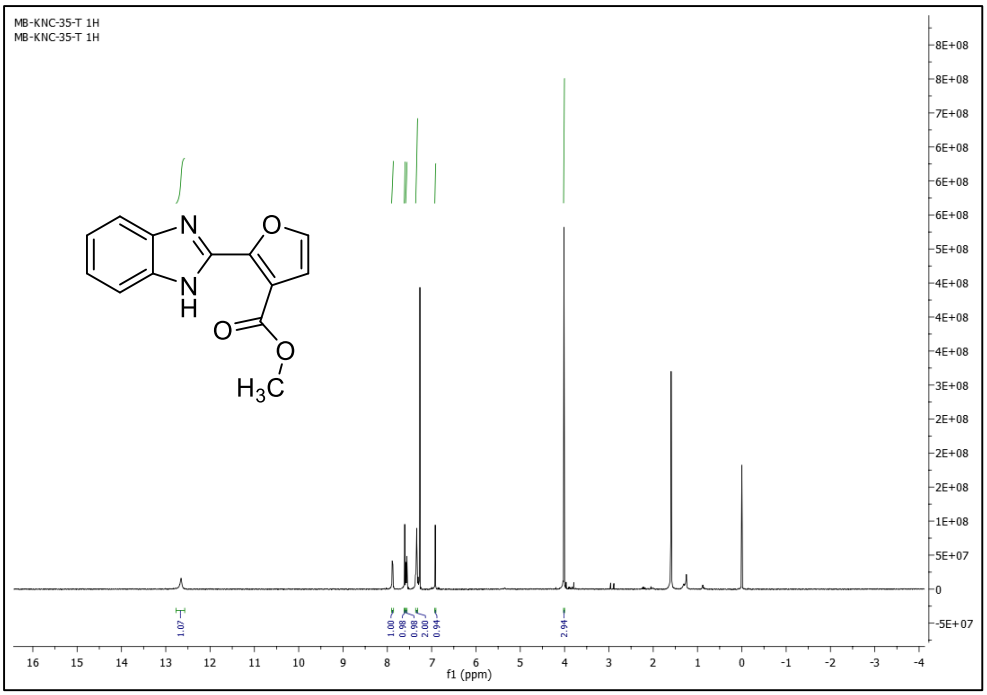

Figure 124. ^{1}H-NMR spectrum of compound **117**

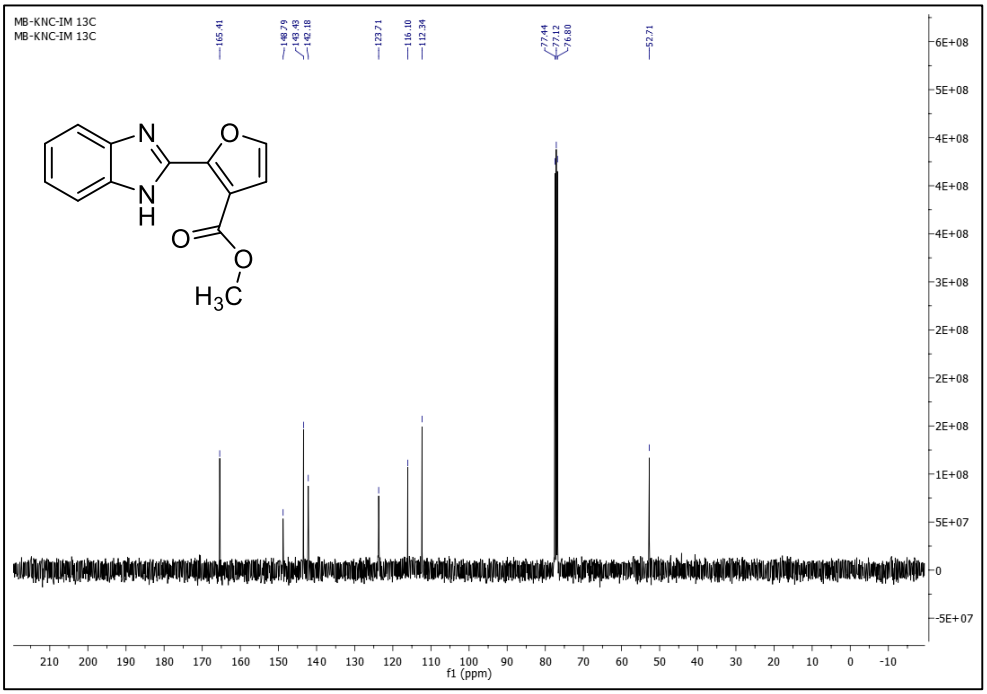

Figure 125. ^{13}C-NMR spectrum of compound **117**

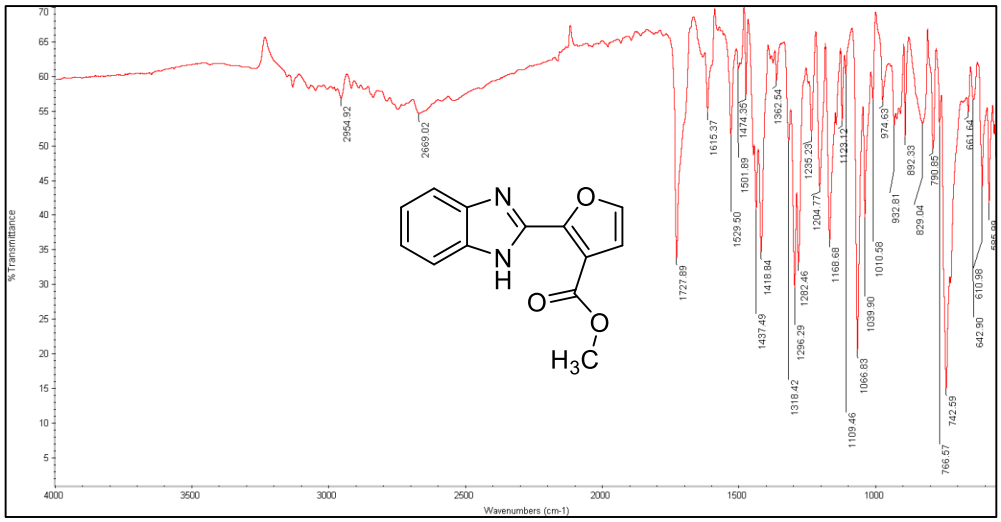

Figure 126. IR spectrum of compound **117**

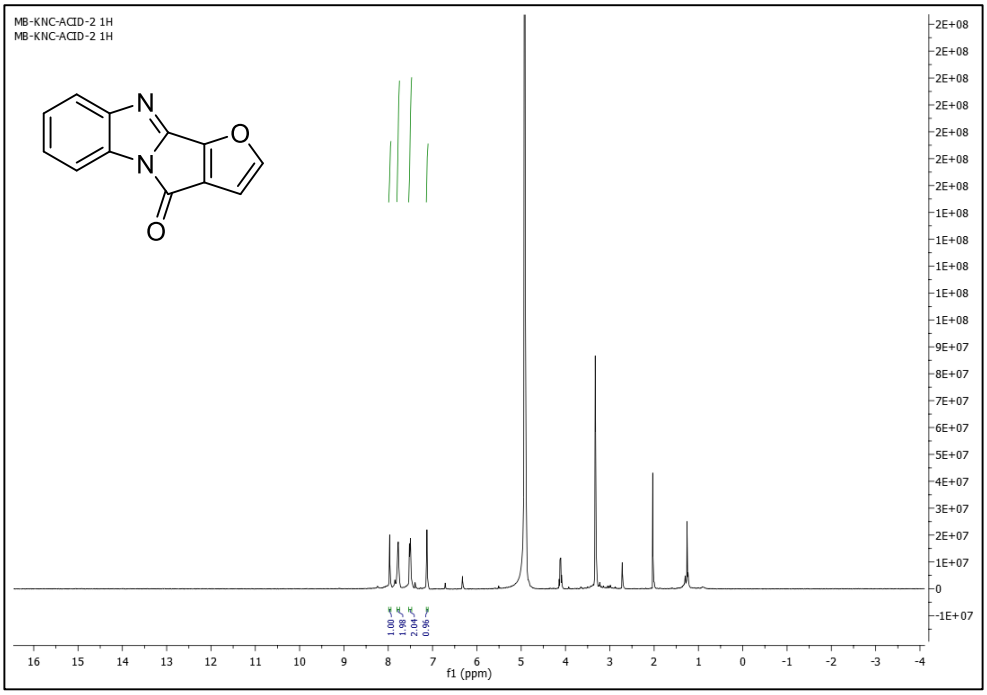

Figure 127. ^{1}H-NMR spectrum of compound **118**

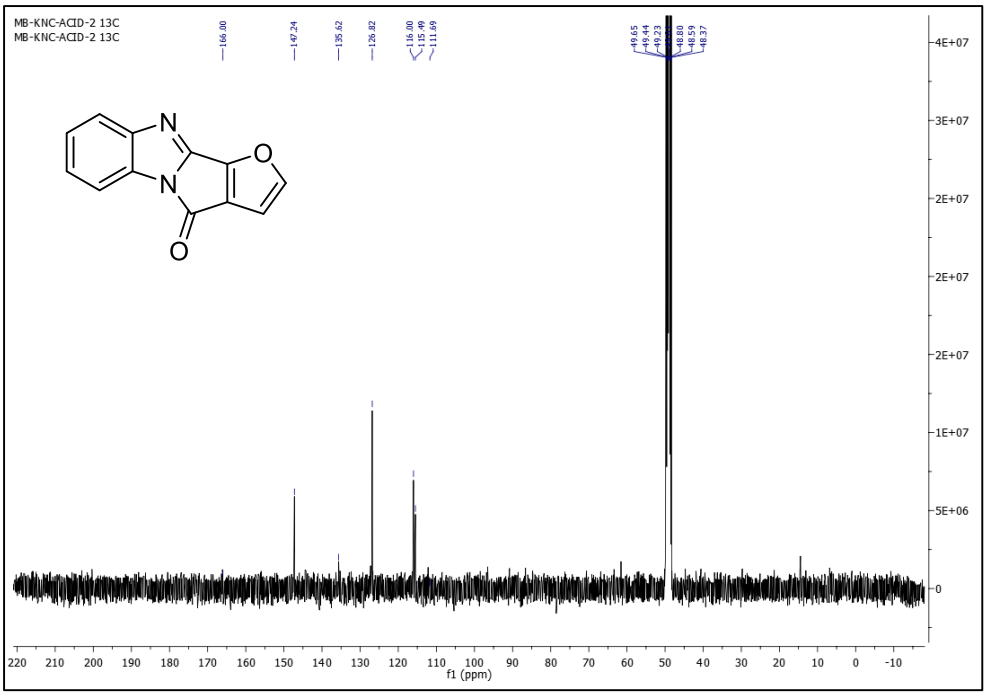

Figure 128. ^{13}C-NMR spectrum of compound **118**

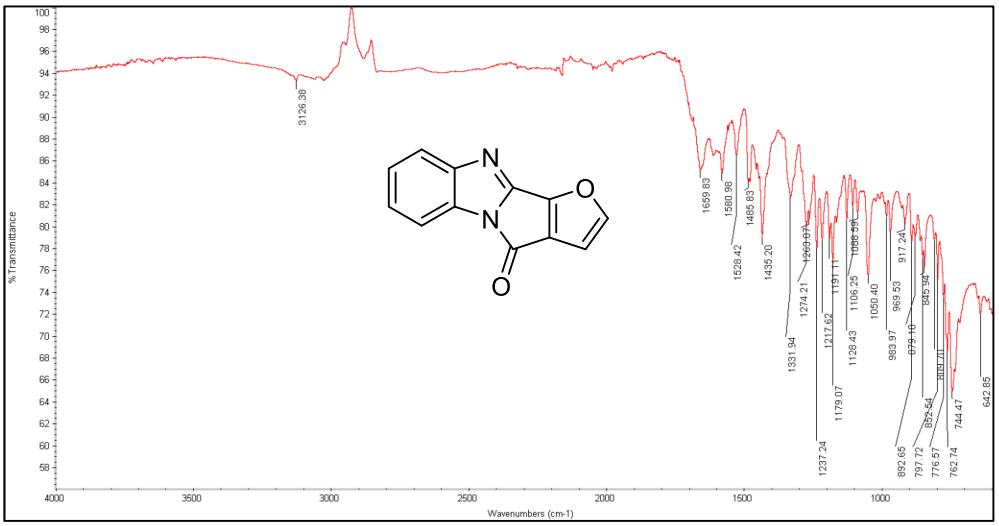

Figure 129. IR spectrum of compound **118**

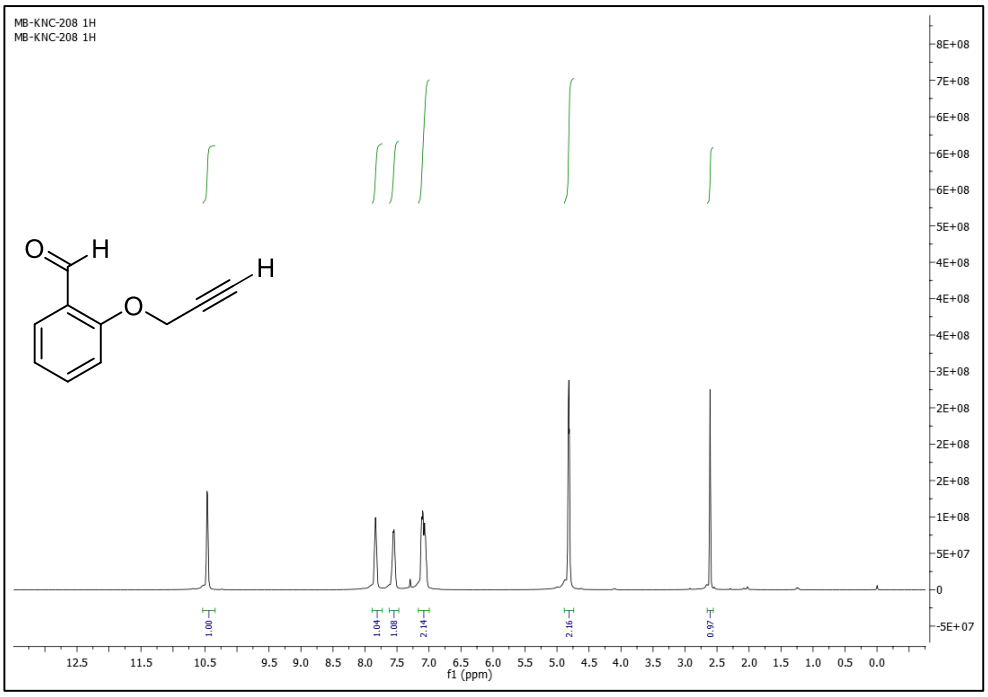

Figure 130. ^{1}H-NMR spectrum of compound **120a**

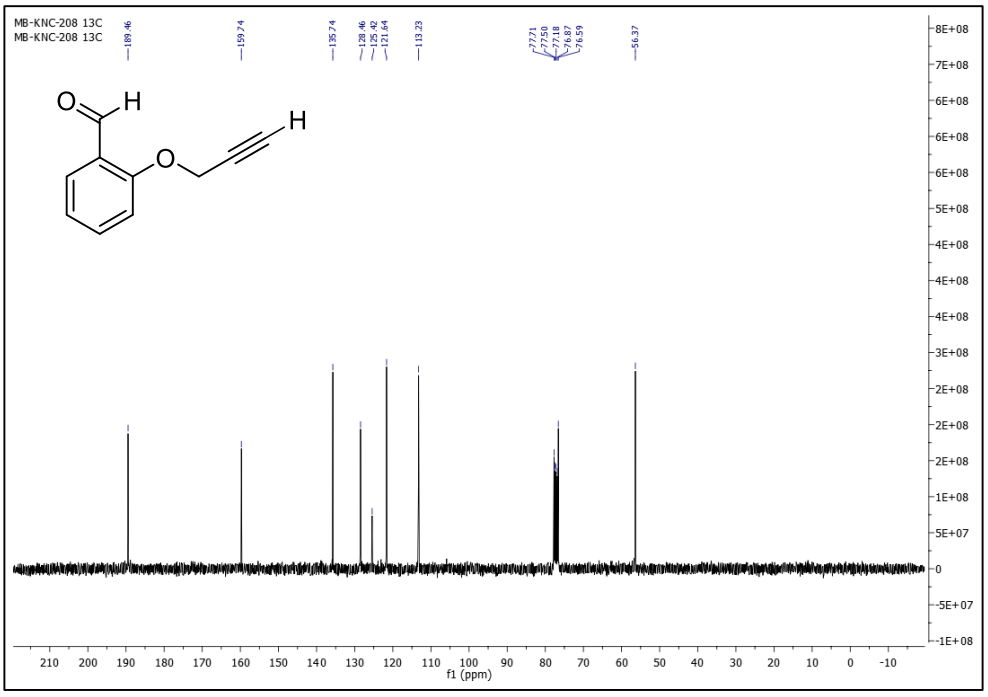

Figure 131. ^{13}C-NMR spectrum of compound **120a**

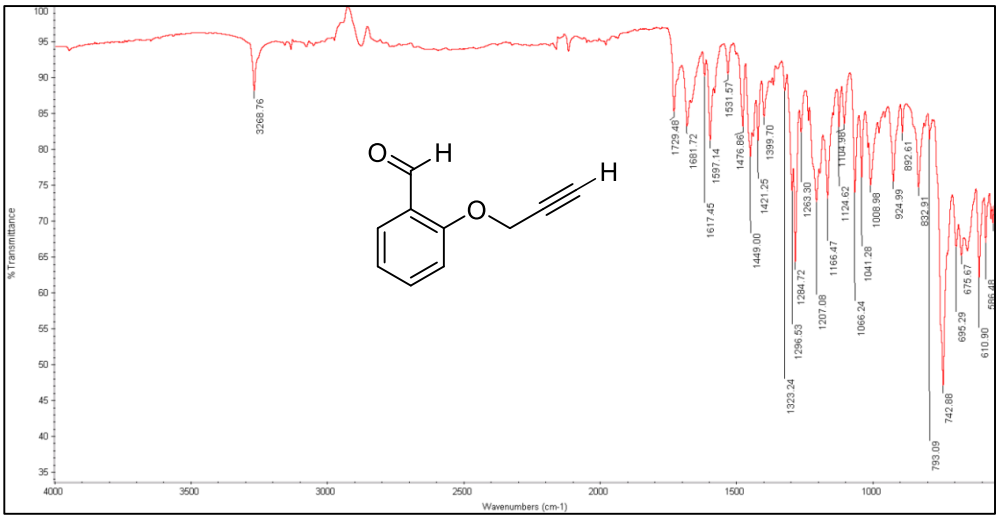

Figure 132. IR spectrum of compound **120a**

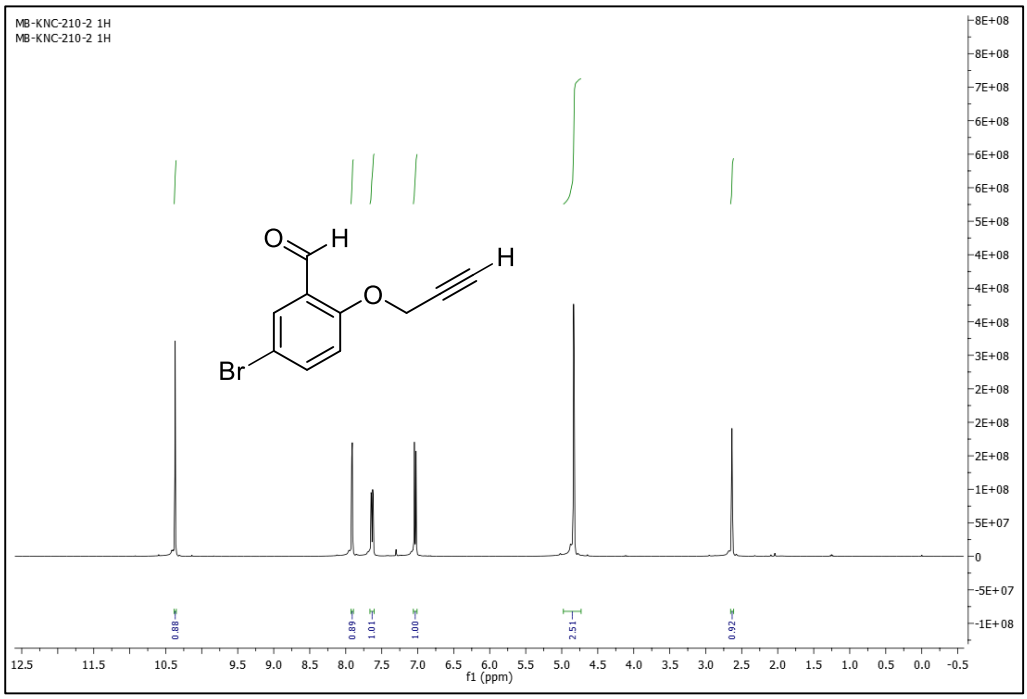

Figure 133. ^{1}H-NMR spectrum of compound **120b**

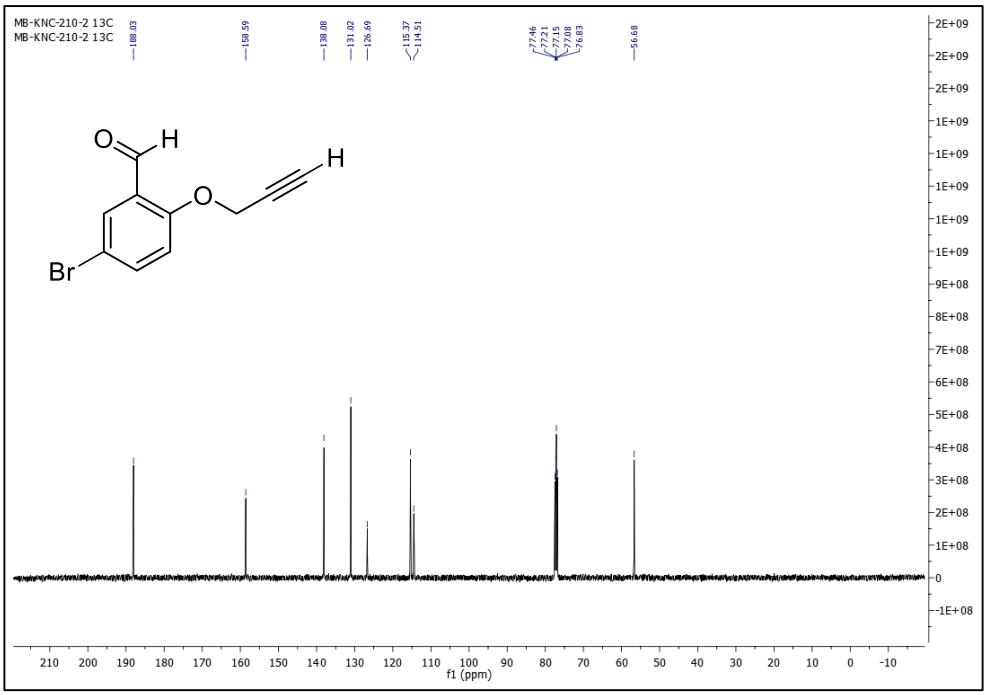

Figure 134. ^{13}C-NMR spectrum of compound **120b**

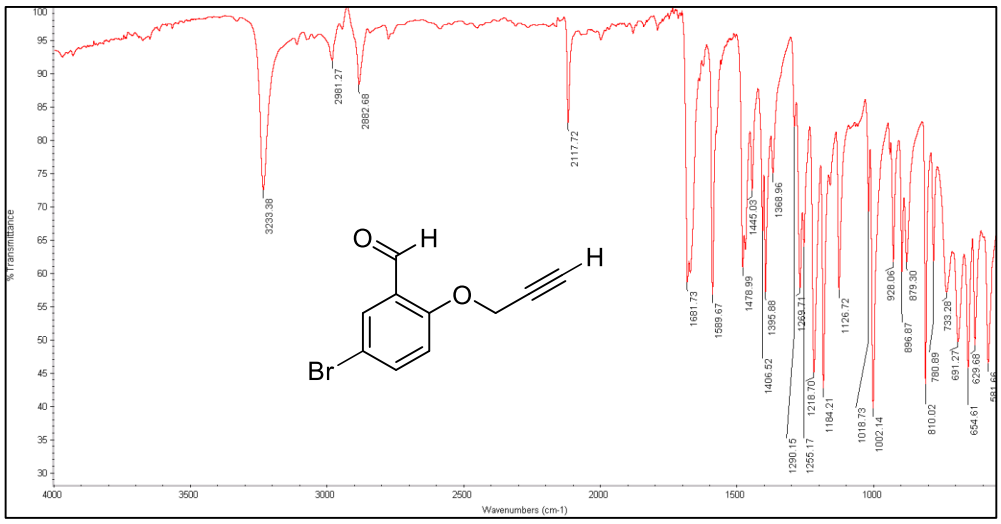

Figure 135. IR spectrum of compound **120b**

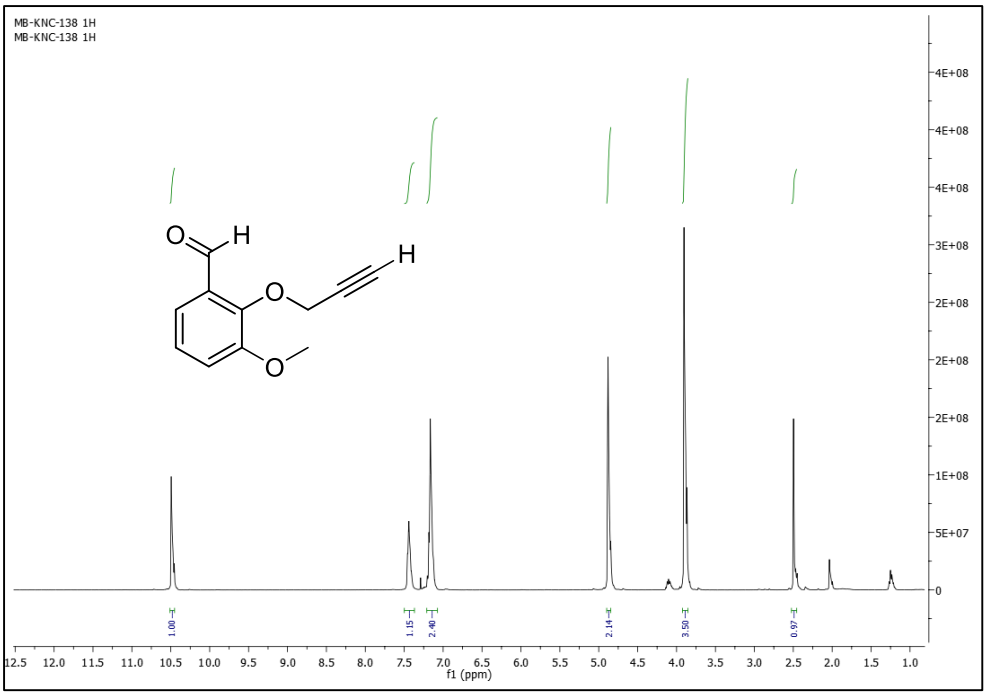

Figure 136. ^{1}H-NMR spectrum of compound **120c**

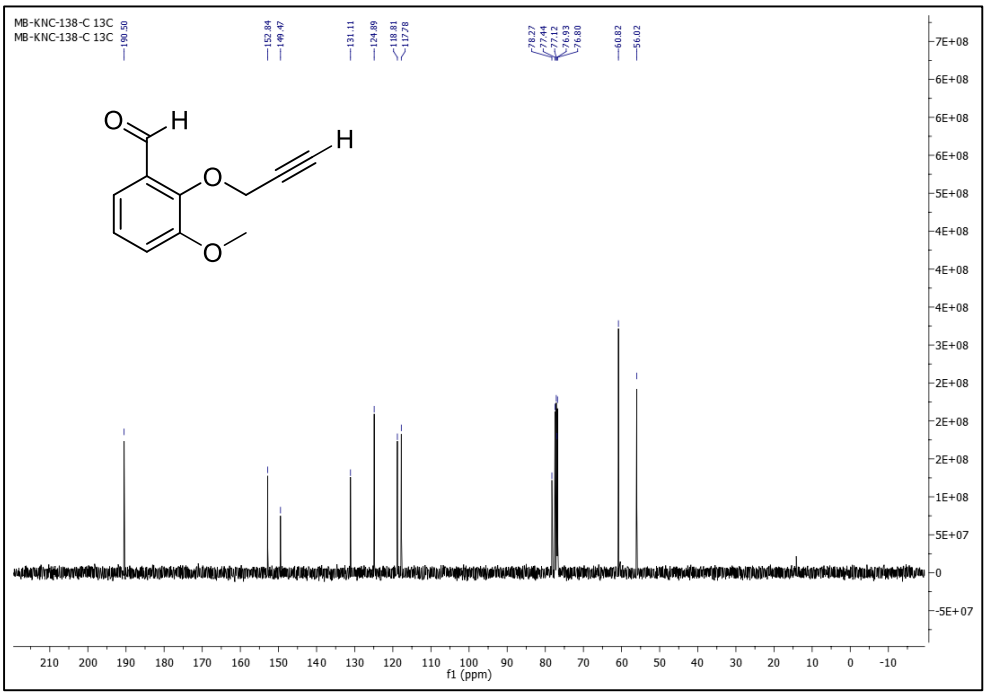

Figure 137. ^{13}C-NMR spectrum of compound **120c**

Figure 138. IR spectrum of compound **120c**

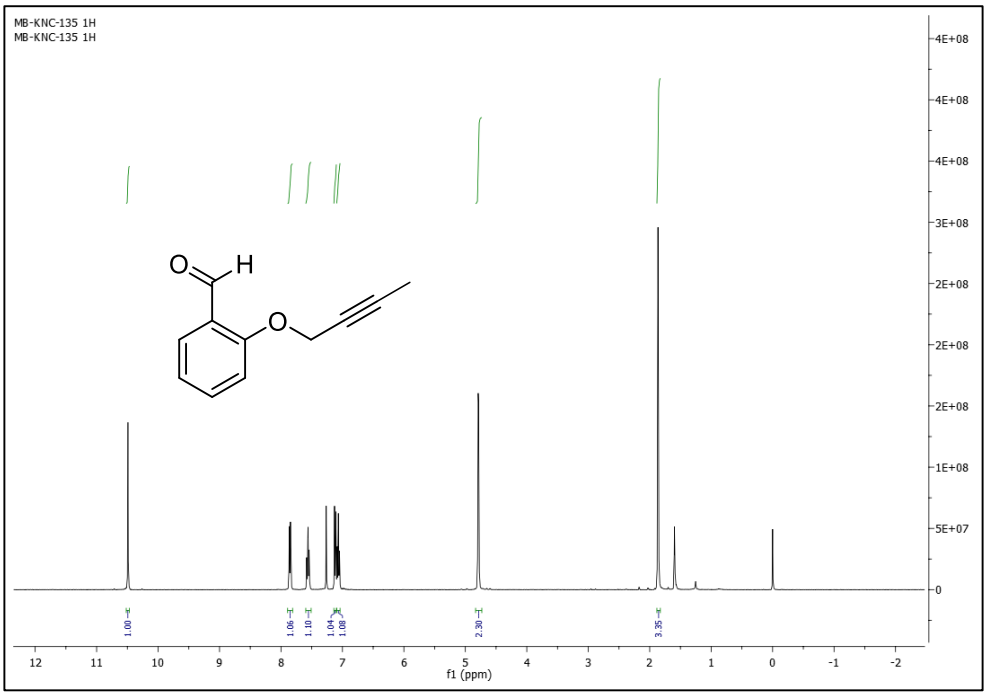

Figure 139. ^{1}H-NMR spectrum of compound **120f**

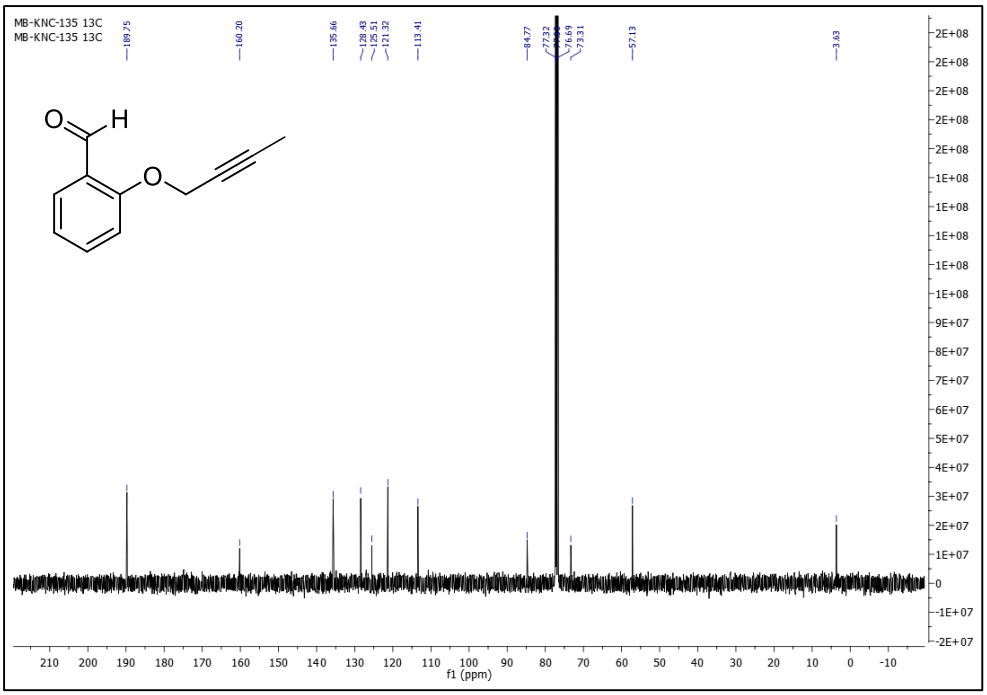

Figure 140. ^{13}C-NMR spectrum of compound **120f**

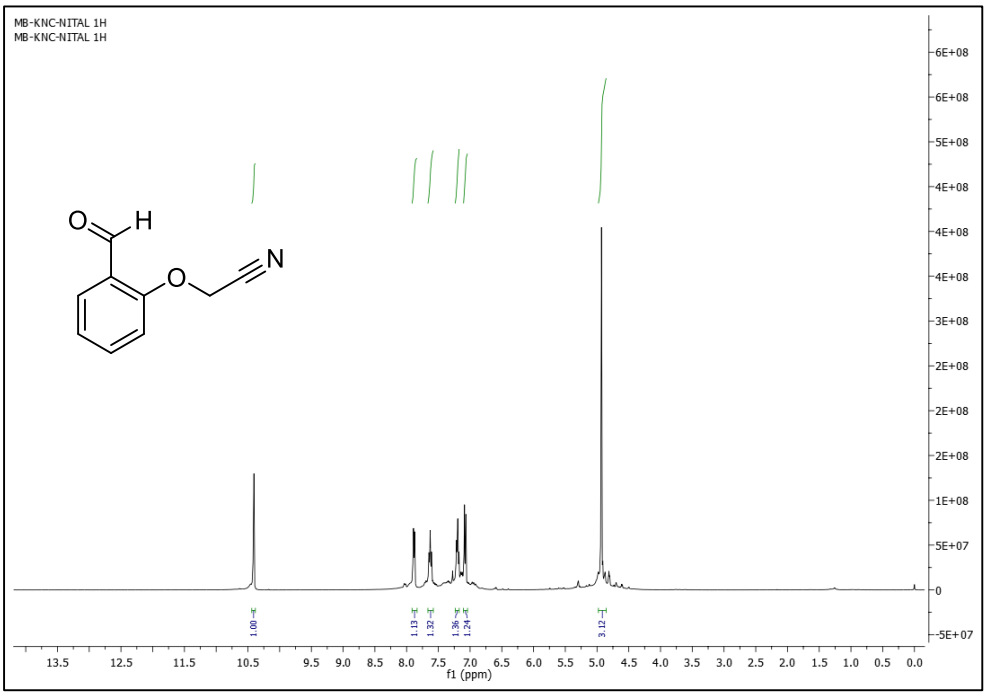

Figure 141. ^{1}H-NMR spectrum of compound **120g**

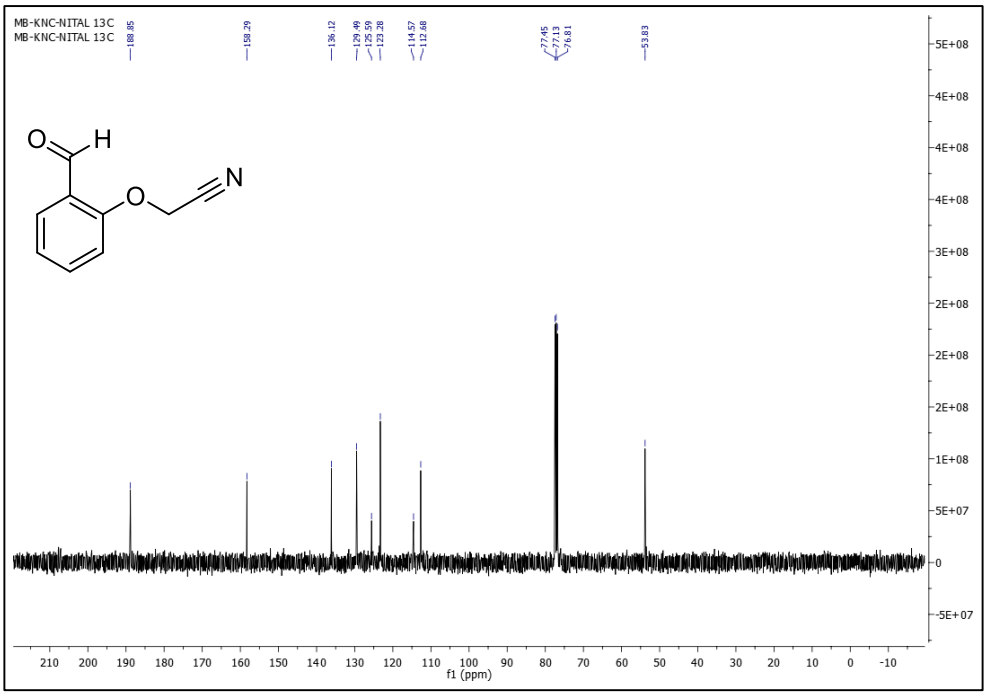

Figure 142. ^{13}C-NMR spectrum of compound **120g**

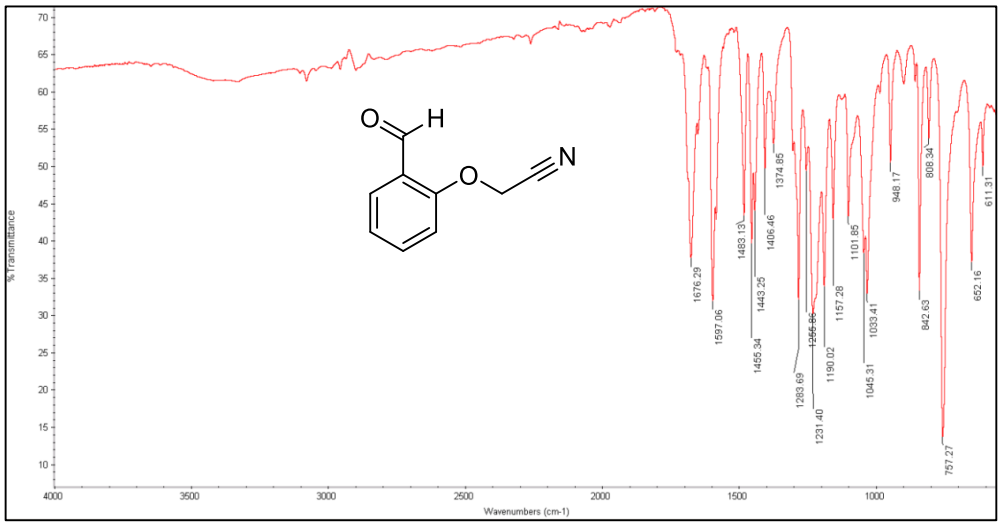

Figure 143. IR spectrum of compound **120g**

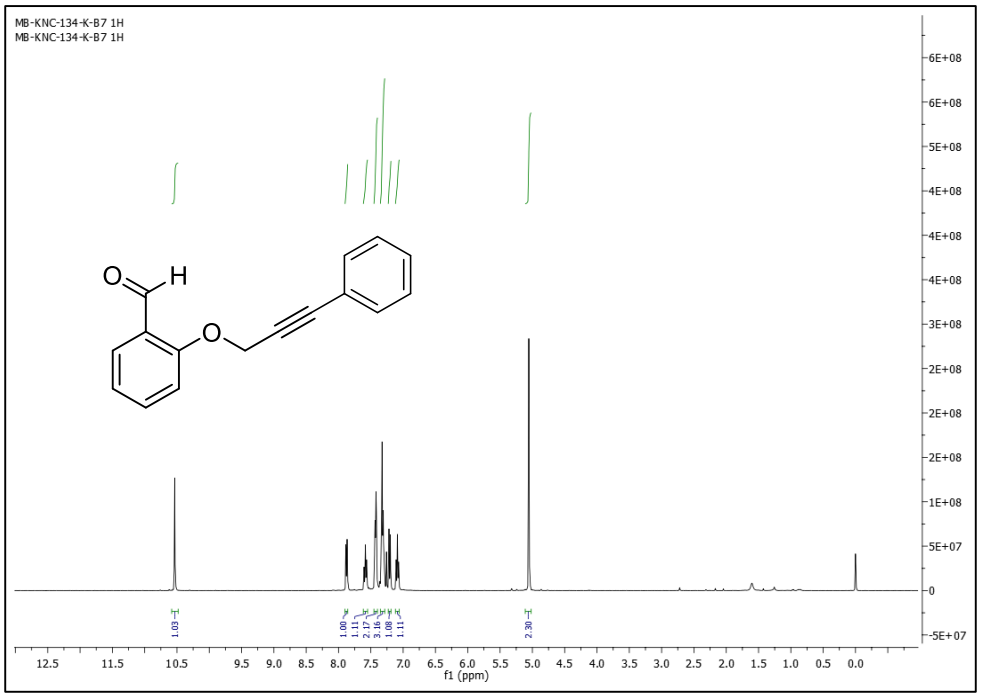

Figure 144. ^{1}H-NMR spectrum of compound **120d**

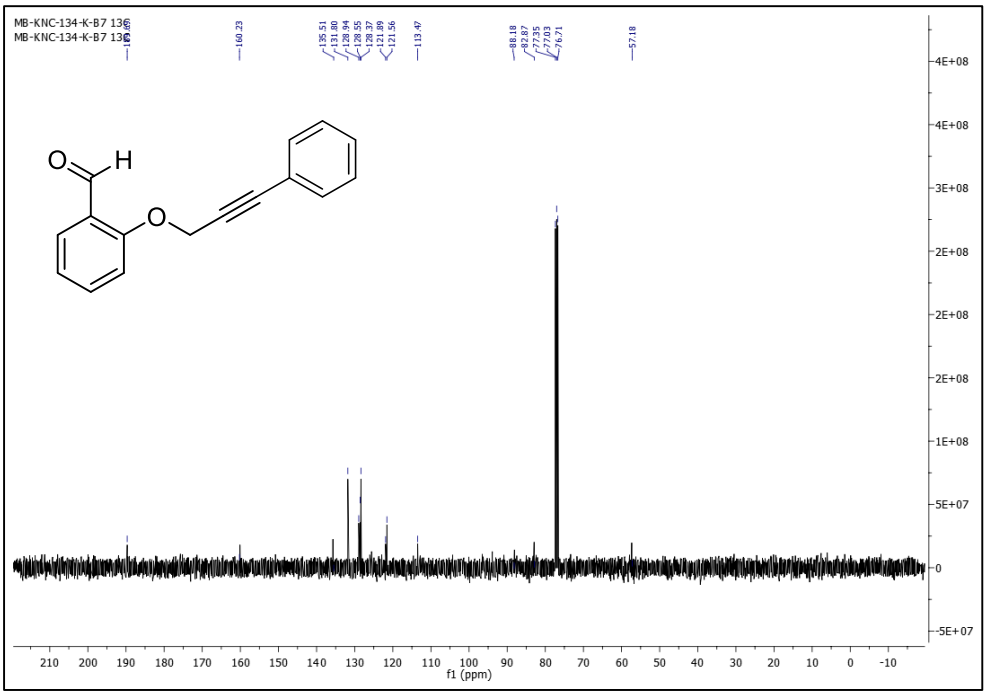

Figure 145. ^{13}C-NMR spectrum of compound **120d**

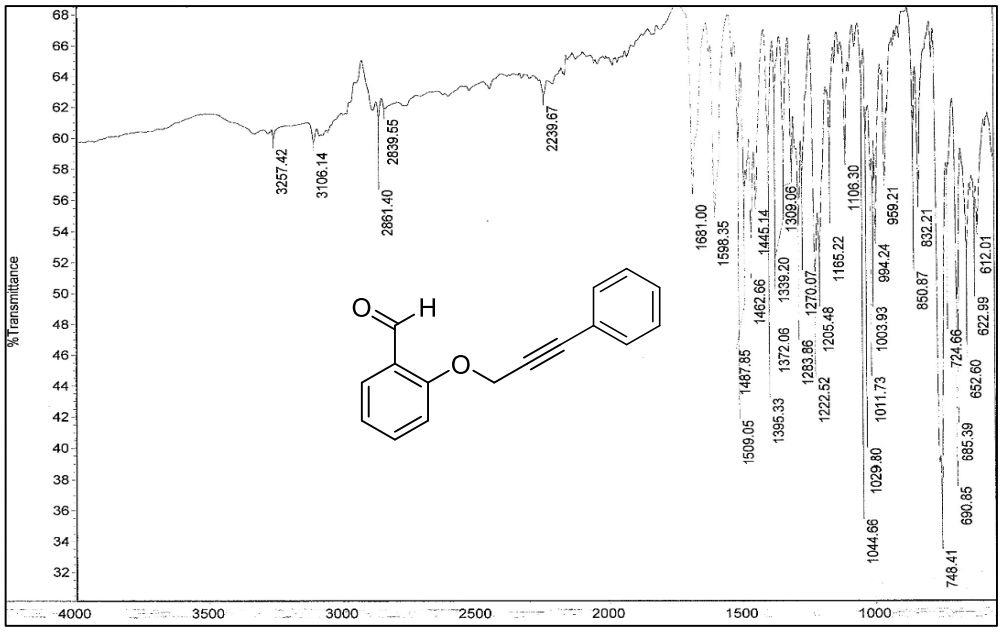

Figure 146. IR spectrum of compound **120d**

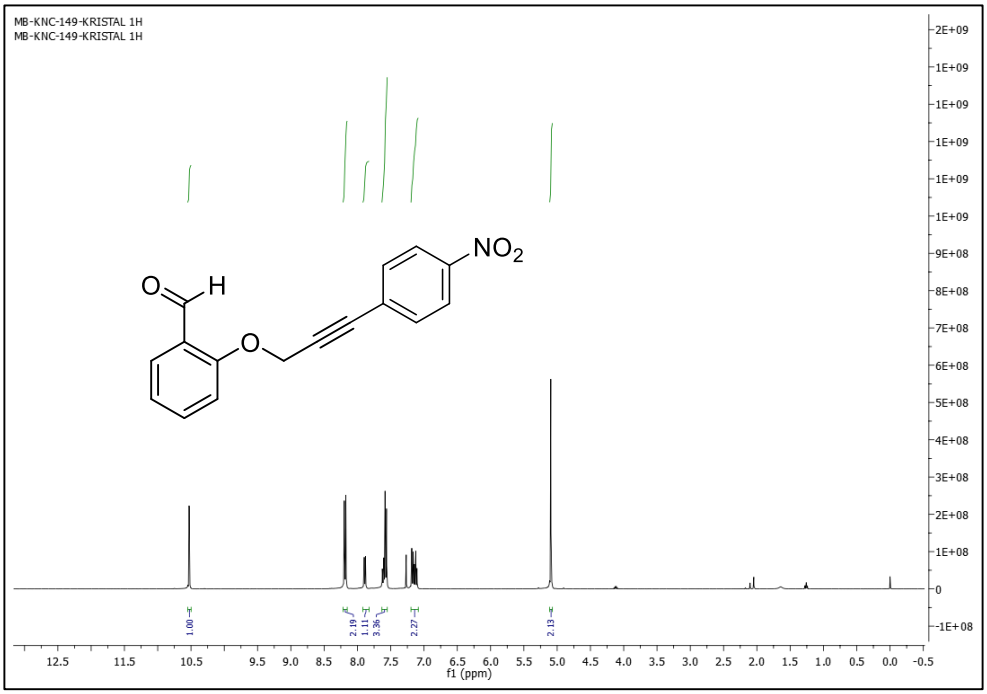

Figure 147. ^{1}H-NMR spectrum of compound **120e**

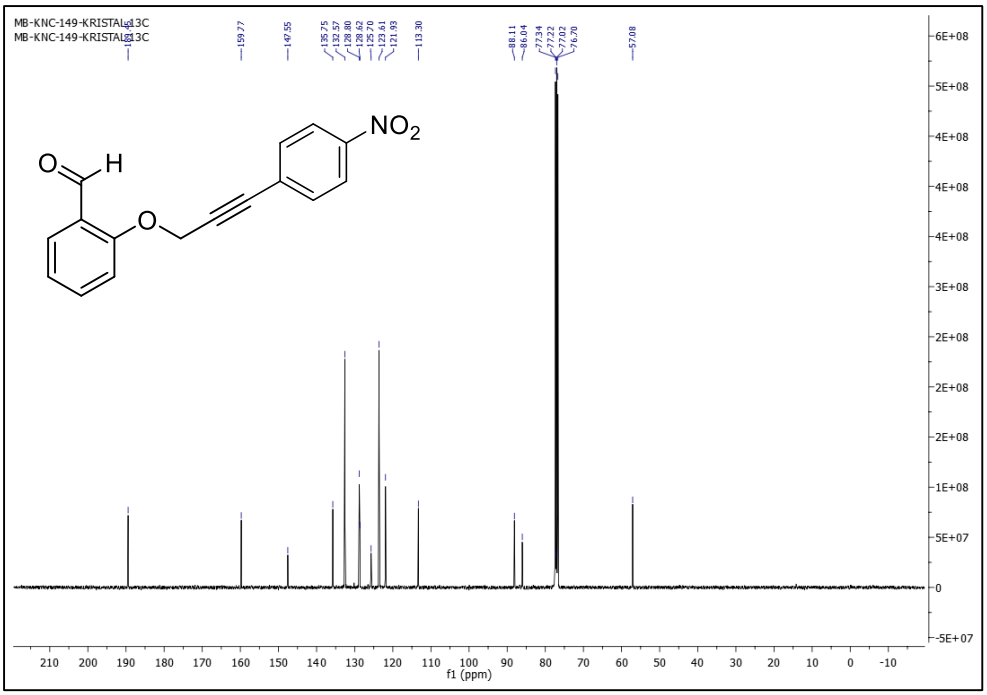

Figure 148. ^{13}C-NMR spectrum of compound **120e**

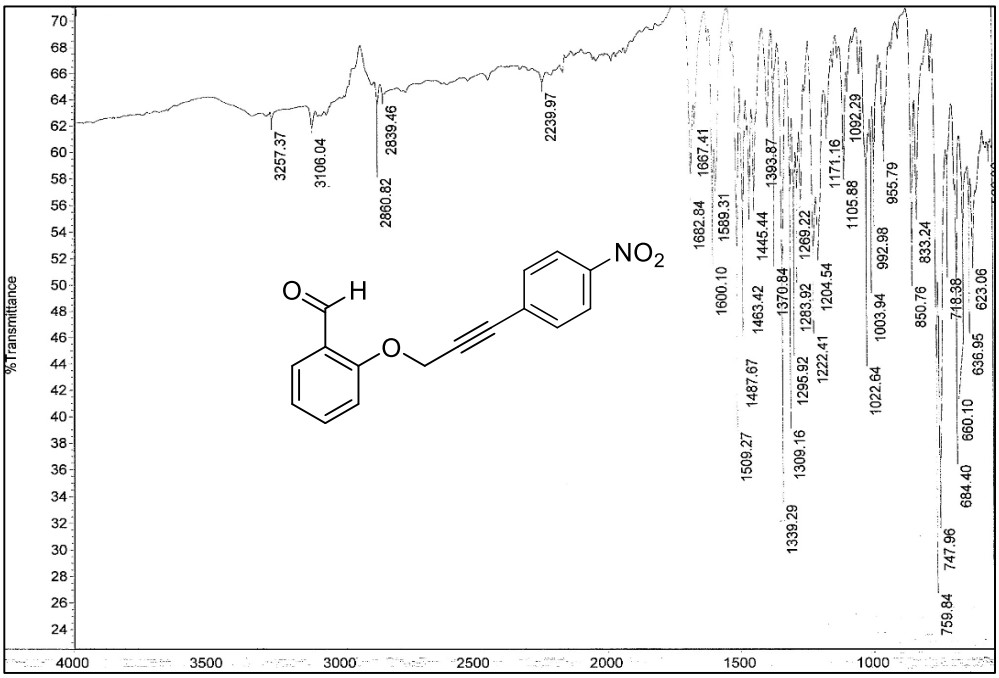

Figure 149. IR spectrum of compound **120e**

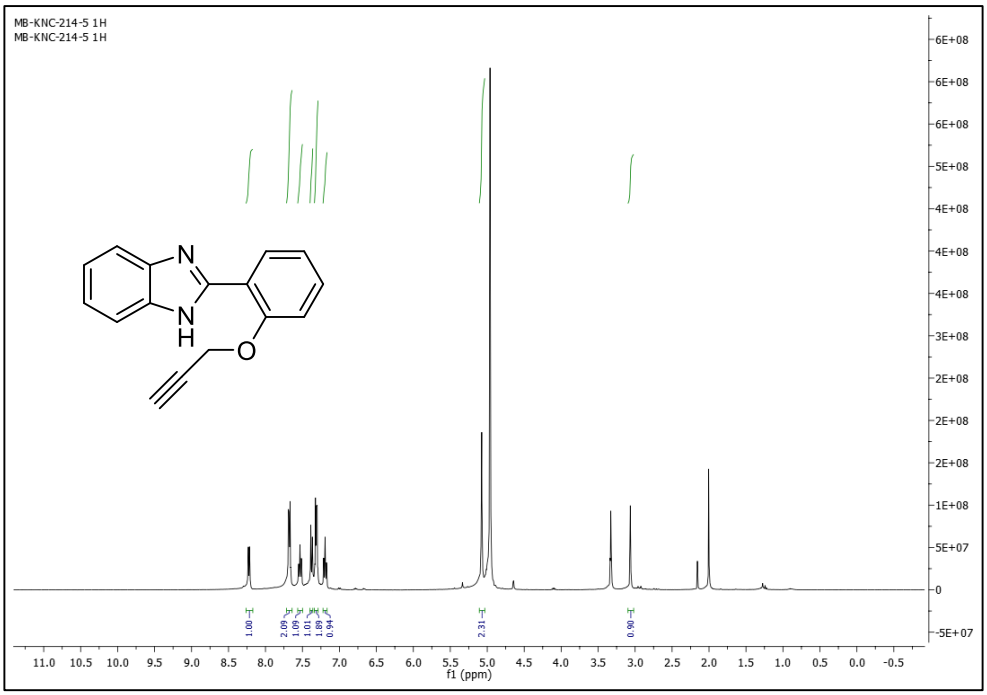

Figure 150. ^{1}H-NMR spectrum of compound **121a**

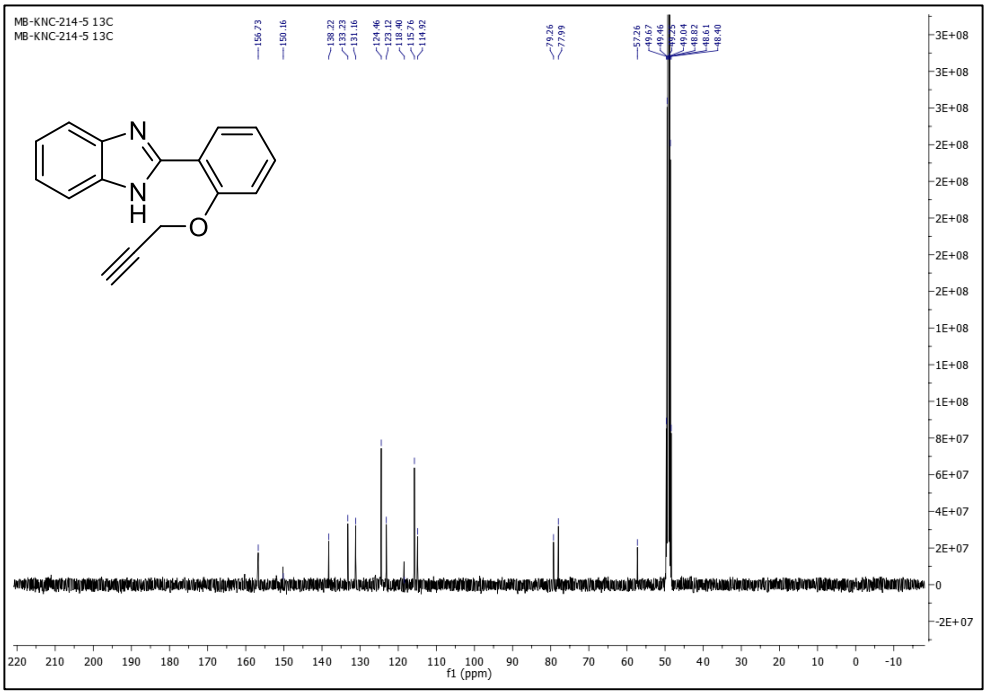

Figure 151. ^{13}C-NMR spectrum of compound **121a**

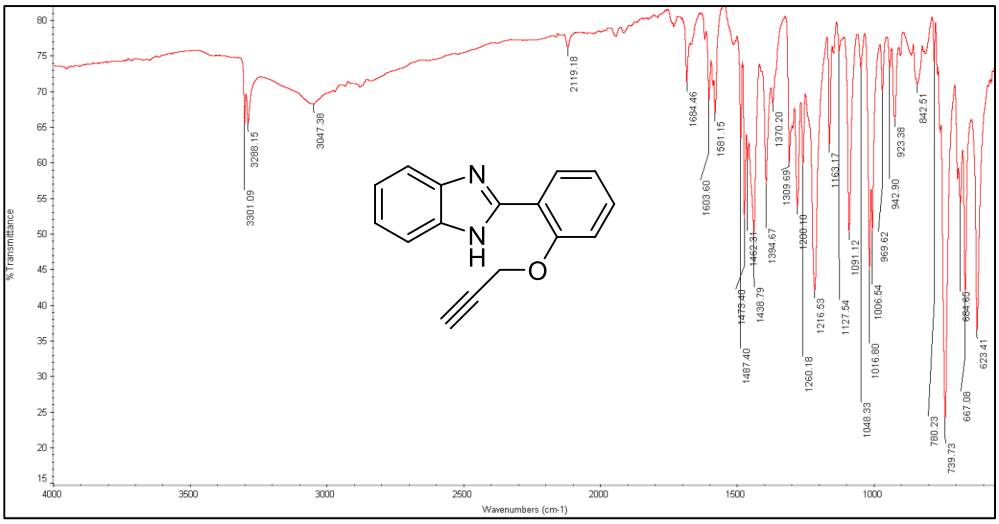

Figure 152. IR spectrum of compound **121a**

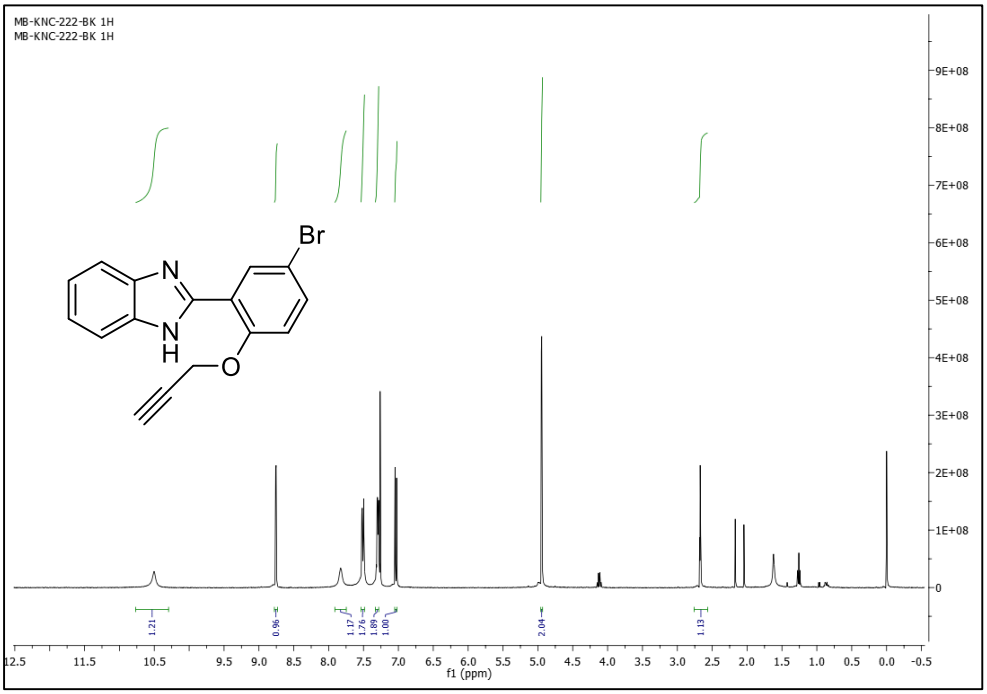

Figure 153. ^{1}H-NMR spectrum of compound **121b**

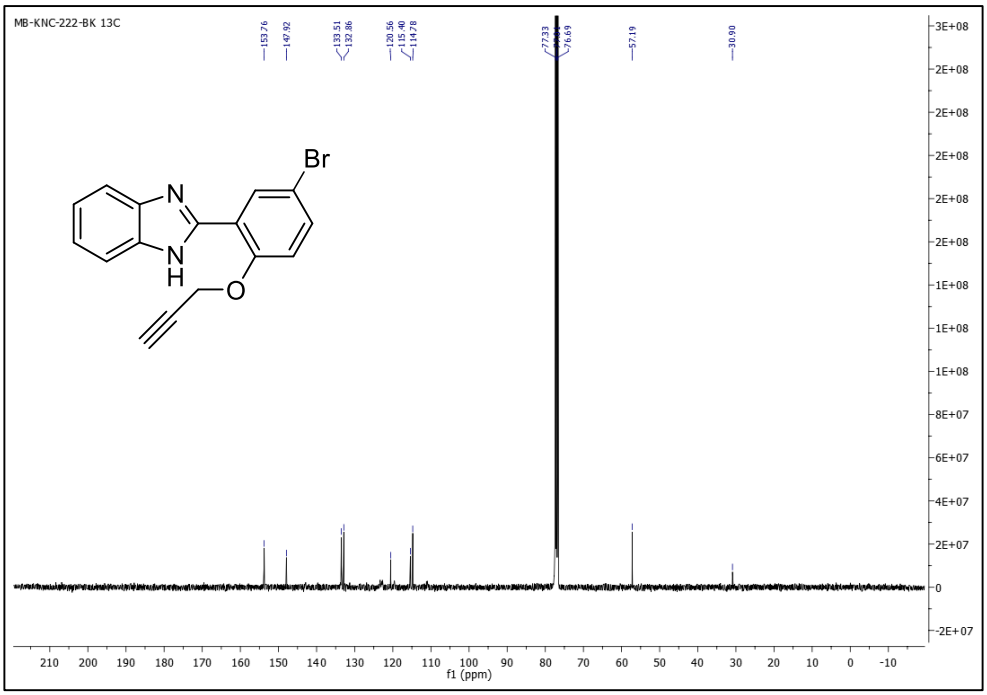

Figure 154. ^{13}C-NMR spectrum of compound **121b**

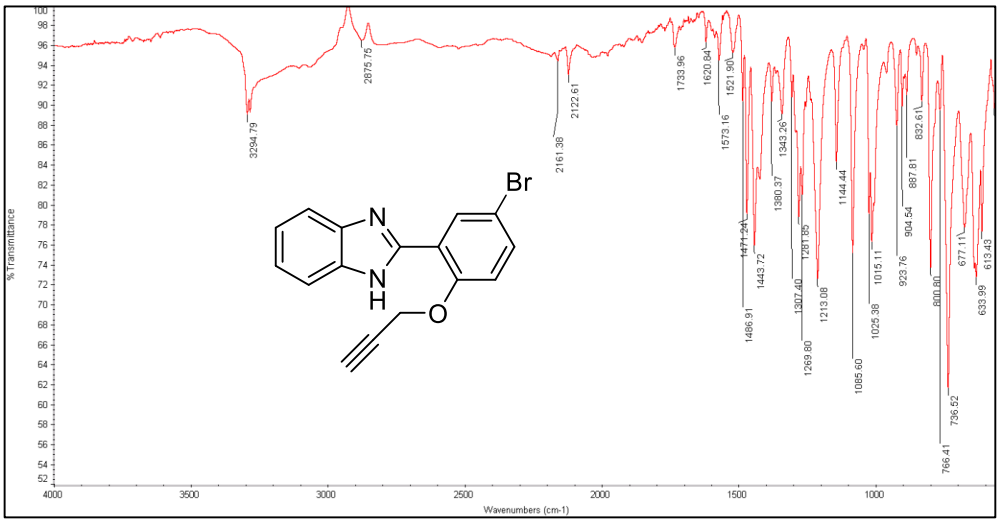

Figure 155. IR spectrum of compound **121b**

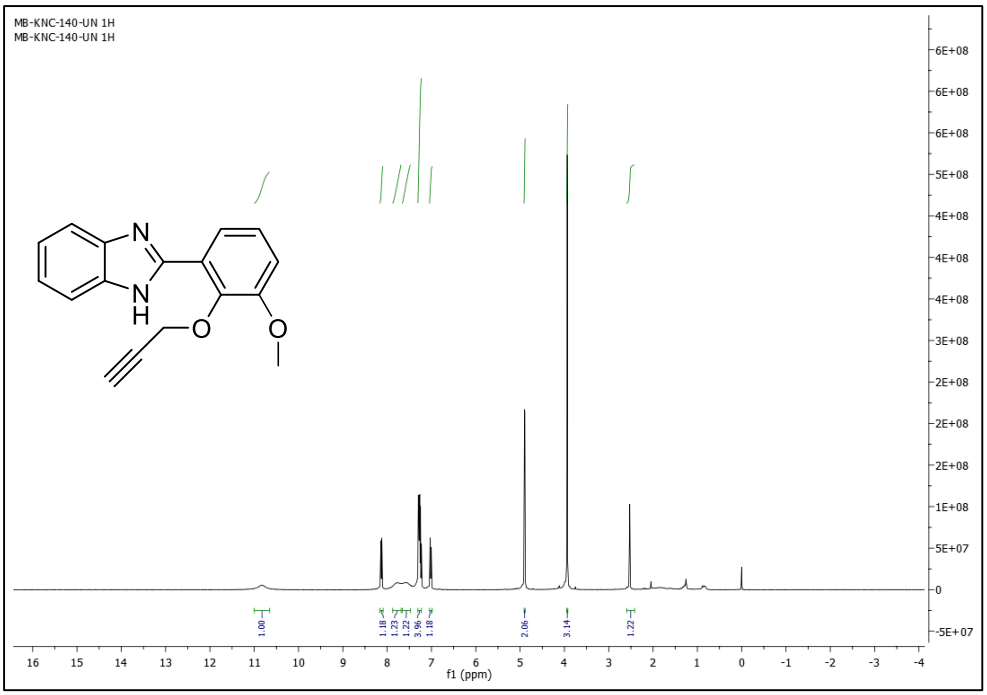

Figure 156. ^{1}H-NMR spectrum of compound **121c**

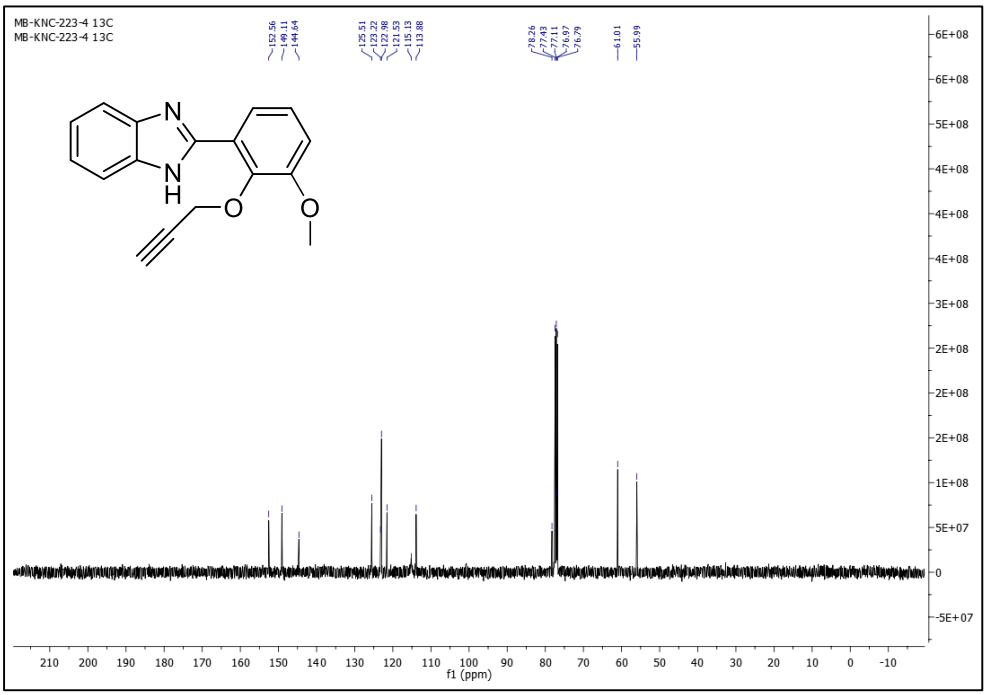

Figure 157. ^{13}C-NMR spectrum of compound **121c**

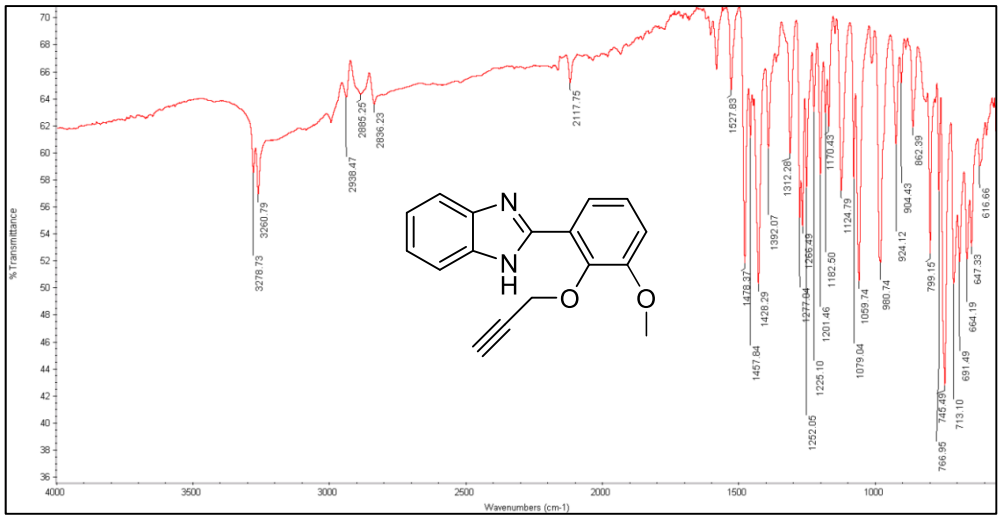

Figure 158. IR spectrum of compound **121c**

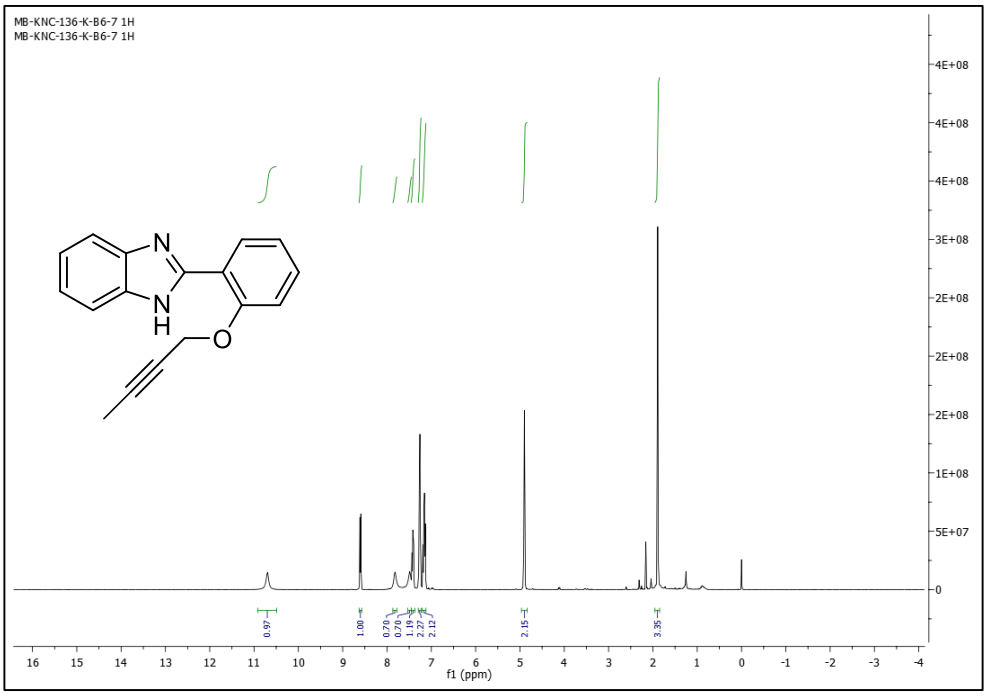

Figure 159. ^{1}H-NMR spectrum of compound **121f**

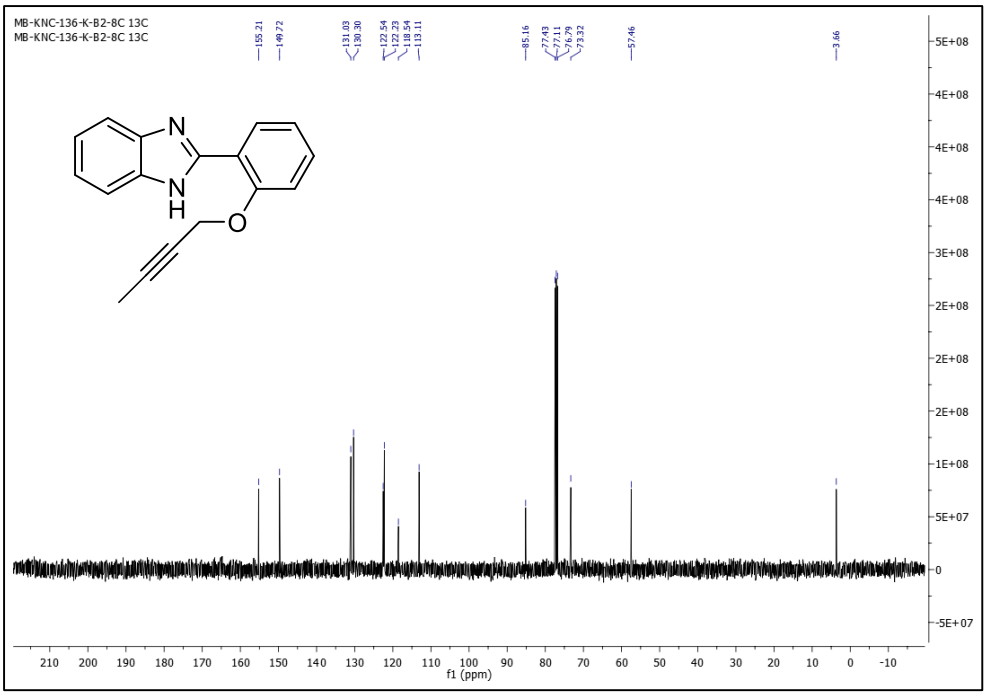

Figure 160. ^{13}C-NMR spectrum of compound **121f**

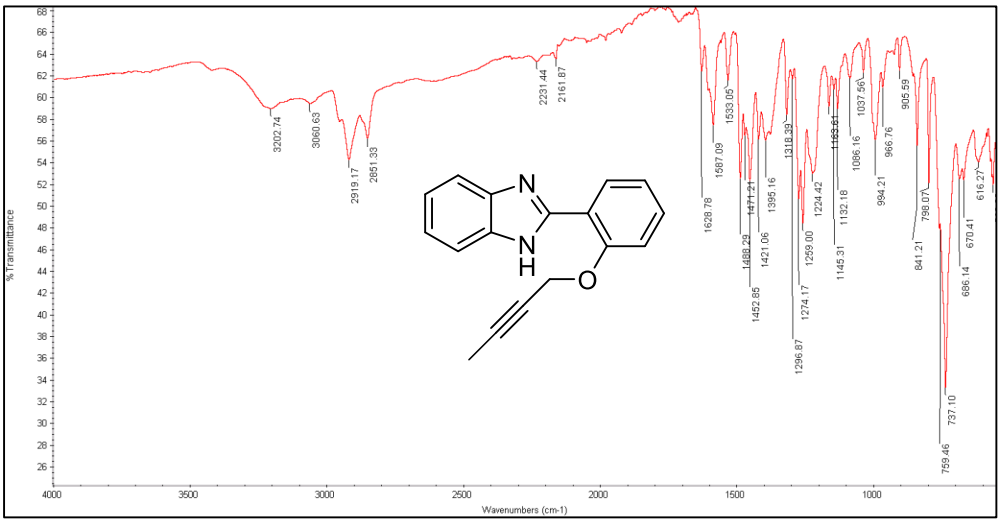

Figure 161. IR spectrum of compound **121f**

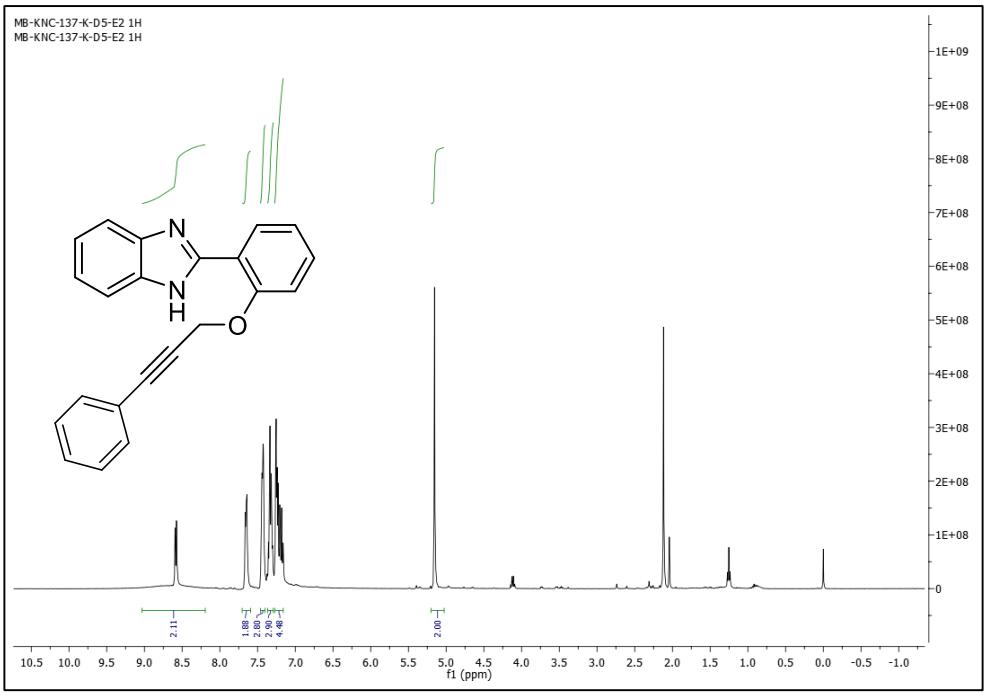

Figure 162. ^{1}H-NMR spectrum of compound **121d**

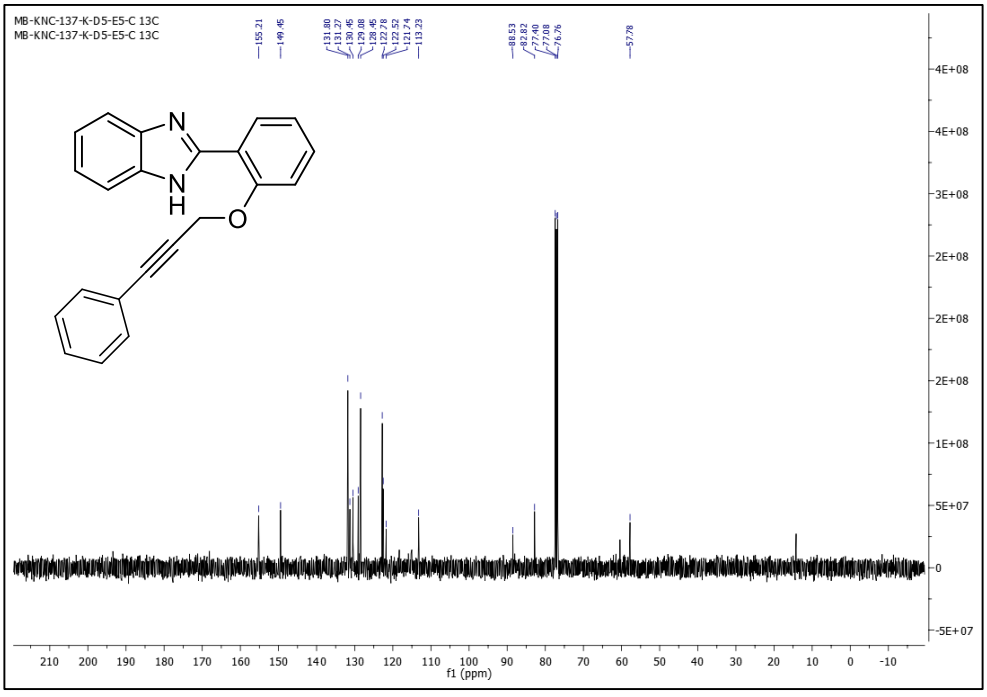

Figure 163. ^{13}C-NMR spectrum of compound **121d**

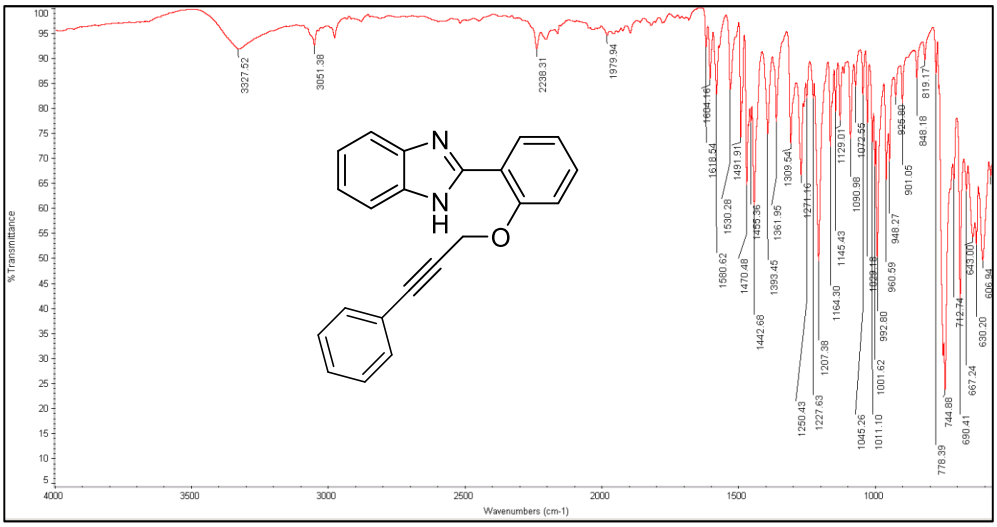

Figure 164. IR spectrum of compound **121d**

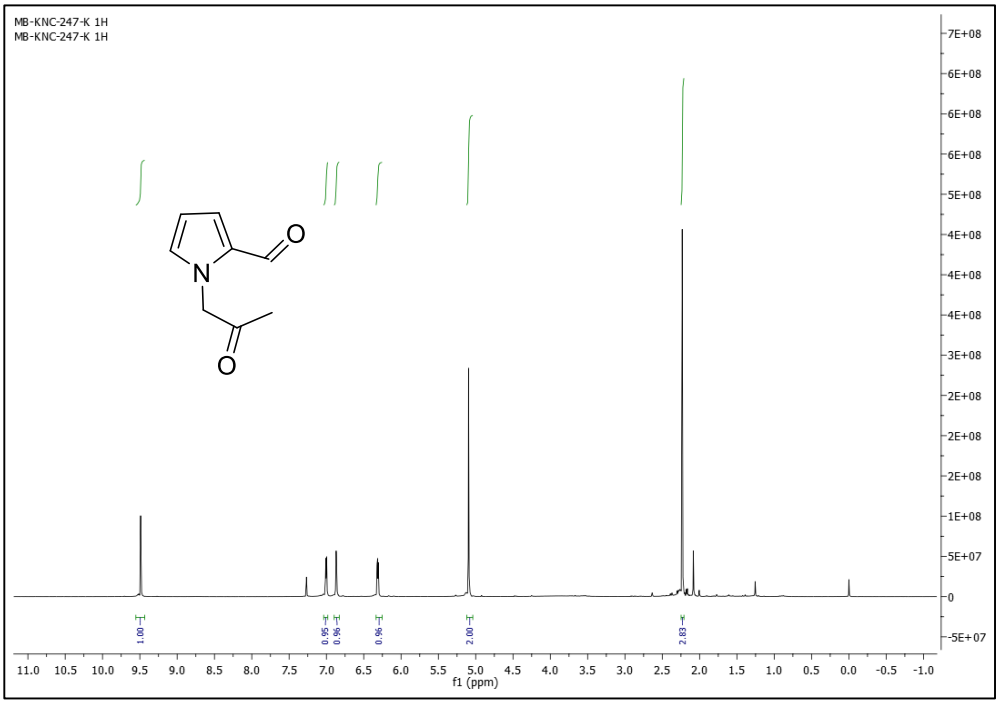

Figure 165. ^{1}H-NMR spectrum of compound **143**

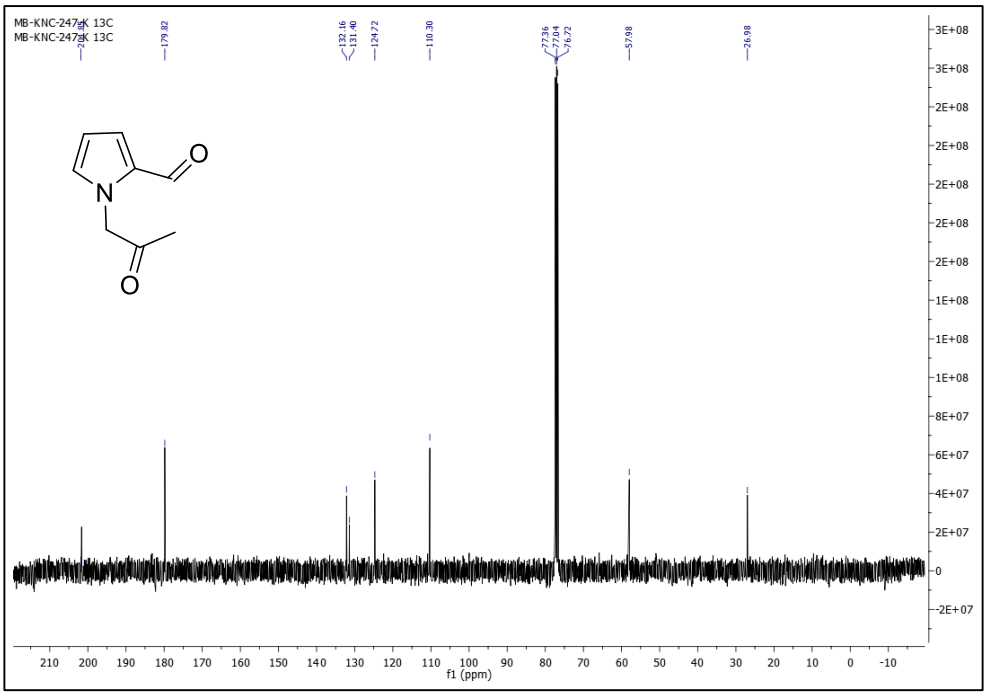

Figure 166. ^{13}C-NMR spectrum of compound **143**

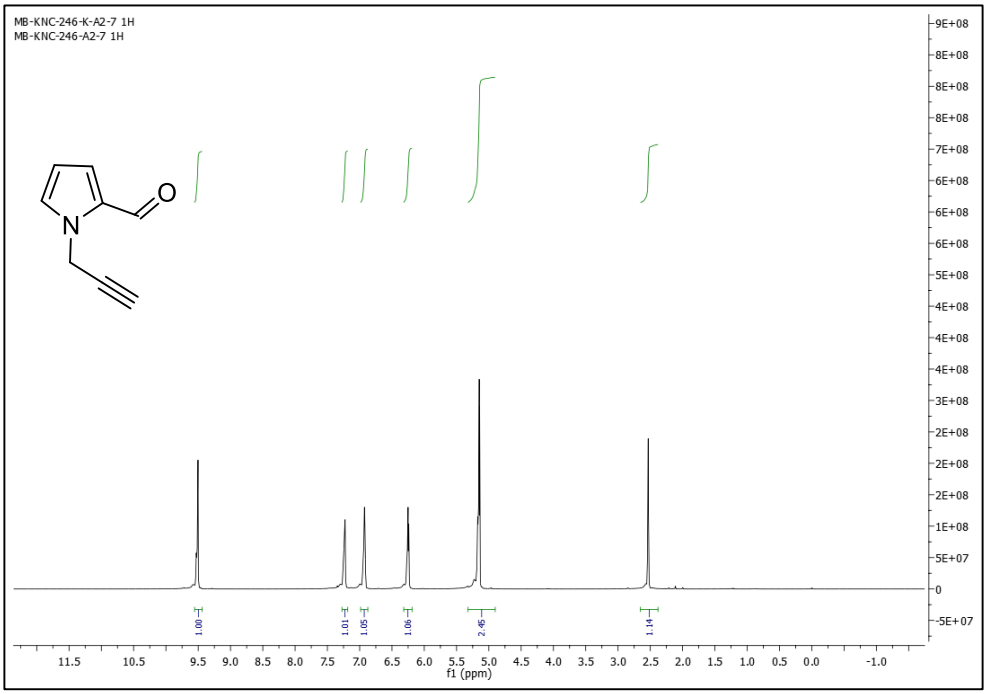

Figure 167. ^{1}H-NMR spectrum of compound **144**

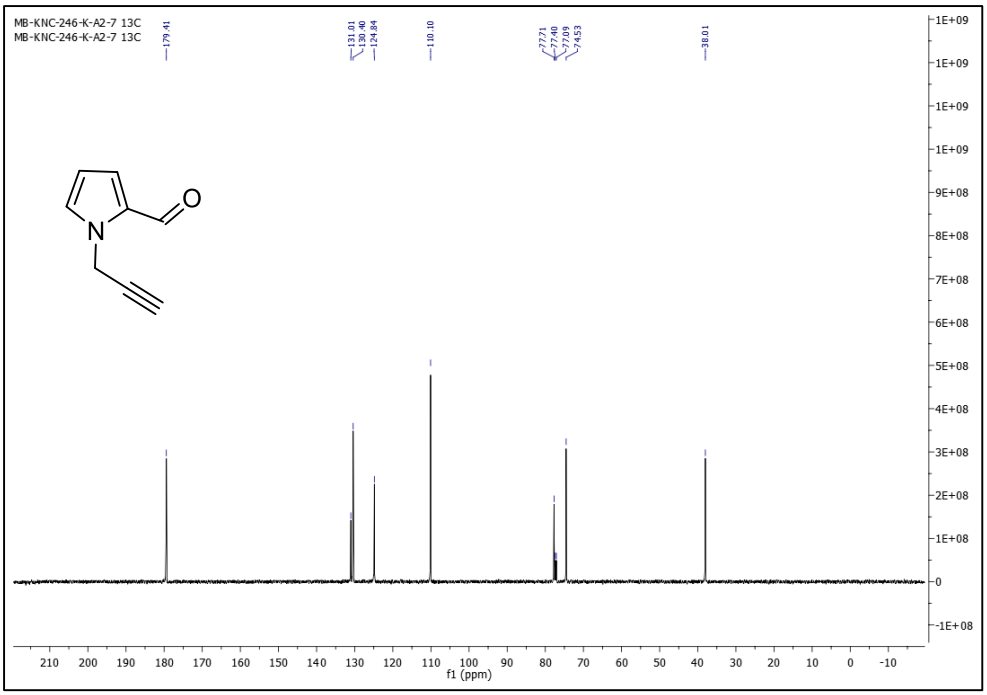

Figure 168. ^{13}C-NMR spectrum of compound **144**

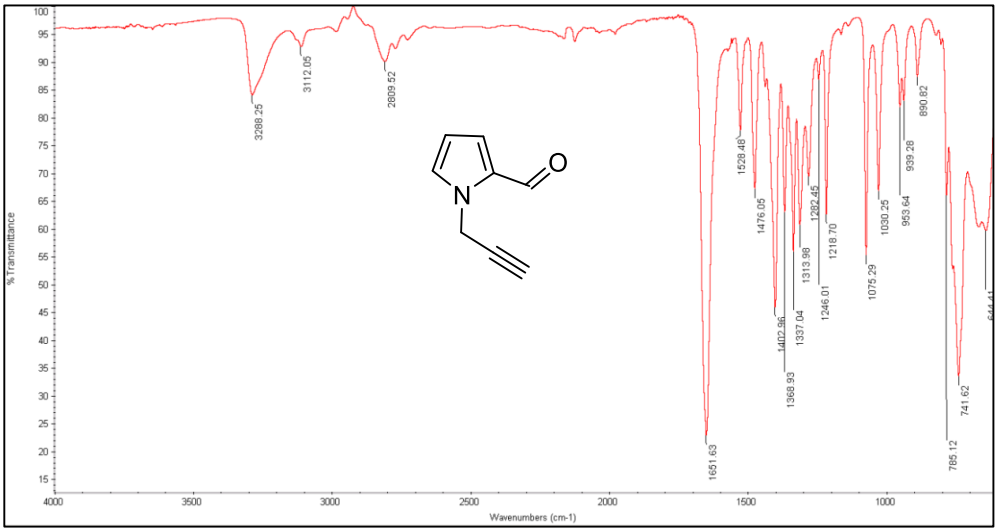

Figure 169. IR spectrum of compound **144**

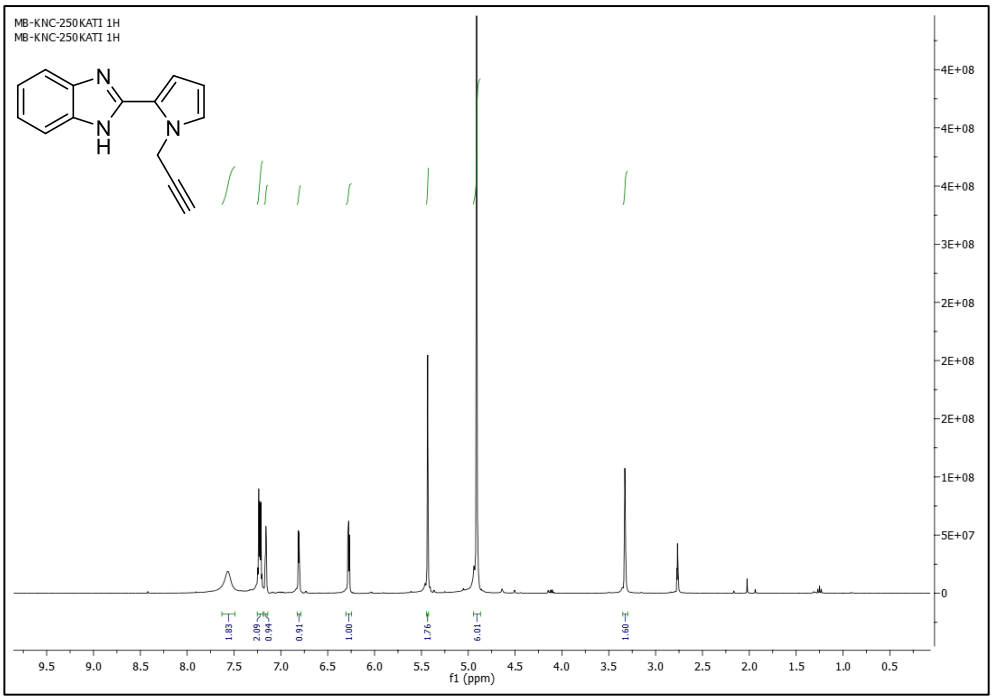

Figure 170. ^{1}H-NMR spectrum of compound **145**

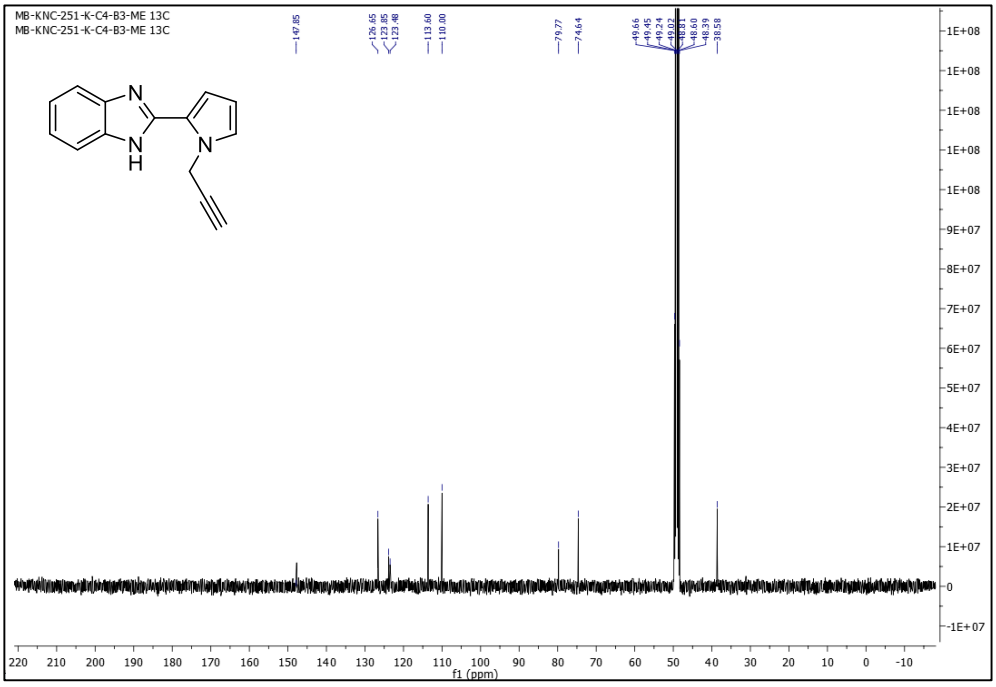

Figure 171. ^{13}C-NMR spectrum of compound **145**

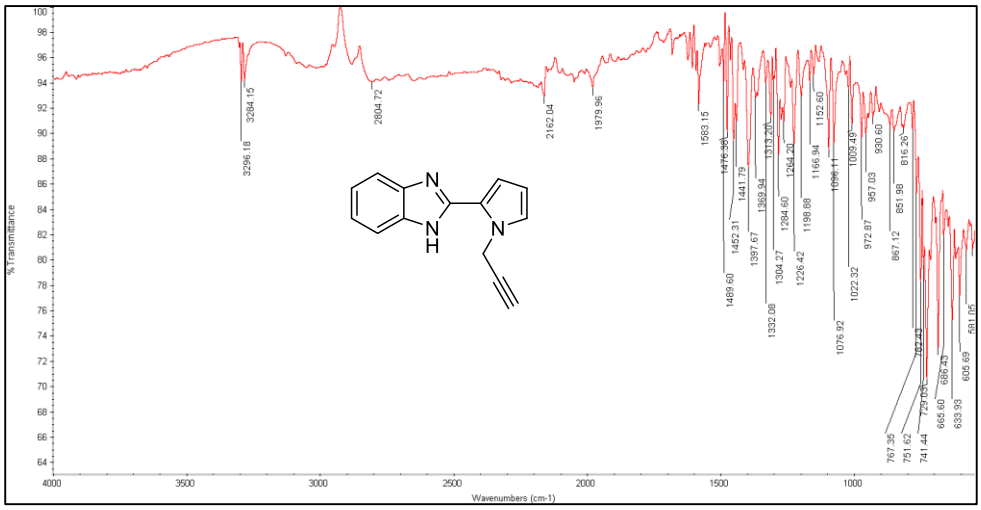

Figure 172. IR spectrum of compound **145**

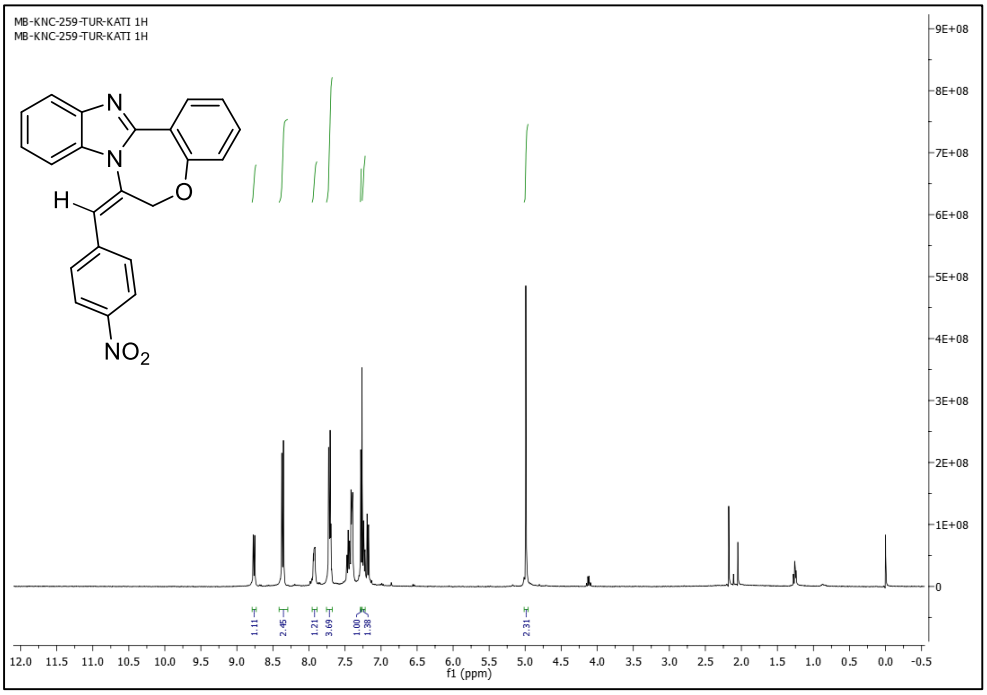

Figure 173. ^{1}H-NMR spectrum of compound **122e**

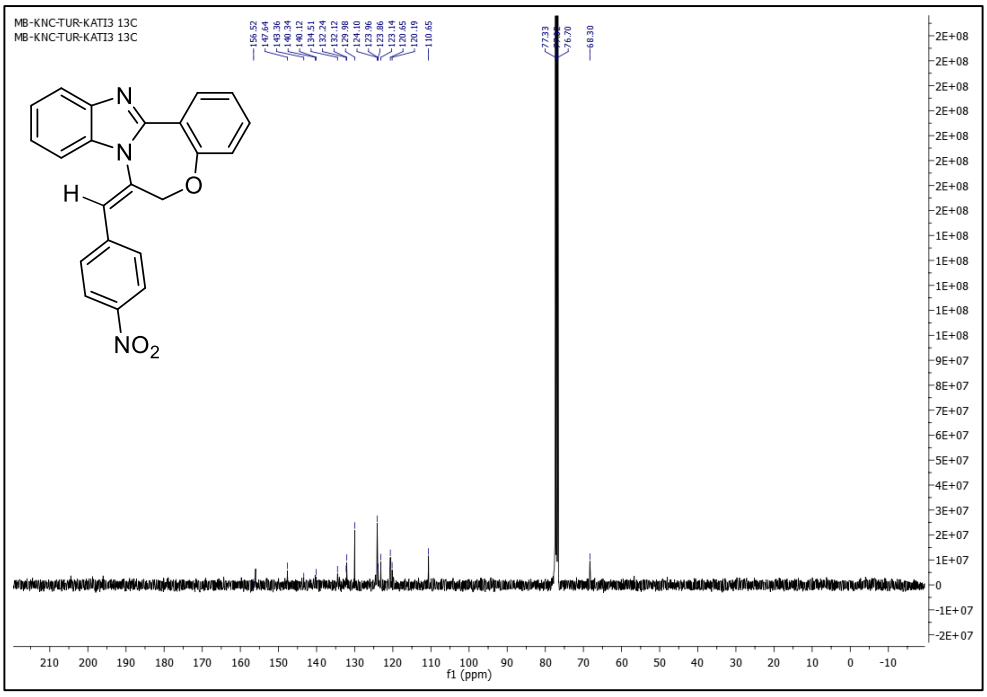

Figure 174. ^{13}C-NMR spectrum of compound **122e**

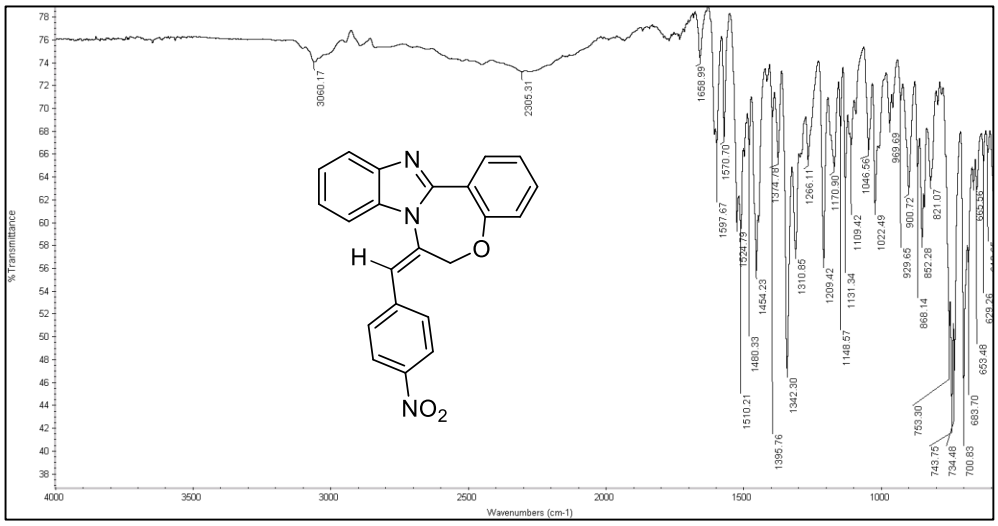

Figure 175. IR spectrum of compound **122e**

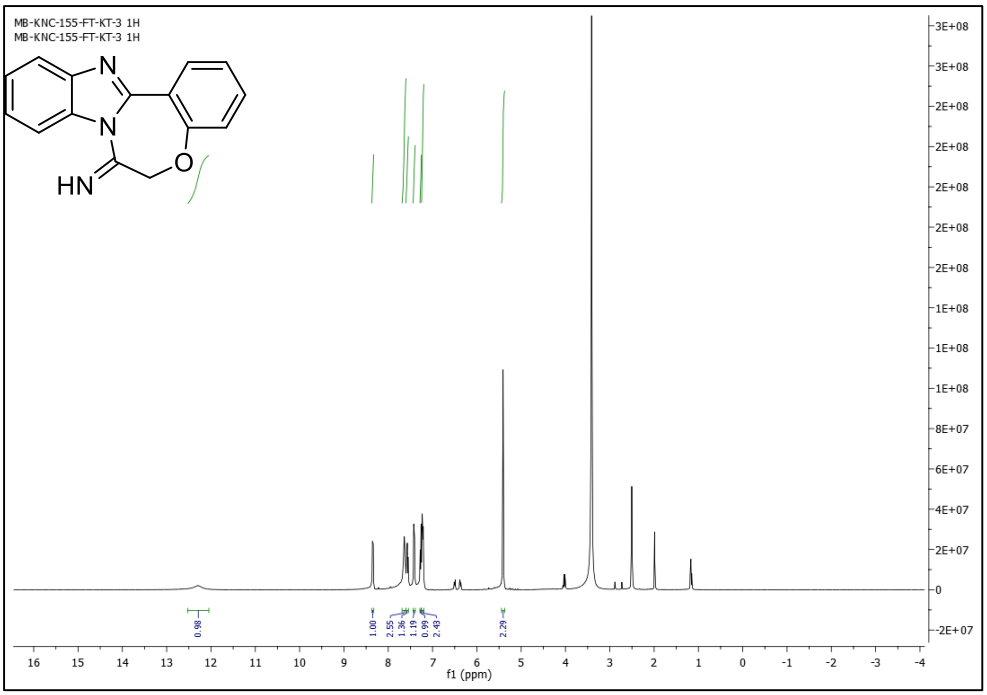

Figure 176. ^{1}H-NMR spectrum of compound **122g**

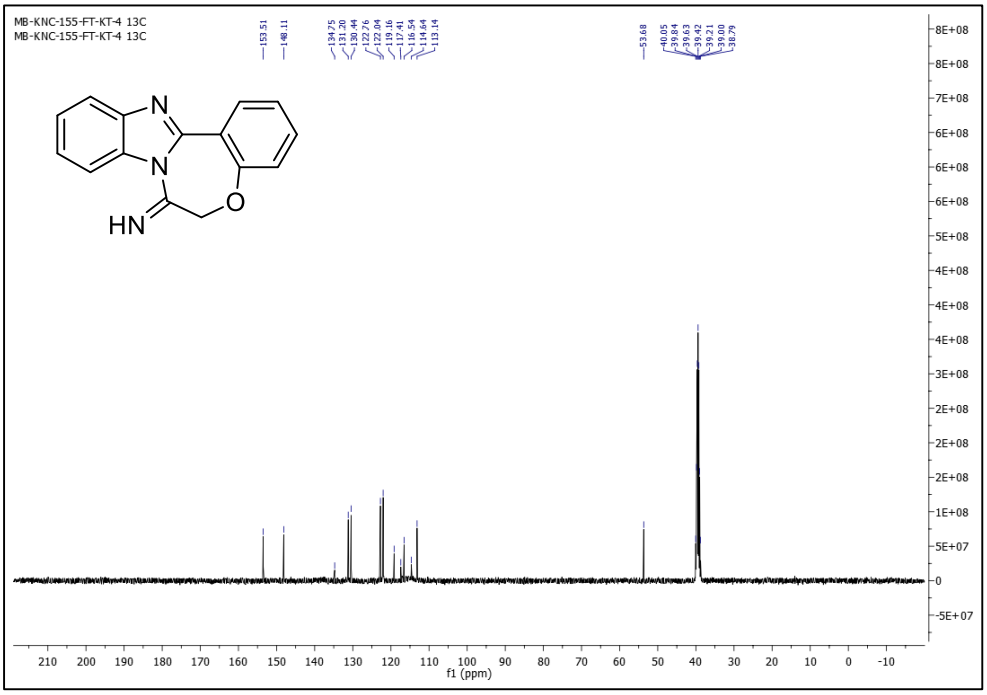

Figure 177. ^{13}C-NMR spectrum of compound **122g**

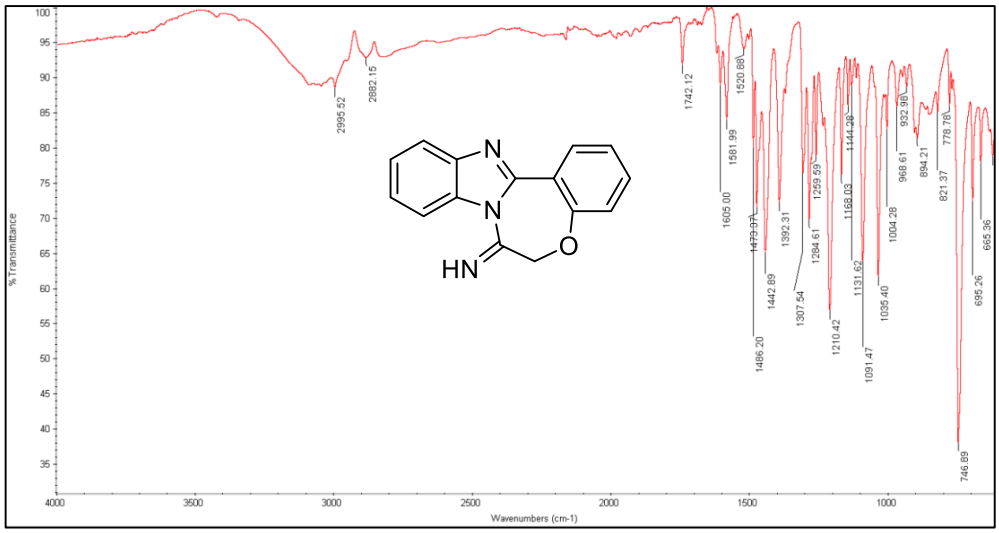

Figure 178. IR spectrum of compound **122g**

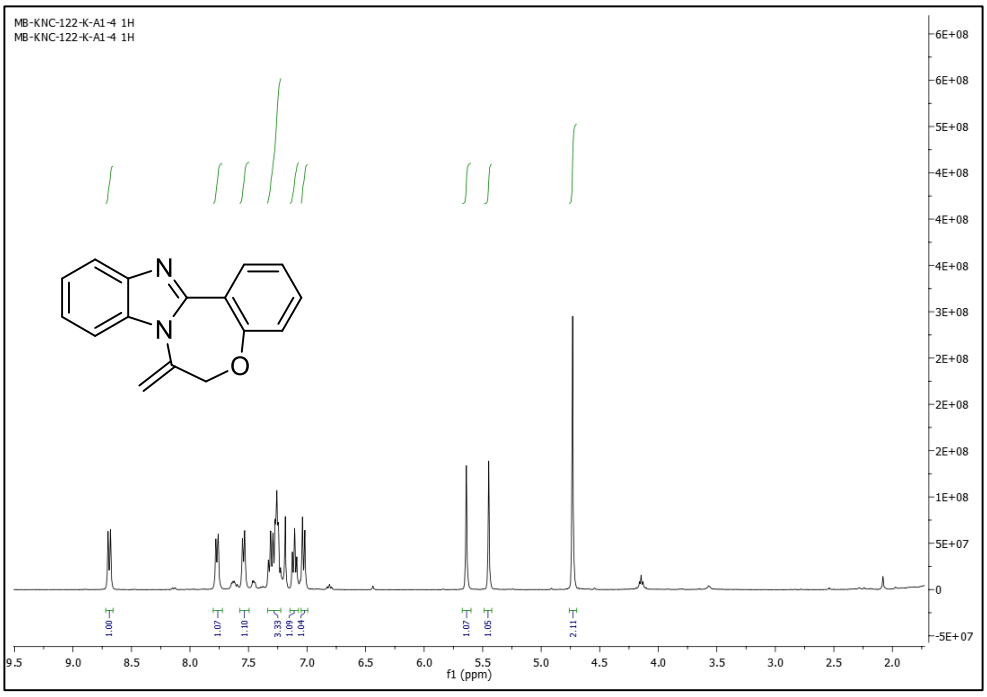

Figure 179. ^{1}H-NMR spectrum of compound **122a**

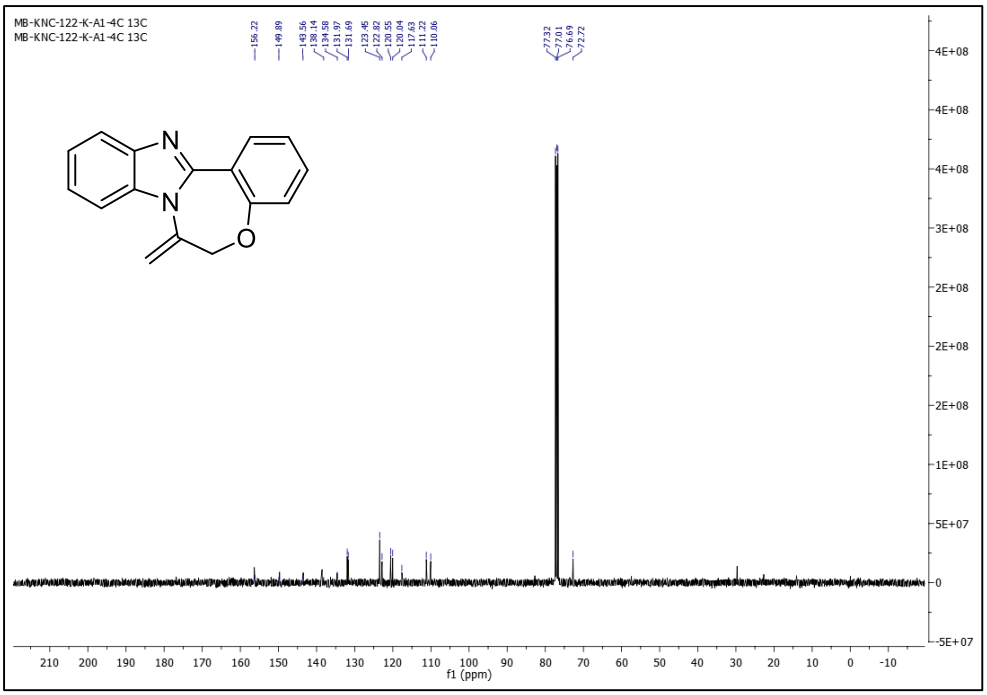

Figure 180. ^{13}C-NMR spectrum of compound **122a**

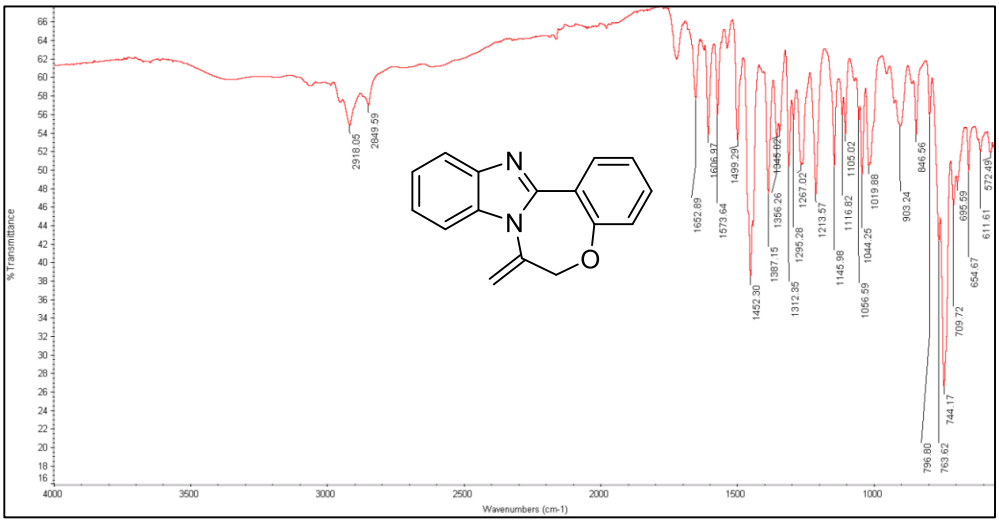

Figure 181. IR spectrum of compound **122a**

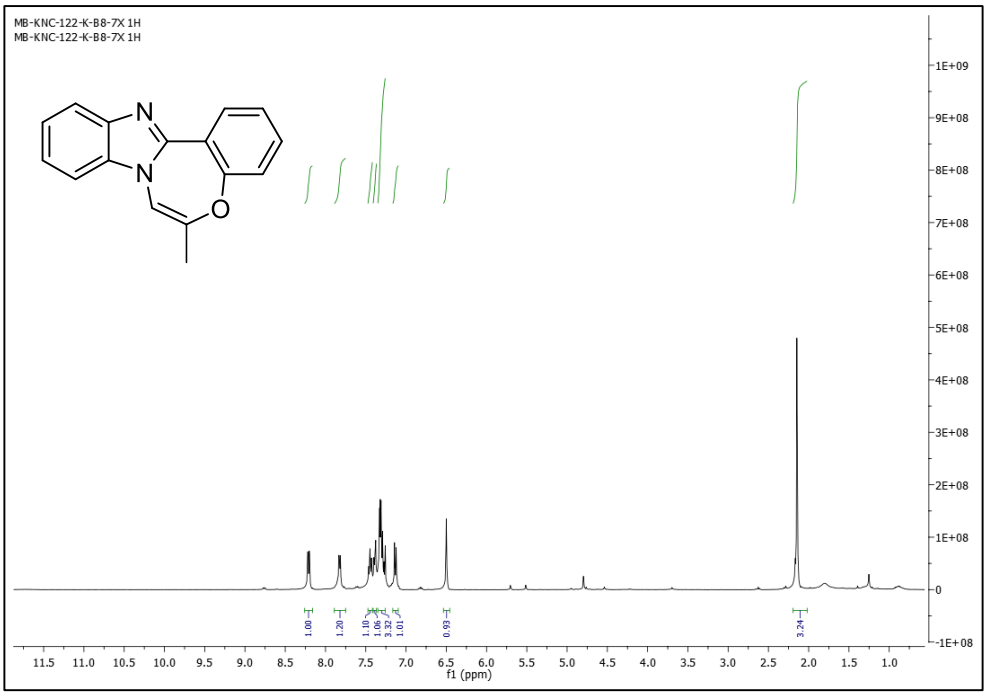

Figure 182. ^{1}H-NMR spectrum of compound **140b**

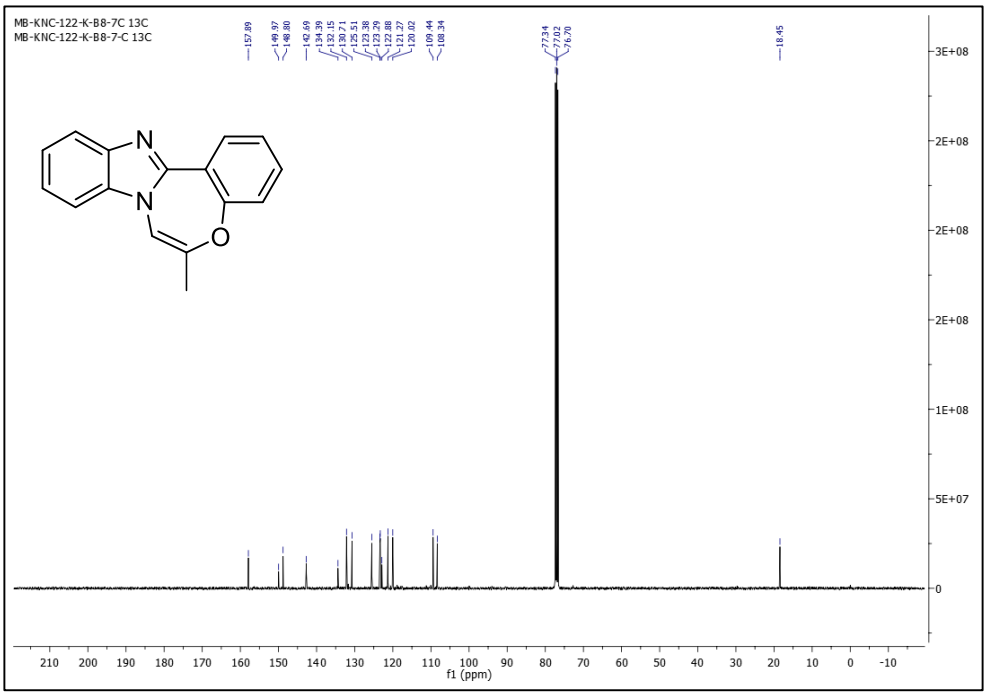

Figure 183. ^{13}C-NMR spectrum of compound **140b**

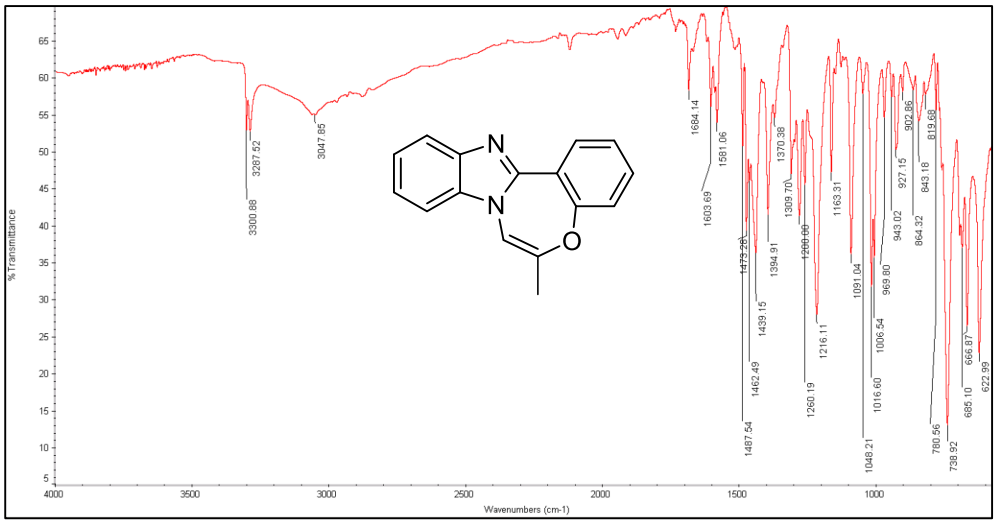

Figure 184. IR spectrum of compound **140b**

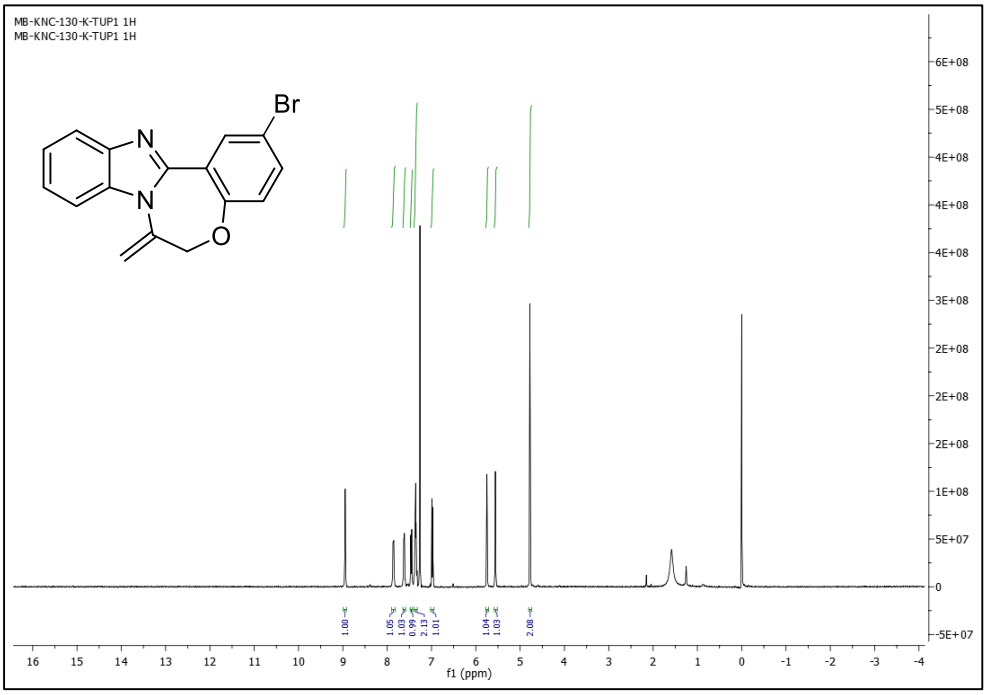

Figure 185. ^{1}H-NMR spectrum of compound **122b**

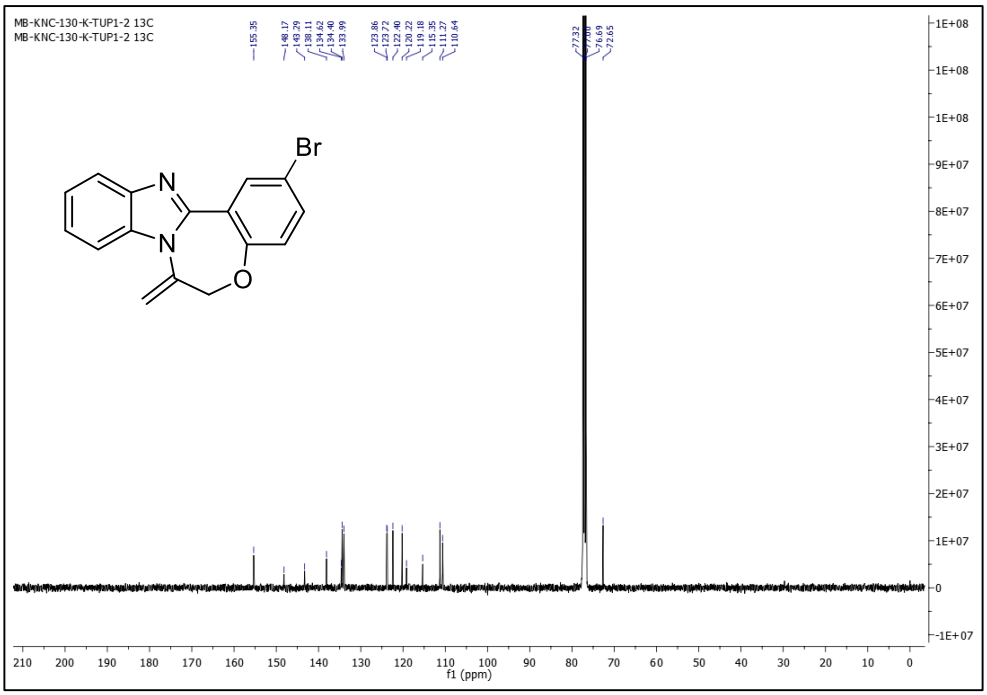

Figure 186. ^{13}C-NMR spectrum of compound **122b**

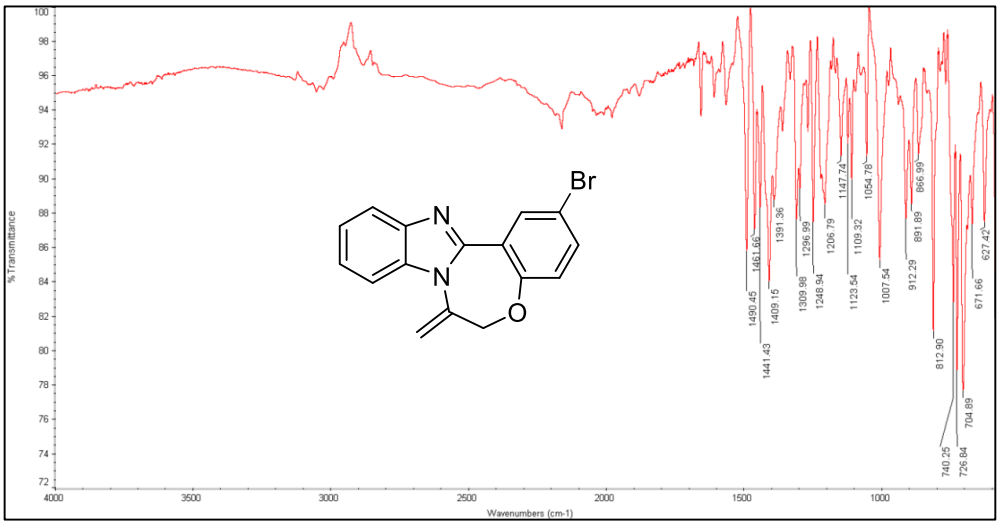

Figure 187. IR spectrum of compound **122b**

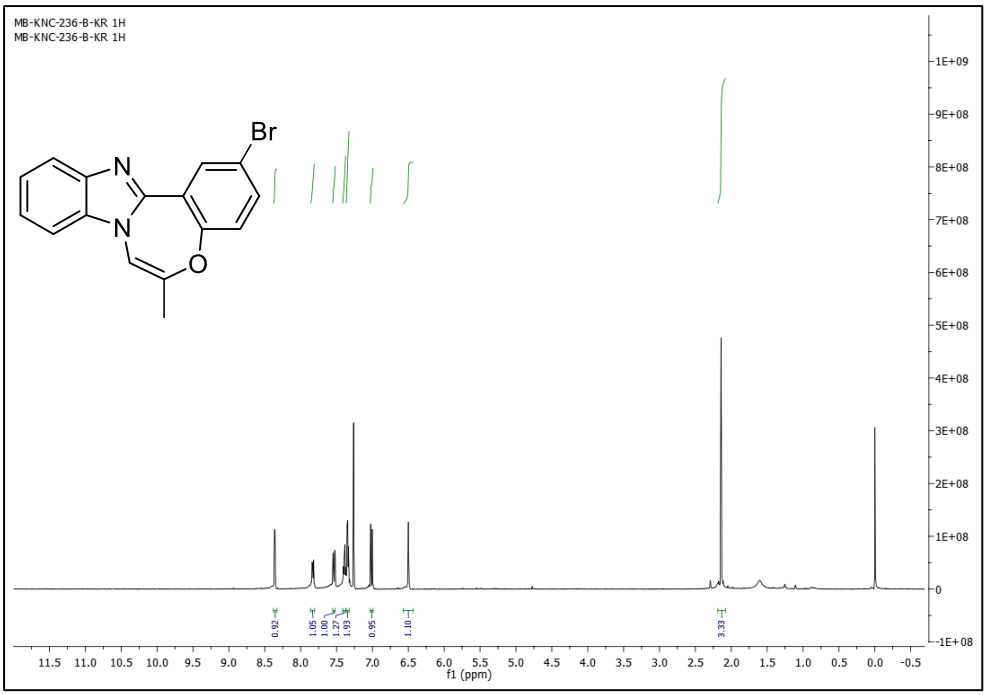

Figure 188. [1]H-NMR spectrum of compound **141b**

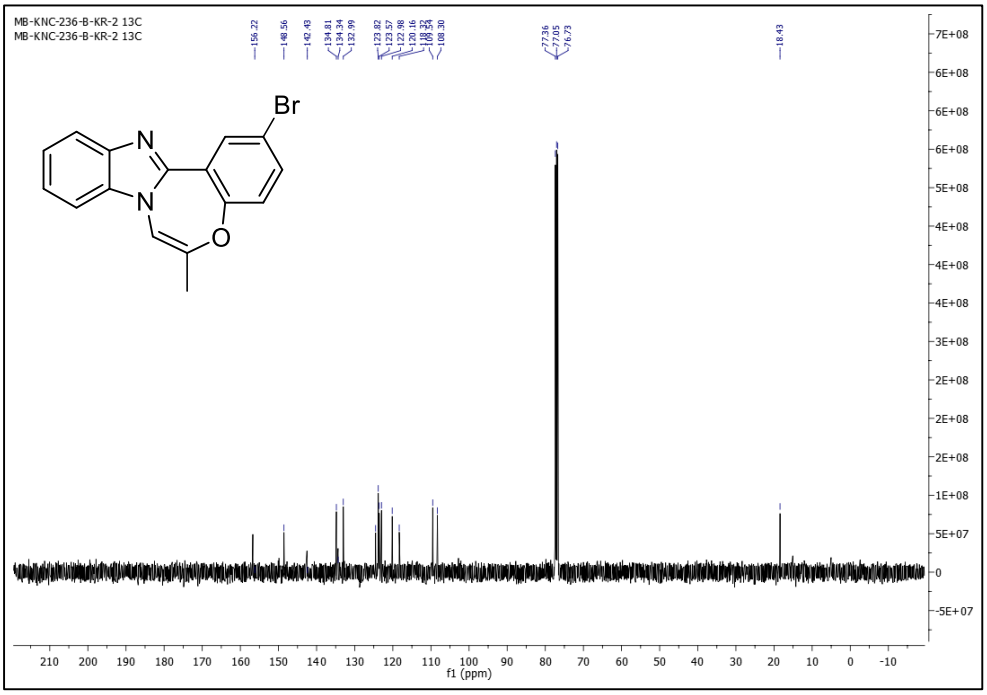

Figure 189. [13]C-NMR spectrum of compound **141b**

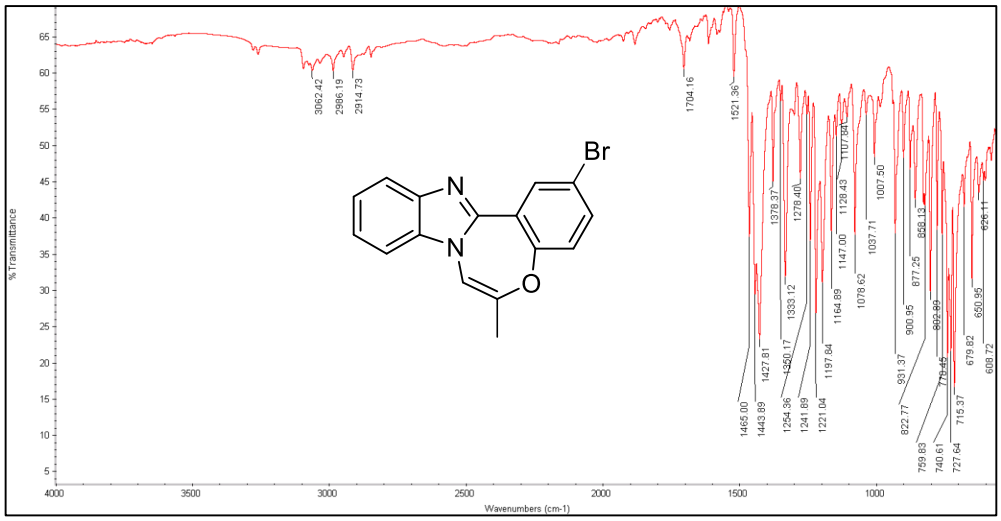

Figure 190. IR spectrum of compound **141b**

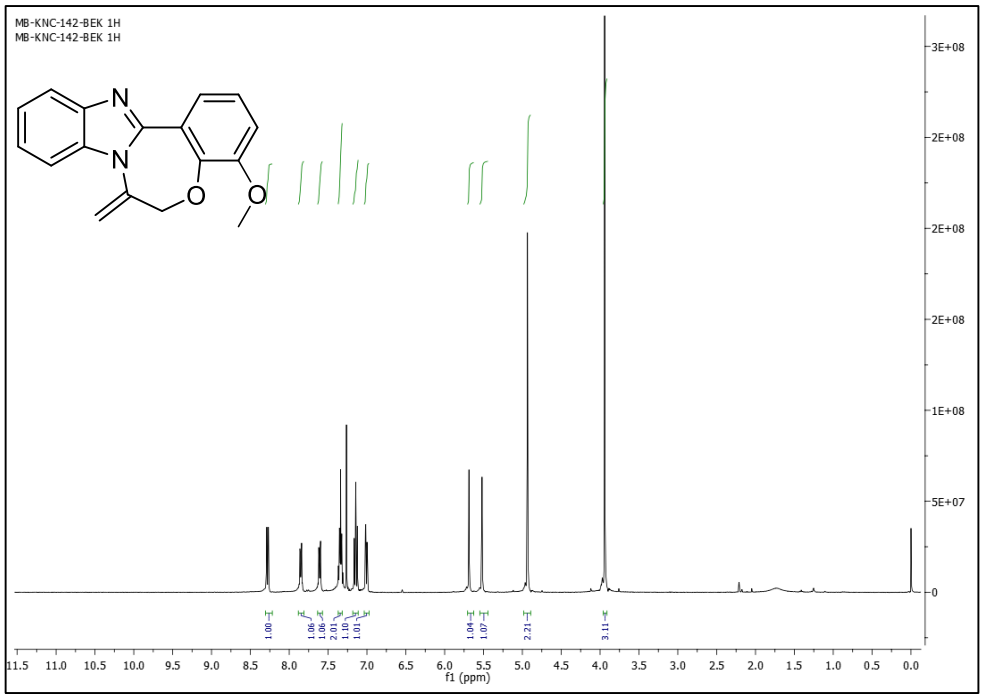

Figure 191. ^{1}H-NMR spectrum of compound **122c**

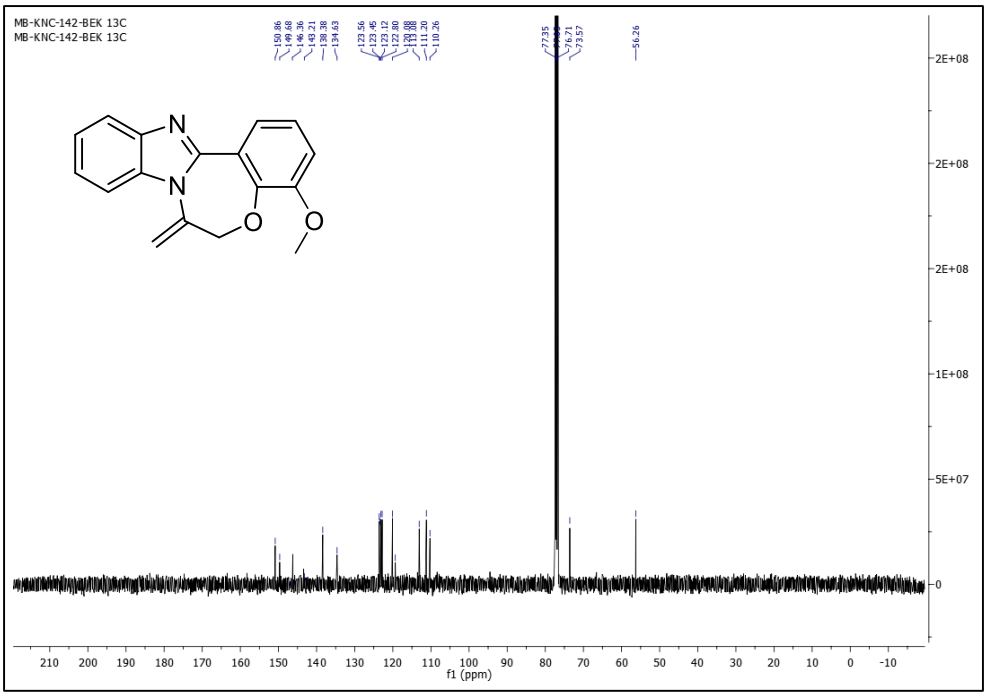

Figure 192. ^{13}C-NMR spectrum of compound **122c**

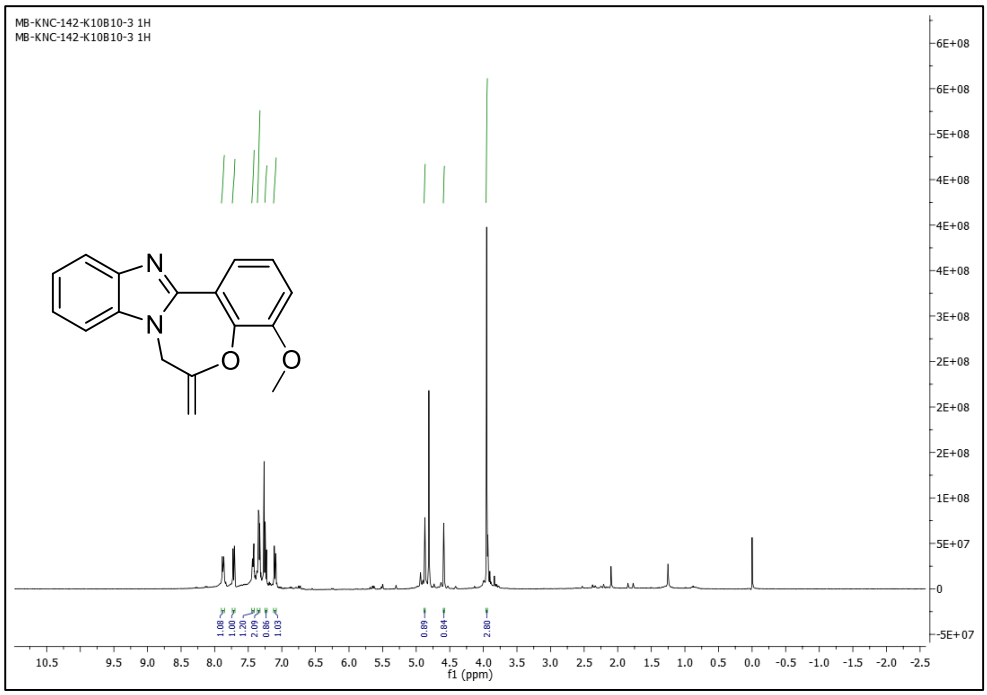

Figure 193. ^{1}H-NMR spectrum of compound **135a**

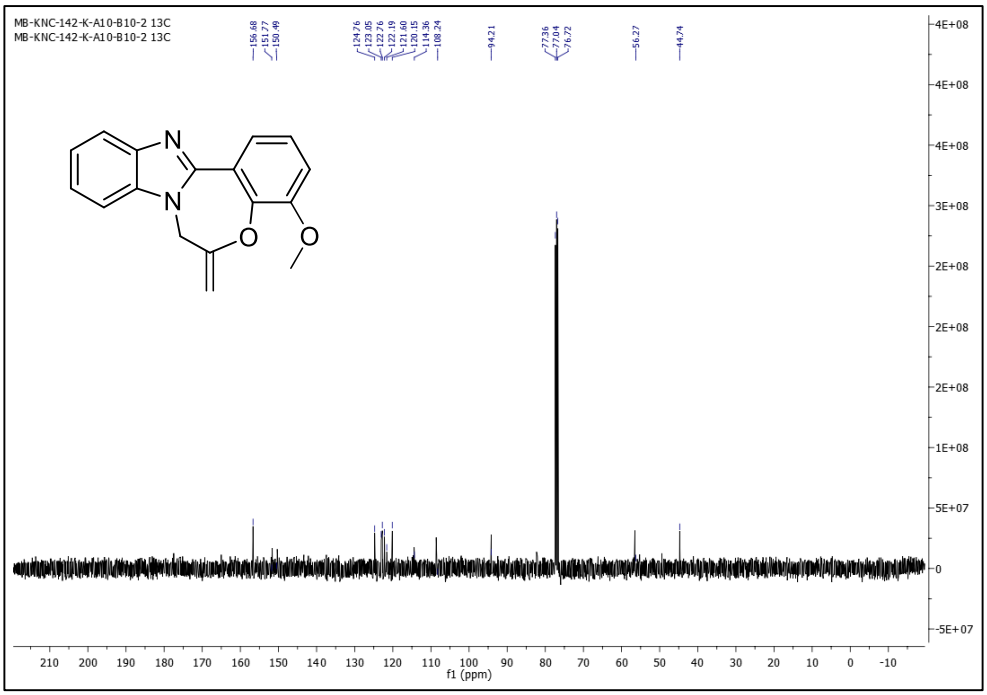

Figure 194. ^{13}C-NMR spectrum of compound **135a**

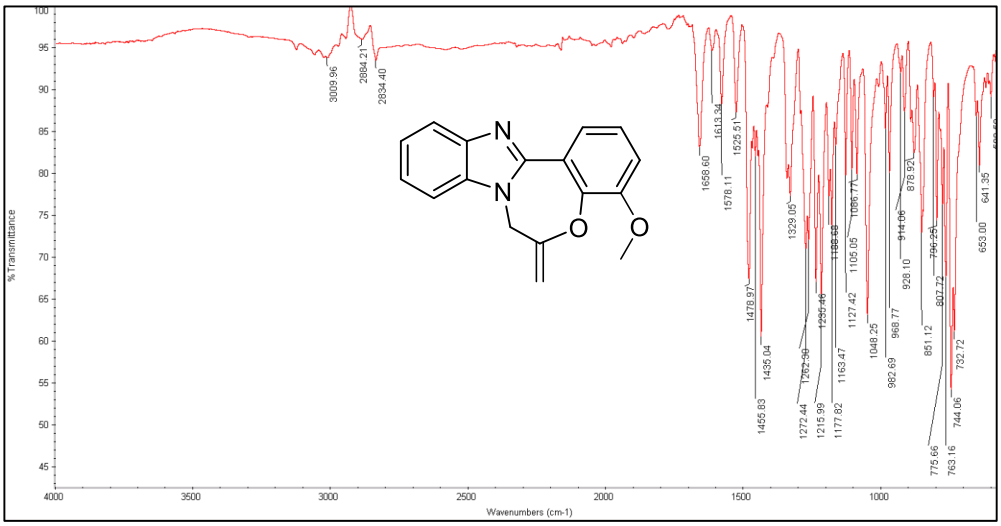

Figure 195. IR spectrum of compound **135a**

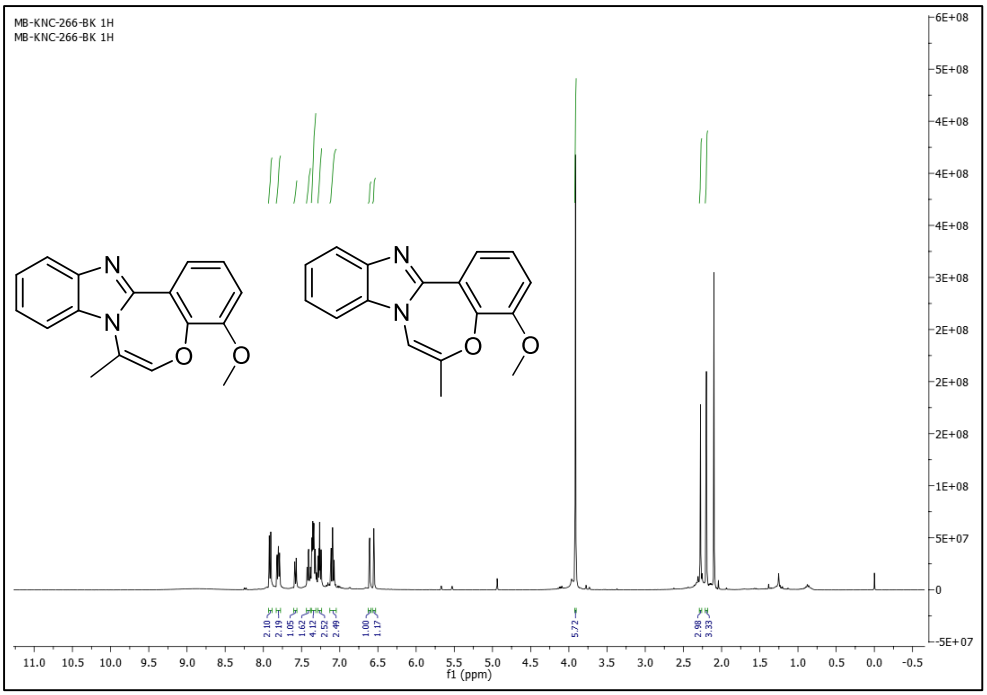

Figure 196. ^{1}H-NMR spectrum of compound **123c** and **135b**

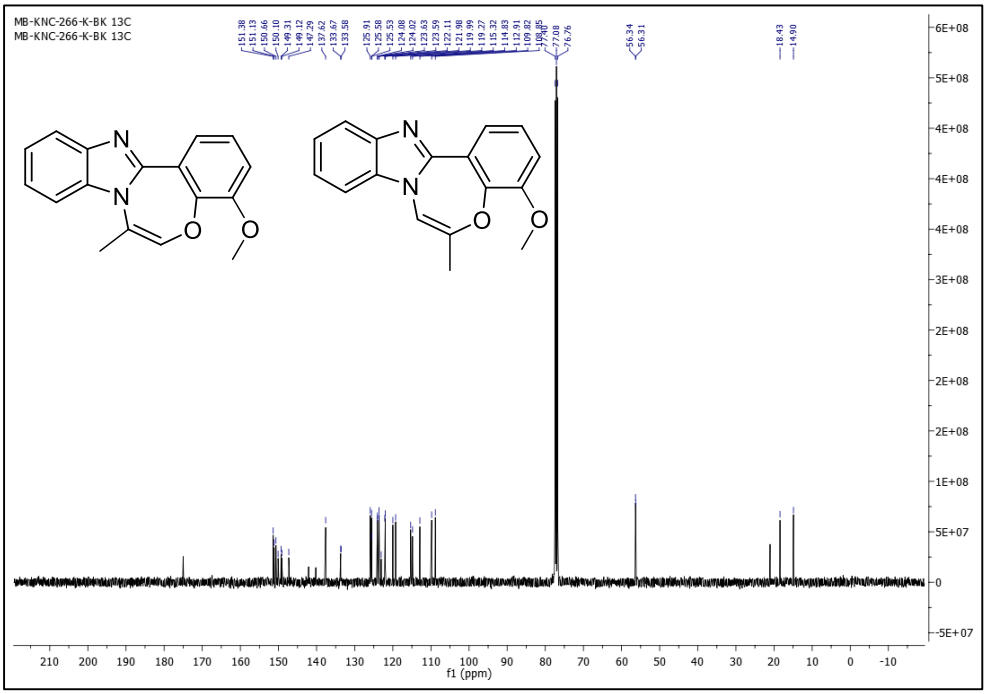

Figure 197. ^{13}C-NMR spectrum of compound **123c** and **135b**

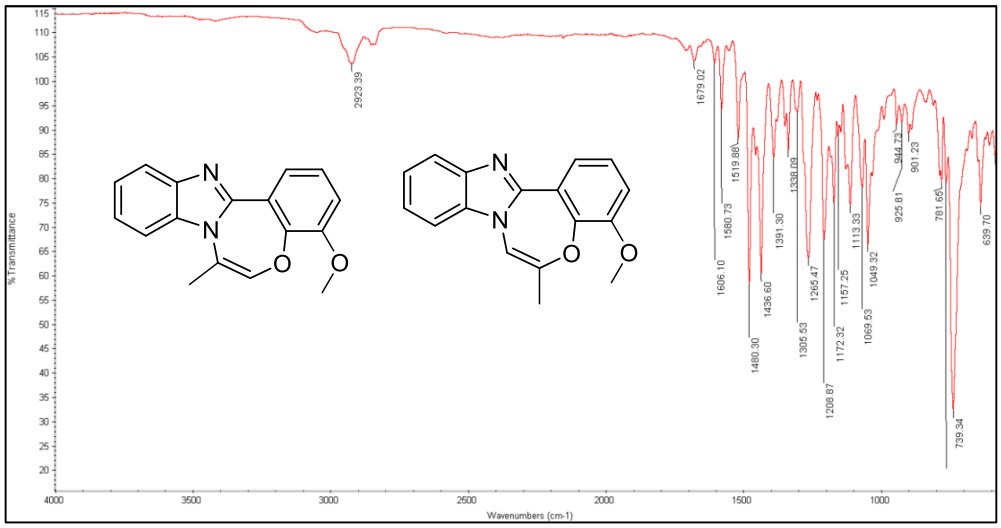

Figure 198. IR spectrum of compound **123c** and **135b**

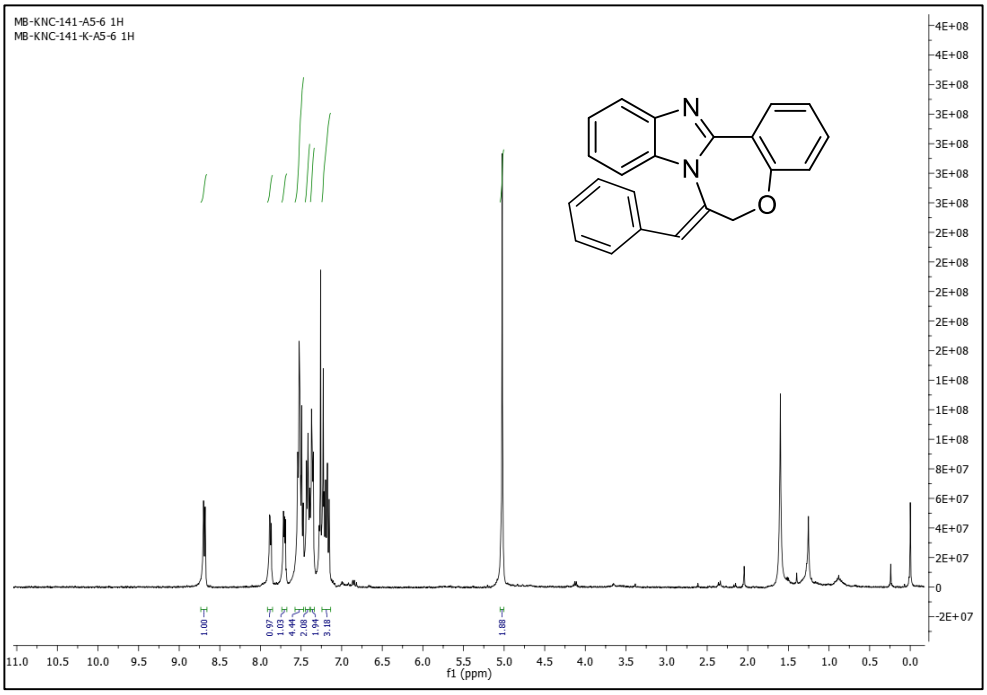

Figure 199. ^{1}H-NMR spectrum of compound **122d-*Z***

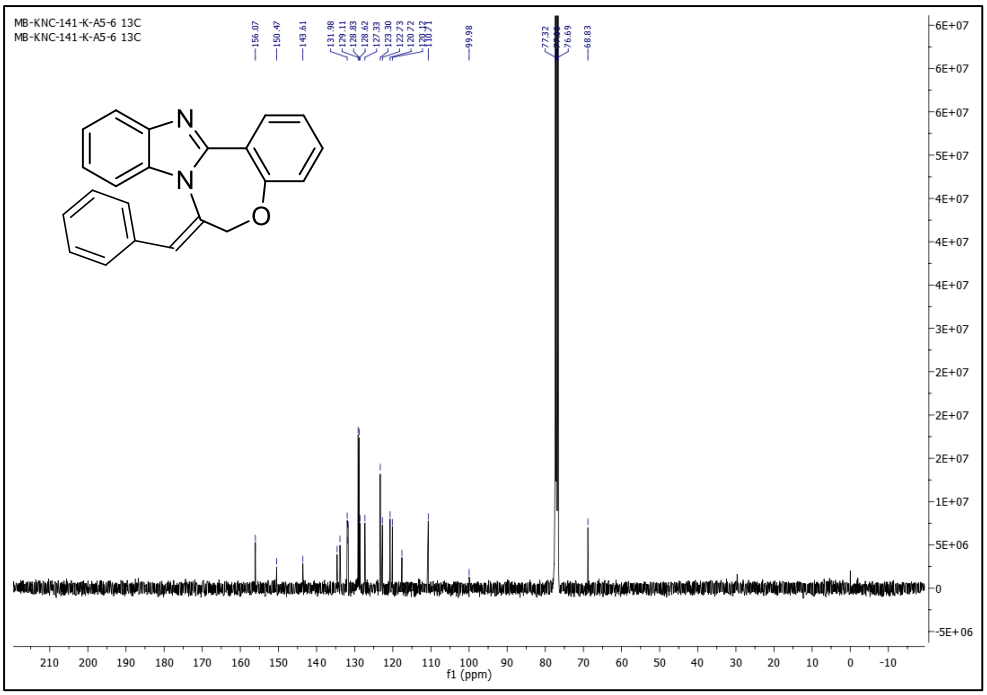

Figure 200. ^{13}C-NMR spectrum of compound **122d-*Z***

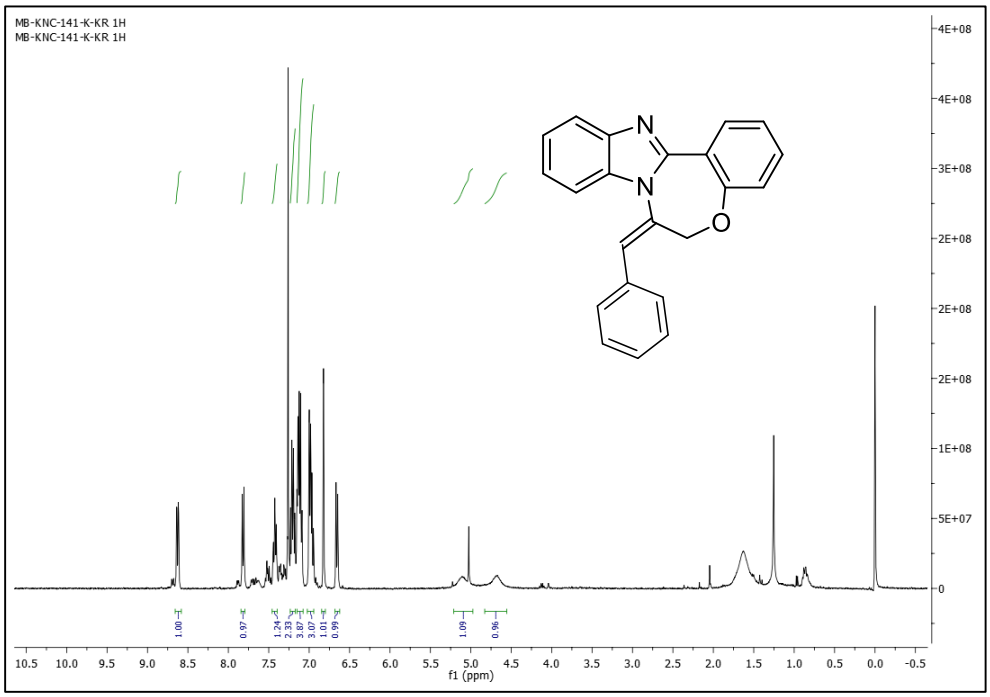

Figure 201. ^{1}H-NMR spectrum of compound **122d-*E***

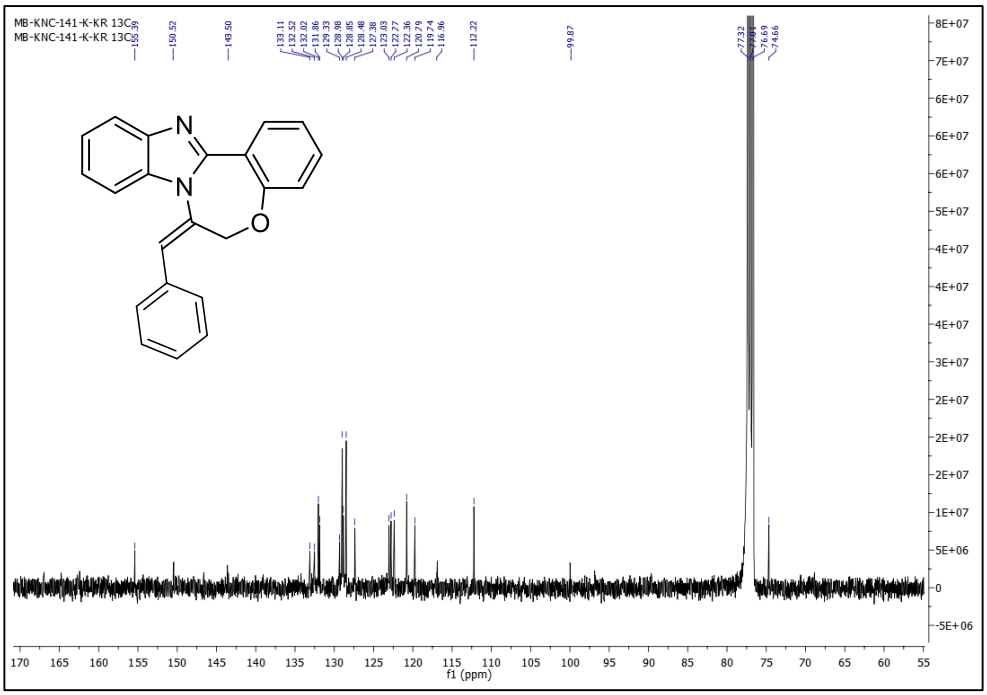

Figure 202. ^{13}C-NMR spectrum of compound **122d-*E***

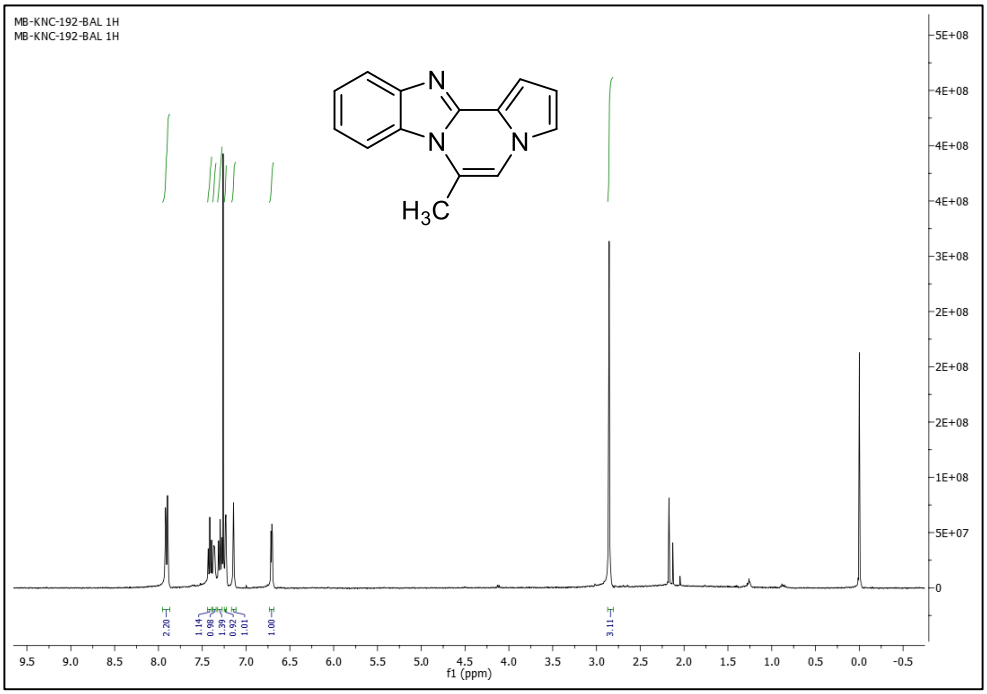

Figure 203. ^{1}H-NMR spectrum of compound **146**

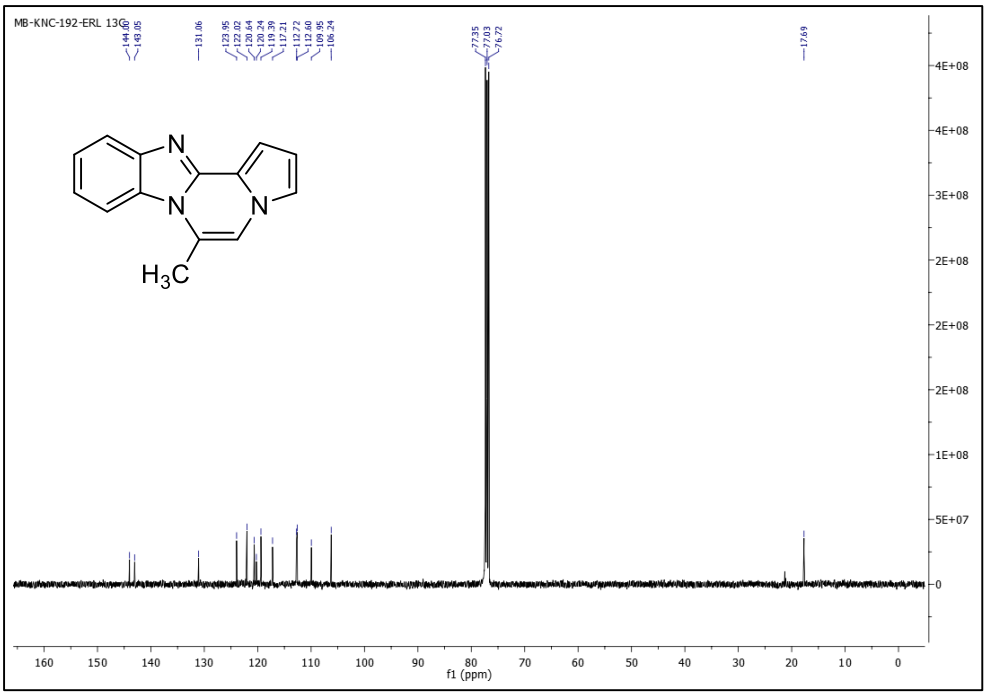

Figure 204. ^{13}C-NMR spectrum of compound **146**

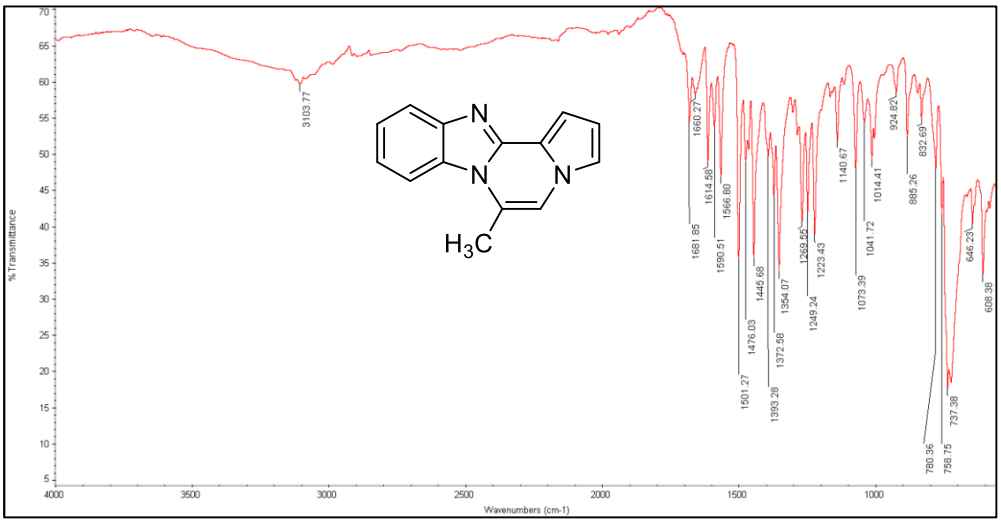

Figure 205. IR spectrum of compound **146**

CURRICULUM VITAE

PERSONAL INFORMATION:

Date and Place of Birth: 20/09/1985, Istanbul (TURKEY)

Marital Status: Married

Nationality: Republic of Turkey

E-mail: korkmaz.nalan@gmail.com

EDUCATION

Ph.D.: METU Department of Chemistry, Ankara (3.93/4.00)

Date of Graduation: September, 2018

M.S.: METU Department of Chemistry, Ankara (3.79/4.00)

Date of Graduation: October, 2011

B.S.: METU Department of Chemical Engineering (Minor), Ankara (2.74/4.00)

Date of Graduation: January, 2010

B.S.: METU Department of Chemistry (Major), Ankara (3.30/4.00)

Date of Graduation: June, 2009

High School: Sakarya Anatolian High School, Sakarya (5.00/5.00)

Date of Graduation: June, 2003

EXPERIENCE:

19.01.2016 – 03.10.2017:	**METU**
	CHEMISTRY DEPARTMENT
	Research and Teaching Assistant
16.09.2013 – 15.01.2016:	**TUBITAK – SAGE**
	TGTB-ESG-PYROTECHNICS SYSTEM DIVISION
	Mamak/ANKARA
	Research Engineer
09.11.2010 - 15.09.2013:	**METU**
	CHEMISTRY DEPARTMENT
	Research and Teaching Assistant
15.06.2008 - 15.09.2008:	**MIT (Massachusetts Institute of Technology)**
	CHEMICAL ENGINEERING DEPARTMENT
	Massachusetts-Boston/USA
	Internship

PUBLICATION:

1. **Korkmaz Cokol, N**.; Kaya, S.; Balci, M.; A new synthon for the synthesis of aminoinositol derivatives, *Tetrahedron Lett.* **2017**, *58*, 2732-2735

PROFESSIONAL MEETINGS AND ACTIVITIES:

29.06 - 07.02.2010:	24. National Chemistry Congress
	Zonguldak Karaelmas University-Zonguldak
07.06 - 02.07.2011:	25. National Chemistry Congress
	Erzurum Atatürk University-Erzurum
09-18.07.2011:	43. International Chemistry Olympics
	METU-Ankara
19-21.10 2011:	Chemistry Symposium
	METU-Ankara
01-06.10.2012:	26. National Chemistry Congress
	Muğla Sıtkı Kocman University-Muğla

29-31.03.2013:	1. Medicinal Chemistry Congress
	Chemistry Society-Antalya
16.09.2013:	Security And Privacy Education for Defensive Industry
	TUBITAK-SAGE-Ankara
24.09.2013:	General Health And Safety Training
	TUBITAK-SAGE-Ankara
22.11.2013:	Explosive Materials Workshop
	MKEK-Ankara
12.07.2014:	11. Workshop Pyrotchnics Combustion Mechanisms
	IPSUSA-Colorado Springs/Colorado-USA
13-18.07.2014:	40th International Pyrotechnics Seminar
	IPSUSA-Colorado Springs/Colorado-USA
20-24.08.2017:	254th ACS National Meeting Society
	Washington D.C-USA